



**Interactions between  $\beta$ -lactoglobulin and  
nutraceutical ligands riboflavin,  
vitamin D<sub>3</sub> and Lysozyme  
Formation, physico-chemical and biological characterization of  
functional delivery scaffolds**

**Thèse**

**Fatoumata Diarrassouba**

**Doctorat en sciences et technologie des aliments**  
Philosophiae Doctor (Ph.D)

Québec, Canada

© Fatoumata Diarrassouba, 2013



## Résumé

La protéine majeure du lactosérum, la  $\beta$ -lactoglobuline ( $\beta$ lg) est bien reconnue pour ses propriétés structurales intéressantes lui permettant d'établir des interactions avec des ligands de taille et de caractéristiques différentes. La riboflavine (RF) et la vitamine D<sub>3</sub> (D<sub>3</sub>) ont été sélectionnées comme modèles de petits nutraceutiques amphiphiles et hydrophobes, respectivement, et le lysozyme (Lyso), comme ligand protéique de plus grande taille.

La capacité de la  $\beta$ lg à lier la RF a été étudiée par des méthodes spectroscopiques. La  $\beta$ lg et la RF forment le complexe  $\beta$ lg-RF dont la photoactivation génère une activité antiproliférative contre les cellules cancéreuses de la peau, démontrée en utilisant le protocole du NCI/NIH Developmental Therapeutics Program. La cytotoxicité serait probablement due à la génération d'espèces oxydatives réactives résultant de l'interaction entre la RF et la  $\beta$ lg.

L'impact de la formation du  $\beta$ lg-D<sub>3</sub> sur la solubilité et stabilité de la D<sub>3</sub> a été étudié en utilisant des méthodes spectroscopiques et de chromatographie. Les résultats ont démontré que le complexe  $\beta$ lg-D<sub>3</sub> était stable aux pHs gastrique et intestinal et augmentait la solubilité de la D<sub>3</sub>. De plus, une matrice protéique appelée coagulum enrichie en D<sub>3</sub> ( $94.5 \pm 1.8$  % de taux d'encapsulation) été formée à partir du complexe  $\beta$ lg-D<sub>3</sub> grâce à l'aptitude de la  $\beta$ lg à s'auto-associer.

Les images de microscopie électronique ont montré que les interactions électrostatiques entre la  $\beta$ lg et Lyso ont pour leur part, abouti à la formation de microsphères pouvant encapsuler la D<sub>3</sub> à un taux élevé ( $90.8 \pm 4.8$  %).

La capacité des matrices à base de  $\beta$ lg à transporter, protéger et à améliorer la solubilité, la stabilité et la biodisponibilité de la D<sub>3</sub> a été évaluée en effectuant des expériences *in vitro* et *in vivo* chez des modèles animaux. Les matrices protéiques à base de  $\beta$ lg ont significativement augmenté la solubilité, stabilité et biodisponibilité de la D<sub>3</sub> ( $p < 0.001$ ). Ces études prouvent que la  $\beta$ lg, grâce à ses

caractéristiques suturales, pourrait former des matrices protéiques compatibles avec une administration orale et les aliments, tout en préservant l'activité biologique de la RF, de la D<sub>3</sub> et donc possiblement d'autres molécules bioactives.

## Abstract

The major whey protein,  $\beta$ -lactoglobulin ( $\beta$ lg) is well recognized for its interesting structural properties and ability to interact with ligands with varying size and characteristics. Riboflavin (RF) and vitamin D<sub>3</sub> (D<sub>3</sub>) were selected as small amphiphilic and hydrophobic nutraceutical models, respectively, and Lysozyme, as a larger size ligand model.

Spectroscopic methods were used to demonstrate interaction between  $\beta$ lg and RF.  $\beta$ lg and RF form a complex, which was irradiated according to the NCI/NIH Developmental Therapeutics Program. The  $\beta$ lg-RF complex exhibited an important anti-proliferative activity against skin melanoma cancer cell lines, probably due to the generation of reactive oxygen species as the result of the interaction between RF and  $\beta$ lg.

The impact of the  $\beta$ lg-D<sub>3</sub> complex on the solubility and stability of the D<sub>3</sub> was studied using spectroscopic methods and chromatography. The findings indicate that the  $\beta$ lg-D<sub>3</sub> complex is stable at the gastric and intestinal pHs and increases the solubility of the vitamin. A  $\beta$ lg-based scaffold, named coagulum, enriched with D<sub>3</sub> ( $94.5 \pm 1.8$  % of encapsulation efficiency) was prepared by using the capacity of  $\beta$ lg to self-aggregate.

Electronic microscopy images showed that microspheres, with high D<sub>3</sub> encapsulation efficiency ( $90.8 \pm 4.8$  %), were formed as the result of electrostatic interactions between  $\beta$ lg and Lyso.

The efficiency of  $\beta$ lg-based scaffolds to improve the solubility, stability and bioavailability of the D<sub>3</sub> was evaluated by performing *in vitro* and *in vivo* experiments using animal model. The  $\beta$ lg-based scaffolds significantly increased the solubility, stability bioavailability of D<sub>3</sub> ( $p < 0.001$ ). Overall, the present study showed that  $\beta$ lg, due to its structural properties, can be used to form protein-based

matrices compatible with a food and an oral administration while preserving the biological activity of RF, D<sub>3</sub> and possibly other bioactive molecules.

# Preface

The present thesis is submitted to the Faculty of Graduate Studies of Laval University (Faculté des études supérieures de l'Université Laval) to meet the requirements for achieving the *Philosophiae Doctor es Sciences* (Ph. D.) degree at the Faculty of Agriculture and Food Science (Faculté des Sciences de l'Agriculture et de l'Alimentation).

The research was mostly conducted at the Department of Food Science and Technology, Faculty of Agriculture and Food Science, Laval University. Additional experimental work was performed at the EA-CIDAM (Ingénierie Développement Aliment Médicament), Laboratoire de Biopharmacie, Faculté de Pharmacie, Clermont-Ferrand, France, with Professor Eric Beyssac, Associate Professor PhD Ghislain Garrait, PhD Li Liang and PhD Pedro Alvarez, as collaborators. PhD Garbiel E. Remondetto and Professor Muriel Subirade were the co-supervisor and supervisor, respectively.

In the introduction section, the work presented in this thesis describes the use of bovine milk whey  $\beta$ -lactoglobulin in the formulation of food grade oral delivery platforms. The first chapter of the thesis is a literature review on  $\beta$ -lactoglobulin – based delivery scaffolds, a version of which will be published in the book titled '*Engineering Foods for Bioactives Stability and Delivery*' to be published by Springer.

The rationale for this work, hypothesis and objectives are presented in the second chapter. The main experimental work of this thesis has been published or submitted for publication in relevant scientific journals. Versions of seven manuscripts were presented in chapters 3 to 9 as follows:

- Chapter 3. Fatoumata Diarrassouba, Gabriel Remondetto, Li Liang and Muriel Subirade. 2013. Nanocomplex formation between riboflavin and  $\beta$ -lactoglobulin: spectroscopic investigation and biological characterization. *Food Research International*. 52(2):557–567.

- Chapter 4. Fatoumata Diarrassouba, Gabriel Remondetto, Li Liang, Ghislain Garrait, Eric Beyssac and Muriel Subirade. 2013. Effects of gastrointestinal pH conditions on the stability of the  $\beta$ -lactoglobulin/vitamin D<sub>3</sub> complex and on the solubility of vitamin D<sub>3</sub>. *Food Research International*. 52(2):515 – 521.

- Chapter 5. Fatoumata Diarrassouba, Ghislain Garrait, Gabriel Remondetto, Pedro Alvarez, Eric Beyssac and Muriel Subirade. 2014. Increased stability and protease

resistance of the  $\beta$ -lactoglobulin/vitamin D<sub>3</sub> complex. Food Chemistry. 145:646-652.

- Chapter 6. Fatoumata Diarrassouba, Gabriel Remondetto, Ghislain Garrait, Pedro Alvarez, Eric Beyssac and Muriel Subirade. Increased water solubility, stability and bioavailability of vitamin D<sub>3</sub> upon sequestration in  $\beta$ -lactoglobulin - Based Coagulum. Submitted to the Journal of Controlled Release.

- Chapter 7. Fatoumata Diarrassouba, Ghislain Garrait, Gabriel Remondetto, Pedro Alvarez, Eric Beyssac and Muriel Subirade. Self-assembly of  $\beta$ -lactoglobulin and egg white lysozyme as a potential carrier for nutraceuticals. Submitted to the Journal of Physical Chemistry B. Manuscript ID jp-2013-08298b.

- Chapter 8. Fatoumata Diarrassouba, Ghislain Garrait, Gabriel Remondetto, Pedro Alvarez, Eric Beyssac and Muriel Subirade. Food proteins-based microspheres for increased uptake of vitamin D<sub>3</sub>. Submitted to the Journal of Controlled Release.

- Chapter 9. Fatoumata Diarrassouba, Ghislain Garrait, Gabriel Remondetto, Pedro Alvarez, Eric Beyssac and Muriel Subirade. Comparative study between different  $\beta$ -lactoglobulin-based scaffolds for the delivery of vitamin D<sub>3</sub>. This manuscript is still in preparation. A comparative study was performed between the  $\beta$ lg-based scaffolds prepared in the present thesis, the  $\beta$ lg/vitamin D<sub>3</sub> complex, and the free vitamin D<sub>3</sub>. The efficiency of the different systems to stabilize and enhance the bioavailability of vitamin D<sub>3</sub> were evaluated.

Finally, the conclusion of this work including the main findings and research outcome and perspectives are presented in chapter 10, which is followed by the references and appendices. Appendix I represents the list of contributions including the list of manuscripts and conferences. Appendices 2 to 6 represent the posters and oral presentations at different conferences and oral presentation competitions.

*To my beloved dad Soumana Diarrassouba,*

*Humble and accomplished scientist,  
your exceptional human and scientific  
qualities are recognized worldwide.  
You have deeply touched everyone  
who has been in contact with you,  
You are my inspiration, role-model,  
and mentor. You are my hero dad.*



# Acknowledgements

The present PhD thesis is the outcome of converging efforts of many years of hard work and dedication, which would have not been possible without the constant support and love from my family, friends, supervisors and co-workers.

## **Family and friends.**

First and foremost, I would like to express all my love and gratitude to my son Soumana for being such a great, loving and compassionate human being. He is always supportive, always ready to give me hug whenever he feels like I need comfort and warmth. Thank you son and know that I am so grateful to be your mom and so proud of you.

To moms Assitan Samaké and Heidi Rempel, dads Irv Rempel and Soumana Diarrassouba, without whom I would not have been at this stage of my personal and professional live. I love you dearly and I thank you so much for your unconditional love and support. This PhD thesis is the result of your joined blessings. God bless you all. A special 'thank you' to Mom Heidi for your patience and precious help in proofreading all my papers during these years, from my Masters degree to the present PhD thesis. You have been a great inspiration for me, a role model who will always inspire me in all areas in my life.

To my brothers Ibrahim, N'Faly, Jamy, Brad and sister Kim, thank you for being so supportive and thoughtful.

I am very much grateful to my dear friends Anne and David Ehret for all the help and invaluable support, encouragement and advice. David I have no word strong enough to express all my gratitude for all your help in editing my work. Your contribution to this thesis was deeply appreciated. Anne thank you for motivating me, your invaluable support and commitment to our twining project Teriya.

I am deeply thankful to my dear friend Earla Legault for all the love, good spirit, beautiful smile and for introducing me to the group of the 'Healing Chicks': Darlene, Irene, Debbie, Patsy, Roxanne, Carmen, Margot, Leigh-Ann, Jinder, Paula, Christine and Osa. Thank you for all the positive thoughts, great and unique moments we shared. Thank you Earla for your help and priceless contribution to our twining project Teriya.

I would like to specially dedicate this PhD thesis to Amine, Alya, Tamou Jelti and Adama Berthe. You are my family, my friends and I love you dearly. Thank you for being there at any moment of the day and night for me and Soumana.

My deep appreciation and love to my dear buddies Mariama Abdou Goubé and Fatou Thiam. Thank you for all the inspiring discussions, great moments we shared and unforgettable memories.

Thank you to my friends Ibrahima and Kadiatou Sow, OumouTouré Fall, Solange N’Gazo and Rémy and Hapsatou Maiga.

I am very grateful to my friends and colleagues who made this PhD a very enjoyable ride that was rich in learning opportunities, pleasant encounters and new friendships: Massama, Raquel, Romain, Li Liang, Pedro Álvarez, Ahmed Gomez, Shyam Suwal, Luis Felipe Gutiérrez, Luca Lo Verso, Sébastien Goumon, Abdelbasset Atia (Abdel), Élodie Rozoy, Sandra Laneuville, Sabrine, Nassim, Juan, Sergei Mikhailyn, Hasna Hanchi, Rima Atoum, Hany Geagea, Hélène Gaudreau, Charles Edmonds, Sophie Banville, Marina Bergoli, Mónica Araya-Farías and Franck.

To all my Teriya friends, in Mali, the Commune of Sanakoro – Djitumu, and the cities of Agassiz and Harrison-Hot-Springs: thank you for your enthusiastic commitment and accepting to be part of this exciting ride. Special ‘thank you’ to Monica for translating most of our documents for the twinning project.

I would like to thank Ghislain Garrait, Rachel, Quentin and Alexis for all the help and warm welcome which made me feel like I was home any time I traveled to Clermont-Ferrand (France). I am so grateful to you Ghislain and so glad that I was coached by you. Thank you so very much for your great and invaluable scientific contribution to my work.

## **Supervisors and co-workers.**

I am deeply grateful to my supervisor, Professor Muriel Subirade for accepting me as a PhD student in her prestigious Canadian Research Chair and team. Muriel impressed me with her pragmatism and dynamism. She inspired me with her excellent management skills. I learned a lot from her and acquired useful tools for my future academic carrier.

I am very thankful to my co-supervisor, Gabriel E. Remondetto for accepting to work with me despite his busy schedule and professional commitment. I was mesmerized by Gabriel's multidisciplinary competence. He has a vast knowledge in so many research areas and is very knowledgeable. With his contribution, my work gained in meaningful insights and considerable depth.

I would like to thank Professor Jean Amiot for agreeing to pre-read this thesis and for his valuable comments.

I am thankful to Dr Michel Britten, for evaluating this thesis. Dr Britten is world-class scientist well known for his work in the dairy industry, on milk components, milk by-products and processed foods.

I am grateful Professor D errick Rousseau for agreeing to be the external examiner of this thesis. I feel very privileged to receive an evaluation and a feedback on my work from such a world class and well renowned scientist in food research.

I am deeply grateful to Profesor Odile Chambin for accepting to take the trip to Qu ebec city to evaluate this thesis, despite her extremely busy agenda. I am very appreciative for having such a well-known scientist in Pharmaceutical and polymeric delivery technologies to evaluate my work.

I must also thank Professor Eric Beyssac for inviting to carry out important parts of my research in his lab EA – CIDAM ( quipe d'Accueil, Conception Ing enierie D veloppement Aliment M dicament) at Clermont-Ferrand, France. Prof. Beyssac was always available to provide any support, scientific advice or resources, which helped my greatly to reach important results during both of my stays in his lab.

I am thankful to the team of the EA – CIDAM lab: Xie, Roselyne, Pascale, Sandrine, Professor Cardot and Val erie for the good moments in the lab and positive encouragement in my studies.

It my absolute pleasure to thank Mr Bernard Pouliot for all the laughter and very joyful moments in his office when we were working on my different PowerPoint presentations and scientific posters. I am profoundly thankful for all the advice and learning opportunities, both socially and professionally. It was such an honor for me to get to know such a unique human being.

Finally, I would like to express my sincere acknowledgements and deep appreciation to the technicians without whom this PhD thesis would have never been completed with such an ease and an efficiency: Diane Gagnon, Pascal Dubé, Alain Gaudreau and Richard Janvier.

This thesis was sponsored by the Canada Research Chair on Proteins, Biosystems and Functional Foods and the Natural Sciences and Engineering Research Council of Canada (NSERC) through the Vanier Canada Graduate Scholarships (Diarrassouba, F.). Experimental works in France (EA-CIDAM Faculté de Pharmacie, Clermont-Ferrand, France) were funded by the Canada Graduate Scholarships – Michael Smith Foreign Study Supplements (Diarrassouba, F.) and Fonds de Recherche Nature et Technologies Québec (FRQNT) – International Training Program (Diarrassouba, F.).

Thank you God for helping me all along.

# Table of contents

Résumé.....	iii
Abstract.....	v
Preface.....	vii
Acknowledgements.....	xi
Table of contents.....	xv
List of abbreviations.....	xxvi
Introduction.....	1
Chapter 1. Literature review.....	5
1.1. Abstract.....	6
1.2. Introduction.....	6
1.3. Manufacture of whey proteins.....	8
1.4. Fractionation of $\beta$ lg from the whey proteins.....	9
1.5. Structure of $\beta$ lg.....	11
1.5.1. Basic structure of $\beta$ lg.....	11
1.5.2. Structural transitions of $\beta$ lg.....	17
1.6. Functionality of $\beta$ lg.....	18
1.7. Formation and characterization of the $\beta$ lg-ligand complexes.....	20
1.7.1. Structural basis for the formation of the $\beta$ lg-ligand complexes.....	20
1.7.2. Fluorescence quenching upon ligand binding.....	21
1.7.2.1. Theoretical explanation.....	21
1.7.2.2. Fluorescence emission of $\beta$ lg.....	23
1.7.3. Circular dichroism.....	24
1.7.3. Blg-ligand complexes.....	25
1.8. Blg-biopolymer self-assembly.....	29
1.8.1. Blg auto-association.....	29
1.8.2. Blg-based delivery systems: from molecule to particles.....	30
1.8.3. Blg-based microparticles for oral delivery.....	34
1.8.4. Characterization of $\beta$ lg-based nano and microparticles.....	38
1.9. Conclusion.....	41
Chapter 2.....	43
Problem statement.....	43
Hypothesis and objectives.....	43
2.1. Problem statement.....	44
2.2. Hypothesis.....	46
2.3. Objectives.....	46
2.3.1. General objective.....	46
2.3.2. Specific objectives.....	46
Chapter 3. Nanocomplex formation between riboflavin and $\beta$ -lactoglobulin: spectroscopic investigation and biological characterization.....	51
3.1 Abstract.....	52
3.2 Introduction.....	52

3.3. Experimental section .....	54
3.3.1. Materials .....	54
3.3.2. Sample preparation.....	54
3.3.3. Circular dichroism measurement.....	55
3.3.4. Steady state fluorescence measurement.....	55
3.3.4.1. Protein fluorescence spectra .....	55
3.3.4.2. Synchronous fluorescence spectra .....	56
3.3.5. Biological characterization of the $\beta$ lg/RF nanocomplex.....	56
3.3.5.1. Cell line culture .....	56
3.3.5.2. Anti-proliferative activity assay.....	56
3.3.5.4. Light stability of the $\beta$ lg/RF nanocomplex .....	58
3.4. Results and discussion.....	58
3.4.1. Influence of $\beta$ lg–RF interaction on the structure of the protein.....	58
3.4.2. Influence of RF on fluorescence spectra of $\beta$ lg .....	61
3.4.3. Analysis of fluorescence quenching mechanism.....	63
3.4.4. Fluorescence resonance energy transfer from $\beta$ lg to RF .....	66
3.4.5. Binding constants and binding points of RF to $\beta$ lg .....	71
3.4.6. Influence of RF on the synchronous fluorescence of $\beta$ lg.....	78
3.4.7. Anti-proliferative activity assay the $\beta$ lg/RF nanocomplex .....	80
3.4.8. Light stability of the $\beta$ lg/RF nanocomplex.....	85
3.5. Conclusion.....	87
3.6. Acknowledgments .....	88
Chapter 4. Effects of gastrointestinal pH conditions on the stability of the $\beta$ -lactoglobulin/vitamin D <sub>3</sub> complex and on the solubility of vitamin D <sub>3</sub> .....	90
4.1. Abstract .....	91
4.2. Introduction.....	92
4.3. Materials.....	95
4.3.1. Sample preparation.....	95
4.3.2. Influence of the pH on the stability of the $\beta$ lg/D <sub>3</sub> complex .....	95
4.3.3. Influence of the $\beta$ lg/D <sub>3</sub> complex formation on the solubility of vitamin D <sub>3</sub> .....	97
4.3.4. Statistical analysis.....	97
4.4. Results and discussion.....	98
4.4.1. Influence of the pH on the interaction between $\beta$ lg and D <sub>3</sub> .....	98
4.4.2. Influence of the pH on the stability of the $\beta$ lg/D <sub>3</sub> complex .....	106
4.4.3. Influence of the pH on the fractional residual fluorescence.....	109
4.4.4. Influence of the $\beta$ lg/D <sub>3</sub> complex formation on the solubility of D <sub>3</sub> .....	109
4.5. Conclusion.....	111
4.6. Acknowledgements .....	112
Chapter 5. Increased stability and protease resistance of the $\beta$ -lactoglobulin/vitamin D <sub>3</sub> complex .....	115
5.1. Abstract.....	116
5.2. Introduction.....	116
5.3. Experimental section .....	118
5.3.1 materials .....	118

5.3.2 sample preparation .....	118
5.3.3. Stability of the $\beta$ Ig/D <sub>3</sub> complex in refrigerated conditions .....	119
5.3.4. Uv – stability of the $\beta$ Ig/D <sub>3</sub> complex .....	119
5.3.5. Intestinal stability of the $\beta$ Ig/d <sub>3</sub> complex .....	120
5.3.6. <i>In vitro</i> study of the permeability of the $\beta$ Ig/D <sub>3</sub> complex .....	120
5.3.7. <i>In vivo</i> study of the intestinal absorption of the $\beta$ Ig/D <sub>3</sub> complex .....	121
5.3.7.1. Animal models .....	121
5.3.7.2. <i>In vivo</i> experiments .....	122
5.3.8. Statistical analysis .....	122
5.4. Results and discussion .....	123
5.4.1. Stability of the $\beta$ Ig/D <sub>3</sub> complex in refrigerated conditions .....	123
5.4.2. UV-light - stability of the $\beta$ Ig/D <sub>3</sub> complex .....	126
5.4.3. Intestinal stability of the $\beta$ Ig/D <sub>3</sub> complex .....	130
5.4.4. <i>In vitro</i> study of the permeability of the $\beta$ Ig/D <sub>3</sub> complex .....	137
5.4.5. <i>In vivo</i> study of the intestinal absorption of the $\beta$ Ig/D <sub>3</sub> complex .....	140
5.5. Conclusion .....	143
5.6. Acknowledgements .....	144
Chapter 6. Increased water solubility, stability and bioavailability of vitamin D <sub>3</sub> upon sequestration in $\beta$ -lactoglobulin - based coagulum .....	146
6.1. Abstract .....	147
6.2. Introduction .....	148
6.3. Experimental section .....	150
6.3.1. Materials .....	150
6.3.2. Sample preparation .....	150
6.3.3. Encapsulation of D <sub>3</sub> in the $\beta$ Ig-based coagulum .....	150
6.3.4. Stability of D <sub>3</sub> during long term storage at 4 °c .....	151
6.3.5. Stability of D <sub>3</sub> to uv-light irradiation .....	151
6.3.6. Kinetic release of D <sub>3</sub> in simulated intestinal fluid .....	152
6.3.7. <i>In vivo</i> study of the intestinal absorption of the D <sub>3</sub> containing $\beta$ Ig/lyso .....	152
6.3.8. Statistical analysis .....	153
6.4. Results and discussion .....	153
6.4.1. Encapsulation efficiency of D <sub>3</sub> in the $\beta$ Ig-based coagulum .....	153
6.4.2. Impact of the $\beta$ Ig-based coagulum on the long term stability of D <sub>3</sub> .....	154
6.4.4. Impact of the $\beta$ Ig-based coagulum on the uv-light stability of D <sub>3</sub> .....	157
6.4.5. Impact of the $\beta$ Ig-based coagulum on the intestinal kinetic release of D <sub>3</sub> .....	159
6.4.6. <i>In vivo</i> study of the bioavailability of D <sub>3</sub> .....	162
6.5. Conclusion .....	165
6.6. Acknowledgements .....	166
Chapter 7. Self-assembly of $\beta$ -lactoglobulin and egg white lysozyme as a potential carrier for nutraceuticals .....	168
7.1. Abstract .....	169
7.2. Introduction .....	170
7.3. Experimental section .....	172
7.3.1. Materials .....	172

7.3.2. Sample preparation.....	172
7.3.3. Effect of protein ratio on the formation of the $\beta$ lg/Lyso co-precipitate .	173
7.3.4. Effect of the ph on the formation of the $\beta$ lg/Lyso co-precipitate .....	173
7.3.5. Characterization of the $\beta$ lg/Lyso co-precipitate .....	174
7.3.5.1 size and surface charge.....	174
7.3.5.2 scanning and transmission electron microscopy for the determination of surface and interior morphology .....	174
7.3.6. Model nutraceutical loading studies .....	175
7.3.7. Statistical analysis.....	176
7.4. Results and discussion.....	176
7.4.1. Effect of the protein concentration on the formation of the $\beta$ lg-Lyso co-precipitates.....	176
7.4.2. Effect of the pH on the formation of the $\beta$ lg-Lyso co-precipitates.....	182
7.4.4. Characterization of the $\beta$ lg/Lyso co-precipitates .....	188
7.4.4.1 scanning and transmission electron microscopy of surface and interior morphology .....	188
7.4.4.2. Determination of the amounts of proteins in the $\beta$ lg/Lyso microspheres .....	190
7.4.5. Vitamin D <sub>3</sub> encapsulation in $\beta$ lg/Lyso microspheres.....	192
7.5. Conclusion.....	195
7.6. Acknowledgments .....	196
Chapter 8. Food proteins-based microspheres for increased uptake of vitamin D <sub>3</sub> .....	198
8.1. Abstract.....	199
8.2. Introduction.....	200
8.3. Experimental section .....	202
8.3.1. Materials .....	202
8.3.2. Sample preparation.....	202
8.3.3. Encapsulation of D <sub>3</sub> in the $\beta$ lg/Lyso microspheres .....	202
8.3.4. Stability of D <sub>3</sub> during long term storage at 4 °c.....	203
8.3.5. Stability of D <sub>3</sub> to UV-light irradiation.....	203
8.3.6. Kinetic release of D <sub>3</sub> in simulated intestinal fluid .....	203
8.3.7. <i>In vitro</i> study of the permeability of the D <sub>3</sub> .....	204
8.3.8. <i>In vivo</i> study of the intestinal absorption of the d <sub>3</sub> containing $\beta$ lg/Lyso	204
8.3.9. Statistical analysis.....	205
8.4. Results and discussion.....	206
8.4.1. Stability of D <sub>3</sub> during long-term storage at 4 °c.....	208
8.4.2. Stability of D <sub>3</sub> in response to uv-light irradiation .....	209
8.4.3. Kinetic release of D <sub>3</sub> in simulated intestinal fluid .....	214
8.4.4. <i>In vitro</i> study of the permeability of D <sub>3</sub> .....	221
8.4.5. <i>In vivo</i> study of the bioavailability of D <sub>3</sub> .....	224
8.5. Conclusion.....	226
8.6. Acknowledgments .....	226
Chapter 9. Comparative study between different $\beta$ -lactoglobulin-based scaffolds for the delivery of vitamin D <sub>3</sub> .....	228
9.1. Abstract.....	229

9.2. Introduction .....	230
9.3. Experimental section.....	232
9.3. Experimental section.....	232
9.3.1 materials .....	232
9.3.2 sample preparation .....	233
9.3.3. Stability in refrigerated conditions .....	233
9.3.4. Uv – stability of the $\beta$ Ig-based scaffolds .....	234
9.3.5. Intestinal stability of the $\beta$ Ig-based scaffolds.....	234
9.3.6. <i>In vivo</i> study of the bioavailability of D <sub>3</sub> .....	235
9.3.6.1. Animal models.....	235
9.3.6.2. <i>In vivo</i> experiments .....	235
9.3.7. Statistical analysis .....	236
9.4. Results and discussion .....	236
9.6. Conclusion .....	246
9.7. Acknowledgments.....	247
Chapter 10. Concluding chapter.....	248
10.1. Research outcome.....	249
10.2. Perspectives and future trends .....	252
References.....	255
Appendices .....	277
Appendix 1 .....	278
Appendix 2 .....	281
Appendix 3 .....	283
Appendix 4 .....	285
Appendix 5 .....	287
Appendix 6 .....	288

# Index of tables

## Chapter 1

Table 1.1. Major whey proteins content in bovine milk, unprocessed whey (UPW), whey protein concentrates (WPC) and whey protein isolates (WPI) ..... 9

## Chapter 3

Table 3.1. Stern–Volmer quenching constants  $K_{SV}$  and dynamic quenching rate constant at different temperatures ..... 65

Table 3.2. Energy efficiency transfer and distance between the donor  $\beta$ lg and the acceptor RF ..... 68

Table 3.3. Binding constant and binding number for static quenching of native and pre-denatured  $\beta$ lg by RF, at different temperatures and at neutral pH (7.4) ..... 72

## Chapter 4

Table 4.1. Influence of pH on the emission maximum wavelength of  $\beta$ lg and the  $\beta$ lg/D<sub>3</sub> complex ..... 103

## Chapter 5

Table 5.1. TEER of the Caco-2 cells monolayers ..... 139

## Chapter 7

Table 7.1. Average Size (three measurements) of the  $\beta$ lg/Lyso self-assembly at ratio 2:1 and different pH values before and after overnight agitation ..... 187

## Chapter 8

Table 8.1. TEER of the Caco-2 cells monolayers ..... 223

# Index of figures

## Chapter 1

Figure 1.1. Dimer of $\beta$ Ig with di-sulfides bonds in blue .....	13
Figure 1.2. Central cavity of $\beta$ Ig monomer with hydrogen bonds .....	15
Figure 1.3. Structures of $\beta$ Ig displaying the EF-loop in the closed (left) and open (right) conformation in the green circle. The conical $\beta$ -barrel is formed by two sheets consisting of $\beta$ -strands A-D and strands E-H.....	16
Figure 1.4. Different structures of microparticles obtained by microencapsulation: (a) microcapsule, (b) multilayer microcapsule, (c) microsphere and (d) multishell and multicore microsphere .....	35

## Chapter 3

Figure 3.1. (A) Far-UV, (B) near-UV circular dichroic spectra of $\beta$ Ig in the absence and presence of increasing concentration of riboflavin in 10 mM phosphate buffer at pH 7.4. The concentrations of $\beta$ Ig are 10 $\mu$ M for the far-UV region and 20 $\mu$ M for the near-UV region. The concentrations of RF vary from 0 to 40 $\mu$ M.....	60
Figure 3.2. Fluorescence emission spectra of $\beta$ Ig in the presence of different concentrations of RF; (A) [ $\beta$ Ig] = 5 $\mu$ M; (B) [ $\beta$ Ig] = 10 $\mu$ M; [RF] in $\mu$ M, curves: 0, 1, 2.5, 5, 10, 15 and 20 ( $\lambda$ EX = 280 nm, T = room temperature, pH = 7.4). Insets: Stern–Volmer plots for the quenching of $\beta$ Ig by RF (A): [ $\beta$ Ig] = 5 $\mu$ M; (B): [ $\beta$ Ig] = 10 $\mu$ M.....	62
Figure 3.3. Overlap of the fluorescence emission spectra of $\beta$ Ig (A) with the absorption spectra of RF (B).....	70
Figure 3.4. The structure of $\beta$ Ig was updated from PBD (ID # 3BLG)	70
Figure 3.5. The evolution of fluorescence intensity of $\beta$ Ig alone as a function of temperature (20, 35, 45 and 55 °C). (A) [ $\beta$ Ig] = 5 $\mu$ M, (B) [ $\beta$ Ig] = 10 $\mu$ M; phosphate buffer 10 Mm at pH 7.4. Excitation at 280 nm. ....	75
Figure 3.6. The synchronous fluorescence spectra of $\beta$ Ig at 5 (A and B) and 10 $\mu$ M(C and D). On panels A and C, $\Delta\lambda$ = 15 nm; on panels B and D, $\Delta\lambda$ = 60 nmin the presence of [RF] = 0, 1, 2.5, 5, 10, 15 and 20 $\mu$ M. Solvent: phosphate buffer 10 mM at pH 7.4. Fluorescence scans were carried out from 200 to 400 nm. ....	79

Figure 3.7. Cytotoxicity RF containing solutions on skin melanoma M21 cell lines irradiated in the absence and presence of  $\beta$ Ig (25 min at 365 nm). The treatment consisted in the  $\beta$ Ig/RF complex and RF solutions, each at a final concentration of 5, 2.5 and 1.25  $\mu$ M. Growth inhibition and cytotoxicity were evaluated after an incubation period of 48 h for recovery. .... 82

Figure 3.8. Effect of irradiation of the  $\beta$ Ig/RF complex,  $\beta$ Ig and RF solutions during 25 min at 365 nm (4 W);  $\beta$ Ig (20  $\mu$ M): not irradiated (A) and irradiated (B); RF (20  $\mu$ M): not irradiated (C) and irradiated (D);  $\beta$ Ig/RF (20  $\mu$ M): not irradiated (E) and irradiated (F). .... 84

Figure 3.9. Influence of light on the stability of the  $\beta$ Ig/RF nanocomplex for a two week period. UV-vis spectra of RF (A) compared to that of the  $\beta$ Ig/RF nanocomplex (B). C represents the impact of explosion to light on the concentration RF alone and the  $\beta$ Ig/RF nanocomplex. UV-vis spectra and concentrations were determined at 445 nm. .... 86

## Chapter 4

Figure 4.1. Fluorescence intensity of  $\beta$ Ig (a and c) and the  $\beta$ Ig/D<sub>3</sub> complex (b and d) at different pH (1.2, 2.0, 3.0, 5.0, 6.8, 7.0 and 8.0). Excitation at 280 nm (a and b) and 290 nm (c and d). .... 99

Figure 4.2. Synchronous fluorescence of Trp using  $\Delta\lambda = 60$  nm of  $\beta$ Ig in absence (a) and presence of vitamin D<sub>3</sub> (b). .... 101

Figure 4.3. Vitamin D<sub>3</sub> binding capacity of  $\beta$ Ig at different (1.2, 2.0, 3.0, 5.0, 6.8, 7.0 and 8.0). B. Fractional residual fluorescence of  $\beta$ Ig.  $F_{\max}$  is the intensity at the emission maximum ( $\lambda_{\max}$ ) and  $F_0$  is the intensity for  $\beta$ Ig at  $\lambda_{\max}$ . Excitation at 280 and 290 nm. .... 105

Figure 4.4. Relative solubility of vitamin D<sub>3</sub> in the presence and absence of  $\beta$ Ig. A static concentration of vitamin D<sub>3</sub> of 20  $\mu$ M was incubated overnight at 4 °C with increasing concentration of  $\beta$ Ig (0, 1.25, 2.5, 5, 10, 20, 30, 60 and 80  $\mu$ M). .... 110

## Chapter 5

Figure 5.1. Stability of D<sub>3</sub> and the  $\beta$ Ig/D<sub>3</sub> complex in refrigerated conditions (4°C) during five weeks. A : Plot of the fitted curves of D<sub>3</sub> and the D<sub>3</sub>/ $\beta$ Ig. B. Equivalence between D<sub>3</sub> and the D<sub>3</sub>/ $\beta$ Ig. The level of  $\alpha$  was set at 0.05. The lower decision limit (LDL) was 0.8 and the upper decision limit (UDL) was set at 1.25 (representing 25% difference). .... 125

Figure 5.2. UV-light Stability of D<sub>3</sub> and the  $\beta$ Ig/D<sub>3</sub> complex during 24 hours ( $\lambda = 254$  nm). A: Graph of the stability and B. the equivalence between D<sub>3</sub> and the  $\beta$ Ig/D<sub>3</sub> complex. .... 129

Figure 5.3. Stability of D<sub>3</sub> and the D<sub>3</sub>/βlg complex in Simulated Intestinal Fluid without pancreatin at pH 6.8, 37°C (USP-2 apparatus). A: Graph of the intestinal stability and B. The equivalence between D<sub>3</sub> and the βlg/D<sub>3</sub> complex. .... 133

Figure 5.4. Stability of D<sub>3</sub> and the D<sub>3</sub>/βlg complex in Simulated Intestinal Fluid with pancreatin at pH 6.8, 37°C (USP-2 paddle apparatus). A: Graph of the intestinal stability and B. The equivalence between D<sub>3</sub> and the βlg/D<sub>3</sub> complex..... 136

Figure 5.5 A. Mean 25(OH)D<sub>3</sub> in the plasma samples of the rats receiving water (control), D<sub>3</sub> and the βlg/D<sub>3</sub> complex. Each error bar is constructed using 1 standard error from the mean (JMP, SAS Institute, Inc.). B. The equivalence between D<sub>3</sub> and the βlg/D<sub>3</sub> complex..... 141

## Chapter 6

Figure 6.1. Long term stability of D<sub>3</sub> and the D<sub>3</sub>-loaded βlg-based coagulum in refrigerated conditions (4°C). .... 155

Figure 6.3. Stability of D<sub>3</sub> and the D<sub>3</sub>-loaded βlg-based coagulum in the simulated intestinal fluid without and with pancreatin at 37°C. .... 161

Figure 6.4. Bioavailability of D<sub>3</sub> in the rat experiment. Mean 25(OH)D<sub>3</sub> (± SEM) in rats forced fed the water (control), D<sub>3</sub>, the βlg/D<sub>3</sub> complex and D<sub>3</sub>-loaded βlg-based coagulum. D<sub>3</sub> was measured by dosage of the serum level of the 25(OH)D<sub>3</sub> was significantly enhanced for the D<sub>3</sub> entrapped in the βlg-based coagulum..... 163

## Chapter 7

Figure 7.1. Impact of the βlg:Lyso concentration ratio (v/v) on the protein self-assembly determined by the turbidity at 600 nm. .... 177

Figure 7.2. Impact of the βlg:Lyso concentration ratio (v/v) on the surface charge of the protein self-assembly at pH 6.8..... 179

Figure 7.3. Impact of the pH on the formation of βlg/Lyso self-assembly as determined by turbidity at 600 nm. The βlg:Lyso concentration ratio was 2:1 and the pH values were 4, 5, 6.8, 7.5, 8, 9, 10 and 11..... 183

Figure 7.4. Impact of pH on the charge of the βlg/Lyso self-assembly at varying pH: 4, 5, 6.8, 7.5, 8, 9, 10 and 11. The βlg:Lyso concentration ratio was 2:1. .... 185

Figure 7.5A. TEM image of the βlg/Lyso self-assembly at pH 7.5, ratio 2:1..... 189

Figure 7.5B. SEM image of the βlg/Lyso self-assembly at pH 7.5, ratio 2:1..... 189

Figure 7.6. RP-HPLC profiles of amounts of  $\beta$ Ig and Lyso in the supernatant (A) and the pellet (B) after centrifugation (5000 x g for 5 min) of the  $\beta$ Ig/Lyso microspheres prepared using ratio 2:1 at pH 7.5. Absorbance for the proteins at 280 nm and D<sub>3</sub> at 265 nm..... 191

Figure 7.7. RP-HPLC profiles of D<sub>3</sub> recovered from the supernatant (A) and the pellet (B) after centrifugation (5000 x g for 5 min) of  $\beta$ Ig/Lyso microspheres - containing D<sub>3</sub>. Absorbance for the proteins at 280 nm and D<sub>3</sub> at 265 nm. .... 194

## Chapter 8

Figure 8.1. Stability of D<sub>3</sub> and the  $\beta$ Ig/D<sub>3</sub>/Lyso microspheres in refrigerated conditions (4°C) during five weeks. A: Plot of the fitted curves of D<sub>3</sub> and the  $\beta$ Ig/D<sub>3</sub>/Lyso microspheres. B. Equivalence between D<sub>3</sub> and the  $\beta$ Ig/D<sub>3</sub>/Lyso microspheres. The level of  $\alpha$  was set at 0.05. The lower decision limit (LDL) was 0.8 and the upper decision limit (UDL) was set at 1.25 (representing 25% difference)..... 208

Figure 8.2. UV-light stability of D<sub>3</sub> and the  $\beta$ Ig/D<sub>3</sub>/Lyso microspheres over 24 hours ( $\lambda$  = 254 nm). A: Graph of the stability of D<sub>3</sub>. B. The equivalence between D<sub>3</sub> and the  $\beta$ Ig/D<sub>3</sub>/Lyso microspheres..... 212

Figure 8.3. Stability of D<sub>3</sub> and the  $\beta$ Ig/D<sub>3</sub>/Lyso microspheres in Simulated Intestinal Fluid without pancreatin at pH 6.8, 37°C (USP-2 apparatus). A: Graph of the intestinal stability and B. The equivalence between D<sub>3</sub> and the  $\beta$ Ig/D<sub>3</sub>/Lyso microspheres..... 216

Figure 8.4. Stability of D<sub>3</sub> and the  $\beta$ Ig/D<sub>3</sub>/Lyso microspheres in Simulated Intestinal Fluid with pancreatin at pH 6.8, 37°C (USP-2 apparatus). A: Graph of the intestinal stability and B. The equivalence between D<sub>3</sub> and the  $\beta$ Ig/D<sub>3</sub>/Lyso microspheres. 219

Figure 8.5. Bioavailability of D<sub>3</sub> in the rat experiment. Mean 25(OH)D<sub>3</sub> in rats forced fed the water (control), D<sub>3</sub> and D<sub>3</sub> - entrapped  $\beta$ Ig/Lyso microspheres. Each error bar is constructed using 1 standard error from the mean. .... 225

Figure 8.6. Stability of the unprotected D<sub>3</sub> and in the  $\beta$ Ig/D<sub>3</sub> complex,  $\beta$ Ig/D<sub>3</sub>/Lyso microspheres and  $\beta$ Ig-based coagulum. and the  $\beta$ Ig/D<sub>3</sub>/Lyso microspheres in refrigerated conditions (4 °C) during five weeks. .... 237

Figure 8.7. UV-light stability of D <sub>3</sub> of the unprotected D <sub>3</sub> and in the βlg/D <sub>3</sub> complex, βlg/D <sub>3</sub> /Lyso microspheres and βlg-based coagulum. ....	239
Figure 8.8. Stability of the unprotected D <sub>3</sub> and in the βlg/D <sub>3</sub> complex, βlg/D <sub>3</sub> /Lyso microspheres and βlg-based coagulum in Simulated Intestinal Fluid without pancreatin at pH 6.8, 37 °C (USP-2 apparatus). ....	241
Figure 8.9. Stability of the unprotected D <sub>3</sub> and in the βlg/D <sub>3</sub> complex, βlg/D <sub>3</sub> /Lyso microspheres and βlg-based coagulum in Simulated Intestinal Fluid with pancreatin at pH 6.8, 37 °C (USP-2 apparatus). ....	242
Figure 8.10. <i>In vivo</i> experiment of the bioavailability of D <sub>3</sub> . Mean 25(OH)D <sub>3</sub> in rats forced fed the water (control), unprotected D <sub>3</sub> , βlg/D <sub>3</sub> complex, βlg/D <sub>3</sub> /Lyso microspheres and βlg-based coagulum in the rat experiment. Each error bar is constructed using 1 standard error from the mean. ....	244

## Chapter 9

Figure 9.1. Stability of the unprotected D <sub>3</sub> and in the βlg/D <sub>3</sub> complex, βlg/D <sub>3</sub> /Lyso microspheres and βlg-based coagulum. and the βlg/D <sub>3</sub> /Lyso microspheres in refrigerated conditions (4 °C) during five weeks. ....	237
Figure 9.2. UV-light stability of D <sub>3</sub> of the unprotected D <sub>3</sub> and in the βlg/D <sub>3</sub> complex, βlg/D <sub>3</sub> /Lyso microspheres and βlg-based coagulum. ....	239
Figure 9.3. Stability of the unprotected D <sub>3</sub> and in the βlg/D <sub>3</sub> complex, βlg/D <sub>3</sub> /Lyso microspheres and βlg-based coagulum in Simulated Intestinal Fluid without pancreatin at pH 6.8, 37 °C (USP-2 apparatus). ....	241
Figure 9.3. Stability of the unprotected D <sub>3</sub> and in the βlg/D <sub>3</sub> complex, βlg/D <sub>3</sub> /Lyso microspheres and βlg-based coagulum in Simulated Intestinal Fluid with pancreatin at pH 6.8, 37 °C (USP-2 apparatus). ....	242
Figure 9.5. <i>In vivo</i> experiment of the bioavailability of D <sub>3</sub> . Mean 25(OH)D <sub>3</sub> in rats forced fed the water (control), unprotected D <sub>3</sub> , βlg/D <sub>3</sub> complex, βlg/D <sub>3</sub> /Lyso microspheres and βlg-based coagulum in the rat experiment. Each error bar is constructed using 1 standard error from the mean. ....	244

## List of abbreviations

ACN	Acetonitrile
a.u.	Arbitrary Units
$\beta$ Ig	$\beta$ -lactoglobulin
cm	centimeter
Da	Dalton
D3	Vitamin D3
DTP	Development Therapeutics Program
HPLC	High performance liquid chromatography
hr	Hour(s)
IU	International units
KDa	Kilo-dalton
L	Liter
m	Meter
mA	Milliampere
mg	Milligram
MeOH	Methanol
mm	Millimeter
mM	Millimolar
min	Minutes
mL	Milliliters
nm	Nanometer
PBS	Phosphate-buffered saline
pI	Isoelectric point
pH	Potential of Hydrogen
RF	Riboflavin
RP-HPLC	Reversed – phase HPLC
rpm	Revolutions per minute
s	Seconds
SDS	Sodium dodecyl sulfate
SEM	Scanning electron microscopy
TEER	Trans Epithelial Electric Resistance
TEM	Transmission electron microscopy
TFA	Trifluoroacetic Acid
$\mu$ L	Microliter
$\mu$ g	Microgram
$\mu$ m	Micrometer
$\mu$ mol	Micromole
$\mu$ M	Micromolar
UV	Ultraviolet
V	Volts
v/v	Volume/volume
W	Watt
w/v	Weight per volume

x g

Relative centrifugal force

Common amino acid abbreviations

A	Ala	Alanine
C	Cys	Cysteine
D	Asp	Aspartic acid
E	Glu	Glutamic acid
F	Phe	Phenylalanine
G	Gly	Glycine
H	His	Histidine
I	Ile	Isoleucine
K	Lys	Lysine
L	Leu	Leucine
M	Met	Methionine
N	Asn	Asparagine
P	Pro	Proline
Q	Gln	Glutamine
R	Arg	Arginine
S	Ser	Serine
T	Thr	Threonine
V	Val	Valine
W	Trp	Tryptophan
Y	Tyr	Tyrosine



## Introduction

Active compounds such as probiotics, bioactive peptides and proteins, antioxidants, vitamins with physiological benefits resulting in enhanced general well-being and/or reduced risk of chronic disease beyond basic nutritional functions, are often referred to as nutraceuticals [1, 2]. In Canada, they fall under the regulation of the natural health products (NHPs), which came into effect on January 1, 2004 sites [3]. The market of NHPs is rapidly increasing worldwide. Since 2004, Health Canada has authorized over 50,000 NHPs for sale in Canada as well as 1,250 manufacturing sites [3]. According to the same source, within only five months (October 2011 to March 2012), the number of product applications completed per month has increased 109 %. The market value is estimated around 117 billion US dollars only from the three most important sources, including the United States, Japan and Western Europe [4]. This value increases between 300 and 400 billion US dollars, when other areas such as East Europe, Latin America, Asia or Africa are considered.

Generally, bioactives are labile ingredients that are susceptible to elevated temperature, pressure, oxygen and light during food processing. Furthermore, they are prone to degradation during passage in the gastrointestinal (GI) tract when confronted to the pH, presence of enzymes and other nutrients [2]. Entrapment of bioactives in delivery platforms appears as an effective mean to preserve their integrity, to deliver and modulate their release in the body.

$\beta$ -lactoglobulin ( $\beta$ lg) accounts for about 60 % and thus, is the major protein in bovine milk whey. This whey protein with high nutritional value, related to its high content in essential amino acids, is used in the food industry for its interesting techno-functional and structural properties [5]. Although its true physiological role is still elusive,  $\beta$ lg which is also member of the lipocalin family, has been attributed a transport function for small hydrophobic nutraceutical ligands as well as larger molecules. The interesting structural properties and physicochemistry of  $\beta$ lg

provide this protein with the ability to establish various types of interactions, including hydrophobic and electrostatic interactions, with ligands of different characteristics [5]. Reports indicate that the biological properties such as water solubility or photoreactivity of some of these ligands are improved upon binding to  $\beta$ lg [6-8].

Riboflavin (RF) and vitamin D<sub>3</sub> (D<sub>3</sub>) are both small nutraceutical ligands with important biological activities, but with dissimilar physico-chemical characteristics. RF is an endogenous photosensitizer, which implies that upon light irradiation at a certain wavelength, it can be photoactivated in aqueous solution and produce reactive oxidative species [9, 10]. Since  $\beta$ lg is composed of aromatic amino acids, including tryptophan and tyrosine, which are also capable of generating oxidative species, the association of the  $\beta$ lg and RF may produce cascade or cumulative oxidative reactions [11, 12]. While RF is an amphiphilic vitamin which binding to  $\beta$ lg has not yet been described in the literature, reports indicate that two molecules of D<sub>3</sub> can bind to  $\beta$ lg to form a complex [13]. D<sub>3</sub> is highly hydrophobic and sensitive to light, which is problematic in food formulation. In Canada, foods that are currently fortified with D<sub>3</sub> are dairy products or margarine, which have high fat content [14, 15]. The binding of D<sub>3</sub> with  $\beta$ lg might improve these shortcomings and thus extend some of its applications to foods with low fat contents.

$\beta$ lg – based vehicles of varying can be formed by promoting hydrophobic interactions or through an electrostatically-driven process, which could lead to the self-aggregation of  $\beta$ lg or co-assembly with other food grade biopolymers of opposite charge [16-20]. The cationic protein Lysozyme (Lyso) offers such a possibility. Its isoelectric point is around 10.7, which provides a wide range for electrostatic interactions with  $\beta$ lg, which isoelectric point is 5.3 [5, 21]. Additionally, Lyso is one of the main components of airway fluid where it assumes the host defense [22]. As an enzyme, it damages or kills bacteria by lysing their cell wall peptidoglycan. Its antibacterial activity is therefore limited to gram positive bacteria. Lyso can also bind small ligands with pharmaceutical interest [23, 24]. Therefore, the complex formation between  $\beta$ lg and Lyso might lead to formation of a

surpamolecular matrix which can be used for the encapsulation of small bioactives that bind to both proteins. However,  $\beta$ lg is sensitive to environmental factors including the pH and temperature, which are inherent to the process of foodstuffs preparation. This instability can considerably impede the effectiveness of the delivery platform, especially those intended for food applications. The formation of complexes could contribute to enhance the stability of  $\beta$ lg.

Despite the challenges and limitations related to use of  $\beta$ lg in the formulation of delivery scaffolds, there is still a high interest in  $\beta$ lg-based vehicles for oral delivery of biologically active molecules. Ongoing research is seeking new alternatives to overcome such drawbacks and develop  $\beta$ lg-based carriers systems for optimal delivery of biologically active molecules of nutritional importance.

The following chapter presents an extensive work on the production of  $\beta$ lg, its structure and functionality as a platform of nano and microsize for the oral delivery of bioactives.



# CHAPTER 1

## Literature review

### **$\beta$ -Lactoglobulin-based nano and microparticulate systems for bioactives protection and delivery**

A version of this literature review will be published as a chapter in the book on *Engineering Foods for Bioactives Stability and Delivery* to be published by Springer.

By :

Fatoumata Diarrassouba<sup>a</sup>, Ghislain Garrait<sup>b</sup>, Gabriel Remondetto<sup>c</sup>  
and Muriel Subirade<sup>a</sup>

<sup>a</sup>Chaire de Recherche du Canada sur les Protéines, les Bio-systèmes et les Aliments Fonctionnels, INAF/STELA, Université Laval, Québec, QC, Canada

<sup>b</sup> ERT-CIDAM, Lab Biopharmacie, Faculté de Pharmacie, 28 Place Henri Dunant, 63001 Clermont-Ferrand, France

<sup>c</sup> Centre de Recherche et Développement, Agropur Coopérative, 4700 Armand Frappier, St-Hubert, QC, Canada J3Z 1G5

## **1.1. Abstract**

The new paradigms in human nutrition and ever increasing demand of consumers for safe and healthy food products encourage research for functional foods and nutraceuticals as pharmaceutical surrogates. Food proteins are abundant and from renewable sources, with functional groups conferring interesting structural and functional properties. Their ability to bind small ligands, form aggregates and electrostatic complexes with other food macromolecules provides numerous applications for oral delivery technology. The current review focuses on the major milk protein  $\beta$ -lactoglobulin, its fractionation and isolation from whey proteins, techno-functional properties and applications in the formulation of nano and micro-sized oral delivery platforms.

## **1.2. Introduction**

The development of the ideal oral delivery system has become the focus of tremendous research worldwide, particularly in food and pharmaceutical sciences. Along with the field of functional foods and nutraceuticals, the market of which is skyrocketing, the popularity of oral delivery systems has soared and the sales were already expected to reach over \$ 67 billion a few years ago [25, 26]. The designation of 'oral delivery system' rhymes usually with 'controlled delivery' of bioactive compounds, which involves the efficiency of delivery and the enhancement of solubility, absorption, bioavailability, safety and duration of action [26]. In addition to increasing patient comfort and compliance, oral delivery systems can achieve sustain, controlled and site-specific release of bioactives [25-28]. Consequently, on a pharmaceutical point of view, serum concentrations are less prone to fluctuations; toxicity and the frequency of dosing are reduced [26]. In the food industry, delivery systems are used as carriers for functional ingredients which are hence protected from hostile environmental factors including heat, light, oxygen, high pressure and shear forces during processing, storage and utilization

until the intact bioactive ingredient is delivered in the intestines; the list of advantages is not exhaustive. The release rate of the bioactive molecule can then be modulated via the control of conditions including temperature, ionic strength, pH and digestive enzymes [29].

The release kinetics from the oral delivery system relies on the chemical composition and/or the structure of the carrier system. In general, mechanisms of release such as diffusion results from the physical (erosion) or chemical decomposition (degradation); swelling and osmotic pressure lead to an expansion of the carrier system, thus expelling the bioactive out of the carrier matrix [26, 28]. Therefore, the chemical composition and structure of the oral delivery system are of utmost importance to achieve effective release of bioactives. With the size of oral delivery systems decreasing dramatically, concerns have been raised regarding the toxicity of such carriers and the resulting degradation products. Indeed, reduced size may lead to an increase in toxicity given that small sized carriers might reach and accumulate in regions within cells or tissue inaccessible to macroscopic particles of the same composition [30]. In fact, the size of oral delivery systems decreased from capsules, tablets or powder forms to microparticles, nanoparticles and nanocomplexes. Microparticles are less than about 1000  $\mu\text{m}$  while nanoparticles and nanocomplexes are less than 100 nm in size [2, 29]. Therefore, biopolymers which are biocompatible and biodegradable with negligible to null toxicity are increasingly used to fabricate oral delivery systems. Milk whey proteins fit well to this criteria and as such, whey proteins – based delivery systems have been the focus of countless peer-reviewed articles [2, 18, 31-36]. However, whey proteins are composed of diverse proteins with different structures, properties and functions, which makes undistinguishable the role and degree of participation of each protein in the formation of the carrier system [37]. Most functional properties of whey isolates, including aggregates and gel formation, are attributed to its major protein that is  $\beta$ -lactoglobulin ( $\beta\text{lg}$ ) [17, 38]. The present review is therefore consecrated on the major whey protein  $\beta$ -lactoglobulin ( $\beta\text{lg}$ ) and its functionality as micro and nano-based oral delivery system.

### **1.3. Manufacture of whey proteins**

Whey is the by-product of cheese production consisting of the serum recovered after isoelectric precipitation of the caseins [39]. The cow milk batch is initially centrifuged to separate the cream to obtain the skim milk, which pH is then decreased to 4.6 in order to precipitate the caseins or the curd, used for cheese production. The resulting serum contains the so-called whey proteins. Sweet whey results from a renneting process in which, the rennet enzyme cleaves kappa-casein liberating high levels of the caseino-macropeptide (13 mg/mL or 22 %). This protein is present in much lower quantities (0.25 mg/mL or 5 %) in acid whey, a by-product of acid caseins [38]. The protein content in whey depends essentially on two methods which are used to concentrate the different proteins at a yield of about 80 % purity [38]. Whey protein concentrates (WPC) are mainly obtained via ultrafiltration using a membrane with a cut-off of about 10,000 Da. Whereas, whey protein isolates (WPI) with higher protein content result from subsequent diafiltration of the WPC [39]. Individual proteins, including the major whey protein  $\beta$ lg, can then be separated from the whey proteins (Table 1.1).

**Table 1.1. Major whey proteins content in bovine milk, unprocessed whey (UPW), whey protein concentrates (WPC) and whey protein isolates (WPI)**

Protein	Milk (g/l)	UPW (%)	WPC (%)	WPI (%)	Molecular Weight (KDa) / (pI)
$\beta$ – lactoglobulin ( $\beta$ lg)	2 – 4	3.1 (61)	31 (51)	71 (80)	18.3 (pI = 5.3)
$\alpha$ – lactalbumin ( $\alpha$ -lac)	1 – 1.5	0.76 (15)	11 (18)	11 (12)	14.2 (pI = 4.4)
Bovine serum albumin (BSA)	0.1 – 0.4	0.15 (3)	1.1 (1.8)	2.6 (3)	66 (pI = 4.7)
Immunoglobulin(IgG)	0.6 – 1.0	0.37 (7)	3.3 (5.4)	3.3 (4)	146 - 1,030
Total milk whey protein	5 – 7				

**Note:** Adapted from [38-41]. Values are expressed as % w/w in powder, mg/ml in whey and % of measured protein (in brackets) for whey protein concentrates (nominally 80% protein) in cheese whey and whey protein isolates obtained by ion exchange of the cheese whey. Lactoferrine, proteose peptone and caseinomacropetide which are minor proteins also constituting whey proteins, are not presented in the table. Traces of IgA and IgM also exist in bovine milk, usually at around 1/10 the level of IgG.

#### 1.4. Fractionation of $\beta$ lg from the whey proteins

A number of separation methods have been optimized to produce high purity levels of  $\beta$ lg. Some of these methods have been scaled up for commercial applications while most of them remain at the laboratory scale, certainly due to their relatively high cost, low productivity, poor selectivity, presence of unwanted denatured proteins and inappropriateness for industrial implementation [41-43]. Mehra and O'Kennedy summarized the current fractionation methods into five categories: the selective precipitation, addition of salts or precipitants, ion-exchange chromatography, enzymatic hydrolysis and membrane filtration [41].

Variants of each method were published; however, their principles are presented as follows. The selective precipitation consists in adjusting the pH (4.65) of the whey protein which is then demineralized (reduction of the ionic strength) by electro dialysis or diafiltration before recovering  $\beta$ lg by centrifugation. The yield of this method is mitigated with 51.6 % of dried  $\beta$ lg concomitantly with 30.9 % of lipids, which is disadvantageous for some food applications (foaming or whipping). A recovery of 84 % of pure  $\beta$ lg from whey proteins was obtained by salting out at acidic pH (2.0) and increasing concentration of salt (NaCl from 7.0 to 30 %). Various salts (ferric chloride -  $\text{FeCl}_3$  – at pH 4.2) and precipitants have also been used [41, 42]. Anion-exchange chromatography at higher pH values (6.0 and above) or cation-exchange chromatography at a lower pH value (3.0) allow the selective binding and improved recovery of  $\beta$ lg (96 % to 100%) with high purity (67.7 to 99 %). The acidic and peptic resistance of  $\beta$ lg was exploited to optimize a method which allowed the production of high purity protein in its native conformation. In fact, during peptic digestion,  $\beta$ lg remains stable and thus is not hydrolyzed, which is not the case for other whey proteins. Finally, whey protein components of similar molecular weight can also be separated by membrane filtration in response to ionic strength (electrostatic forces) and pH modification. Subsequently additional microfiltration or other types of membrane of controlled pores can be used to further separate proteins of similar size.

Research is still ongoing to develop methods that ally speed, sensitivity, resolution, user-convenience with high efficiency. The challenge now resides in separating genetic variants of  $\beta$ lg (mainly variants A and B), given that milk source has a great impact on the protein composition of both milk and whey, and in term, on the molecular structure of the protein [44, 45].

## **1.5. Structure of $\beta$ lg**

The structure and amino acid composition of  $\beta$ lg have been the focus of extensive research [5, 46-48]. Thus, only the structural characteristics and physico-chemical properties related to bioactive protection and delivery are detailed in the present review.

### **1.5.1. Basic structure of $\beta$ lg**

Well defined crystal structures indicate that  $\beta$ lg is a globular protein pertaining to the lipocalin family, with a molecular weight of 18,3 KDa and an isoelectric point ( $pI$ ) of 5.3 [5, 38, 48]. The two main genetic variants of  $\beta$ lg, A and B, differ from a mutation occurring at amino-acid sequence position 64 ( $Asp_A \rightarrow Gly_B$ ) and 118 ( $Val_A \rightarrow Ala_B$ ). The overall conformation of the molecule remains fairly the same, although the substitutions lead to dissimilarities in properties such as heat stability and resistance to pressure denaturation [48, 49]. The information presented in the current review will refer to  $\beta$ lg variant B.

The protein is constituted of 162 amino acids, including all 20 amino acids in relative amounts that make it exceptional and valuable nutritionally. In fact, compared to theoretical common values computed for proteins,  $\beta$ lg comprises about 17 % more essential amino acids [41]. The tertiary structure of  $\beta$ lg is

composed of 8 % of  $\alpha$ -helix, 45 % of  $\beta$  -sheet and 47 % of random coil, as represented by the dimeric protein in Figure 1.1 [5, 47, 48].



Figure 1.1. Dimer of  $\beta$ lg with di-sulfides bonds in blue. Adapted from PDB 1B8E [48].

$\beta$ lg has an overall radius of 2 nm, with almost 90 % of its mass within 1 nm of the surface and nearly 60 % within 0.5 nm [50]. The structure of the monomer of  $\beta$ lg is composed of nine strands of antiparallel  $\beta$  – sheets (strands A to I), eight (strands A to H) of which wrap around to form a flattened, conical barrel also called central calyx (Figure 1.2).



**Figure 1.2. Central cavity of  $\beta$ lg monomer with hydrogen bonds (--). Adapted from PDB 1B8E [48].**

The cylindrical shaped calyx has a length of 15 Å, with hydrophobic walls composed of two sheets made of stands A - D and stands E - H (Figures 1.2 and 1.3).

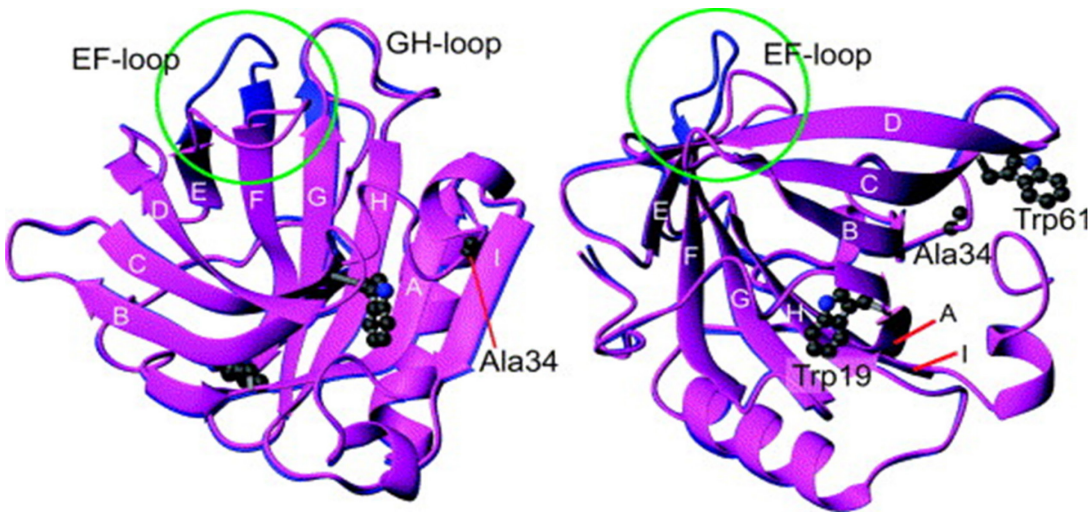


**Figure 1.3. Structures of β<sub>l</sub>g displaying the EF-loop in the closed (left) and open (right) conformation in the green circle. The conical β-barrel is formed by two sheets consisting of β-strands A-D and strands E-H. Adapted from Sakurai and Goto 2006 [51].**

Strand A (residues 16 – 27) participates in both sheets due to its 90° bend at its midpoint (Ser21), while the ninth strand (I) extends the EFGHA sheet. The neighboring strands within the sheets are connected via a loop [52]. The dimer interface is formed in part by strand I and the loop connecting strand A to B. Strand A is preceded by a 3-turn  $\alpha$ -helix while another one lies in the A-B loop. The structure of  $\beta$ lg contains two disulfide bridges consisting of Cys66 – Cys160, connecting the C-D loop to the carboxyl-terminal region, and Cys106-Cys119 links strands G and H. An additional Cys at position 121 is buried and thus, remains free. At pH values from 5 to about 7, including that of the milk (~ pH 6.6),  $\beta$ lg exists in as a dimer in solution, below pH 3 and above 7, the monomeric conformation predominates [5, 52]. Upon modification of the pH,  $\beta$ lg undergoes different structural transitions categorized into distinct classes (M, Q, N and R) and their interrelation is as follows:  $M \leftrightarrow Q \leftrightarrow N \leftrightarrow R$  [53].

### **1.5.2. Structural transitions of $\beta$ lg**

Reports indicate that moderate to considerable pH-induced structural transitions of  $\beta$ lg occur between pH 2.5 and 8, while above pH 9,  $\beta$ lg undergoes significant and irreversible structural modification, also called base-induced unfolding of the protein [52-54]. Below pH 2, the volume and compressibility of the protein decrease, providing a more compact structure to  $\beta$ lg [54]. It is believed that further structural transition continues at pH values less than 1.0, even though no report exists at the moment. Between pH 2.5 to 8, the overall conformation of the protein is conserved extraordinarily well, despite significant structural changes.

The dimer-to-monomer transition occurring between pH 4.5 and 2.5 is the acid induced dissociation of the dimeric  $\beta$ lg into monomers. It includes the  $\beta$ lg transition from the monomeric (M) to the acidic form (Q) around pH 3, where the protein is believed to dimerize [53, 54]. This transition triggers a different orientation of the  $\alpha$ -helix, thus affecting only the surface electrostatic properties of  $\beta$ lg. The native

dimeric (N) to the acidic (Q) form transition occurs between pH 6.0 and 4.5. This transition is accompanied with a change in the compactness of the protein translated into a slight expansion of the hydrodynamic volume of  $\beta$ lg [53, 54]. It also includes the pH 5 transition (dimer to octamer transition from pH 3.9 to 5), at which  $\beta$ lg undergoes an octamerization without significantly affecting its secondary structure. Above pH 5, the dimerization of  $\beta$ lg is due to the electrostatic interactions between Asp130 and Glu134 of one monomer with corresponding lysine residues of other monomers. The Tanford (N - R) transition occurs between pH 7 and 8 [53, 54]. This transition involves a conformational change of the EF loop (residues 85–90), probably due to the cleavage of hydrogen bonds between the F and G strands [53]. Finally, the transition at pH 9.0 or above where  $\beta$ lg undergoes an irreversible base-induced unfolding [54]. These structural transitions are important for understanding the functional properties of the protein.

## **1.6. Functionality of $\beta$ lg**

The physiological role of  $\beta$ lg, albeit not fully understood, seems to be intimately related to its amino acid composition and tertiary structure. The health benefits of  $\beta$ lg and derived peptides go far beyond its undeniable nutritional value and well justify its use as functional food ingredients and nutraceuticals. Their effects on a number of disease conditions have been reviewed elsewhere [41, 55]. Examples of beneficial activities on human health include their role as hypotensive, anticancer, immunomodulatory, opioid agonist, mineral binding, antimicrobial, gut health enhancing, hypocholesterolemic, insulinotropic and psychomodulatory agents.

Functional advantages of  $\beta$ lg reside in its properties such as gel formation, foaming, emulsion stabilization, all of which find numerous applications in the food industry [2, 17, 56]. Gelation remains one of the most important techno-functional properties of  $\beta$ lg and is traditionally achieved through thermal treatment. The sequential gelation steps consists of the unfolding of polypeptide chains with

concomitant exposure of initially buried hydrophobic amino acid residues and subsequent self-aggregation of protein molecules into a three-dimensional network that entraps water by capillary forces [2]. Contributing forces are hydrophobic effects, van der Waals, hydrogen bonding, and covalent interactions, which impact can be determined via the use of destabilizing agents. As such, urea can be used to block the formation of the hydrogen bonds, sodium dodecyl sulfate (SDS) to block the formation of the hydrophobic interactions, and 2-mercaptoethanol to block the formation of the disulfide bridge [57]. In absence of salt,  $\beta$ lg forms transparent 'fine stranded' gels at extreme pH values away from its  $pI$  and opaque 'particulate' gels near its  $pI$ .

Salt was used to induce cold-set gels made by prior heat denaturation of  $\beta$ lg [2, 57]. The solubility of  $\beta$ lg is greatly enhanced in presence of salt due its surface charge distribution at neutral pH, thus explaining the harvesting of the protein by dialysis or precipitation upon salting out and further growing of X-ray crystal structures [5, 58].

The structure of  $\beta$ lg justifies its classification as a member of the lipocalin family and calycin subclass, which is naturally involved in the transportation of small hydrophobic bioactives [59]. Reports indicate that  $\beta$ lg binds retinol, triglyceride and long chain fatty acids such as palmitic acid, resulting in enhanced intestinal uptake of these ligands.  $\beta$ lg might also have an important role in carrying implicated ligands in food systems and pharmaceutical preparations, as well as in digestion, absorption and metabolism of some of implicated ligands in neonates [41]. However, the sequence similarity of  $\beta$ lg with glycodelin, an important protein for fetal development expressed in the endometrium during the first trimester of human pregnancy, suggests further important biological functions [5, 51]. This is confirmed by the absence of  $\beta$ lg from human and rodents milk and its presence in the whey of ruminant's milk including cow, thus making its true function still elusive [5, 43]. However, there is a general consensus about its role as ligands transporter.

Intensive literature exists on the large selection of ligands that bind to  $\beta$ lg [5, 46, 58]. This ligand binding property is mainly ascribed to the presence of the central calyx, which plays the role of a receptacle for small hydrophobic and amphiphilic molecules, consequently forming  $\beta$ lg-ligand complexes [6, 7].

## **1.7. Formation and characterization of the $\beta$ lg-ligand complexes**

### **1.7.1. Structural basis for the formation of the $\beta$ lg-ligand complexes**

The folding of the two  $\beta$ -sheets (A - D and E - H) into a central cavity paneled with hydrophobic amino acids (Figure 1.2 and 1.3) resembles a barrel with the EF loop (residues 85-90) acting as the gate [59]. The EF loop folds over the entrance of the calyx to form a closed conformation at pH lower than 6.5 and at pH above 7, it adopts an open conformation which exposes the interior of the calyx [60]. This conformational flexibility is attributed to the Tanford transition which is accompanied by the deprotonation of the carboxyl group of Glu 89, located on the EF loop. Glu 89 that has an anomalous  $pK_a$  of 7.3 is normally buried and protonated in the “close conformation” at acidic pH. At pH values above 7, Glu 89 is exposed and deprotonated, thus triggering the opening of the EF loop. This consequently offers access to the central calyx [59]. The pH-controlled flipping of the EF loop seems to be crucial for the physiological significance of  $\beta$ lg since in the closed conformation, bound ligands might be protected in the acidic stomach in order to be further released within the intestines at higher pH value [5, 46, 53].

A number of methods have been used to study the binding of the ligands to  $\beta$ lg [7, 47, 61-64]. However, spectroscopic methods are among the most user-friendly, rapid, accurate and less cumbersome techniques used to investigate the protein-ligand interaction. Fluorescence spectroscopy is preferred to study the binding stoichiometric of the  $\beta$ lg-ligand complex while circular dichroism is interesting for

studying the influence of the ligand binding on the secondary and tertiary structure of the protein.

## **1.7.2. Fluorescence quenching upon ligand binding**

### **1.7.2.1. Theoretical explanation**

Fluorescence spectroscopy is principally used to study the microenvironment of species with intrinsic fluorescence emission aptitude, called chromophores or fluorophores, which typically contain aromatic molecules [65]. The fluorescence spectral data constitutes the emissions spectra, which is largely influenced by the chemical structure of the fluorophore and the solvent in which it is dissolved. By definition, the fluorescence emission spectrum is a plot of the fluorescence intensity versus wavelengths, usually in nanometers [65]. Fluorescence spectroscopy and mostly fluorescence quenching, is commonly used to characterize ligand binding to proteins. Fluorescence quenching refers to any process that decreases the fluorescence intensity of a sample caused by processes such as inner-filter effect, energy transfer, ground state complex formation and collisional processes [66, 67]. The inner-filter effect occurs when the fluorescence emission of the fluorophore is affected by the presence of an absorbing substance that absorbs the radiation going towards (excitation) or emanating from (emission) the fluorophore [68]. The resulting fluorescence quenching will thus arise from the reduction of the radiation intensity that excites the fluorophore. The inner-effect can be corrected by carefully selecting the concentration of the ligand, so that the absorbance of the ligand at the excitation and emission wavelength is below 0.1 [68].

Collisional or dynamic quenching results from collisions involving both the fluorophore and quencher during the lifetime of the excited state, while static quenching refers to ground-state fluorophore–quencher complex formation [67]. In the case of collisional quenching, the quencher diffuses to the fluorophore during

the lifetime of the excited state and upon contact, the fluorophore returns to the ground state, without emission of a photon [65]. Important parameters such as the association constant and binding number can be computed using various equations such as the well-known Stern-Volmer equation (in the case of non-fluorescent complex formation) or its modified version derived for a dynamic quenching process, in which there is a constant contribution of fluorescence of the non-quenchable fraction. These equations and variants are well described elsewhere [65, 67, 68].

Variants of the fluorescence spectroscopy include the synchronous fluorescence and fluorescence resonance energy transfer (FRET). The synchronous fluorescence is a scan that provides important information about the molecular environment in the vicinity of fluorophores in general, a shift in the position of the emission maximum corresponding to the changes of the polarity around the fluorophore [69]. The synchronous fluorescence spectra is obtained by recording the fluorescence spectra resulting from the difference between the excitation wavelength and emission wavelength at 15 or 60 nm intervals, corresponding to the changes of the polarity around tyrosine (Tyr) and tryptophan (Trp) residues, respectively [69]. Upon ligand binding, a stronger fluorescence quenching for a scan at  $\Delta\lambda = 60$  nm (Trp) than for  $\Delta\lambda = 15$  nm (Tyr) is indicative of the binding of the ligand closer to the Trp residues [69]. This information is extremely important since it confirms the formation of a ground-state complex that can be further analyzed in the context of the fluorescence resonance energy transfer (FRET) [65, 68, 69]. FRET occurs when there is overlap between the fluorescence emission spectrum of a donor fluorophore (in the excited state) with the absorption spectrum of an acceptor ligand (in the ground state). FRET can provide accurate structural information about protein-ligand binding. The transfer rate is affected by any condition that affects the distance between the donor and acceptor biomolecules, owing to FRET the name of 'spectroscopic ruler' [70]. Thus, the Förster distance, that is the distance for a specific donor-acceptor pair where 50% of the fluorescence energy of the donor (fluorophore) is transferred to the acceptor

(ligand), can be computed to suggest the localization of the ligand on the protein [65, 68].

### 1.7.2.2. Fluorescence emission of $\beta$ Ig

The fluorescence of  $\beta$ Ig arises mainly from Trp and Tyr residues. At physiological pH, the dimeric form of  $\beta$ Ig possesses four Trp residues (Figure 1.3), two on each monomer (Trp19 and 61). Trp61 is exposed to the solvent, thus explaining the almost complete quenching of its fluorescence. It has also been suggested that the location of Trp61, close to disulfide bond (Cys66–Cys160) and near the guanidine group of Arg124, both considered as strong quenchers, and the possible self-quenching of Trp61 of the other monomer in the  $\beta$ Ig dimeric form, might all contribute to the reduction of its fluorescence emission [71]. Trp19 contributes the most (80%) to the total intrinsic fluorescence, mainly due to its position in the hydrophobic cavity of the native conformation of the protein [6]. It is thus a highly sensitive probe that is used for monitoring conformational modification in  $\beta$ Ig. Figure 1.3 shows well Trp19, at the bottom of the calyx and Trp61 residues [51]. Typically, 280 nm is used as the excitation wavelength with Trp contributing to major fluorescence intensity and a maximum emission peak around 335 nm for  $\beta$ Ig [72]. While Tyr residues contribute to the fluorescence when excited at 280 nm, only the environment of Trp is studied at the excitation wavelength of 290 nm. The intrinsic fluorescence emission of  $\beta$ Ig can typically be either quenched or enhanced and shift to a shorter wavelength (blue shift) or a longer wavelength (red shift). The enhancement of the fluorescence emission results from a reduction of intra molecular quenching of Trp residue, for instance when the protein unfolds [71]. Conversely, the quenching occurs when the fluorescence emission of the Trp residue is hindered by the increased intra molecular interactions or upon binding of a ligand. The red shift of the peak indicates that the Trp residue moved from an apolar environment to a more polar region and when surrounded by a more hydrophobic environment the peaks are blue shifted [71, 73].

### 1.7.3. Circular dichroism

Circular dichroism (CD) is extensively used to monitor and understand the structural changes occurring during interactions of proteins with other biological molecules because of its high conformational sensitivity [74]. The CD signal is a radiation with elliptical polarization that results from the difference of unequal absorption between the left and right components of polarized light [75, 76]. Proteins exhibit a CD spectrum that is conveniently divided into specific spectral regions, each of which is dominated by different types of chromophores and provides different kinds of information. The secondary structure can be determined by the far UV that ranges from about 170 to 240 nm and the information is provided by the amide group, which is the dominant chromophores [74, 75]. The near UV from 250 to 300 nm, protein CD is dominated by aromatic side chains and provides information about tertiary structure [74, 75].

The protein CD spectrum that arises from the far UV is composed of secondary structural elements consisting of  $\alpha$ -helix,  $\beta$ -sheets and unordered conformation or random coils. These structural elements in the peptide bonds undergo specific transitions which are well detailed elsewhere [74, 76]. Briefly, it can be indicated that the  $\alpha$ -helix characteristic CD spectrum exhibits two negative bands of comparable magnitude at about 222 and 208 nm, plus a stronger positive band near 190 nm. The  $\beta$ -sheet conformation is characterized by two negative bands near 217 and 195 nm and a positive band near 195 nm. Finally, the unordered polypeptides have a weak positive CD band at  $\sim$  217 nm and a strong negative band at  $\sim$  197 nm [74, 77]. The near-UV CD spectra of proteins arise primarily from the packing of side-chain chromophores including the three aromatic side chains (Phe, Tyr, and Trp) and the disulfide group of cysteine [78]. The near-UV CD is greatly perturbed by conformational changes or ligands binding that affect the geometry or environment of one or more aromatic side chains [74]. This information is important given that the biological functions of proteins rely on their structural characteristics, thus the smallest change in the structure may result in functional modifications.

### 1.7.3. $\beta$ lg-Ligand complexes

To date, four binding sites have been recognized on  $\beta$ lg which include the central calyx formed by the  $\beta$ -barrel, the surface hydrophobic pocket in the groove between the  $\alpha$ -helix and the  $\beta$ -barrel, the outer surface near tryptophan (Trp)19 - arginine (Arg)124, close to the entrance of the  $\beta$ -barrel, and the monomer-monomer interface of the dimer [6, 50, 79]. There is a plethora of literature on  $\beta$ lg – based complexes with ligands of biological importance.  $\beta$ lg can bind ligands of varied nature, going from metal ions [80], fatty acids [81], vitamins [79, 82], pharmaceuticals [83], flavour compounds [84], polyphenols [6, 63, 85]. This list is far from being exhaustive and research for relevant  $\beta$ lg–ligand complexes is still ongoing.

The complexation with  $\beta$ lg is believed to improve the biological properties and the stability to environmental factors of both the ligand and the protein. An interesting feature of  $\beta$ lg is its extraordinary stability to pepsin digestion in the stomach whilst being sensitive to proteolytic activity in the intestines [52, 86]. Indeed, the structure of  $\beta$ lg is remarkably well preserved at lower pH values similar to that of the gastric juice [54]. This acid resistance confers to  $\beta$ lg its functional role as carrier of small hydrophobic ligands which are thus protected during transit in the stomach.  $\beta$ lg then releases its cargo charge at higher pH value in the intestine upon proteolytic activity of chymotrypsin, trypsin and minor proteases present in pancreatin [86, 87]. Consequently, a function of  $\beta$ lg might consist in facilitating the digestion of milk fat during in neonates [87]. It is important to notice that closed conformation of the EF loop at acidic pH confirms the physiological role of  $\beta$ lg as a transporter of small bioactives since bound ligands might be protected in the acidic stomach and later be released within the basic small intestine when the EF loop is in the 'open' conformation [51, 58].

Evidence suggests that binding of ligands to  $\beta$ lg is beneficial for both the protein and bound bioactive molecule. Binding of naturally occurring phosphatidylcholine did not influence the resistance of  $\beta$ lg to gastric pepsinolysis but protected the

protein from subsequent degradation under duodenal condition [88]. It has also been established that complexation with tea polyphenols extracts resulted in an increase in  $\beta$ -sheet and  $\alpha$ -helix leading to an alteration of the protein's conformation, which consequently stabilized the structure of  $\beta$ lg [89]. This finding was recently confirmed by the protection of the secondary structure of  $\beta$ lg upon binding to coffee, cocoa and tea polyphenols [90]. Substantial research indicates that upon binding to  $\beta$ lg, hydrophobic ligands are better protected against oxidative degradation and the solubility of some of them is enhanced, which might improve the biological properties of the bioactives [6, 8]. The photostability of folic acid was improved upon binding to the surface of  $\beta$ lg, in the groove between the  $\alpha$ -helix and the  $\beta$ -barrel [7].

Riboflavin is a natural occurring photosensitizer, and as such, is capable of absorbing energy directly from visible light at a specific wavelength (UV-A at around 365 nm) and transferring it to molecular oxygen in order to generate lethal cytotoxic agents such as the singlet oxygen [91]. Irradiation of riboflavin generates reactive oxygen species, riboflavin radicals through type I reaction and singlet oxygen, superoxide, peroxide, and hydroxyl radical through type II reaction. Type I mechanism involves the generation of reactive oxygen species such as the hydroxyl radical  $\text{OH}^\bullet$  and superoxide ion  $\text{O}_2^{\bullet-}$ , while type II mechanism consists mainly in an energy transfer from the  $^3\text{RF}^*$  to the molecular ground state  $\text{O}_2$ , thus generating the singlet state oxygen  $^1\text{O}_2$ . This oxygen species is highly electrophilic and can oxidize directly electron-rich double bonds in biomolecules or participate in electron-transfer reactions, initiating radical-induced damage in macromolecules, which leads to cell death [91]. Although the singlet oxygen is among the most reactive and aggressive oxidative species, both mechanisms can also be involved simultaneously, the predominance of one depending on the reaction system. Other mechanisms, involving direct oxidation of substrates by electron abstraction in anaerobic conditions can also prevail [92, 93].

RF has been suggested as a sensitizer for the treatment of tumors, some dermal and cornea infections that are refractive to conventional therapy, and as an effective method for hygienic process *in vitro* in photodynamic therapy [9, 12, 94, 95]. This natural vitamin could represent a good alternative to synthetic photosensitizers currently used in clinic such as Porfimer-sodium and 5-aminolevulinic acid. These photosensitizers are potentially toxic and require irradiation at longer wavelengths and important equipment that are costly [95, 96].

Reports also indicate that Tyr, Trp and their peptides react with the photoexcited  $^3\text{RF}^*$  by electron transfer from the Tyr and Trp moieties [97]. It has been demonstrated that these amino acids, which are also present in  $\beta\text{lg}$ , enhance the photoactivation of riboflavin [98]. Particularly, it was found that when RF was used as sensitizer in presence of Trp, an 'exceptional efficiency' for the photo-oxidation of Trp residue was observed, due to the higher quantum yield of the photoproducts resulting from the reaction between the photodegradation products of both compounds [11]. According to Silva and co-workers, the photodegradation products include aggregates forms of RF, indolic products associated to flavins, indolic products of higher molecular weight than Trp, N-formylkynurenine and other products of photodecomposition of Trp of lower molecular weight [11]. Among these photodegradation products, N-formylkynurenine seems to have better photosensitizing properties than Trp and RF, which may result in greater cellular damage [99]. Therefore, RF can be associated to a Trp-containing protein such as  $\beta\text{lg}$  in order to trigger the formation of reactive oxygen species upon light irradiation and induce damage in biological systems as a consequence of its photoactivation.

Another ligand of interest is vitamin D<sub>3</sub> (D<sub>3</sub>). Contrary to RF, D<sub>3</sub> is highly hydrophobic and it has been demonstrated that  $\beta\text{lg}$  binds this vitamin with the subsequent formation of the  $\beta\text{lg}$ -vitamin D<sub>3</sub> complex [13, 79]. The  $\beta\text{lg}$ -vitamin D<sub>3</sub> complex represents an excellent model that confirms the existence of multiple binding sites on the protein. In fact, vitamin D<sub>3</sub>,  $\alpha$ -tocopherol, as well as phosphatidylcholine, each binds two different sites on  $\beta\text{lg}$  – which are: (i) the

surface hydrophobic pocket in the groove between the  $\alpha$ -helix and (ii) the  $\beta$ -barrel, and central calyx [50, 79, 88]. The binding of hydrophobic ligands to the surface site via hydrophobic interactions might provide an additional protection to  $\beta$ lg against proteases due to steric encumbrance [88]. Furthermore, the existence of a secondary surface site might be beneficial to the carrier function of  $\beta$ lg since the disruption of the central calyx upon heat treatment can trigger the release of the bioactive bound inside the cavity [13, 50]. In fact,  $\beta$ lg undergoes irreversible denaturation with concomitant loss of its tertiary structure above 80 °C, which consequently disallows the binding of  $D_3$  to the central calyx [79]. The binding to the central cavity of  $\beta$ lg can also be hampered by pH-induced transitions and particularly by the Tandford transition. At lower pH values, the EF loop – that is the gate of the calyx is in the ‘close conformation’, thus preventing binding of  $D_3$ , which can have access again to the central cavity by raising the pH value. Whereas the surface hydrophobic pocket still remains accessible regardless of the modification of the pH or the temperature [13, 59, 79].

The effect of the pH and the structural transitions on the binding capacity of  $\beta$ lg has been well evaluated whilst very few studies have evaluated the impact of the pH on the  $\beta$ lg-ligand complex. Recently, the impact of the pH on the complexes formed between  $\beta$ lg and folic acid (hydrophilic), resveratrol (amphiphilic) and  $\alpha$ -tocopherol (hydrophobic) has been evaluated [50]. The findings reveal that the  $\beta$ lg-resveratrol complex (binding site located at the outer surface of  $\beta$ lg near Trp19–Arg124) remains stable at acidic pH. The binding of folic acid which occurs in the surface hydrophobic pocket is disturbed by decreasing the pH from 7.0 to 2.0, whereas acidification caused the release of  $\alpha$ -tocopherol bound to the internal cavity but had no influence on that bound to a site at the surface of  $\beta$ lg. Hence, it seems that the behavior of individual ligand depends on its physico-chemical characteristics and binding site on  $\beta$ lg. The effect of the pH, especially that at which the structural transitions occur, on the  $\beta$ lg- $D_3$  complex is unknown. If generated, the information may set up new strategies for food supplementation with  $D_3$ , since the  $\beta$ lg- $D_3$  complex could be formed in dairy products [15].

It has been clearly established that  $\beta$ lg might have a functional advantage in the transport of vitamin D<sub>3</sub> since supplementing milk with vitamin D<sub>3</sub> effectively enhances its uptake [61]. The improvement of the uptake of D<sub>3</sub> is sought by public health authorities, particularly those in North America and countries where sun exposure is limited during the winter [100]. Intakes higher than 400 IU of D<sub>3</sub> are required daily in order to maintain adequate levels of the serum values of its biological marker 25-hydroxyvitamin D<sub>3</sub>, which is around 80 nmol/L [101]. Attaining appropriate serum levels of the biomarker may prevent D<sub>3</sub> deficiency, which is implicated in various skeletal and non-skeletal diseases [102].

It is worth noting that the incorporation of fat-soluble vitamins like D<sub>3</sub> is challenging for the food industry, especially for formulation of beverage or foods with high water content. Therefore, increasing the solubility of D<sub>3</sub> would be highly valued considering the ever-increasing demand for healthy food products with low fat content.

## **1.8. $\beta$ lg-biopolymer self-assembly**

### **1.8.1. $\beta$ lg auto-association**

$\beta$ lg can self-assemble to form aggregates, depending on protein concentration, the ionic forces, pH and temperature of the solution. The mechanisms of  $\beta$ lg self-aggregation have been extensively reviewed [16, 17, 103, 104]. Thermal gelation of  $\beta$ lg served to develop environment-sensitive hydrogels with specific microstructural properties and desired bioactives release profiles [2, 105]. The advantage of thermally induced gels is their capacity to entrap bioactive molecules within the gel matrix, stabilize food texture, swell in water and hold it in a well maintained network structure. These characteristics confer protection from hostile environments to bioactives which can subsequently be released as a response to environmental triggers such as pH (acidic in the stomach and neutral in the intestine), temperature and digestive enzymes [2]. However, heat-sensitive

bioactives cannot be encapsulated in thermal gels. This drawback can be bypassed by using cold-set gels, formed by pre-denaturing the proteins using heat treatment and subsequently using salt to induce gelation. Particulate or fine stranded gels sets can then be obtained depending on the ionic force and pH [57]. The use of cold-induced gelation of  $\beta$ lg for oral delivery of nutraceuticals has been the focus of intense research [2, 39, 57, 106, 107]. The pre-heating of  $\beta$ lg exposes functional groups which can be used to create interactions with bioactives and unfolded polypeptide chains as well as to confine the size of delivery matrix into nano and micro-particulate systems.

The size of the biopolymer-based delivery devices can be controlled via two main processes categorized as 'top down' and 'bottom up' approaches [108]. The 'top down' approach consists of breaking up bulk materials into reduced sized matrices whereas the 'bottom up' approach allows structures to be built from molecules capable of self-assembly [2, 108-110]. Food proteins and particularly  $\beta$ lg have great potential to self-assemble due in part to their polyelectrolyte character which offers the possibility to conveniently manipulate their surface charge and establish non covalent interactions (hydrogen bonding, electrostatic and van der Waals forces). Furthermore, the presence of thiol groups permits covalent interactions and finally, hydrophobic amino acids allow the establishment of hydrophobic interactions upon unfolding of the structure [111]. The promotion of such interactions between the polypeptides of  $\beta$ lg can trigger spontaneous self-aggregation of the protein for form site-specific delivery scaffolds of controlled size.

### **1.8.2. $\beta$ lg-based delivery systems: from molecule to particles**

Generally, nanoparticles refer to functional materials at a length scale of less than 100 nm, although a larger definition includes particles of size inferior to the 1  $\mu$ m [2, 112-114]. Beneficial features of nanoparticles include target and site-specific delivery, ability to penetrate cells and circulating systems, bioactives entrapment

and dispersion throughout the dense polymeric network [105]. The dense matrix formed by entanglement of the polypeptide chains is believed to provide a reinforced resistance to proteolytic attack in simulated gastrointestinal conditions. As such,  $\beta$ lg nanoparticles of sub-100 nm size exhibit an improved resistance to digestive proteases at neutral and acidic pH [105]. The size of the  $\beta$ lg nanoparticles was reduced to about 60 nm upon pre-heating the protein solution. The use of cross-linking agents such as glutaraldehyde can significantly improve the density of the nanoparticle matrix, which in turn impedes the penetration of the proteolytic enzymes into the platform and subsequently, retards the degradation of the protein matrix [115]. Degradation of protein-based delivery platforms by intestinal proteases is a major issue in oral delivery of bioactives, particularly for  $\beta$ lg-based systems. The Tanford transition at intestinal pH provides access for enzymes trypsin and chymotrypsin to the target amino acid groups, consequently degrading the protein [53, 59, 86]. Therefore, the development of  $\beta$ lg-based controlled-release formulations which can efficiently retard the intestinal degradation are advantageous on numerous aspects: (i) increased residence time in the intestines resulting to enhanced adsorption; (ii) improved intimacy of contact with the epithelial membrane and/or at the absorption site; (iii) enhanced bioavailability [116]. The carrier system can be tailored to improve its attachment to the epithelial membrane at the target site, also termed as mucoadhesion, which is important for enhanced uptake and bioavailability of biomolecules.

Mucoadhesion is an important characteristic that motivated research for  $\beta$ lg-based formulations with improved adhesion to the mucus layer in the intestines [18, 39, 117, 118]. Indeed, the mucus layer represents the first membrane barrier that covers the gastrointestinal (GI) tract, obstructs direct adhesion to the epithelial cells and hinders the transport of bioactives [116]. The mucus layer is a viscoelastic protective lining of the epithelium, mainly composed of water (~ 95 %) and up to 5 % of mucins. Mucins are glycoproteins of high molecular weight constituted of peptide backbone with important number of carbohydrate side chains attached to the peptide backbone. Whereas the protein core and formation of the disulfides

bridges between the peptides backbones are responsible for the hydrophobic and viscoelasticity character of the mucins, respectively, the carboxylic side chains confer a strong negative charge to the mucus layer [116]. Recently, cationic  $\beta$ lg nanoparticles of size comprised between 75 and 94 nm were developed as bioavailability enhancer for poorly absorbed bioactive [119]. The cationic  $\beta$ lg nanoparticles were formed by substituting 11 amino acid residues by ethylenediamine, which resulted in positive surface charge and significantly increased surface hydrophobicity. The positively charged  $\beta$ lg nanoparticles improved the mucoadhesion and were proposed as bioavailability enhancers of nutra- and pharmaceuticals [120].

A number of pH sensitive, biocompatible and biodegradable polysaccharides have been used as mucoadhesive agents and it was proved that an increased charge density enhances the adhesion [121, 122]. Interestingly, evidence also indicates that both anionic (e.g. alginate) and cationic (e.g. chitosan) can quite strongly interact with mucins. This can be probably explained by the presence of both charge groups on the backbone and side chains with different pKa, which changes the global charge of the mucin molecules when the pH varies between pH 1 and 7. Thus, while the mucins are fully negatively charged in the intestines, they carry neutral to weak charge in the stomach, the pKa (2.6) of sialic acid (at the end of the carboxylic groups) being used as cut-off point [116]. Nano-sized delivery platforms including electrostatic complexes and coacervates formation between  $\beta$ lg and polysaccharides have been developed. These platforms result from the electrostatic interactions between oppositely charged molecules under particular pH and ionic force [117, 123-126]. Nanoparticles, with the core constituted of chitosan and shell formed by  $\beta$ lg were developed as nutraceutical carriers [18]. When the native  $\beta$ lg was used to form the shell, the resistance to acid and pepsin degradation property of the protein was preserved.

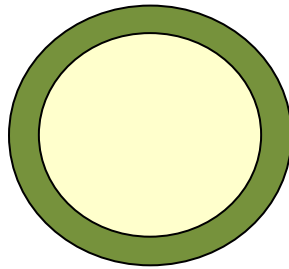
Heat denatured  $\beta$ lg was used to form electrostatic complexes with pectin, an anionic polysaccharides that is only degraded in the colon by the pectinases and

resists proteases and amylase in the upper GI tract [121, 127]. The resulting nanoparticle was suggested for colon delivery purposes for a wide range of bioactives including pharmaceuticals and nutraceuticals. Vitamin D<sub>2</sub>, docosahexaenoic acid and major catechin in green tea ((-)-Epigallocatechin-3-gallate) were successfully entrapped in nanoparticles of size varying from 50 to about 100 nm prepared upon promotion of electrostatic interactions between  $\beta$ lg and pectin [20, 118, 128]. The authors suggested that these nanovehicles could serve as carriers for hydrophobic nutraceuticals in non-fat foods and clear beverages. The encapsulated bioactives benefited from significant protection against oxidative degradation, probably due to mild antioxidant activity of  $\beta$ lg conferred by the free thiol group [20, 129]. In addition, the physical entrapment and reduced mobility of light or oxygen sensitive bioactives within the protein matrix might provide addition resistance to oxidizing agents such as oxygen or free radicals by restricting their access to the encapsulated bioactive molecule [20]. The ability of  $\beta$ lg to absorb UV-light can also contribute in improving the light stability of the entrapped bioactives that absorb at a proximate wavelength range [130].

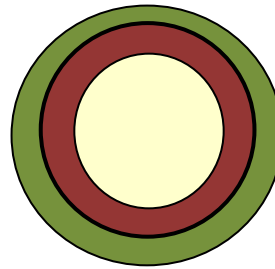
Nanoparticles, particularly of size equal or inferior to 100 nm, have the functional advantage of diffusing readily though both the epithelial and lymphatic tissue at target sites where the entrapped bioactive is uptake with high efficiency [131]. However, the release of the bioactive can also be effectively modulated by larger submicron particles, with slower release profiles and retarded residence time at the mucosal lining [2, 131, 132].

### **1.8.3. $\beta$ lg-based microparticles for oral delivery**

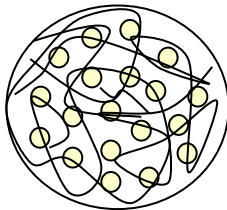
Microparticles are spherical shaped scaffolds of size inferior to 1 000  $\mu\text{m}$  isolating a variety of sensitive bioactive substances from the surrounding environment by a membrane coating [133]. Biopolymers and bioactive ingredients can be combined to form microparticulate structures including multishell, multilayer, microspheres or microcapsules platforms (Figure 1.4).



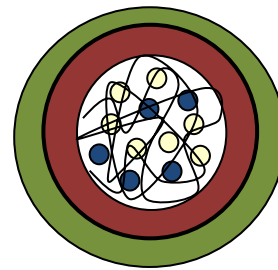
**(a) Microcapsule**



**(b) Multilayer microcapsule**



**(c) Microsphere**



**(d) Multishell and multicore microsphere**

○ Bioactive substance

● ● ~ Microencapsulation material (e.g. biopolymers)

**Figure 1.4. Different structures of microparticles obtained by microencapsulation: (a) microcapsule, (b) multilayer microcapsule, (c) microsphere and (d) multishell and multicore microsphere. Adapted from Nesterenko et al. 2013 [133].**

In the food industry, microparticles have been used to mask unpleasant taste and flavor, convert liquids to solids and protect sensitive ingredients from the harsh external medium including light, moisture, pH and oxidation; the list is not exhaustive [2, 133]. Currently, there is an important amount of reports on the use of microparticle as delivery vehicles for nutraceuticals and pharmaceuticals. The use of non-toxic food grade materials is of particular interest for oral delivery and as such, a large volume of research on  $\beta$ lg-based microparticulate systems exists in the literature. Furthermore,  $\beta$ lg pertains to the lipocalin family, explaining its recognition and internalization by the human lipocalin-interacting membrane receptor that is expressed in the intestine [5]. Therefore, its uptake by intestinal cells is advantageous in formulation of oral delivery platforms that entrap and release bioactives within the intestine. Microparticles can be formulated to prolong residence time of bioactives at the target site and improve their bioavailability, as a result of enhanced mucoadhesion. Coacervates of  $\beta$ lg with naturally occurring polysaccharides with mucoadhesive property such as alginate, pectin, arabic gum, acacia gum have been used for the encapsulation of probiotics, vitamins, etc. [2, 18, 33, 134-136].

Despite important potential applications in delivery technology, the use of coacervates is restricted to a narrow window of pH and ionic strength, a range beyond which the microparticles are unstable and thus can lead to premature release of the bioactive cargo charge [134]. Solutions to this issue include formation of Maillard type conjugates consisting of non-enzymatic browning involving the terminal or a side chain amine group of  $\beta$ lg and the reducing end of a sugar such as dextran [137, 138]. Crosslinking including glutaraldehyde or formaldehyde have been used to stabilize coacervates, however they are not authorized for food application due to their toxicity.

Biocompatible alternatives such as rennet, genipin, glyceraldehyde or transglutaminases are available. They are all capable of stabilizing coacervates by covalently bridging proteins matrices, but with a yield well below that of the toxic ones [39, 134]. However, it is important to ensure that crosslinking does not

impede on the bioaccessibility and release of the active molecule entrapped within the carrier matrix which then forms a barrier against diffusion and inward access of digestive enzymes [39]. Maillard conjugates, the use of cross-linking agents for improved microparticles stability as well as emulsion and lipid-based particulate systems are out of the scope of the present review.

The development of protein based delivery systems is attracting increasing interest due in part to their GRAS status and the possibility to entrap bioactives with different physico-chemical properties. Particularly,  $\beta$ lg naturally interacts with small ligands as well as food macromolecules to form complexes of which size and surface properties can be controlled. Recent reports indicate that  $\beta$ lg and food proteins such as egg white proteins including Lysozyme (Lyso) can form electrostatic complexes at pH comprised in between the  $pI$  of the two biopolymers [139]. Electrostatic complexes were formed between Lyso and  $\beta$ lg and both charge and hydrophobic forces were found to play a major role in the co-precipitation of the two proteins [21, 140].

Lysozyme is an interesting ligand as it is a cationic protein that acts as a lytic enzyme. It acts by lysing the peptidoglycan or murein, a glycosidic polymer composed of N-acetyl muramate and N-acetyl glucosamine in the bacteria cell wall. This in turn will disrupt bacterial membranes, consequently damaging or killing the bacteria [22]. Lyso is found in numerous human fluids, but more specifically in airways secretions. Although its interaction with  $\beta$ lg may involve the active catalytic site (glutamic acid 35 and aspartic acid 52 in Lyso and lysine 138 and 141 at the dimerization site of  $\beta$ lg), other types of interaction, including disulfide bonding, may also take place [21, 140]. Further characterization of the supramolecular structure formed by the co-precipitation of  $\beta$ lg and Lyso could provide more insights on the mechanism of formation of this protein-based matrix.

Evidence strongly suggests that the self-assembly of two proteins into delivery scaffolds will constitute a significant research field in the near future due mostly to

the nutritional advantage, generation of bioactive peptides and simplicity of the process, which offers a variety of applications including bioactive encapsulation and delivery, proteins co-precipitation and isolation [141]. Formulation of bioactive-loaded protein carriers, with controlled size and release profile, require the full understanding of the behavior of the delivery platform in food systems as well as in the GI tract, at the site of absorption. The physico-chemical characteristics including surface properties such as size, surface charge, interior and surface morphology are important parameters to consider for an optimal bio-interaction, uptake and bioavailability of the bioactive substance.

#### **1.8.4. Characterization of $\beta$ Ig-based nano and microparticles**

Most  $\beta$ Ig-based nano and microparticulate carriers with a dense matrix result from electrostatic complexes formed between soluble biopolymers. Typically, the self-assembly is promoted by mixing clear solutions under controlled pH, temperature and ionic forces conditions. This in turn leads to a modification of the light scattering (turbidity) of the resulting solution, which increases rapidly as a consequence of formation of large aggregates or co-precipitates [142]. The theory behind turbidity measurement is the Rayleigh's theory which indicates that the scattering of light is brought upon by particles which are smaller in diameter than the wavelength of the light itself, the upper limit being considered to be about 1/10 of the wavelength [142, 143]. The increase in turbidity is normally associated to an increase in the size of the particles and is commonly measured by UV-vis spectroscopy as optical density in the 340–360 nm range and 550 to 600 nm [20, 118, 142]. The optical property of a solution is a function of the particles present to scatter and absorb light [142]. However, turbidity data should be interpreted carefully, since various environmental factors including temperature, pH (near the pI) and protein concentration can influence the size of  $\beta$ Ig-biopolymer self-assembled structures. The size determination is also based on the optical property of a solution which depends on the ability of the particles dispersed in the solution

to scatter and absorb light. Particle size (1 to 10  $\mu\text{m}$ ) and size distribution are frequently determined using laser light scattering which encompasses static and dynamic light scattering. Detailed information on these optical techniques has been well described in the literature [142-144].

The surface charge of particle is estimated using the zeta potential that is an indication for the particle stability measured by electrophoretic light scattering [143]. Values of zeta potential above +30 mV and below -30 mV are indicative of a stable colloidal system. Instability arises from pH, which affects the surface charge and repulsion/attraction forces between particles, and the ionic strength, which can modify the particle's charge density [143]. The interior and surface aspect of particulate systems can be characterized using transmission (TEM) and scanning electron microscopy (SEM), respectively [2, 18, 144]. Larger size particle or visible particles can be observed using optical microscopy techniques equipped with epifluorescence and optical fluorescent filters for improved discrimination between distinct biopolymers which are beforehand stained [31, 32]. Finally, the encapsulated bioactive can be extracted from the carrier scaffold and its concentration quantitatively determined (encapsulation efficiency) using techniques such as UV-vis spectroscopy at specific wavelengths or high pressure liquid chromatography (HPLC) [20, 118].

The intestinal uptake and bioavailability of the bioactive substance developed for oral administration are commonly evaluated by performing permeability tests using cell culture or *in vivo* experiments using animal or human models. The behaviour of the oral delivery system in the GI tract and the *in vitro* bioavailability of a bioactive can be monitored using *in vitro* digestion methods or dissolution tests following the US Pharmacopeia/Food and Drug Administration (USP/FDA) guidelines [132]. Briefly, digestion at 37 °C in an acidic solution (pH 1.2) in presence of pepsin represents the gastric conditions while digestion at pH 6.8 in presence of pancreatin simulates the intestinal conditions [31, 32, 132]. More specifically, the fate of the  $\beta\text{lg}$ -based carrier systems in the stomach and intestines corresponds to

the behaviour of the protein in different compartments in the GI tract. Native  $\beta$ lg is resistant to acid and pepsin in the stomach while is degraded at higher pH and by the pancreatin in the intestines [5, 58, 59]. Shell/core chitosan/ $\beta$ lg microparticles with the shell formed by native  $\beta$ lg resist under the gastric conditions while are degraded in the intestines by enzymes. However, the microparticles' shell made of denatured  $\beta$ lg were rapidly degraded under both gastric and intestinal conditions [18].

Cell cultures with adenocarcinoma cell lines derived from human colon epithelia (Caco-2 cells) are among the most frequently used means for *in vitro* permeability tests. The Caco-2 cells have similar biophysical properties similar to that of the epithelial cells of the intestines and as such, mimic well the absorption of the bioactives through the intestinal membrane [132]. Therefore, the Caco-2 cells can be used to evaluate the efficiency of controlled-release formulations [106, 131, 145]. Better information on the uptake and bioavailability of the bioactive substance can be generated using *in vivo* experiments with rats, mice or human beings. In food systems, the concept of bioavailability is most of the time erroneously restricted to the biopharmaceutical phase, which includes the release of the bioactive upon physical erosion or chemical degradation of the carrier system and pays little attention to the biopharmaceutical phase (distribution, metabolism and elimination) and biological responses of the encapsulated bioactive [146]. Careful attention should be given in interpreting bioavailability data resulting from *in vitro* experiments. Optimum bioavailability and biological response result necessarily from an accurate understanding of the relationship between the structure of the carrier platform, biophysical characteristics of both the bioactive and encapsulating material, and good knowledge of physiology of the intended target site.

## 1.9. Conclusion

Indolic amino acids such as Trp are present in the structure of  $\beta$ lg. They can be directly photoactivated upon absorption of UV radiation, or indirectly via energy transfer from chromophores such as RF, which may generate reactive oxidative species [147]. Some of the resulting photodecomposition products are better photosensitizers than the initial compounds, due to their higher stability and quantum yield [99, 147]. Since RF is a known photosensitizer which has been successfully essayed in photodynamic therapy (ribophototherapy) against skin affections [95], the combination of  $\beta$ lg and RF may also generate photooxidation products that can damage dermal cells upon proper irradiation in aqueous solution.

The interaction of  $\beta$ lg with  $D_3$  although well studied in the literature, still requires information on the stability of the  $\beta$ lg- $D_3$  complex in varying pH conditions and the effects of the complex formation on the solubility, stability and bioavailability of the vitamin are unknown.  $D_3$  represents a typical model of small hydrophobic bioactive with important clinical significance [148, 149]. Since hydrophobic interactions play an important role in the self-aggregation of  $\beta$ lg at its pI [17], the  $\beta$ lg- $D_3$  complex and in particular  $D_3$  might gain in stability, if entrapped within the dense protein matrix.

Lastly, Lyso could represent a good model of larger ligand for  $\beta$ lg. This is even more relevant with the existence of reports on the formation of electrostatic complexes between Lyso and  $\beta$ lg [21]. The resulting protein-based scaffold could serve for the delivery of bioactives, which could be pertinent if the bioactive binds to both proteins. However, careful characterization of the protein scaffold is required since its fate in the digestive system could be uncertain because of the presence of proteases.

Like almost all animal proteins, the use of  $\beta$ lg as delivery platform might undergo careful consideration, as it may also be implicated in the spreading of

neurodegenerative diseases such as bovine spongiform encephalitis (mad cow disease). Moreover, potential risks for allergic reactions prompted research for alternatives from natural sources such as vegetable proteins [150]. Nevertheless,  $\beta$ lg is widely used in the food industry, and because of its nutritional importance, its functionality as a carrier system remains very attractive.

## **CHAPTER 2**

### **Problem statement**

### **Hypothesis and Objectives**

## 2.1. Problem Statement

The development of protein-based carrier systems is attracting interest due to their biocompatibility, biodegradability and food grade status. The milk whey protein  $\beta$ lg is a well-recognized carrier for small hydrophobic bioactives, the biological properties of which are believed to be improved upon binding to the protein. RF, is an amphiphilic vitamin and also a photosensitizer with potential applications in photodynamic therapy. It generates photodegradation products upon UV or visible light absorption, inducing damage in biological systems. This activity is important in photodynamic therapy, currently used in clinic to treat tumors or other localized affections. However, current photosensitizers such as Porfimer-sodium and 5-aminolevulinic acid are potentially toxic and require irradiation at longer wavelengths, which necessitates costly equipment. The photoactivation of RF is achieved by using equipment that are user friendly and that use cheap light sources.  $\beta$ lg contains amino acids such as Trp that can also be photoactivated upon light absorption. The association between RF and  $\beta$ lg could generate highly reactive oxidative species due to a cumulative effect and trigger a cascade reaction leading to damage in biological systems.

The binding of  $\beta$ lg to  $D_3$  has been extensively studied. However, reports on the stability of  $D_3$  after complex formation and that of the  $\beta$ lg- $D_3$  complex at varying pH values are scarce. Additionally, there is few information on the impact of complex formation on the solubility, intestinal stability, absorption and bioavailability of  $D_3$ . This information is important because  $D_3$  deficiency is quite common in North American and high latitude countries, where exposure to sun is reduced during the winter. Food fortification seems to be insufficient to maintain adequate levels of the circulating  $D_3$  (25-hydroxy- $D_3$ ). The reasons for low  $D_3$  intake include the limited range of foods that are fortified, which is mainly composed of dairy products. Furthermore, in addition to its classical effects on skeletal diseases (e.g. rickets),  $D_3$  deficiency is increasingly implicated in non-skeletal diseases such as cancer. Therefore, means of increasing the uptake and the bioavailability of  $D_3$  are sought.  $\beta$ lg can self-aggregate under mild acidic conditions, with hydrophobic interactions

playing an important role, which also are implicated in the binding of  $D_3$  to  $\beta$ lg. Therefore, the self-aggregation of the  $\beta$ lg- $D_3$  complex could be beneficial for the stability of the vitamin. To date, there is no report in the literature on the self-aggregation of the  $\beta$ lg- $D_3$  complex.

Electrostatic complexes resulting from the interaction between oppositely charged biopolymers such as polysaccharides and proteins have been used for oral delivery purposes. However, for increased stability, most of these carriers require the use of toxic crosslinking agents such as glutaraldehyde and formaldehyde, which are not compatible with a food administration. Food grade crosslinking agents including genipin, rennet or glyceraldehyde have been used as good alternatives, but with shortcomings. Conversely, food proteins and particularly milk proteins are readily available, from cheap, abundant and renewable sources. In addition to their high nutritional value, these proteins have interesting structural and functional properties, which make them good candidates for the formulation of delivery platforms with a GRAS (generally recognized as safe) status. Lyso is a cationic protein with enzymatic and antibacterial activities. Its positive charge and the existence of numerous functional groups could be exploited to establish electrostatic interactions with  $\beta$ lg and thus, Lyso could become a larger sized ligand for the former protein. In fact,  $\beta$ lg and Lyso are two food proteins that offer a wide range for electrostatic complex formation. The  $pI$  of  $\beta$ lg is 5.3 while that of Lyso is 10.7, indicating that at pH values comprised within this interval, the two compound can co-precipitate to form a supramolecular structure. This protein-based matrix could be further characterized and may have potential application in the delivery of bioactives such  $D_3$ , which already is known to bind  $\beta$ lg.

## 2.2. Hypothesis

The present study hypothesizes that  $\beta$ lg, due to its structural properties, can serve as a versatile food grade carrier for small and larger sized bioactives with different physico-chemical characteristics; the biological activities of the small ligands can be improved upon binding to  $\beta$ lg while the larger sized ligand, of opposite charge, can serve to form an electrostatic driven protein – based platform which can be used to encapsulate a bioactive that has affinity with one of the proteins.

## 2.3. Objectives

The following objectives were formulated to verify the research hypothesis.

### 2.3.1. General objective

The present work aims at studying the interactions between  $\beta$ lg and model ligands RF, D<sub>3</sub> and Lyso, including the effects of complex formation on the photoactivation of RF, the impact of complexation with  $\beta$ lg and self-aggregation of the  $\beta$ lg on the stability of D<sub>3</sub>, and the use of Lyso to form a protein – based matrix that can encapsulate D<sub>3</sub>.

### 2.3.2. Specific objectives

- Investigate the interaction between riboflavin and  $\beta$ -lactoglobulin and its impact on the structure of the protein and on the photoactivation of riboflavin.
- Determine the pH and intestinal stability of the  $\beta$ -lactoglobulin – vitamin D<sub>3</sub> complex and impact on the solubility of vitamin D<sub>3</sub>.
- Optimize and characterize the self-aggregation of the  $\beta$ -lactoglobulin – vitamin D<sub>3</sub> complex with concomitant encapsulation of the vitamin in the  $\beta$ -lactoglobulin based matrix.

- Optimize and characterize the formation of micro-sized electrostatic complexes between oppositely charged  $\beta$ -lactoglobulin and egg white Lysozyme for the delivery of biological actives of nutritional importance (using vitamin D<sub>3</sub> as model nutraceutical).



## **Contextual transition**

The following chapter outlines the findings from the spectroscopic studies on the interaction between riboflavin and  $\beta$ -lactoglobulin, which corresponds to the first specific objective of the present thesis. Riboflavin is a vitamin with both hydrophobic and hydrophilic moieties that is also a natural occurring photosensitizer. Its binding to  $\beta$ -lactoglobulin, which normally binds small hydrophobic ligands, was investigated using fluorescence spectroscopy and the impact of the interaction on the protein structure was analyzed using circular dichroism. This work also reports the impact of the  $\beta$ -lactoglobulin – riboflavin interaction on the photoactivation of riboflavin, which was performed by assaying the antiproliferative activity of the complex against skin melanoma cancer cell lines.



## CHAPTER 3

# **Nanocomplex formation between riboflavin and $\beta$ -lactoglobulin: Spectroscopic investigation and biological characterization**

A version of this work has been published in Food Research International, Volume 52, Issue 2, July 2013, Pages 557–567.

By :

Fatoumata Diarrassouba<sup>a</sup>, Gabriel Remondetto<sup>b</sup>, Li Liang<sup>a</sup> and Muriel Subirade<sup>a</sup>

<sup>a</sup>Chaire de recherche du Canada sur les protéines, les bio-systèmes et les aliments fonctionnels, Institut de recherche sur les nutraceutiques et les aliments fonctionnels (INAF/STELA), Université Laval, Québec, QC, Canada

<sup>b</sup>Centre de recherche et développement, Agropur Coopérative. 4700 rue Armand Frappier, St-Hubert, QC, J3Z 1G5, Canada

### **3.1 Abstract**

Light activated drug delivery systems with the use of photosensitizers are attracting increasing interest in both the medical and non-medical fields. Riboflavin (RF) is an endogenous photosensitizer that interacts with proteins located in the cell membrane and induces damages to biological systems including tumor tissues. Spectroscopic methods were used to demonstrate interaction and energy transfer between  $\beta$ -lactoglobulin ( $\beta$ lg), the major bovine milk protein, and RF. The findings reveal the formation of a ground-state nanocomplex between  $\beta$ lg and RF with minor impact on the structure of the protein.  $\beta$ lg can bind and transport RF, which has great implications for the food industry in terms of food fortification. The impact of these interactions on RF was determined by assessing the anti-proliferative activity of the  $\beta$ lg/RF nanocomplex by irradiating skin melanoma cancer cell lines with UV-A light according to the NCI/NIH Developmental Therapeutics Program. The  $\beta$ lg/RF nanocomplex exhibited important anti-proliferative activity in the micromolar range. The cytotoxicity is likely due to the generation of reactive radical and oxygen species as the result of the interaction between RF and  $\beta$ lg. This study provides important information on the potential use of the  $\beta$ lg/RF nanocomplex in photodynamic therapy, which is applied in the medical field against tumor cells as well as in the food industry against food-borne pathogens.

### **3.2 Introduction**

The development of light activated drugs — that is photodynamic therapy (PDT) is gaining increasing interest in both oncology and non-oncologic applications as well as in controlling microbial growth on surfaces in the food processing industry and decontamination of foods [151, 152]. The photoactivation of the photosensitizer (PS) leads to the production of molecules in the excited state that can transfer energy to molecular oxygen with the generation of reactive oxygen species including the most aggressive singlet oxygen ( $^1\text{O}_2$ ), a process known as the type II

pathway [153]. The type I mechanism is mainly predominant in oxygen depleted conditions and consists of a transfer of electron or atomic hydrogen to create free radicals which initiate radical-induced damage in biomolecules [154, 155]. Advantages of conventional PDT include effectiveness in destroying diseased tissues with negligible damage to healthy ones [156]. However, controversy still surrounds the selectivity of these PS which consequently results in the restriction of the application of PDT to only certain types of cancers [96, 157]. Additionally, most PS are hydrophobic, have enhanced cell permeability but poor solubility in water and thus, tend to aggregate in aqueous solutions. This characteristic affects their photochemical activity and cell-targeting properties [154]. Furthermore, light delivery devices are costly and require heavy investment. These limitations can be overcome possibly by using indirect photodynamic processes resulting from the cascade oxidation of biological systems, which can be generated by the photooxidation of biomacromolecules that is triggered by endogenous PS such as riboflavin (RF). RF is a soluble vitamin, biocompatible and readily available in nature [158]. RF can cause damage to DNA, proteins and other biomolecules upon light activation through both type I and type II pathways upon the absorption of light energy under aerobic conditions and generation of the triplet excited state ( $3RF^*$ ) [11]. Consequently, the RF/light combination is efficient against numerous antibiotic resistant pathogens found in foods and against cancers such as leukemia [159, 160]. Another advantage for the use of riboflavin is that its excitation wavelength is located within the UV-A range, which requires much lower capital and running costs than the current photosensitizers used in clinics, and most importantly is far from the absorption peak of hemoglobin (around 600 nm), which preferably should not absorb during irradiation treatment [153].

The major protein from bovine milk,  $\beta$ -lactoglobulin ( $\beta$ lg), is recognized as a versatile carrier for small bioactive molecules [46]. Different binding sites for ligands have been located on  $\beta$ lg, most of which are in the vicinity of the Trp residue [6]. Furthermore, according to Davies, the photo-oxidation products of the amino acid tryptophan (Trp) have been detected in both the free amino acid and

from the Trp residues in peptides and proteins, and most importantly, the degradation products are better PS than Trp itself and can trigger the formation of the  $^1\text{O}_2$  during continued light exposure [99]. Therefore, the generation and gradual accumulation of the Trp photo-oxidation products in proteins can result in cascade damage in biological systems [99]. Additionally,  $\beta\text{lg}$  also contains other amino acids such as tyrosine and phenylalanine, capable of energy or electron transfer to RF to generate the  $^3\text{RF}^*$  and  $^1\text{O}_2$  upon light exposure [161]. Therefore, upon irradiation, the cumulative effect of RF/ $\beta\text{lg}$  may potentially generate the formation of reactive oxygen and radical species that can be used against localized surface tumor tissues and against pathogens in the food system, for disinfection purposes. The objectives of this study were to evaluate if  $\beta\text{lg}$  could bind RF to form a nanocomplex and the impact of the resulting interactions on both the structure of  $\beta\text{lg}$  and the photoactivation of RF. The stability of the photoactivated  $\beta\text{lg}/\text{RF}$  nanocomplex and its effect on skin melanoma cells were evaluated in vitro.

### **3.3. Experimental Section**

#### **3.3.1. Materials**

$\beta$ -Lactoglobulin (B variant, purity  $\geq 90\%$ ) and riboflavin were purchased from Sigma-Aldrich Chemical and Co. (St. Louis, MO, USA) and used without further purification.

#### **3.3.2. Sample preparation**

$\beta$ -Lactoglobulin ( $\beta\text{lg}$ ) and riboflavin (RF) stock solutions were prepared daily by dissolving each compound in 10 mM phosphate buffer at pH 7.4 to obtain a concentration of 100  $\mu\text{M}$ . The concentrations of RF and  $\beta\text{lg}$  were determined spectrophotometrically using a molar extinction coefficient of 10,000  $\text{M}^{-1} \text{cm}^{-1}$  for

RF and  $17,600 \text{ M}^{-1} \text{ cm}^{-1}$  for  $\beta\text{lg}$  [6, 162]. Samples were prepared fresh prior to each analysis by mixing native  $\beta\text{lg}$  and RF stock solutions in varying proportions (Section 3.3.3), and were allowed to incubate at room temperature in the dark. Denaturation of  $\beta\text{lg}$  was achieved by heating the protein to  $85 \text{ }^\circ\text{C}$  for 30 min at the appropriate concentration followed by cooling to room temperature [57]. Then the denatured  $\beta\text{lg}$  and RF stock solutions in varying proportions prior to analysis (Section 3.3.3). Each experiment was repeated at least three times.

### **3.3.3. Circular dichroism measurement**

Circular dichroism (CD) measurements were carried out using a Jasco J-710 spectropolarimeter. Influence of RF on  $\beta\text{lg}$  secondary and tertiary structures was analyzed in the far-UV (190 to 250 nm) and near-UV (250 to 350 nm) regions of the CD spectra, using  $\beta\text{lg}$  at concentrations of  $10 \text{ }\mu\text{M}$  and  $20 \text{ }\mu\text{M}$ , respectively. Increasing concentrations of RF (0, 1, 2.5, 5, 10, 20 and  $40 \text{ }\mu\text{M}$ ) were used for both protein concentrations. Path lengths were 0.1 cm and 1 cm for the far-UV and near-UV regions, respectively. Differences in molar absorbance ( $\Delta\epsilon$ ) were recorded at a speed of 100 nm/min, 0.2 nm resolution, 10 accumulations and 1.0 nm bandwidth. Buffer and RF backgrounds were subtracted from the raw spectra. Each experiment was repeated at least three times.

### **3.3.4. Steady state fluorescence measurement**

#### **3.3.4.1. Protein fluorescence spectra**

Steady-state fluorescence measurements were carried out on a Cary Eclipse 300 fluorescence spectrophotometer (Varian Inc., Englewood, CO, USA) equipped with a temperature-controlled bath. The fluorescence spectra were recorded at different temperatures (20, 35, 45 and  $55 \text{ }^\circ\text{C}$ ) for  $\beta\text{lg}$ . Two different concentrations of the non- and pre-heat-treated protein were assayed ( $5$  and  $10 \text{ }\mu\text{M}$ ) in the presence of

increasing concentrations of RF (0, 1, 2.5, 5, 10, 15 and 20  $\mu\text{M}$ ). The fluorescence emission spectra in the range of 290 to 450 nm were recorded at an excitation wavelength of 280 nm. RF has no fluorescence in the range of 300–450 nm [69]. Spectra resolution was 5 nm for both excitation and emission.

#### **3.3.4.2. Synchronous fluorescence spectra**

The synchronous fluorescence of native  $\beta\text{Ig}$  (after mixing with RF at varying concentration) was obtained by recording the fluorescence spectra resulting from the difference between the excitation wavelength and emission wavelength at 15 or 60 nm intervals, corresponding to the changes of the polarity around tyrosine and tryptophan residues, respectively [69].

#### **3.3.5. Biological characterization of the $\beta\text{Ig}/\text{RF}$ nanocomplex**

##### **3.3.5.1. Cell line culture**

M21 human skin melanoma cells were cultured in DMEM medium (Dulbecco's Modified Eagle Medium) containing sodium bicarbonate, a high concentration of glucose, glutamine, and sodium pyruvate (Hyclone, Logan, UT) supplemented with 5 % fetal calf serum. The cells were maintained at 37 °C in a water-saturated atmosphere containing 5 %  $\text{CO}_2$  [163].

##### **3.3.5.2. Anti-proliferative activity assay**

The  $\beta\text{Ig}/\text{RF}$  nanocomplex was formed directly in phosphate-buffered saline (PBS), pH 7.4 (GIBCO, Burlington, ON). Briefly, RF and  $\beta\text{Ig}$  solutions were prepared in PBS solution as described above, mixed at a final concentration of 20  $\mu\text{M}$  each and incubated at room temperature for about 2 h. Solutions of 20  $\mu\text{M}$  RF and  $\beta\text{Ig}$  were used as control solutions. The anti-proliferative activity was assessed using the in

vitro cell line screening procedure described by the National Cancer Institute for the Development Therapeutics Program (DTP) anticancer drug discovery initiative [164]. One hundred microliters of M21 skin melanoma cells in DMEM medium were seeded in 96-well plates. Plates were incubated for 24 h. Aliquots (100  $\mu$ L) containing increasing concentrations of the  $\beta$ Ig/RF nanocomplex, as well as RF and  $\beta$ Ig solutions solubilized in PBS were diluted in fresh medium and added to the cells for a final concentration of 1.25, 2.5 and 5  $\mu$ M, respectively. The plates were then exposed for 25 min to monochromatic light at 365 nm within the UV-A zone (4-W, PL Series, UVP®, Upland, CA). Irradiated plates were incubated for 48 h. Plates containing attached cell lines were then fixed and stained using the sulforhodamine B method [163]. In brief, cells were fixed by the addition of cold trichloroacetic acid to the wells (10% (w/v) final concentration), for 30 min at 4 °C. Plates were washed five times with tap water and dried. Sulforhodamine B solution (50  $\mu$ L) at 0.1 % (w/v) in 1 % acetic acid was added to each well, and plates were incubated for 15 min at room temperature. Unbound dye was removed by washing five times with 1% acetic acid. Bound dye was solubilized in 10 mM Trisbase, and the absorbance was read using a  $\mu$ Quant Universal microplates spectrophotometer (Biotek, Winooski, VT) at a wavelength 548 nm. The experiments were performed at least twice in triplicate.

### **3.3.5.3. Reversed-phase high performance liquid chromatography**

In order to investigate the behavior of the irradiated  $\beta$ Ig/RF nanocomplex, the nanocomplex, RF, and  $\beta$ Ig solutions were irradiated at 365 nm in PBS, without the cancer cell lines. The irradiation products were analyzed by reversed phase high performance liquid chromatography (RP-HPLC) fitting with a Phenomenex Kinetex 1.7  $\mu$ m 2.1  $\times$  75 mm XB-C18 column (Phenomenex, Torrance, California, USA) using an Agilent1260 HPLC Series system (Agilent technologies, Palo Alto, CA, USA). The gradient elution was 0–2 min, 20–65 % B; 2–2.25 min, 65–100 % B; 2.25–4.85 min isocratic 100 % B; 4.85–5 min, 100–20 % B; 5–8 min isocratic 20 % B. Mobile phases were A: H<sub>2</sub>O + 0.1 % TFA and B: acetonitrile + 0.1 %TFA (v/v).

The mobile phase flow rate was 0.4 mL min<sup>-1</sup>. After separation on the Kinetex column, detection was achieved at 280 nm.

#### **3.3.5.4. Light stability of the $\beta$ Ig/RF nanocomplex**

In order to evaluate the light stability of the  $\beta$ Ig/RF nanocomplex, a two-week degradation study was conducted. Fifty mL of the  $\beta$ Ig/RF nanocomplex, RF, and  $\beta$ Ig solutions were prepared as described above in clear 50 mL-falcon tubes. The solution of  $\beta$ Ig and RF was bubbled with a stream of dry nitrogen and protected from light for 2 h to allow complex formation between  $\beta$ Ig and RF. The RF and  $\beta$ Ig solutions, each concentrated at 20  $\mu$ M, were used as controls and were submitted to the same treatment as the  $\beta$ Ig/RF nanocomplex. After the incubation period, the falcon tubes were exposed to day light for two weeks. Bacterial growth was prevented by the addition of 0.1 % of sodium azide to the solutions. At day 0, 1, 3, 7 and 14, samples were withdrawn for spectrophotometric determination of the RF and  $\beta$ Ig concentrations using the method described above for both RF and  $\beta$ Ig. The UV-vis spectra of  $\beta$ Ig were subtracted from the spectra obtained for the  $\beta$ Ig/RF nanocomplex at each sampling period.

### **3.4. Results and discussion**

#### **3.4.1. Influence of $\beta$ Ig-RF interaction on the structure of the protein**

The structural integrity of  $\beta$ Ig is essential for exercise of its transport properties [81]. The binding of small ligands on  $\beta$ Ig can generate minor to important perturbation in the secondary and tertiary structure of the protein [6]. Therefore, it is essential to study the impact of RF on the structure of  $\beta$ Ig, which can be achieved using the circular dichroism (CD). The secondary structure of  $\beta$ Ig can be determined in the 190 to 240 nm range of the CD spectra, whereas the tertiary

structure is determined between 250 and 350 nm [75]. The far-UV spectra arising from the peptide bonds did not change significantly with the increasing concentrations of RF (Figure 3.1A), suggesting that the interaction occurring between RF and  $\beta$ Ig does not modify the secondary structure of the protein.

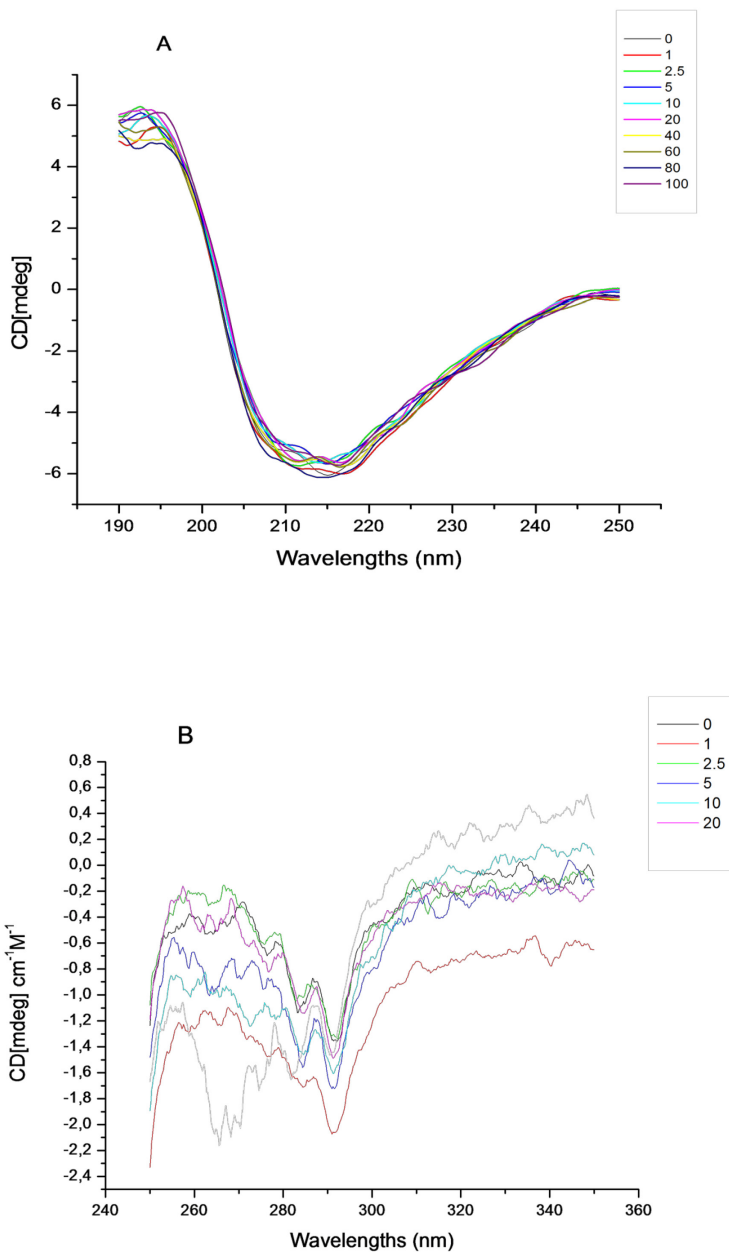


**Figure 3.1. (A) Far-UV, (B) near-UV circular dichroic spectra of  $\beta$ Ig in the absence and presence of increasing concentration of riboflavin in 10 mM phosphate buffer at pH 7.4. The concentrations of  $\beta$ Ig are 10  $\mu$ M for the far-UV region and 20  $\mu$ M for the near-UV region. The concentrations of RF vary from 0 to 100  $\mu$ M for the Far-UV and 0 to 40  $\mu$ M for the near-UV spectra.**

On the other hand, the near-UV CD arising from the environment of each aromatic amino acid side chain and probably disulfide bonds, showed very minor perturbations (panels B). The peaks at 286 and 293 nm, a signature of tryptophan residues in  $\beta$ lg in its native conformation, remained similar at concentrations of RF below 40  $\mu$ M (Figure 3.1B). Therefore, this finding suggests that RF at concentrations below 40  $\mu$ M did not significantly modify the tertiary structure of  $\beta$ lg. References related to the far and near UV CD of flavins including RF are scarce. A study conducted in the late 1960s on the far- and near-UV CD signal of RF indicated that since the chromophoric group in the flavins (i.e. the isoalloxazine ring) is optically inactive, environmental perturbations may be responsible for any CD signal arising from theoretically active ribityl side chains [165]. Therefore, in the current study, the dramatic alteration of the CD signals at higher RF concentrations (data not shown) may be indicative of important modifications to the environment of the ribityl side chain of RF. Consequently, the isoalloxazine ring may be involved in the interaction with  $\beta$ lg at the binding site, modifying the environment of the ribityl side chain of RF. An excess of RF leads to the saturation of the apo-protein and CD signals. This may allow the determination of the concentration of both the apo and holoprotein, especially when combined with other spectroscopic methods such as fluorescence measurement as it was demonstrated with the RF-binding protein [166].

#### **3.4.2. Influence of RF on fluorescence spectra of $\beta$ lg**

The fluorescence spectra of 5 and 10  $\mu$ M  $\beta$ lg with varying concentrations of RF up to 20  $\mu$ M are shown in Figure 3.2A and B, respectively.

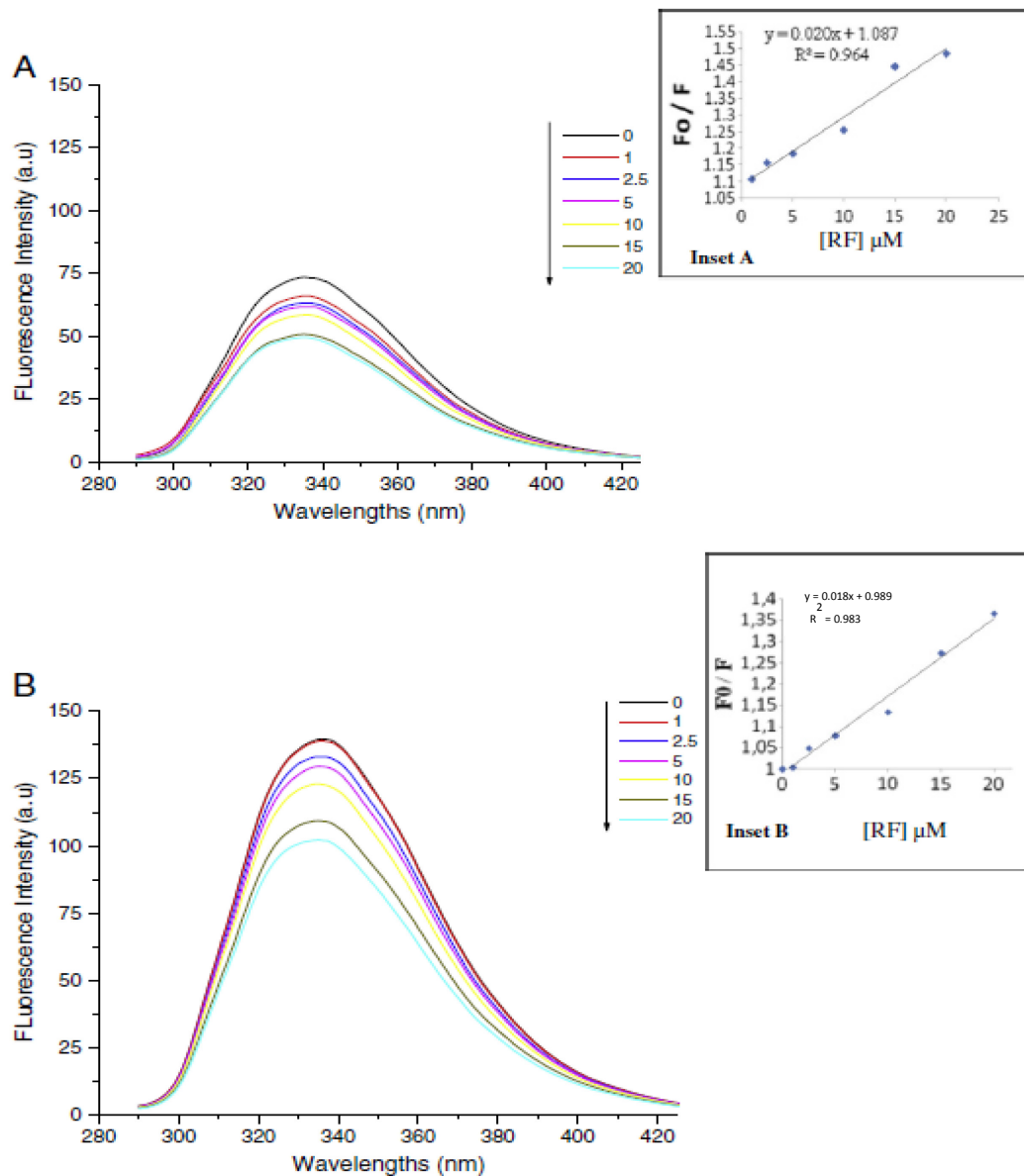


**Figure 3.2.** Fluorescence emission spectra of  $\beta\text{Ig}$  in the presence of different concentrations of RF; (A)  $[\beta\text{Ig}] = 5 \mu\text{M}$ ; (B)  $[\beta\text{Ig}] = 10 \mu\text{M}$ ; [RF] in  $\mu\text{M}$ , curves: 0, 1, 2.5, 5, 10, 15 and 20 ( $\lambda_{\text{EX}} = 280 \text{ nm}$ ,  $T = \text{room temperature}$ ,  $\text{pH} = 7.4$ ). Insets: Stern–Volmer plots for the quenching of  $\beta\text{Ig}$  by RF (A):  $[\beta\text{Ig}] = 5 \mu\text{M}$ ; (B):  $[\beta\text{Ig}] = 10 \mu\text{M}$ .

The fluorescence intensity of  $\beta$ lg at both concentrations decreased with increasing RF concentration whereas the fluorescence of RF was enhanced (data not shown). The red shift (333 to 336 nm) observed for both concentrations of  $\beta$ lg. The maximum emission peak of  $\beta$ lg is typically around 335 nm. This suggests that the chromophoric group is still in a hydrophobic environment, although slightly more hydrophilic relative to native protein [6]. The occurrence of interactions between these two biomolecules can also be supported by the analysis of fluorescence quenching.

### 3.4.3. Analysis of fluorescence quenching mechanism

Collisional or dynamic quenching results from collisions involving both the fluorophore and the quencher during the lifetime of the excited state, while static quenching refers to ground-state fluorophore–quencher complex formation [67]. Dynamic quenching can be estimated using the Stern–Volmer equation and consequently, by computing the Stern–Volmer quenching constant (KSV), which gives the ratio between fluorescence intensities in the presence or absence of a quencher as a function of its concentration, taking into account the fluorophore life time in the quencher's absence. The duration of the static and collisional quenching provided by the KSV allows a differentiation between the two events, the collisional quenching constant of various kinds of quenchers with biopolymer generally being around  $2.0 \times 10^{10} \text{ L mol}^{-1} \text{ s}^{-1}$  [69]. It is possible to distinguish between the static and dynamic quenching mechanisms by measuring their duration. However, assuming that there is a formation of a non-fluorescent complex between RF and  $\beta$ lg, the Stern–Volmer formula (Equation 3.1) can be applied [67] :

$$F_0/F = 1 + K_q T_0 [\text{RF}] = 1 + K_{sv} [\text{RF}]$$

where,  $F$  and  $F_0$  are the fluorescence intensities of  $\beta$ lg with and without RF, respectively,  $K_q$  is the fluorescence quenching rate constant of the protein,  $K_{SV}$  is the Stern–Volmer quenching constant,  $\tau_0$  is the average fluorophore lifetime without quencher and  $[RF]$  is the concentration of quencher. The fluorescence lifetime of the Trp residues of  $\beta$ lg is  $1.28 \times 10^{-9}$  s at neutral pH [6].

The plots of  $F_0/F$  versus  $[RF]$  (intercept = 1, slope =  $K_{SV}$ ) are displayed in inset A ( $\beta$ lg 5  $\mu$ M) and B ( $\beta$ lg 10  $\mu$ M) of Figure 3.2. The linear correlation coefficient shows a good linear relationship and thus the fluorescence quenching rate constant can be inferred easily from the Stern–Volmer quenching constant. The values for  $K_q$  were  $1.43 \times 10^{13} \text{ M}^{-1} \text{ s}^{-1}$  and  $1.62 \times 10^{13} \text{ M}^{-1} \text{ s}^{-1}$  for  $\beta$ lg 10 and 5  $\mu$ M, respectively (Table 3.1). This finding implies that dynamic quenching plays a minor role compared to static quenching. In order to confirm this result, Stern–Volmer plots of the quenching of  $\beta$ lg by RF at different temperatures (35, 45 and 55 °C) were determined (Table 3.1). It is well recognized that elevated temperature results in larger diffusion coefficients, hence the dynamic quenching rate constant should increase with increasing temperature [6]. In the present study, the slope of the Stern–Volmer plots and the  $K_{SV}$  remained fairly similar with increase in temperature (Table 3.1), confirming that the interaction between RF and  $\beta$ lg results in the formation of a  $\beta$ lg–RF ground state complex.

**Table 3.1. Stern–Volmer quenching constants  $K_{SV}$  and dynamic quenching rate constant at different temperatures, as per Equation 3.1**

$\beta I_0$ ( $\mu\text{M}$ )	Temperature ( $^{\circ}\text{C}$ )	Stern-Volmer Equation	Correlation coefficient	$K_{SV}$ ( $10^{-3} \text{ L x mol}^{-1}$ )	$K_q$ ( $10^{12} \text{ L x mol}^{-1} \text{ x s}^{-1}$ )
5	20	$Y = 1.087 + 0.020 X$	0.964	20	16.2
	35	$Y = 1.161 + 0.023X$	0.998	23	18.1
	45	$Y = 1.139 + 0.024X$	0.997	24	19.2
	55	$Y = 1.118 + 0.022X$	0.995	22	18.0
10	20	$Y = 0.989 + 0.018 X$	0.983	18	10.4
	35	$Y = 1.034 + 0.022 X$	0.968	22	17.5
	45	$Y = 1.029 + 0.022 X$	0.978	22	17.6
	55	$Y = 1.017 + 0.021 X$	0.986	21	17.3

In the case of bovine serum albumin (BSA), both static and dynamic quenching mechanisms were implicated in the quenching of BSA fluorescence by RF [67]. In order to obtain further proof of the formation of a ground-state complex between RF and  $\beta$ lg, a study of the occurrence of an energy transfer between these two molecules was carried out.

#### 3.4.4. Fluorescence resonance energy transfer from $\beta$ lg to RF

Fluorescence resonance energy transfer (FRET) can be used to determine the efficiency of energy transfer and to estimate the distance between donor tryptophan residues on  $\beta$ lg and the acting acceptor RF, following Equation 3.2 [69]:

$$E = 1 - \frac{F}{F_0} = \frac{R_0^6}{R_0^6 + r^6}$$

Where, E is the efficiency of energy transfer between the donor and the acceptor,  $R_0$  is the Förster distance (in Å) representing the distance at which resonance energy transfer is 50 % efficient (ranging typically from 2 to 9 nm for biological macromolecules), and r is the distance between the donor ( $\beta$ lg) and the acceptor (RF).  $R_0^6$  ( $\text{cm}^6$ ) is given by Equation 3.3 [70]:

$$R_0^6 = 8.79 \times 10^{-25} (K^2 n^{-4} \phi J), \text{ thus } R_0 = 9.78 \times 10^3 (K^2 n^{-4} \phi J)^{1/6}$$

Where,  $K^2$  ( $K^2 = 2/3$ ) is a factor describing the relative orientation in space of the transition dipoles of the donor and acceptor (n), the refractive index of the solution which is typically assumed to be 1.33 for biomolecules in aqueous solution ( $\phi$ ), is the fluorescence quantum yield of the donor ( $\beta$ lg), and (J) is the spectral overlap integral between the fluorescence emission spectrum of the donor and the

absorption spectrum of the acceptor.  $J$  ( $M^{-1} \text{ cm}^{-3}$ ) can be calculated by using Equation 3.4 [69, 70] :

$$J = \int_0^{\infty} F(\lambda) \varepsilon(\lambda) \lambda^4 d\lambda$$

Where  $F(\lambda)$  is the corrected fluorescence intensity of the donor ( $\beta\text{lg}$ ) in the wavelength range from  $\lambda$ ,  $\varepsilon(\lambda)$  is the molar absorption coefficient of the acceptor (RF) at wavelength  $\lambda$ ,  $n = 1.36$ , and  $\varphi = 2.52$  [70]. However, in the present work, it was assumed that the inner filter effect due to the absorbance of RF has a minor effect on the quenching mechanism.

The efficiency of energy transfer ( $E$ ) is described as the fraction of photons absorbed by the donor which are transferred to the acceptor [70, 167]. This efficiency increases when the transfer rate is much faster than the decay rate and is greatly influenced by the distance between the donor and the acceptor ( $r$ ) in the vicinity of the Fröster distance ( $R_0$ ), as can be seen in Equation 3.2. From Equations 3.2, 3.3 and 3.4,  $J$  values were computed and presented in Table 3.1, along with  $E$ ,  $R_0$ , and  $r$  values for both  $\beta\text{lg}$  concentrations (5 and 10  $\mu\text{M}$ ). There is a clear influence of the protein concentration and ratio of RF to  $\beta\text{lg}$  on the calculated parameters (Table 3.2).

**Table 3.2. Energy efficiency transfer ( $E$ ) and distance between the donor  $\beta\text{lg}$  and the acceptor RF ( $r$ ), as per Equation (3)**

$\beta\text{lg}$ ( $\mu\text{M}$ )	Ratio RF / $\beta\text{lg}$	$E$	$J$ ( $10^{-18} \text{ M}^{-1} \text{ cm}^{-3}$ )	$R_0$ (nm)	$r$ (nm)
<b>5</b>	0.1	0.126	3.72	1.098	1.495
	0.2	0.147	3.63	1.093	1.444
	0.4	0.178	3.50	1.086	1.382
	1	0.251	3.19	1.070	1.265
	1.5	0.339	2.82	1.048	1.154
	2	0.381	2.64	1.036	1.108
<b>10</b>	0.1	0.0087	7.99	1.246	2.706
	0.2	0.058	7.58	1.236	1.936
	0.4	0.086	7.36	1.230	1.797
	1	0.146	6.88	1.216	1.608
	1.5	0.250	6.05	1.190	1.410
	2	0.323	5.45	1.169	1.304

The  $J$ ,  $R_0$ , and  $r$  values decrease while  $E$  increases along with increasing concentration of RF. Furthermore,  $r$  is in the interval (1 to 10 nm) within which the energy transfer takes place. The binding distance is also between  $0.5 R_0$  and  $1.5 R_0$  (except for the ratio of RF to  $\beta$ lg at 10  $\mu$ M below 0.2, which are less than  $2 R_0$ ), indicating that the energy transfer from RF to  $\beta$ lg is efficient and highly probable, and that the binding distance  $r$  calculations are reliable [70]. The monomer radius is estimated to be around 1.75 nm, which is much larger than the calculated values of  $R_0$  and close to  $r$  in the current study [67, 70]. It is also interesting to note that  $J$  almost doubles with a doubling of the concentration of the protein, indicating an increase in the spectral overlap at the higher protein concentration (Table 3.2). These findings are confirmed with the spectral overlap between the fluorescence emission spectrum of  $\beta$ lg and the absorption spectrum of RF as seen on Figure 3.3.

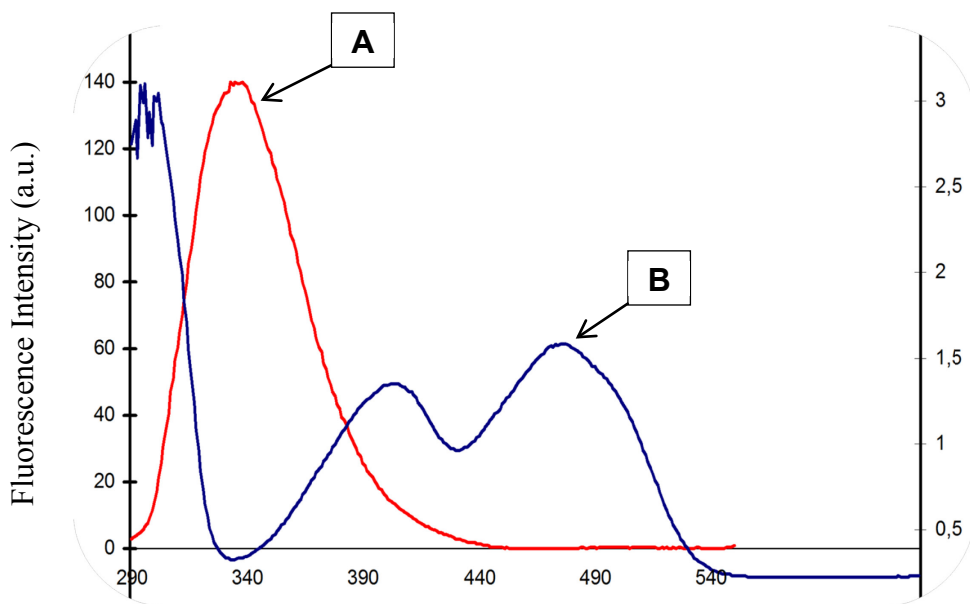


**Figure 3.3. Overlap of the fluorescence emission spectra of  $\beta$ lg (A) with the absorption spectra of RF (B).**

Therefore, it can be concluded that energy transfer occurs between  $\beta$ Ig and RF, as previously observed between RF and albumins [67]. Therefore, there is a formation of a ground state nanocomplex between RF and  $\beta$ Ig. This result hence allows the calculation of parameters such as the binding constant and binding points of the vitamin to the protein.

#### 3.4.5. Binding constants and binding points of RF to $\beta$ Ig

As shown on Figure 3.2, the complexation of RF to  $\beta$ Ig leads to modification in the fluorescence properties of the protein. Furthermore, it was demonstrated that static quenching was the dominant mechanism involved in this interaction. Therefore, it is possible to determine the binding constant for a non-fluorescent complex [69]. The binding constant ( $K_S$ ) and the binding number ( $n$ ) can be computed using the formula (Equation 3.5) derived from the equilibrium between free and bound molecules, when ligands bind independently to a set of equivalent sites on a larger biomolecule [68] :

$$\log\left(\frac{F_0 - F}{F}\right) = \log K_S + n \log[RF]$$

Where,  $K_S$  is the binding constant to a site and  $n$  is the number of binding sites per  $\beta$ Ig molecule. The binding parameters can be obtained by plotting  $\log[(F_0 - F) / F]$  against  $\log[RF]$ . The slope and the intercept of the straight line allow calculation of  $n$  and the binding constant  $K_S$ , respectively [6, 67]. The values of the  $K_S$  and  $n$  computed from the plot of  $\log[(F_0 - F) / F]$  against  $\log[RF]$  were  $1.0 \times 10^2 \text{ M}^{-1}$ ;  $n = 0.5$  and  $K_S = 1.7 \times 10^6 \text{ M}^{-1}$  and  $n = 1.4$ , for  $\beta$ Ig 5 and 10  $\mu\text{M}$ , respectively (Table 3.3).

**Table 3.3: Binding constant and binding number for static quenching of native and pre-denatured  $\beta$ Ig by RF, at different temperatures and at neutral pH (7.4) as per Equation 3.5**

$\beta$ Ig	Concentration ( $\mu$ M)	Temperature ( $^{\circ}$ C)	Equation (2)	Correlation coefficient	$K_s$ ( $M^{-1}$ )	Binding number ( $n$ )
Native	5	20	$Y = 2.02 + 0.506 X$	0.936	$1.0 \times 10^2$	0.5
		35	$Y = 1.61 + 0.398 X$	0.927	$4.1 \times 10$	0.4
		45	$Y = 1.94 + 0.466 X$	0.974	$9.0 \times 10$	0.4
		55	$Y = 1.851 + 0.457 X$	0.931	$7.1 \times 10$	0.4
	10	20	$Y = 6.22 + 1.403 X$	0.927	$1.7 \times 10^6$	1.4
		35	$Y = 2.873 + 0.685 X$	0.962	$7.5 \times 10^2$	0.7
		45	$Y = 2.735 + 0.660 X$	0.969	$5.4 \times 10^2$	0.7
		55	$Y = 3.010 + 0.726 X$	0.976	$1.0 \times 10^4$	0.7
Pre-denatured	5	20	$Y = 3.87 + 0.910 X$	0.987	$7.4 \times 10^4$	1.0
	10	20	$Y = 6.66 + 1.477 X$	0.962	$4.4 \times 10^6$	1.5

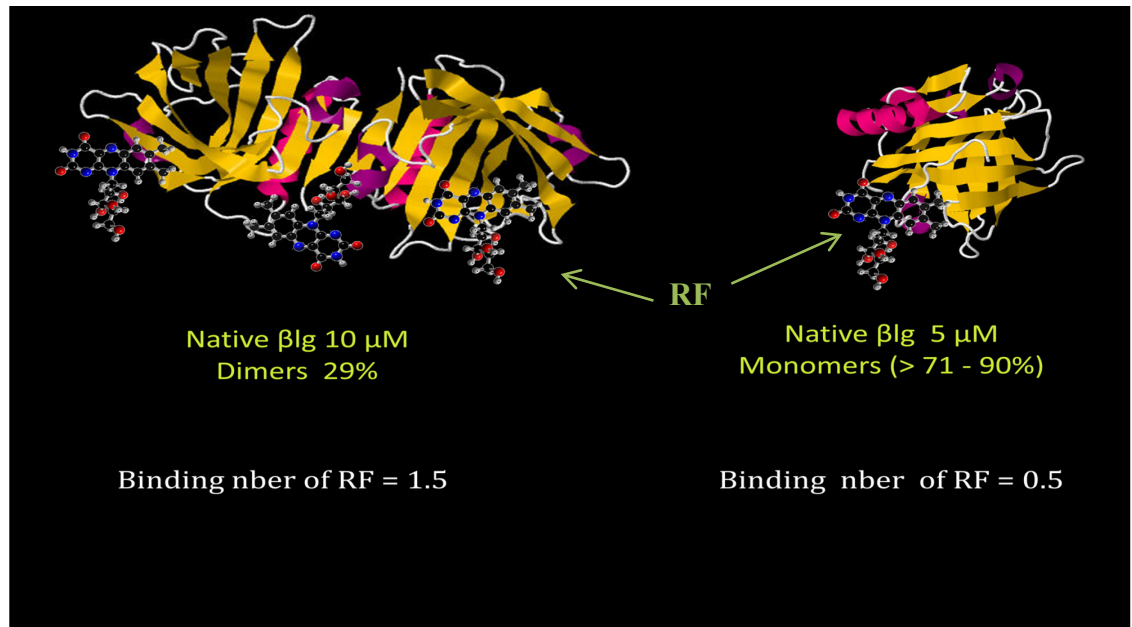
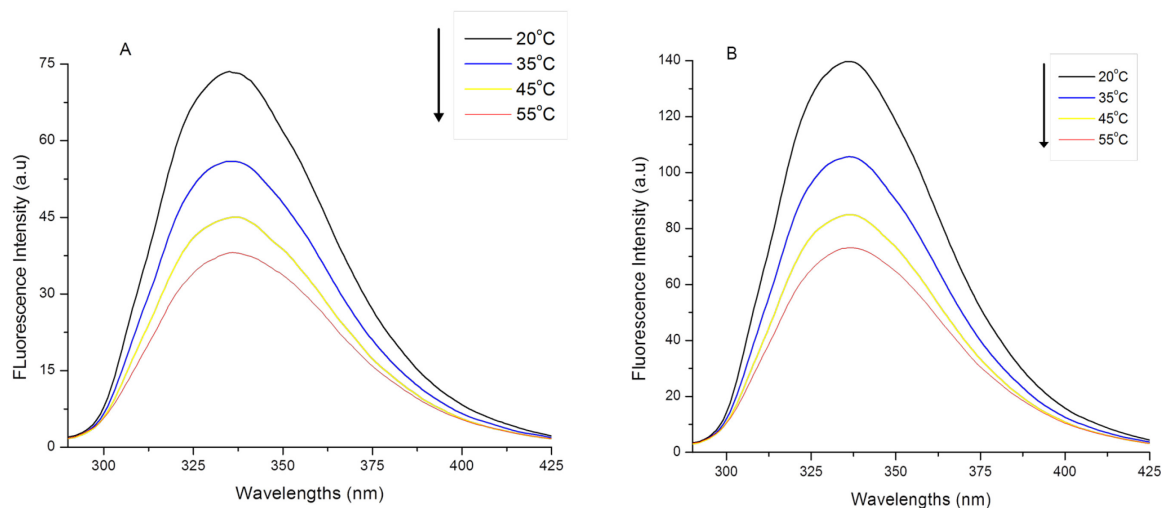


Figure 3.4 is a 3D diagram representing both dimeric and monomeric βlg (PDB ID 3BGL) with the suggested binding sites for RF [60].

Interestingly, both  $K_S$  and  $n$  increased with the increasing concentration of  $\beta$ Ig. It has been suggested that  $\beta$ Ig exists as a mixture of monomers and dimers at neutral pH and the proportion of dimer is 29 % when the protein concentration is 10  $\mu$ M [6]. At 5  $\mu$ M, this proportion could be expected to be even lower. The formation of a dimer by hydrophobic interactions at the monomer contact site eliminates the ligand binding site on the monomer but forms a higher-affinity pocket for binding to the dimer [6]. While the reduction of the binding constant from  $K_S = 1.7 \times 10^6 \text{ M}^{-1}$  to  $K_S = 1.0 \times 10^2 \text{ M}^{-1}$  is consistent with the literature, the decrease in binding number is unexplained.

Evidence suggests that when heating to 56 °C the heat- modifications are reversible and no obvious modification of the behavior of  $\beta$ Ig is observed in aqueous solutions [168]. In the present study, heating did not exceed 55 °C, well below the protein unfolding temperature, but sufficient for dimer dissociation. The intrinsic fluorescence of Trp amino acid residues was monitored to provide information about the slope and intercept as per Equation 3.5.

The binding constants derived from the  $\beta$ Ig–RF interaction at neutral pH and at different temperatures (room temperature, 35, 45 and 55 °C) were consistent with the shift of the protein dimer–monomer equilibrium (Table 3.3). In fact, the binding constants were lower than that of the protein at room temperature and were of similar magnitude, except for 10  $\mu$ M  $\beta$ Ig at 55 °C, which had a binding constant which was two-fold higher ( $1.02 \times 10^4 \text{ M}^{-1}$ ). The higher binding constant was probably due to the beginning of aggregate formation as confirmed by the self-quenching of the intrinsic fluorescence of  $\beta$ Ig with increasing temperature (Figure 3.5A and B).



**Figure 3.5.** The evolution of fluorescence intensity of  $\beta$ Ig alone as a function of temperature (20, 35, 45 and 55 °C). (A)  $[\beta$ Ig] = 5  $\mu$ M, (B)  $[\beta$ Ig] = 10  $\mu$ M; phosphate buffer 10 Mm at pH 7.4. Excitation at 280 nm.

A red shift was also observed for both concentrations of  $\beta$ lg. Therefore, it can be argued that structural modification during the early stages of thermal denaturation, the so-called molten globule state may occur earlier than indicated in the literature, at temperatures above 70 °C [169]. This stable monomeric intermediate exhibits substantial secondary structure but lacks the rigidity of the tertiary structure. Furthermore, as presented in Table 3.3,  $\beta$ lg monomers in the native state have only a partial binding site for RF, that is, the hydrophobic cavity. Since the molten globule state is also a monomer, it was not surprising to observe that the binding number, for  $\beta$ lg at 5  $\mu$ M decreased with increasing temperature (Table 3.3). The results of this study are consistent with the findings of previous reports, as such, a greater flexibility of the calyx entrance, which promotes easier binding of small ligands to the central cavity after thermal treatment [162, 170]. The higher binding constant at 55 °C can further be explained by the fact that the molten globule has a less tightly packed tertiary structure which probably affects the value of ligand binding constants. Upon progressive heating, the surface hydrophobicity slowly decreases, which is translated into the dissociation of the dimer [170]. This may be the reason for the greater binding constant and binding number of  $\beta$ lg to RF at room temperature than at temperatures up to 45 °C.

When the calyx of native  $\beta$ lg was disrupted by manipulation with heat treatment, the binding constant and binding number of vitamin D<sub>3</sub> were changed, demonstrating that there was a secondary binding site for the vitamin on the native protein [171]. Table 3.3 shows the results obtained when the protein was heat-unfolded compared to its native conformation. The binding constant ( $1.7 \pm 1.4 \times 10^6$  and  $4.4 \pm 1.4 \times 10^6$ ) and binding number (1.4 and 1.5) for both the native and unfolded protein at a concentration of 10  $\mu$ M were very comparable. This suggests that unfolding of the calyx did not change the binding parameters of RF to 10  $\mu$ M  $\beta$ lg, and that there is one binding site plus another partial binding site of RF to  $\beta$ lg. These binding sites may correspond to the hydrophobic areas of the protein: near the central calyx and at the monomer contact site [46].

In the case of 5  $\mu\text{M}$   $\beta\text{lg}$ , the binding number increased from 0.5 to 1, with concomitant formation of a more stable 1:1 RF- $\beta\text{lg}$  complex accompanied by a significant increase in the binding constant (Table 3.3). Additionally, evidence strongly suggests that RF can penetrate and bind to hydrophobic contacts of the chromophore within serum and the interior of human albumin, resulting in changes in the geometric structure of the proteins [172]. These reported findings are consistent with the later results and with the data obtained from the CD analysis. Most importantly, the binding of RF to riboflavin binding protein in a 1:1 complex yields a binding constant estimated to be  $10^7 \text{ M}^{-1}$  [67]. Although the riboflavin binding protein does not belong to the lipocalin family, a parallel can be made between the binding constants for both the RF-binding protein and RF/ $\beta\text{lg}$  complex, which in the current study, was  $1.7 \times 10^6$  for the native state of  $\beta\text{lg}$  (10  $\mu\text{M}$ ) [173]. This result suggests that RF may be bound at the entrance of the central cavity of the dimeric form of native  $\beta\text{lg}$ , forming a complex of nanometer size.

Conversely, at lower native protein concentration, where monomers predominate in solution, the hydrophobic pocket formed by the hydrophobic interactions at the monomer contact site no longer exists, explaining the fact that the central calyx constitutes the binding site of the isoalloxazine ring of RF to  $\beta\text{lg}$ . This finding indicates that hydrophobic interactions may not be the only type of interaction involved in the binding of RF to  $\beta\text{lg}$ . The ribityl side chain, encompassing four hydroxyl groups, may also contribute to hydrogen bond formation with  $\beta\text{lg}$ , since these interactions are also implicated in dimer stability [174]. Electrostatic interactions could be ruled out since at neutral pH, RF does not carry any charge.

### **3.4.6. Influence of RF on the synchronous fluorescence of $\beta$ lg**

Synchronous fluorescence is a scan that provides important information about the molecular environment in the vicinity of fluorophores tyrosine and Trp, using wavelengths at intervals  $\Delta\lambda = 15$  nm (Figure 3.6, panels A and C) and  $\Delta\lambda = 60$  nm (Figure 3.6, panels B and D), respectively [171].

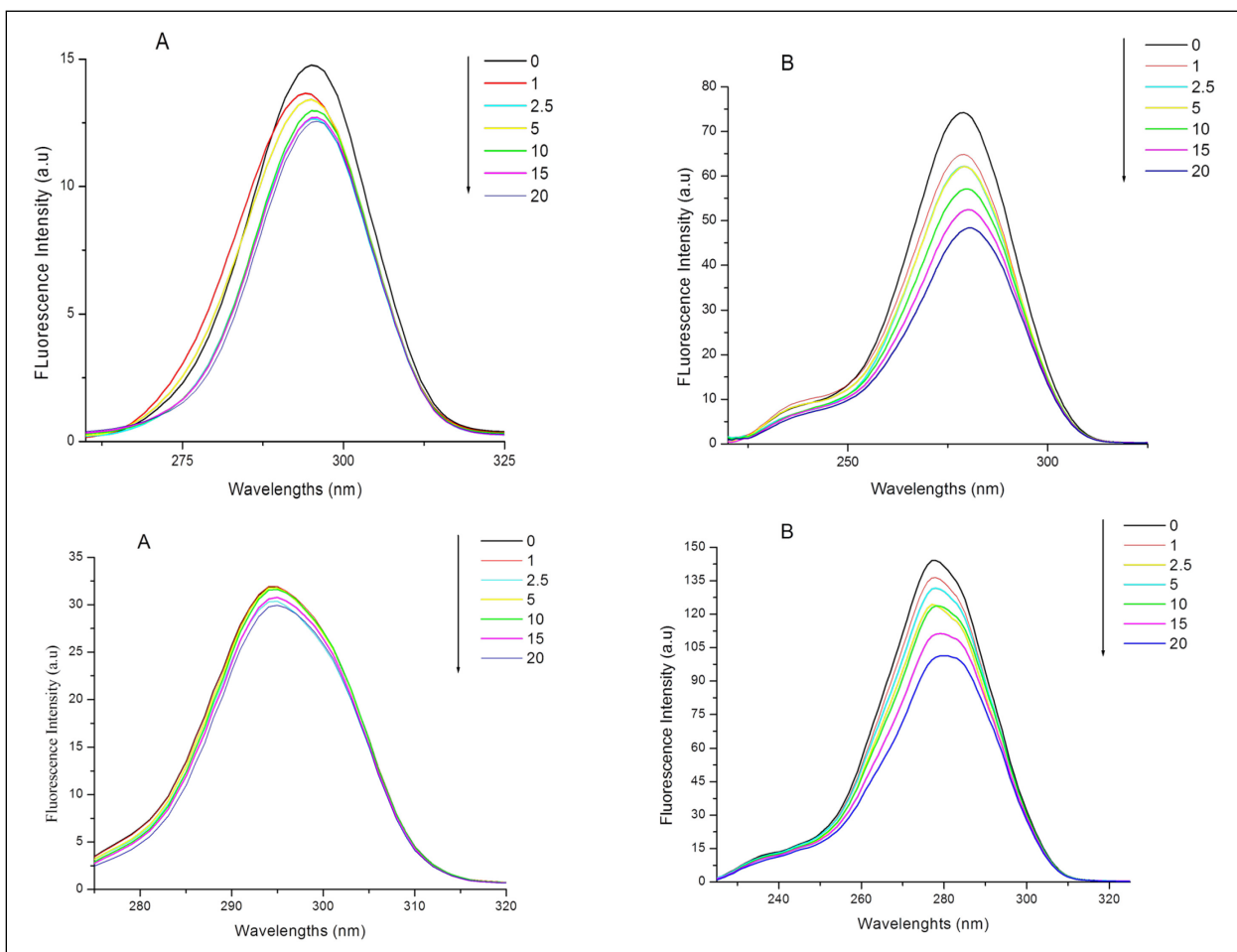


**Figure 3.6. The synchronous fluorescence spectra of  $\beta$ Ig at 5 (A and B) and 10  $\mu$ M(C and D). On panels A and C,  $\Delta\lambda = 15$  nm; on panels B and D,  $\Delta\lambda = 60$  nm in the presence of [RF] = 0, 1, 2.5, 5, 10, 15 and 20  $\mu$ M. Solvent: phosphate buffer 10 mM at pH 7.4. Fluorescence scans were carried out from 200 to 400 nm.**

The results obtained from synchronous fluorescence indicate that the addition of RF resulted in the slight quenching of tyrosine residues but did not yield any shift in the fluorescence maximum intensity, whereas the interaction between RF and Trp residues results in a conformation modification demonstrated by the presence of a red shift (Figure 3.6). These results reveal that upon binding of RF to  $\beta$ Ig, the hydrophobic cavity opens slightly, rendering a more hydrophilic environment for the buried Trp residues. Furthermore, Figure 3.6 shows that the fluorescence of both tyrosine and Trp residues is quenched by the increasing concentrations of RF, but the quenching effect is more significant with Trp residues (Figure 3.6, panels B and D). This result implies that RF is located in the vicinity of tryptophan residues [69]. The binding of RF close to Trp residues has important implications. There is strong evidence that upon UV or visible light irradiation, RF enters an excited state and initiates a photo-activation process which may lead to the degradation of proteins or other bio-macromolecules [69]. Indeed, reports in the literature suggest that the RF triplet excited state ( $^3\text{RF}^*$ ) is generated by near-UV wavelengths. This indicates that at 280 nm, which corresponds to the  $\beta$ Ig excitation wavelength,  $^3\text{RF}^*$  can be formed by energy or electron transfer from the Trp side chains of the  $\beta$ Ig molecule, thus producing protein and RF radicals and subsequent generation of reactive oxygen species. These reactive oxygen species, including singlet state oxygen, can later attack other biological targets and trigger cascading oxidative reactions, leading to cell death [99]. Therefore, it can be hypothesized that protein degradation induced by the photo-activation of RF could be used in photodynamic therapy, to treat tumor and cancer tissues in accessible regions, as previously shown for methylene blue [95, 97, 161]. In order to verify this hypothesis, an anti-proliferative activity assay of the  $\beta$ Ig/RF nanocomplex was conducted.

#### **3.4.7. Anti-proliferative activity assay the $\beta$ Ig/RF nanocomplex**

Since the early 1980s, the toxic effect produced in biological systems directly irradiated in the presence of RF has been described [175]. Currently, the use of RF

in photodynamic therapy (PDT) is well described and the term 'ribo-phototherapy' was even suggested by Sato et al. [95]. There is an ample evidence for the effectiveness of light-activated RF in the inactivation of pathogenic bacteria, and in the treatment of malignant and non-cancerous tissues [11, 12]. Dougherty and collaborators have detailed the mechanism of action of PDT, the subcellular and tumor localization of photosensitizers, and the cellular responses of tumor tissues, and attempted to explain the underlying molecular mechanism of RF in PDT [155].

In the present study, the occurrence of efficient energy transfer between RF and  $\beta$ Ig was demonstrated and its biological implication was assessed by evaluating the anti-proliferative activity of the  $\beta$ Ig/RF nanocomplex on human M21 skin melanoma cell lines, which represents one of the primary embryonic germ layers [99]. The standard procedure from the NCI/NIH Development Therapeutics Program was used to determine cell growth inhibition and cytotoxicity [163]. Negative numbers represent the growth inhibition while the positive numbers that of the inhibitory concentration where cytotoxicity begins (Figure 3.7).

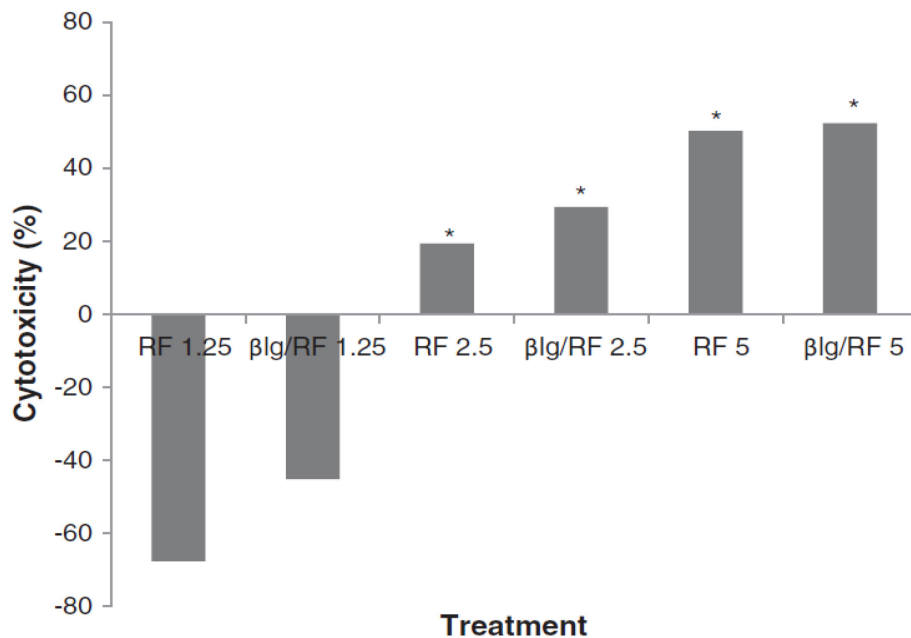


**Figure 3.7. Cytotoxicity RF containing solutions on skin melanoma M21 cell lines irradiated in the absence and presence of  $\beta$ lg (25 min at 365 nm). The treatment consisted in the  $\beta$ lg/RF complex and RF solutions, each at a final concentration of 5, 2.5 and 1.25  $\mu$ M. Growth inhibition and cytotoxicity were evaluated after an incubation period of 48 h for recovery.**

Cell culture and culture media, supplemented with RF,  $\beta$ lg and the  $\beta$ lg/RF nanocomplex were irradiated for 25 min at 365 nm within the UV-A light range. Figure 3.7 represents the relative cell cytotoxicity of the cancer cell lines after irradiation. Control cells incubated with PBS was not affected by irradiation, and neither were the cells supplemented with  $\beta$ lg alone (data not shown). All RF-containing treatments exhibited significant anti-proliferative activity on skin melanoma cells in the micromolar range ( $p < 0.001$ ). There was a significant effect of the  $\beta$ lg/RF nanocomplex and of RF alone at 5 and 2.5  $\mu$ M compared to the same treatment at 1.25  $\mu$ M ( $p < 0.001$ ). The latter concentration inhibited cell growth, with the  $\beta$ lg/RF nanocomplex (almost 46.1 %) providing a higher growth inhibition rate compared to RF alone (68.5 %), but the difference was not significant. The cytotoxicity effect of RF-containing solutions started at 5 and 2.5  $\mu$ M and was comparable for both concentrations, with that of the  $\beta$ lg/RF nanocomplex (Figure 3.7). The values of relative toxicity were 29.4 % and 19.5 % for the  $\beta$ lg/RF nanocomplex and RF alone at 2.5  $\mu$ M, respectively, but were 52.3 % and 50.2 % for the  $\beta$ lg/RF nanocomplex and RF alone at 5  $\mu$ M, respectively. Hence, the concentration for the inhibition of cell growth may be close to 5  $\mu$ M which is presented on Figure 3.7. Furthermore, it is important to note that the formation of the nanocomplex did not affect the biological activity of RF.

The study has clearly demonstrates that the  $\beta$ lg/RF nanocomplex photodynamic damage to the melanoma cell lines. This is probably due to the fact that the protein encompasses all major chromophoric amino acids that are capable of photooxidative damage through type I and type II pathways with the generation of  $^1\text{O}_2$  by the transfer of energy from the protein to the ground state molecular oxygen [164]. This is supported by the findings of Figure 3.8, where RP-HPLC results including irradiated and not irradiated  $\beta$ lg (Figure 3.8A and B), irradiated and not irradiated RF (Figure 3.8C and D), and irradiated and not irradiated  $\beta$ lg/RF nanocomplex (Figure 3.8E and F) are presented.

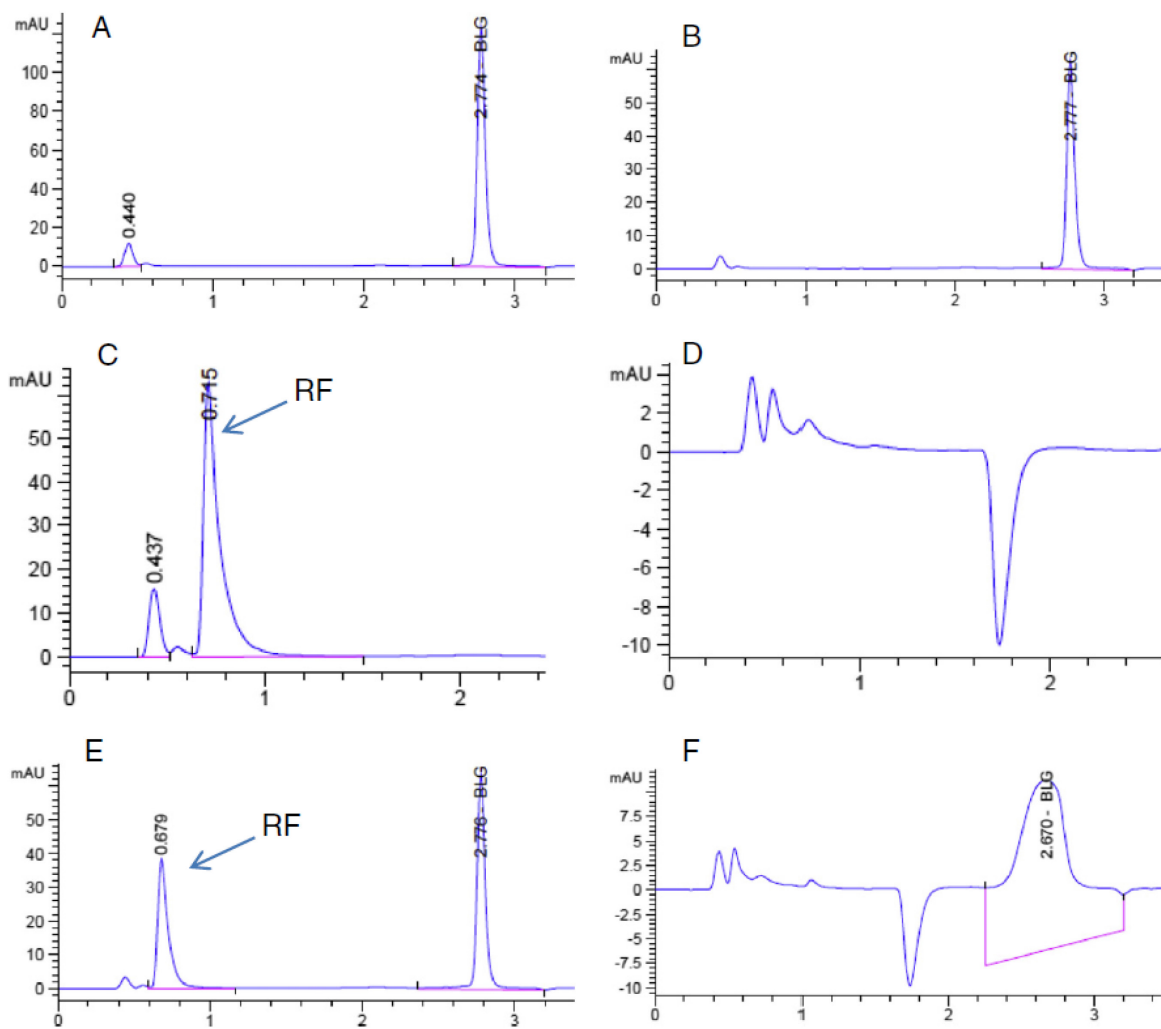


**Figure 3.8. Effect of irradiation of the  $\beta$ Ig/RF complex,  $\beta$ Ig and RF solutions during 25 min at 365 nm (4 W);  $\beta$ Ig (20  $\mu$ M): not irradiated (A) and irradiated (B); RF (20  $\mu$ M): not irradiated (C) and irradiated (D);  $\beta$ Ig/RF (20  $\mu$ M): not irradiated (E) and irradiated (F).**

After irradiation, RF is completely destroyed while  $\beta$ Ig is degraded and its concentration reduced by half, although the degradation products cannot be perceived on the RP-HPLC graph. In fact, the current study has demonstrated that RF binds  $\beta$ Ig in the vicinity of the tryptophan amino acid. Most importantly, Silva et al. showed that aggregate forms of RF, indolic products associated with flavins and those with molecular weights greater than that of tryptophan, formylkynurenine, and other tryptophan photodecomposition products were generated after photodegradation of tryptophan in oxygen-saturated aqueous solution sensitized by RF [11]. Furthermore, Davies suggested that the singlet oxygen-mediated damage to tryptophan can generate numerous degradation products, including N-formylkynurenine and kynurenine, which are better photosensitizers than tryptophan and therefore produce cascade formation of  $^1\text{O}_2$  resulting in greater damage [99]. Therefore, the degradation of the  $\beta$ Ig/RF nanocomplex after irradiation could generate a cumulative damaging effect on targeted cells.

#### **3.4.8. Light stability of the $\beta$ Ig/RF nanocomplex**

The light stability of the  $\beta$ Ig/RF nanocomplex was evaluated by carrying out a degradation study over two weeks. The nanocomplex was exposed to light and samples were withdrawn to assess the content of RF for two weeks. The influence of light on the UV-vis spectra of RF and the  $\beta$ Ig/RF nanocomplex is presented on Figure 3.9.

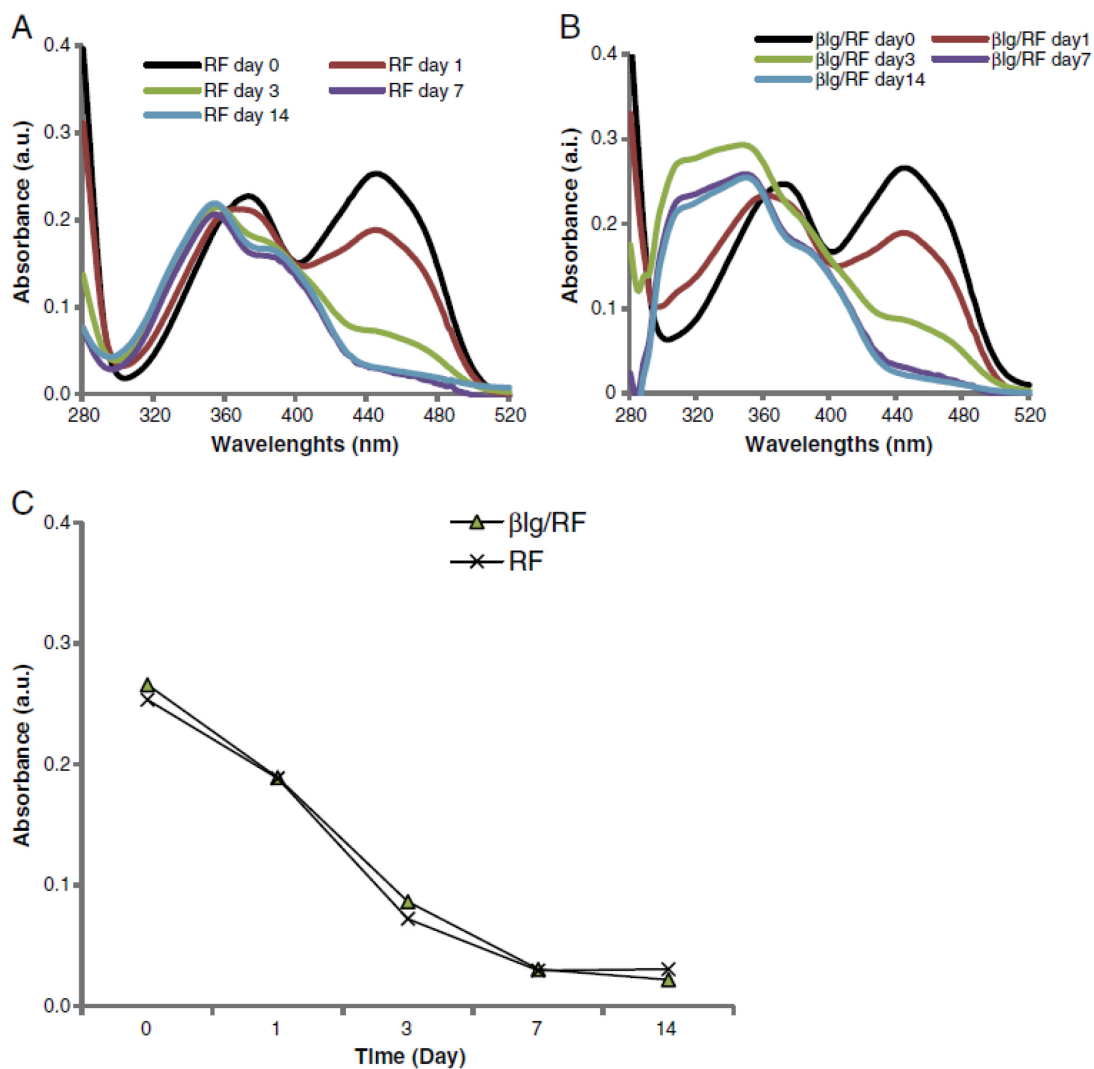


**Figure 3.9. Influence of light on the stability of the  $\beta$ Ig/RF nanocomplex for a two week period. UV-vis spectra of RF (A) compared to that of the  $\beta$ Ig/RF nanocomplex (B). C represents the impact of exposure to light on the concentration RF alone and the  $\beta$ Ig/RF nanocomplex. UV-vis spectra and concentrations were determined at 445 nm.**

The UV–vis spectra of RF (Figure 3.9A) and  $\beta$ Ig/RF nanocomplex (Figure 3.9B) have similar behavior, with more perturbation on the spectra of the later. Degradation for both RF–containing solutions and subsequent formation of degradation products occurred on day 3 and only those photodegradation products could be detected in the solutions at 445 nm (Figure 3.9C). RF and its degradation products all contribute to the UV–vis spectra at 445 nm, which explains the marked decrease in its concentration. The concentration of RF in the  $\beta$ Ig/RF nanocomplex decreased in similar fashion as RF alone, meaning that the presence of  $\beta$ Ig does not hinder the photoactivation of RF. Moreover, photoactivated RF generates the  $^3\text{RF}^*$  excited state that is known to interact with Trp and other chromophoric amino acids through types I and II mechanisms, most of which are present on  $\beta$ Ig [97, 99].

The identification of the photodegradation products of both RF and  $\beta$ Ig was not the focus of the present study. Photoactivation processes occur upon the irradiation of the  $\beta$ Ig/RF nanocomplex, which may lead to the generation of reactive photodecomposition products and could enhance photoactivation processes and most importantly, overcome side effects associated with classic photodynamic therapy [11, 99].

### **3.5. Conclusion**

This study reports for the first time the binding of RF to  $\beta$ Ig with negligible impact on the structure of the protein, the integrity of which is important for its carrier function. The binding results in the formation of a nanocomplex through static quenching mechanism and allows transfer of efficient energy between  $\beta$ Ig and RF. Upon irradiation, the  $\beta$ Ig/RF nanocomplex exhibited important anti-proliferative activity on skin melanoma cells at a dose within the micromolar range. Consequently,  $\beta$ Ig can play a role as a food grade and biocompatible light activated carrier for RF which photoactivation is not affected by complexation with the protein. This system has potential for both the food industry for sanitation purposes

and for biomedical sciences against tumor cells localized in accessible areas such as the skin.

### **3.6. Acknowledgments**

This study was funded by the Canada Research Chair on Proteins, Biosystems and Functional Foods and the Natural Sciences and Engineering Research Council of Canada (NSERC) through the Vanier Canada Graduate Scholarships (F.D.). The authors would like to thank D. Gagnon (Faculté des Sciences de l'Agriculture et de l'Alimentation, Université Laval, Québec, Q.C.), P. Dubé (Institut de recherche sur les nutraceutiques et les aliments fonctionnels (INAF/STELA), Université Laval, Québec, QC, Canada) and J. Lacroix (Unité des Biotechnologies et de Bioingénierie, Centre de recherche, C.H.U.Q., Hôpital Saint-François d'Assise, Québec, QC, Canada) for their valuable technical assistance.

## **Contextual transition**

The physico-chemical and structural characteristics of vitamin D<sub>3</sub> are different from that of RF. Vitamin D<sub>3</sub> binds differently  $\beta$ -lactoglobulin, and thus shows the versatility of  $\beta$ -lactoglobulin as a carrier. Vitamin D<sub>3</sub> is highly hydrophobic and unstable to light. The scope of the following chapter includes stability studies of the  $\beta$ -lactoglobulin/vitamin D<sub>3</sub> complex at varying pH values, including that prevailing in the gastrointestinal tract. The fat solubility of D<sub>3</sub> being an important issue for the fortification of food products with low fat content, the impact of complexation with  $\beta$ -lactoglobulin on the solubility of vitamin D<sub>3</sub> was determined by HPLC. This chapter addresses the second objective of the thesis.

## CHAPTER 4

### **Effects of gastrointestinal pH conditions on the stability of the $\beta$ -lactoglobulin/vitamin D<sub>3</sub> complex and on the solubility of vitamin D<sub>3</sub>**

A version of this work has been published in Food Research International, Volume 52, Issue 2, July 2013, Pages 515 – 521.

By :

Fatoumata Diarrassouba<sup>a</sup>, Gabriel Remondetto<sup>b</sup>, Li Liang<sup>c</sup>, Ghislain Garrait<sup>d</sup>, Eric Beyssac<sup>d</sup> and Muriel Subirade<sup>a</sup>

<sup>a</sup>Chaire de Recherche du Canada sur les Protéines, les Bio-systèmes et les Aliments Fonctionnels, INAF/STELA, Université Laval, Québec, QC, Canada

<sup>b</sup> Centre de Recherche et Développement, Agropur Coopérative, 4700 Armand Frappier, St-Hubert, QC, Canada J3Z 1G5

<sup>c</sup> State Key Lab of Food Science and Technology, School of Food Science and Technology, Jiangnan University, Wuxi, Jiangsu, China

<sup>d</sup> ERT-CIDAM, Lab Biopharmacie, Faculté de Pharmacie, 28 Place Henri Dunant, 63001 Clermont-Ferrand, France

#### 4.1. Abstract

$\beta$ -Lactoglobulin ( $\beta$ lg) is the major bovine milk protein with important biological and functional properties including a transport role for small hydrophobic ligands. However,  $\beta$ lg is prone to structural changes triggered by modification of its environment such as pH variation. An unfavorable environment during formulation, manufacture or storage of food products or transit in the gastrointestinal tract can have a dramatic impact on the stability of the  $\beta$ lg/ligand complex, resulting in the deterioration of its binding ability and premature release of the ligand. This can impair the biological properties of the ligands and reduce their beneficial effects on health. In the present study, vitamin D<sub>3</sub> (D<sub>3</sub>) was used as a nutraceutical ligand model to study the pH-stability of the  $\beta$ lg/D<sub>3</sub> complex as well as the consequences of the complex formation on the solubility of the vitamin. Fluorescence spectroscopy was used to monitor the stability of the  $\beta$ lg/D<sub>3</sub> complex at pH 1.2, 2.0, 3.0, 5.0, 6.8, 7.0 and 8.0. HPLC was used to evaluate the solubility of D<sub>3</sub> by preparing the  $\beta$ lg/D<sub>3</sub> complex in different ratios using a static concentration of D<sub>3</sub> and increasing concentrations of  $\beta$ lg. The binding of D<sub>3</sub> to  $\beta$ lg was not significantly affected by pH. Furthermore, the data allowed determination of the fractional residual fluorescence representing the fraction of  $\beta$ lg not bound to the ligand, which indicated that the  $\beta$ lg/D<sub>3</sub> complex remained stable at all pH values. Therefore, D<sub>3</sub> might be retained during formulation and storage of food products at different pH values and during passage in the stomach, which has important implications for the food industry. The solubility of D<sub>3</sub> was also significantly increased as a result of binding to  $\beta$ lg, which confirms its role as a carrier to improve the uptake of D<sub>3</sub> and consequently the beneficial effects of D<sub>3</sub> on health.

## 4.2. Introduction

As a member of the lipocalin superfamily, the role of the major bovine milk protein  $\beta$ -lactoglobulin ( $\beta$ lg) as a versatile carrier for small bioactive molecules has long been established [6, 46, 50, 61, 79, 81, 176, 177]. The ligands can bind to four sites on the  $\beta$ lg molecule including the central calyx formed by the  $\beta$ -barrel, the surface hydrophobic pocket in the groove between the  $\alpha$ -helix and the  $\beta$ -barrel, the outer surface near tryptophan (Trp)19–arginine (Arg)124, close to the entrance of the  $\beta$ -barrel, and the monomer–monomer interface of the dimer [6, 50, 79]. Evidence suggests that after binding to  $\beta$ lg, hydrophobic ligands are better protected against oxidative degradation and the solubility of some of them is improved [6, 178]. As such,  $\beta$ lg protects retinol and  $\beta$ -carotene from oxidative degradation [178]. The solubility of resveratrol and  $\alpha$ -tocopherol is improved after binding to  $\beta$ lg, which is advantageous for the fortification of foods with low fat content [6, 50]. However, slight structural alterations could affect the binding capacity of  $\beta$ lg and trigger spontaneous release of the ligand, which can impede the transport function of the protein [50, 79]. Indeed, whereas high temperature leads to the unfolding of the protein, disallowing binding of ligands to the calyx, pH plays an important role in controlling the opening–closing of the EF loop or ‘calyx cap’, thus moderating the entrance and release of ligands that bind inside the central cavity [50, 64, 178]. The EF loop (residues 85–90) folds over the entrance of the calyx to form the closed conformation at pH lower than 6.5 and at pH above 7.0 it adopts the open conformation to expose the interior of the calyx [60].

It has been established that moderate to considerable pH-induced structural transitions of  $\beta$ lg occur between pH 2.0 and 8.0, while above pH 9.0,  $\beta$ lg undergoes significant and irreversible structural modification dubbed base-induced unfolding of the protein [52–54]. Despite significant structural modifications, the overall conformation of the protein is conserved extraordinarily well from pH 2.0 to 8.0 [52]. Uhrínová et al. stated that the closed conformation of the EF loop at acidic pH confirms the physiological role of  $\beta$ lg as a transporter of small molecule ligands

since bound ligands might be protected in the acidic stomach and later be released within the basic small intestine when the EF loop is in the 'open' conformation [52]. On the contrary, Ragona et al. indicated that native  $\beta$ lg cannot be considered as such a carrier through the alimentary tract since fatty acids are released at low pH [87]. On the other hand, Liang and Subirade proved that whereas acidification caused the release of  $\alpha$ -tocopherol bound to the internal cavity, it had no influence on that bound to a site at the surface of  $\beta$ lg [50]. The discrepancies between these different studies can be ascribed to binding studies using dissimilar methods and pH values, the smallest variation of which has important effects on the structure of the protein [79]. Most importantly, the binding capacity of  $\beta$ lg alone is evaluated under various pH conditions rather than the stability of the  $\beta$ lg/ligand complex, which is problematic considering that formation of the  $\beta$ lg/ligand complex is expected to take place before or after incorporation in the intended food matrix or oral administration system [79]. Furthermore, in most cases, studies are conducted using pH values that are not representative of those used during the manufacturing and storage of food products and/or conditions prevailing in the gastrointestinal tract. These issues can lead ultimately to the instability of the  $\beta$ lg/ligand complex, deterioration of the binding ability of the protein, premature release and consequent impairment of biological properties of the ligand, and a reduced beneficial effect on health.

In the current study, vitamin D<sub>3</sub> (D<sub>3</sub>) was used as a nutraceutical ligand model. This hormone-like vitamin has sparked interest, especially after its non-skeletal actions were revealed [179, 180]. Classical actions of D<sub>3</sub> on calcium and phosphorus homeostasis regulation have long been established. Recently, a number of beneficial effects on health have been suggested, including the regulation of both innate and adaptive immune response, effects on the cardiovascular system, lung immunity and respiratory diseases, and protection against bacterial infections, inflammatory bowel diseases, breast and colon cancers, leukemia, tuberculosis, multiple sclerosis, various autoimmune disorders and degenerative diseases [181-186]. Milk, fruit juices, and various food products are enriched with D<sub>3</sub> in high

latitude countries to compensate for the significant decrease of the level of this vitamin, particularly during winter [148, 187]. However, fortification practices seem less effective than supplementation in preventing D<sub>3</sub> deficiency among vulnerable populations when exposure to sun is reduced, making the enhancement of the uptake of D<sub>3</sub> a goal of public health agencies [100]. As such, the U.S. Department of Health and Human Services and the Department of Agriculture encourage individuals within the high-risk groups higher daily intakes of vitamin D of about 25 µg or 1000 IU of vitamin D per day in order to reach and maintain serum 25-hydroxyvitamin D values at 80 nmol/L, which was suggested to be the optimal level of the biomarker [101]. Moreover, the incorporation of fat-soluble vitamins like D<sub>3</sub> is challenging for the food industry. Therefore, increasing the solubility of D<sub>3</sub> would be highly valued considering the ever-increasing demand for healthy food products with low fat content.

Two binding sites for D<sub>3</sub> have been clearly identified on βlg, one within the central calyx formed by the β-strands, the other as an exosite located at the pocket between the α-helix and the β-barrel [79]. Therefore, βlg has been suggested as a good carrier candidate for improved D<sub>3</sub> oral delivery [61, 79]. However these studies were conducted at pH 8.0, where βlg is found in its monomeric form, which does not usually represent the regular pH of food products [61, 79]. Additionally, the impact of pH on the binding capacity of βlg was evaluated whereas the stability of the βlg/vitamin D<sub>3</sub> (βlg/D<sub>3</sub>) complex at different pH values still remains unknown. Therefore, the current study aims at investigating the stability of the βlg/D<sub>3</sub> complex under various pH conditions, including that prevailing in the gastrointestinal track, and the impact of complexation with βlg on the solubility of D<sub>3</sub>.

### **4.3. Materials**

$\beta$ lg (B variant, purity  $\geq$  90 % PAGE) from bovine milk and D<sub>3</sub> (purity  $\geq$  98 %, HPLC) were purchased from Sigma-Aldrich Chemical Company (St. Louis, MO, USA) and used without further purification. Methanol (MeOH, HPLC grade) and Trifluoroacetic Acid (TFA) were purchased from EMD International (Gibbstown, NJ, USA).

#### **4.3.1. Sample preparation**

$\beta$ lg stock solution was made daily by dissolving in Milli-Q water to obtain concentrations of 200  $\mu$ M, measured by spectrophotometer (HP 8453 UV–visible, spectrophotometer, Palo Alto, CA) using a molar extinction coefficient of 17,600 M<sup>-1</sup> cm<sup>-1</sup> at 278 nm [6]. Stock solutions of D<sub>3</sub> concentrated at 100 ppm were prepared daily by dissolving 20 mg of the vitamin in 50 mL of methanol followed by a dilution with Milli-Q water to an initial concentration of 40  $\mu$ M, which represents less than 2 % of methanol after mixing with  $\beta$ lg solutions [188]. The  $\beta$ lg/D<sub>3</sub> complex was prepared by mixing  $\beta$ lg and D<sub>3</sub> solutions in varying proportions (Section 4.3.2) and samples were incubated for about two hours at room temperature prior to analysis. All samples containing D<sub>3</sub> were protected from light by using amber tinted conical tubes.

#### **4.3.2. Influence of the pH on the stability of the $\beta$ lg/D<sub>3</sub> complex**

The effects of pH (1.2, 2.0, 3.0, 5.0, 6.8, 7.0 and 8.0) on the stability of the complex were determined after complex formation. The pH of the  $\beta$ lg/D<sub>3</sub> complex-containing solutions was adjusted by adding either 0.5 M HCl or 0.1 M NaOH. The samples were kept at room temperature and allowed to stabilize for at least 10 min after pH

adjustment before proceeding to fluorescence spectroscopy measurements. All solutions were prepared in triplicate for each pH condition. Steady state fluorescence spectroscopy was used to confirm the binding of D<sub>3</sub> to βlg and to determine the influence of pH on the stability of the complex. Additionally, synchronous fluorescence spectra of βlg were obtained by recording the fluorescence spectra resulting from the difference between the excitation wavelength and the emission wavelength at 60 nm intervals, which corresponds to changes of the polarity around tryptophan residues [101]. A Cary Eclipse fluorescence spectrophotometer (Varian Inc.) was used to measure the intrinsic fluorescence of βlg concentrated at 10 μM after complex formation at a constant ratio of [βlg]/[D<sub>3</sub>] of 1/2 [79]. Emission spectra were recorded from 290 to 550 and from 300 to 550 nm with an excitation wavelength of 280 and 290 nm, respectively [6]. Spectral resolution was 5 nm for both excitation and emission wavelengths. Water and ligand backgrounds were subtracted from the raw spectra.

Since titration experiments have established that D<sub>3</sub> binds strongly to both the central hydrophobic calyx and the exosite of βlg, the fractional residual fluorescence can be used to study the stability of the βlg/D<sub>3</sub> [61, 79, 176]. The fractional residual fluorescence ( $F_{\max}/F_0$ ) was used to determine the fraction of the total protein fluorescence that was not quenched by D<sub>3</sub>, and thus the fraction of βlg not bound to the ligand.  $F$  is the fluorescence intensity of βlg versus wavelength,  $F_{\max}$  is the intensity at the emission maximum ( $\lambda_{\max}$ ), and  $F_0$  is the intensity for βlg at  $\lambda_{\max}$  and is proportional to concentration. Thus a low ratio indicates strong binding of the ligand while a ratio of 1 (100 %) indicates no binding at all [50]. All fluorescence measurements were made in triplicate and the values of  $F_{\max}$  and  $F_0$  were computed from the fluorescence intensity at  $\lambda_{\max}$  for each pH point.

#### **4.3.3. Influence of the $\beta$ lg/D<sub>3</sub> complex formation on the solubility of vitamin D<sub>3</sub>**

The capacity of  $\beta$ lg to influence the solubility of D<sub>3</sub> as a consequence of the formation of the  $\beta$ lg/D<sub>3</sub> complex was investigated by high performance liquid chromatography (HPLC). Different ratios of  $\beta$ lg to D<sub>3</sub> were prepared using D<sub>3</sub> at a static final concentration of 20  $\mu$ M and increasing concentrations of  $\beta$ lg (0, 1.25, 2.5, 5, 10, 20, 30, 60 and 80  $\mu$ M). The mixtures were protected from light and kept at 4 °C overnight. The concentration of D<sub>3</sub> was determined after complex formation by U-HPLC, which was performed on a Phenomenex Kinetex 2.6  $\mu$ m 2.1  $\times$  75 mm C18 column (Torrance, California, USA) using an Agilent 1260 HPLC Series system equipped with a diode Array detector (Agilent Technologies, Palo Alto, CA, USA). The gradient elution was 0–2 min, 20–65 % B; 2–2.25 min, 65–100 % B; 2.25–4.85 min isocratic 100 % B; 4.85–5 min, 100–20% B; 5–8 min isocratic 20 % B. Mobiles phases were A: H<sub>2</sub>O + 0.1 % TFA and B: acetonitrile + 0.1 % TFA (v/v). The mobile phase flow rate was 0.4 mL  $\times$  min<sup>-1</sup>. After separation on the Kinetex column, detection was achieved by setting the detector at 280 nm for the protein and 265 nm for D<sub>3</sub>.

#### **4.3.4. Statistical analysis**

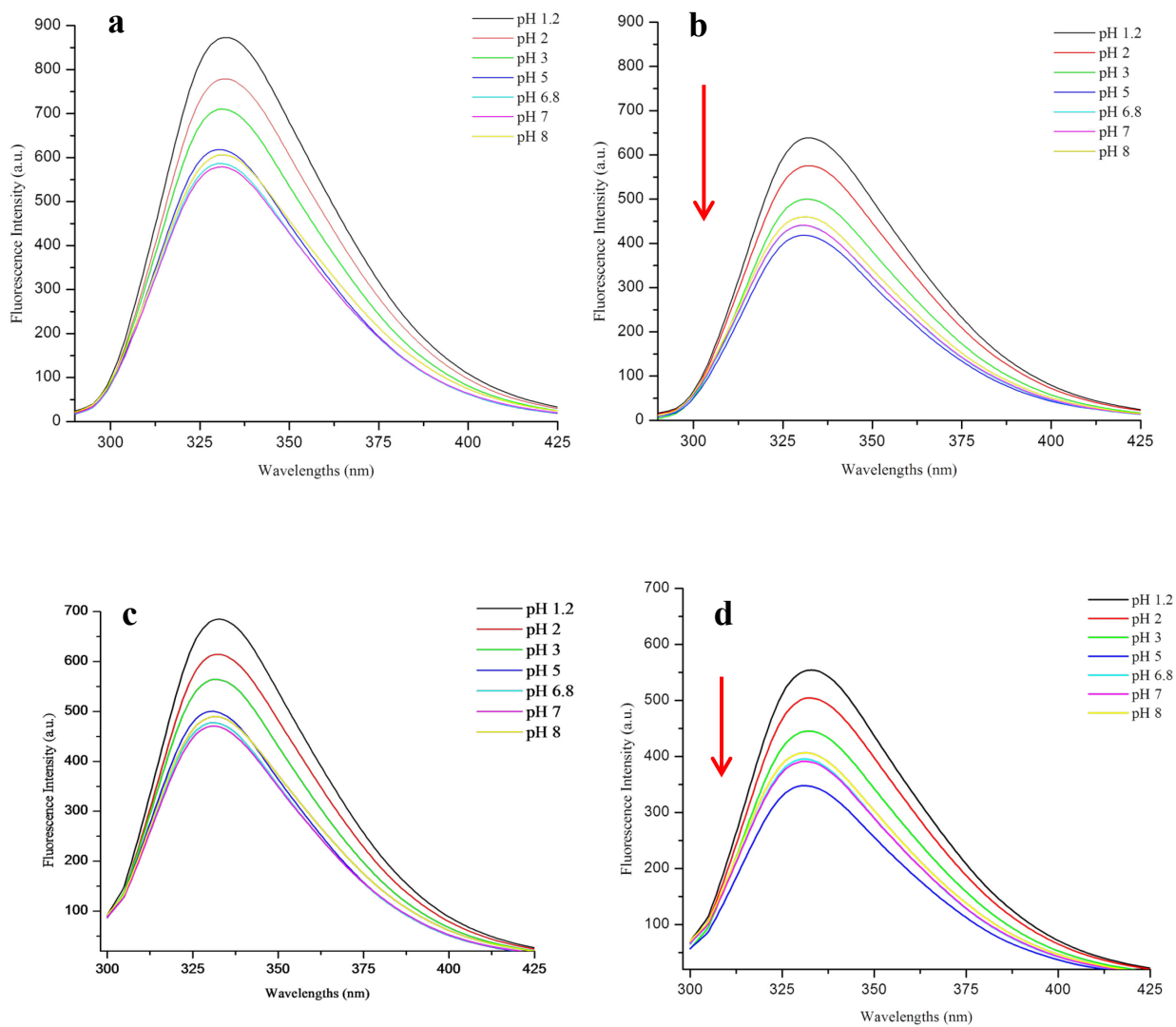
Statistical analysis was performed using the software SAS version 12.0. ANOVA and the Least Significant Difference (LSD) were used to determine differences among means and the significance level was fixed at  $p < 0.05$ . All measurements were made at least in triplicate.

## 4.4. Results and discussion

### 4.4.1. Influence of the pH on the interaction between $\beta$ lg and $D_3$

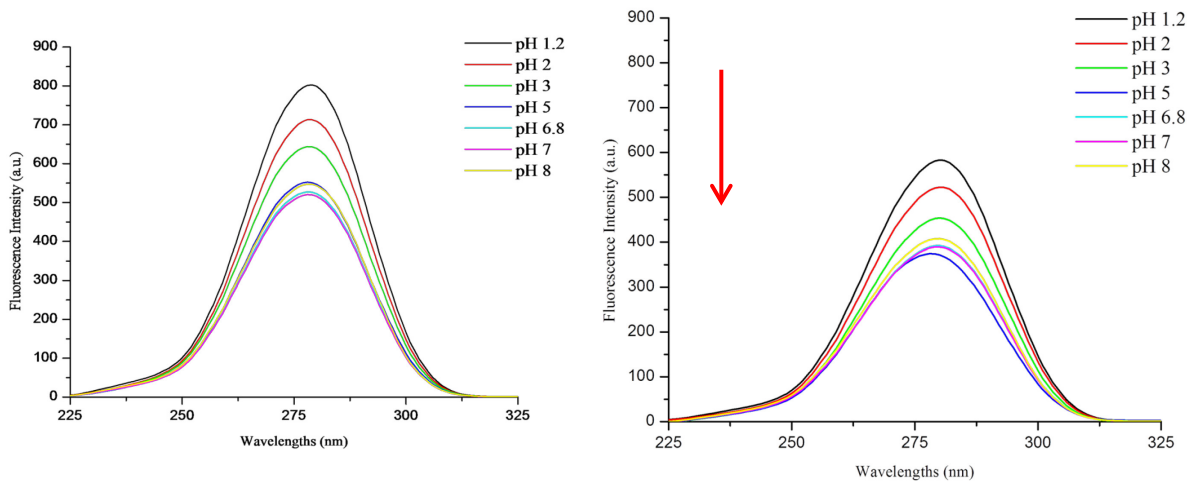
The pH values were specifically selected to be within a range which would not cause appreciable structural modification of the native  $\beta$ -barrel conformation of  $\beta$ lg and also below 9.0, above which an irreversible base-induced unfolding transition occurs leading to the loss of structural integrity of the protein [54]. Unlike previous studies of the effects of pH on the  $D_3$  binding capacity of  $\beta$ lg, the  $\beta$ lg/ $D_3$  complex was first formed and then exposed to specific values of pH. The intrinsic fluorescence spectra for  $\beta$ lg alone and the  $\beta$ lg/ $D_3$  complex were obtained at the different pH values using excitation wavelengths at 280 and 290 nm. The excitation at 290 nm is typically that of Trp19 which is in a non-polar environment and contributes to about 80 % of the total fluorescence of  $\beta$ lg, while excitation at 280 nm provides information on the polarity of the environment of both tyrosine (Tyr) and Trp [6]. Changes in the fluorescence emission spectra can arise from the binding of ligands in the vicinity of the fluorophores, and thus be used to monitor formation of the complex and resulting energy transfer between the protein and the ligand [176].

Figure 4.1 clearly shows the binding of  $D_3$  to  $\beta$ lg, with strong quenching of the intrinsic fluorescence of  $\beta$ lg at all pH values. The highest quenching was observed at pH 5.0, the extent of the quenching being about 32.7 % and 26.3 % at 280 nm and 290 nm, respectively (Figure 4.1c and d). Furthermore, the synchronous fluorescence of  $\beta$ lg alone and the  $\beta$ lg/ $D_3$  complex at intervals of 60 nm, which provides information on the vicinity of the Trp amino acid, also confirms that maximum quenching occurs at pH 5.0 (Figure 4.2a and b).



**Figure 4.1. Fluorescence intensity of  $\beta$ lg (a and c) and the  $\beta$ lg/ $D_3$  complex (b and d) at different pH (1.2, 2.0, 3.0, 5.0, 6.8, 7.0 and 8.0). Excitation at 280 nm (a and b) and 290 nm (c and d).**

This finding may be explained by the fact that pH 5.0 is close to the isoelectric point ( $pI = 5.2$ ) of  $\beta$ lg where octamers are formed by the tetramerization of the protein dimer, implying a decreased electrostatic repulsion and increased hydrophobic interactions between the monomers of the protein [189, 190]. Since  $\beta$ lg binds  $D_3$  essentially through hydrophobic forces, it could be suggested that the auto-association of the monomers reinforces the binding [61]. Although an increased interaction between the monomers of  $\beta$ lg can contribute to the internal quenching of the fluorescence intensity of the protein [50], both Figure 4.1 and Figure 4.2 show that at pH 5.0, the quenching of the fluorescence intensity is much more important for the  $\beta$ lg/ $D_3$  complex than for  $\beta$ lg alone. Therefore, it can be assumed that at pH 5.0,  $D_3$  binds more closely to  $\beta$ lg, and more specifically to Trp.



**Figure 4.2. Synchronous fluorescence of Trp using  $\Delta\lambda = 60$  nm of  $\beta$ Ig in absence (a) and presence of vitamin D<sub>3</sub> (b).**

The quenching of the fluorescence intensity of  $\beta$ lg by  $D_3$  at pH below 5.0 (1.2, 2.0 and 3.0) was greater than at higher pH values (6.8, 7.0 and 8.0). This difference is probably due to the dissociation of dimers into monomers at lower pH, with subsequent reduction of the internal quenching [50]. Interestingly, the quenching of the fluorescence intensity of  $\beta$ lg was minimal at pH 8.0, with a decrease of only 24 % and 13.6 % at 280 nm and 290 nm, respectively. Reduced quenching at high pH may be due to several factors. At pH 8.0, the monomers are formed because of increased electrostatic repulsion and the EF loop, that is the gate of the central calyx, is in the open conformation, which is confirmed by the blue shift observed at higher pH (Table 4.1).

**Table 4.1. Influence of pH on the emission maximum wavelength of  $\beta$ Ig and the  $\beta$ Ig/D<sub>3</sub> complex**

pH	$\lambda_{max}$ (nm)	
	$\beta$ Ig	$\beta$ Ig/D <sub>3</sub> complex
1.2	333	332
2.0	334	334
3.0	331	331
5.0	331	329
6.8	332	330
7.0	331	329
8.0	332	330

This means that the Trp residue is in a more hydrophobic environment caused by the presence of D<sub>3</sub>. It is known that the decrease in polarity in the vicinity of the Trp residue is accompanied by a blue shift in the emission maximum ( $\lambda_{\max}$ ) to shorter wavelengths and an increase in fluorescence intensity [6]. Additionally, Taulier and Chalikian observed that both the volume and compressibility of  $\beta$ lg decreased at acidic pH, whereas at pH above 7.5 there is a loosening in the interior packing of  $\beta$ lg [54]. On the other hand, at pH < 3.0,  $\lambda_{\max}$  for the  $\beta$ lg/D<sub>3</sub> complex is similar to that of  $\beta$ lg in the same conditions, confirming that the EF loop is in the closed conformation (Table 4.1). At pH 1.2, structural changes affecting the tertiary structure of  $\beta$ lg are responsible for the slight shift of  $\lambda_{\max}$  [54]. At pH > 3.0,  $\lambda_{\max}$  shifts to shorter wavelengths (blue shift), confirming that the EF loop is in the open conformation.

At acidic pH where the EF loop is the closed conformation, it can be assumed that the interaction between D<sub>3</sub> and the protein increases as shown in Figure 4.3A.

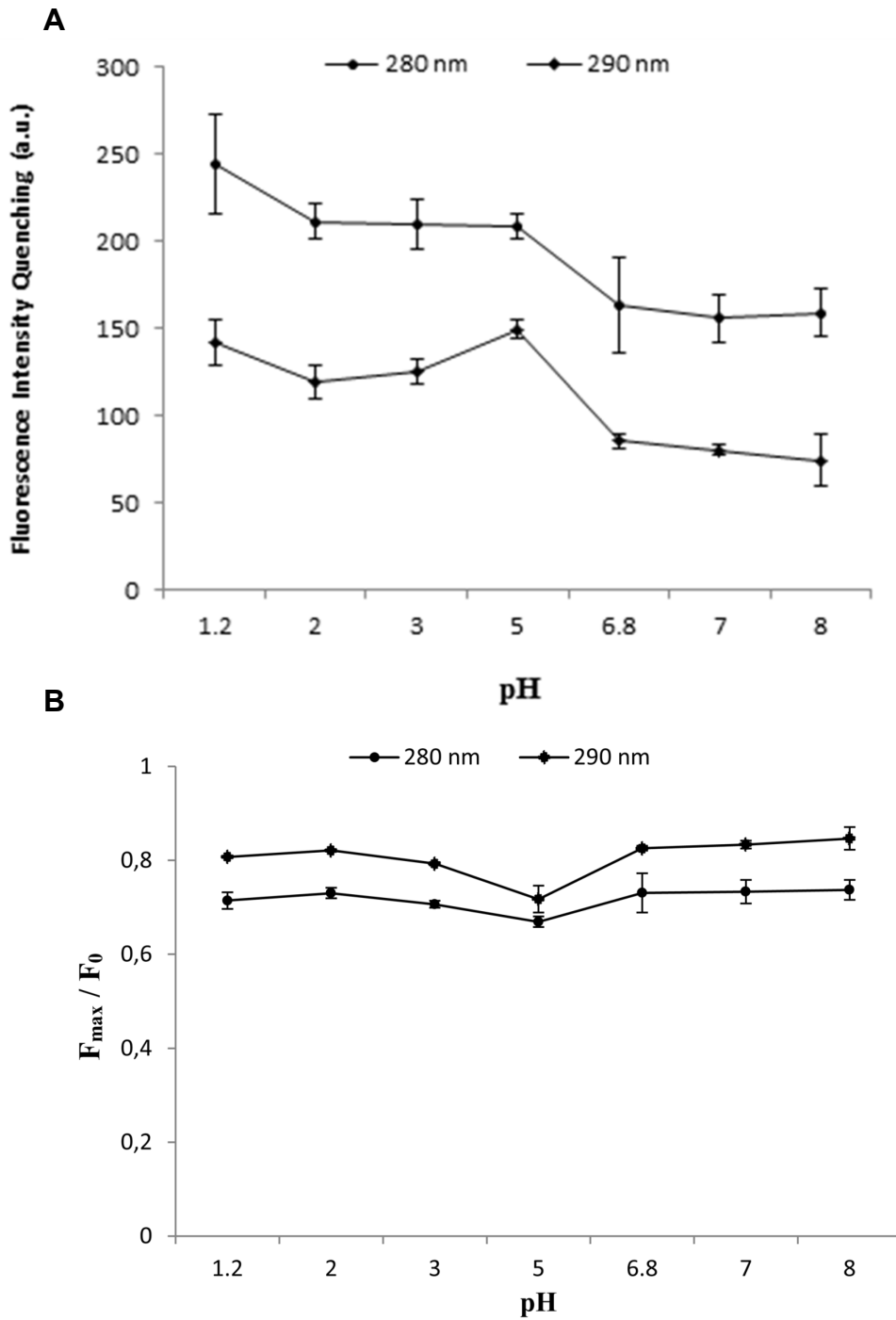


**Figure 4.3.** Vitamin D<sub>3</sub> binding capacity of  $\beta$ lg at different (1.2, 2.0, 3.0, 5.0, 6.8, 7.0 and 8.0). **B.** Fractional residual fluorescence of  $\beta$ lg.  $F_{\max}$  is the intensity at the emission maximum ( $\lambda_{\max}$ ) and  $F_0$  is the intensity for  $\beta$ lg at  $\lambda_{\max}$ . Excitation at 280 and 290 nm.

In summary, the higher quenching at low pH is possibly due to a tighter packing of  $\beta$ lg around  $D_3$  than at high pH. Although the extent of quenching of the fluorescence intensity of  $\beta$ lg is pH-dependent, the interaction between  $\beta$ lg and  $D_3$  does not seem to be affected by pH (Figure 4.1 and Figure 4.2). Rather, the differences in the fluorescence intensity of  $\beta$ lg result from slight structural changes, also called structural transitions, which are triggered by modification of the pH values [60]. These structural transitions are categorized into distinct classes including the transition below pH 2.0, the dimer-to-monomer transition occurring between pH 4.5 and 2.0, the native dimeric (N) to the acidic (Q) form transition which occurs between pH 6.0 and 4.5 (and includes the pH 5.0 transition), the Tanford (N–R) transition occurring between pH 7.0 and 8.0, and the transition at pH 9.0 or above where  $\beta$ lg undergoes an irreversible base-induced unfolding [54]. Given that the interaction of  $\beta$ lg with vitamin  $D_3$  is not significantly affected by pH, it is possible to evaluate the stability of the  $\beta$ lg/ $D_3$  complex in light of the reported pH-induced structural transitions of  $\beta$ lg.

#### **4.4.2. Influence of the pH on the stability of the $\beta$ lg/ $D_3$ complex**

The values of pH were chosen to represent those of the gastrointestinal tract (pH 1.2 and 6.8), acidic food (pH 2.0 and 3.0), the isoelectric point of the protein (pH 5), neutral (pH 7.0), and alkaline (pH 8.0) conditions. At pH 1.2,  $D_3$  was not released from its binding sites on  $\beta$ lg ( Figures 4.1, 4.2 and 4.3). The quenching of the fluorescence intensity of  $\beta$ lg by  $D_3$  was maximal, probably due to the decrease in volume and compressibility of the protein below pH 1.5, which might provide a more compact structure to  $\beta$ lg, as previously reported [54]. According to these authors, this structural transition continues at pH values less than 1.0, although no explanation was suggested. Given the fact that the EF loop is still in the 'closed conformation', there might be a repositioning, rather than a release, of  $D_3$  inside the hydrophobic cavity of the protein closer to the fluorophores. Consequently, the quenching of the fluorescence intensity is high at acidic pH, especially at pH 1.2

compared to more alkaline pH ( $p = 0.0002$ ), as shown in Figure 4.3A. Moreover, fluorescence quenching is higher at 280 nm than at 290 nm probably due to the contribution of both Trp and Tyr amino acids.

The dimer-to-monomer transition of  $\beta$ lg between pH 4.0 and 2.5 is accompanied by a decrease in internal quenching and enhancement of protein fluorescence (Figure 4.1a and c) [50]. The pH 4.0 to 2.5 transition also includes the  $\beta$ lg transition from the monomeric (M) to the acidic form (Q) at pH 3.0 [53, 54]. In the present study, the  $\beta$ lg/ $D_3$  complex remains stable during the pH 4.0 to 2.5 transition (Figures 4.1, 4.2 and 4.3). Figure 4.3A shows that the binding capacity of  $\beta$ lg was not significantly changed from pH 2.0 to 3.0 and was comparable to pH 1.2, although slightly less inferior (Figure 4.3A). This result is consistent with changes induced by the pH 4.0 to 2.5 transition [53]. Indeed, the structural modification results into a different orientation of the  $\alpha$ -helix, thus affecting only the surface electrostatic properties of  $\beta$ lg.  $D_3$  binds to both the internal cavity and surface site, which consists of a pocket formed between the  $\alpha$ -helix and the core of the  $\beta$ -barrel, mainly through hydrophobic interactions [54, 61, 79]. The binding of  $D_3$  is therefore unaffected by the pH 4.0 to 2.5 structural transition.

The structural transition from the native dimeric form (N) to the Q form occurs in the pH 6.0 to 4.5 range and includes the pH 5.0 transition, which is described by [54]. This transition is accompanied with a slight expansion of the hydrodynamic volume of  $\beta$ lg and has minor impact on its structure [53, 54]. Precipitates of octamers form at a pH close to the isoelectric point of  $\beta$ lg (from pH 3.9 to 5.0) [53]. The findings of the present study suggest that the tetramerization of  $\beta$ lg leading to the formation of octamers can be advantageous for the binding of  $D_3$ . In fact, when excited at 280 nm, the behavior of the  $\beta$ lg/ $D_3$  complex is similar from pH 2.0 to pH 5.0 whereas, when excited at 290 nm, the binding capacity of  $\beta$ lg is significantly higher at pH 5.0 (Figure 4.3A). This finding confirms that the self-association of  $\beta$ lg contributes to the increased internal quenching, and most importantly, provides evidence that  $D_3$  is more closely bound to the Trp residues as discussed above.

The well-known Tanford (N–R) transition occurs between pH 7.0 and 8.0 [52-54, 87, 191]. The data generated in the current study indicate that the  $\beta$ lg/D<sub>3</sub> complex remains stable when the pH is varied from pH 6.8 to pH 8.0 (Figure 4.3A). The Tanford transition produces an alteration in the secondary and tertiary structure of  $\beta$ lg, mainly represented by the opening–closing the calyx due to the protonation of the carboxyl group of glutamate side chain of residue 89 (Glu89) located within the EF loop 85–90. Glu89 is inaccessible at pH 6.2, but above pH 7.0, becomes protonated, exposed and accessible to the solvent provoking the displacement of the loop EF which opens the interior of the calyx [52, 60]. In the present study, the shift to the Tanford transition can be seen in Figure 4.3. From pH 6.8 to 8.0, the  $\beta$ lg/D<sub>3</sub> complex presented similar behavior, confirming that the movement of the EF loop leading to the ‘open’ confirmation started at pH 6.8. This finding is important since the N–R transition was suggested to occur above pH 7.0 [60]. Furthermore, the binding of D<sub>3</sub> to  $\beta$ lg was already demonstrated when the protein is in a dimeric form at pH 7.0 and when the dimer dissociates into monomers at pH 8.0 [79, 176]. The pH of the intestine is around pH 6.8, indicating that the  $\beta$ lg/D<sub>3</sub> complex might also remain stable during transit in the gastrointestinal tract. However, whereas  $\beta$ lg is resistant to peptic digestion in the stomach, it is susceptible to proteases prevailing in the intestine [192]. A possible explanation for the intestinal susceptibility of  $\beta$ lg might be the exposure of Tyr amino acids which are sensitive to tryptic and chymotryptic hydrolysis, as the result of the conformation transition at pH greater than 7.0 [192, 193]. Conversely,  $\beta$ lg showed increased stability toward urea unfolding when both sodium dodecyl sulfate and palmitic acid bound the internal cavity of the protein [194]. Moreover, the hydrophobic interaction between these ligands and  $\beta$ lg was enhanced and the exclusion of water from the cavity provided further stability to the protein [194, 195]. It was also shown that surfactant *n*-alkylsulfonate ligands stabilize the monomeric structure of  $\beta$ lg [196]. Consequently, it can be suggested that D<sub>3</sub> binding  $\beta$ lg to both the internal cavity and the surface site through hydrophobic interaction might stabilize the protein. This assertion remained to be proven with further research.

#### 4.4.3. Influence of the pH on the fractional residual fluorescence

The fractional residual fluorescence (FRF) used to determine the proportion of  $\beta$ lg not bound to the ligand provided further proof that  $D_3$  remains bound to  $\beta$ lg at all studied pH values (Figure 4.3B). This suggests that the acid stability of the  $\beta$ lg/ $D_3$  complex might result from the fact that the EF loop remains in the 'closed conformation' when the pH is rapidly decreased or in the 'open conformation' when the pH is increased. In fact, a static concentration of  $\beta$ lg and  $D_3$  was used to initially form the  $\beta$ lg/ $D_3$  complex before quickly proceeding to pH modification to acidic or alkaline conditions. Except at pH 5.0, the proportion of bound  $\beta$ lg was similar from pH 1.2 to 8.0, with about 30% bound protein. At pH 5.0 the proportion of bound protein was significantly higher with about 40 % of  $\beta$ lg bound to  $D_3$  ( $p = 0.02$ ).  $D_3$  was shown to bind at two binding sites on  $\beta$ lg at pH 7.0 as well as at pH 8.0 [79, 176]. In the current study, since the FRF at pH 7.0 and 8.0 had profiles similar to those at lower pH, it can be suggested that  $D_3$  remains at the two different binding sites when the pH is lowered. Comparable results were observed with the  $\beta$ lg/resveratrol complex, for which the FRF at pH 2.0 was similar to that at pH 7.4, indicating that the complex is stable at acidic pH [50].

#### 4.4.4. Influence of the $\beta$ lg/ $D_3$ complex formation on the solubility of $D_3$

U-HPLC measurements were used to determine the impact of complexation with  $\beta$ lg on the solubility of  $D_3$  (Figure 4.4). A fixed concentration of  $D_3$  of 20  $\mu$ M was incubated in the presence or absence of increasing concentration of  $\beta$ lg (1.25 to 80  $\mu$ M). In the absence of  $\beta$ lg, 10% of  $D_3$  was degraded after storage overnight at 4 °C. However, the solubility of  $D_3$  increased steadily when the concentration of  $\beta$ lg was increased from 1.25 to 10  $\mu$ M before reaching a plateau at somewhat higher concentrations of the protein (Figure 4.4).

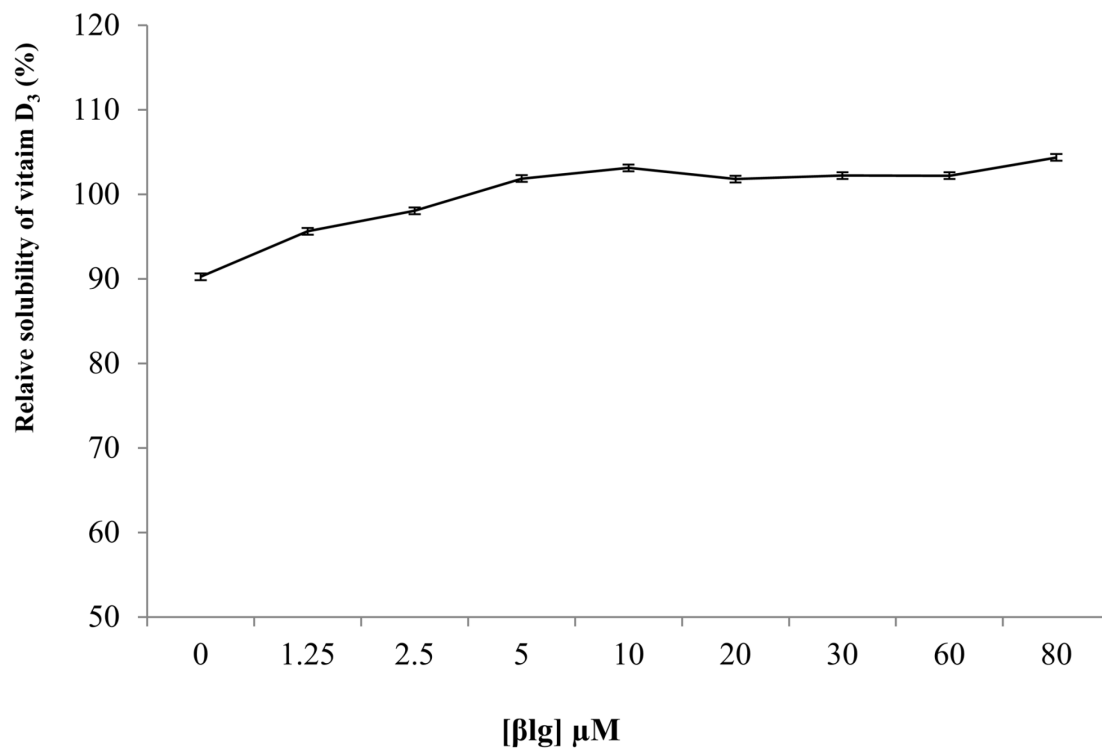


**Figure 4.4. Relative solubility of vitamin D<sub>3</sub> in the presence and absence of  $\beta$ lg. A static concentration of vitamin D<sub>3</sub> of 20  $\mu$ M was incubated overnight at 4 °C with increasing concentration of  $\beta$ lg (0, 1.25, 2.5, 5, 10, 20, 30, 60 and 80  $\mu$ M).**

This result is consistent with previous  $D_3$ - $\beta$ lg binding studies using titration methods, which have shown that the maximal binding of  $D_3$  with  $\beta$ lg was reached at a 2:1 ratio [13, 79, 176]. It was also reported that complexing with  $\beta$ lg significantly increased the hydrosolubility of resveratrol [6]. This beneficial effect is of importance in the food industry where formulation of food products with low fat content can be challenging. It is also worth noting that a U-HPLC method was developed and optimized in the present study to identify and determine the concentrations of both  $D_3$  and  $\beta$ lg in a single run.

#### **4.5. Conclusion**

Overall, the findings indicate that the  $\beta$ lg/ $D_3$  complex remains stable during pH-induced structural transitions occurring between pH 1.2 and 8.0. This pH range encompasses that of the gastrointestinal track, the pH of acidic foods and beverages, transitional values (3.0 and 4.0) and that near the  $pI$  of  $\beta$ lg (5.0), and neutral and alkaline values. These results are in good agreement with the physiological significance of the closing of the EF loop at acidic pH — that is, the putative transport and protective role of  $\beta$ lg on small hydrophobic ligands in the acidic stomach. Additionally, at pH near the  $pI$  of  $\beta$ lg, the tetramerization of  $\beta$ lg which leads to the formation of octamers could be advantageous for the binding of  $D_3$ . Furthermore,  $D_3$  might be retained during formulation and storage of various solid and liquid foods, such as  $D_3$ -containing processed dairy products, which can provide added value to foods. The present study generates new information on the pH-stability of the  $\beta$ lg/ $D_3$  complex, which is valuable for future applications in the food industry. Solubility and subsequent absorption are key determinants for the bioavailability of fat soluble nutrients [14, 197-199]. Therefore, the findings of the current work have implications for the health care system, given that increased solubility of  $D_3$  implies enhancement of its absorption and bioavailability and hence, improved health benefits.

#### **4.6. Acknowledgements**

This work was supported by the Natural Sciences and Engineering Research Council of Canada (NSERC) through the Vanier Canada Graduate Scholarships (F. Diarrassouba) and the Canada research chair in protein, biosystem and functional food physical chemistry. The authors would like to thank Mr Pascal Dubé, Ms Diane Gagnon (Institut de recherche sur les nutraceutiques et les aliments fonctionnels, Université Laval, Québec, QC, Canada) and the EA-CIDAM's team members (Biopharmacie lab, Faculté de Pharmacie, Clermont-Ferrand, France).

## **Contextual transition**

The following chapter also relates to the second objective. Detailed stability study of the  $\beta$ -lactoglobulin/vitamin D<sub>3</sub> complex is presented. The study includes the long term stability in the cold, upon exposure to UV light and intestinal proteases. Permeability and *in vivo* experiments using Caco-2 cells and animals, respectively, were conducted to investigate the intestinal uptake and subsequent effects on the bioavailability of vitamin D<sub>3</sub>.



## CHAPTER 5

# Increased Stability and Protease Resistance of the $\beta$ -Lactoglobulin/Vitamin D<sub>3</sub> Complex

A version of this work was published in Food Chemistry  
Volume 145, February 2014, Pages 646–652.

By :

Fatoumata Diarrassouba<sup>a</sup>, Ghislain Garrait<sup>b</sup>, Gabriel Remondetto<sup>c</sup> Pedro Alvarez<sup>a</sup>,  
Eric Beyssac<sup>b</sup> and Muriel Subirade<sup>a</sup>

<sup>a</sup>Chaire de recherche du Canada sur les protéines, les bio-systèmes et les aliments fonctionnels, Institut de recherche sur les nutraceutiques et les aliments fonctionnels (INAF/STELA), Université Laval, Québec, QC, Canada.

<sup>b</sup>EA-CIDAM, Lab Biopharmacie, Faculté de Pharmacie, 28 Place Henri Dunant, 63001, Clermont-Ferrand, France.

<sup>c</sup>Centre de recherche et développement, Agropur Coopérative. 4700 rue Armand Frappier, St-Hubert, QC, J3Z 1G5, Canada.

## 5.1. Abstract

The stability of the  $\beta$ -lactoglobulin ( $\beta$ lg)/vitamin D<sub>3</sub> (D<sub>3</sub>) complex at 4 °C and upon exposure to UV-C light, and in simulated intestinal fluid, were studied *in vitro*. Caco-2 cells were used to demonstrate the passage of the  $\beta$ lg/D<sub>3</sub> complex across the monolayers. Furthermore, an *in vivo* experiment was conducted by force-feeding rats with the free D<sub>3</sub> and  $\beta$ lg/D<sub>3</sub> complex, with subsequent determination of the plasma concentration of 25-hydroxy-D<sub>3</sub>. The  $\beta$ lg/D<sub>3</sub> complex significantly improved the stability of the vitamin at 4 °C and when exposed to UV-C light. The resistance of  $\beta$ lg to proteases was increased, indicating a mutual protective effect. The  $\beta$ lg/D<sub>3</sub> complex crossed the monolayers, which was confirmed by the significant increase in the concentration of 25-hydroxy-D<sub>3</sub> in rats fed the  $\beta$ lg/D<sub>3</sub> complex compared to the ones fed the free D<sub>3</sub>. Therefore, the current study suggests that the  $\beta$ lg/D<sub>3</sub> complex can effectively be used for the fortification of milk products and low-fat content foods to improve the intake and bioavailability of D<sub>3</sub>.

## 5.2. Introduction

The bovine milk protein,  $\beta$ -lactoglobulin ( $\beta$ lg), is well recognized for its ability to bind and transport small hydrophobic ligands including retinol, fatty acids and vitamin D<sub>3</sub> (D<sub>3</sub>) [46, 61]. To date, four ligand binding sites have been discovered on  $\beta$ lg, including the surface hydrophobic pocket in the groove between the  $\alpha$ -helix and the  $\beta$ -barrel, and central calyx, to which D<sub>3</sub> binds. Upon heat-treatment, the central calyx is disrupted, resulting in the loss of one D<sub>3</sub> molecule. The exosite is unaffected by heat denaturation and thus retains the second molecule of D<sub>3</sub> in its hydrophobic pocket. This makes the fortification of milk and dairy products with D<sub>3</sub> an appropriate means to improve the uptake of this vitamin [61]. However, whilst  $\beta$ lg is resistant to pepsin digestion, it undergoes structural modification at intestinal pH which makes it highly susceptible to proteases in the intestine [58].

Consequently, this may affect the intestinal absorption of D<sub>3</sub> and the bioavailability of the 25-hydroxyvitamin D<sub>3</sub> (25(OH) D<sub>3</sub>), the physiologically active form of D<sub>3</sub> [149]. Although a large number of studies have concentrated on the binding to βlg, there is minimal information on the fate of the βlg/D<sub>3</sub> complex in the gastrointestinal (GI) environment. Indeed, most binding studies focus on the theoretical impact of the complex formation on the structure of βlg, the stability of ligand, and/or the biological implications of the complex formation [6, 195].

There is little information on βlg/ligand complex behavior either under conditions simulating the GI environment, or in a more complex system using an animal model. Instead, many authors have speculated about the intestinal absorption of the complex and/or the ligand alone if released from its carrier [6]. Although Yang and co-workers used a mouse model to confirm the presence of two binding sites for D<sub>3</sub> on βlg and the advantage of supplementing milk with D<sub>3</sub>, the fate of the βlg/D<sub>3</sub> complex in the GI was not studied and the mechanism of the intestinal absorption of D<sub>3</sub> carried by βlg was not elucidated [61].

In previous work, it was established that the βlg/D<sub>3</sub> complex was resistant to the gastric (pH 2.0) and intestinal pH (pH 6.8) [200]. In the present study, the βlg/D<sub>3</sub> complex was formed before evaluating the impact of complex formation on the stability of D<sub>3</sub> in normal and extreme storage conditions over time. Additionally, the βlg/D<sub>3</sub> complex was submitted to simulated intestinal fluid with or without proteolytic enzymes and its permeability through the intestinal cells was studied *in vitro*. Finally, an animal experiment using rats was carried out to study the impact of the complex formation on the intestinal absorption of D<sub>3</sub>.

## 5.3. Experimental Section

### 5.3.1 Materials

$\beta$ -lactoglobulin ( $\beta$ lg) was purchased from Davisco Foods International, Inc. (Le Sueur, MN, USA). The protein was used without further purification. Vitamin D<sub>3</sub> (purity  $\geq$  98%, HPLC) was sourced from Sigma-Aldrich Chemical and Co (Oakville, ON, Canada). Acetonitrile (ACN, HPLC grade), methanol (MeOH, HPLC grade) and trifluoroacetic acid (TFA) were purchased from EMD International (Gibbstown, NJ, USA).

### 5.3.2 Sample preparation

Protein stock solutions (0.2 %) were prepared by dissolving the powder in MilliQ water under mild stirring conditions for 2 h at room temperature and then stored overnight at 4 °C to allow complete rehydration [31]. Vitamin D<sub>3</sub> (D<sub>3</sub>) stock was prepared daily by dissolving 10 mg in 25 mL MeOH [188]. Working solutions of D<sub>3</sub> were obtained by diluting the stock solution in MilliQ water.

The  $\beta$ lg/D<sub>3</sub> complex was prepared by mixing  $\beta$ lg and D<sub>3</sub> solutions using a  $\beta$ lg:D<sub>3</sub> ratio of 1:2 and incubating for about 1.5 to 2 h at room temperature prior to analysis. The final concentration of methanol in the mixture was less than 3 %. All samples containing D<sub>3</sub> were protected from light by using amber-tinted 15 mL conical tubes which were filled to the top with  $\beta$ lg/D<sub>3</sub> complex solution in order to minimize the effect of oxygen on D<sub>3</sub> by eliminating the head space in the tubes.

### **5.3.3. Stability of the $\beta$ lg/D<sub>3</sub> complex in refrigerated conditions**

The  $\beta$ lg/D<sub>3</sub> complex was first formed at room temperature as mentioned above by mixing the same volume (7.5 mL) of both  $\beta$ lg (0.2%) and D<sub>3</sub> (220  $\mu$ M) in six different 15 mL - conical tubes in the dark before covering the tubes with aluminum foil. Each tube corresponded to one of the following sampling periods: week 0, 1, 2, 3, 4 and 5. D<sub>3</sub> concentration on day 0 was immediately determined after the incubation period of about 2 h. Samples for weeks 1 to 5 were stored at 4 °C in a fridge. Each week, a sample was withdrawn for HPLC analysis from the D<sub>3</sub> remaining in the tube, as previously described [200]. Solutions of D<sub>3</sub> diluted in MilliQ water were prepared and analyzed under the same conditions. All the experiments were repeated at least three times.

### **5.3.4. UV – Stability of the $\beta$ lg/D<sub>3</sub> complex**

Each of the  $\beta$ lg/D<sub>3</sub> complex and D<sub>3</sub> solutions were prepared as mentioned in the preceding section and exposed to UV-C light (254 nm, 15 W) in order to assess the UV-light stability of D<sub>3</sub> over 24 h [130]. At each sampling time (t 0, 1, 2, 4, 6, 8, 10 and 24 h), HPLC analysis was performed for D<sub>3</sub> recovery, which represent the amount of the vitamin remaining in solution, using the procedure presented in Section 3. Experiments were performed in triplicate.

### **5.3.5. Intestinal stability of the $\beta$ Ig/D<sub>3</sub> complex**

The stability of the  $\beta$ Ig/D<sub>3</sub> complex was investigated using a USP-2 paddles apparatus (SOTAX Corporation, Westborough, MA, USA). Each of the  $\beta$ Ig/D<sub>3</sub> complex and D<sub>3</sub> solutions (5 mL) were incubated in 95 ml in one of two release media with continuous agitation (at ~ 50 rpm) at 37 °C [18]. In order to minimize D<sub>3</sub> degradation by air, custom-made paraffin discs were used to occlude the top of the mini-vessels with just enough space to allow for the rotation of the paddles. The release media consisted of the simulated intestinal fluid (SIF) as described in the US Pharmacopeia with and without 1.0% pancreatin (w/v) at pH 6.8. Samples (~ 0.1 mL) withdrawn at half-hour or 1-h intervals over 6 h were centrifuged (5,000 x g /5 min) and the concentration of D<sub>3</sub> in the supernatant was determined by HPLC as indicated above. A control with and without enzyme was also run.

### **5.3.6. *In vitro* study of the permeability of the $\beta$ Ig/D<sub>3</sub> complex**

The human Caucasian colon adenocarcinoma cells (CaCo-2) were sourced from the American Type Culture Collection (ATCC, Rockville, MD, USA) at passage 17. Cells were cultured in high-glucose (4.5 g/L) DMEM (Dulbecco's Modified Eagle Medium, Gibco, Grand Island, NY, USA) containing 20 % fetal bovine serum, 2 % vitamins, 2 % non-essential amino acids, 2 % L-glutamine and 2 % of an antibiotic solution consisting of penicillin and streptomycin in addition to an antimycotic agent. Cell lines were maintained at 37 °C in a 5 % CO<sub>2</sub>-95 % air atmosphere and the medium was replaced every second day. A 12 Well Transwell<sup>®</sup> permeable support with polycarbonate membrane insert (24.5 mm diameter, 10  $\mu$ m thickness, 0.4  $\mu$ m pore size) was seeded at  $1 \times 10^5$  cells/insert. All experiments were carried out at 21 days after initial seeding when Caco-2 cells exhibited maximum differentiation.

Before each experiment, the medium was removed and the cell monolayer was washed three times with 1 mL of DPBS 1X (Dulbecco's Phosphate Buffered Saline, Gibco, Grand Island, NY, USA). Solutions (0.5 mL) of D<sub>3</sub> and the βlg/D<sub>3</sub> complex were deposited on the apical side of the monolayer membrane while the basolateral area was submerged in 1.5 mL of the culture media. The final concentration of D<sub>3</sub> on the cells 21.17 µg. DPBS (0.5 mL) was used on cells as a control. HPLC was used to monitor the amount of D<sub>3</sub> recovered in the basolateral site. Trans Epithelial Electric Resistance (TEER) measurements (EVOM - World Precision Instruments (WPI), Inc., Sarasota, FL, USA) were carried out to determine cell integrity before and after the experiment. The toxicity of the test solutions was determined by measuring the TEER at t 30, 60, 90, 120 min and t 24 and 48 h after the experiment.

### **5.3.7. *In vivo* study of the intestinal absorption of the βlg/D<sub>3</sub> complex**

#### **5.3.7.1. Animal models**

Animal studies were conducted at the 'Unité de Stabulation Animale, Ethic Committee-CE-42-12' (Université d'Auvergne, Clermont-Ferrand, France). Adult male Wistar rats ( $n = 25$ ; Elevage Dépré, St. Doulichard, France) weighing  $300 \pm 20$  g at the beginning of the experiment were used. They were housed for an acclimation period of one week in a temperature-controlled room ( $22 \pm 3^\circ\text{C}$ ) and maintained on a 12 h light/12 h dark cycle (lights on from 8:00 a.m. to 8:00 p.m.). Animals were allowed free access to a commercial standard diet (A04, lot 21206, UAR, Epinay-sur-Orge, France) and tap water, as previously reported [201]. The estimated average daily amount of feed intake per adult rat ranged from 25 to 30 g [202].

### 5.3.7.2. In vivo experiments

After the acclimation period, two or three rats were housed per cage for three weeks. The animals had access to feed and water *ad libitum*. The rats ( $n = 15$ ) were divided into 3 groups ( $n = 5$ ) each receiving one of the treatments consisting of MilliQ water supplemented with 0.09 % NaCl (control),  $D_3$ , and the  $\beta$ lg/ $D_3$  complex with the same final concentration of  $D_3$  (110  $\mu$ M or 77  $\mu$ g). Blood samples were collected at T 0, week 1, 2 and 3 in 0.5 mL conical tubes pre-coated with 10  $\mu$ L of sodium heparin (0.1 IU). The plasma was separated by centrifugation at 1000 x  $g$  for 10 min. Plasma samples were stored at  $-20$  °C until analysis of 25(OH) $D_3$  in rat plasma was performed using the 25-Hydroxy Vitamin D Direct EIA kit (IDS Diagnostics, Fountain Hills, AZ, USA) according to the manufacturer's instructions. The one compartment oral dose pharmacokinetics model was used to compute the kinetics of the change in concentration of 25(OH) $D_3$  in the blood samples. The one compartment oral dose pharmacokinetics model was used to compute the kinetics of the change in concentration of 25(OH) $D_3$  in the blood samples.

### 5.3.8. Statistical analysis

Statistical analysis and the  $D_3$  release kinetics were performed using the JMP statistical discovery software (JMP 10, SAS Institute Inc., Cary, NC, USA). Nonlinear regression was performed using the built-in models for nonlinear fitting with fit curve. The equivalence test was also performed to provide an analysis for testing the equivalence of models across levels of the grouping variable ( $D_3$  and the complex  $\beta$ lg/ $D_3$ ). The purpose of this test is to assess whether there is a practical difference between means. The equality of the parameters was tested by analyzing the ratio of the parameters. The decision lines were placed at ratio values of 0.8 and 1.25, representing a 25 % difference. The significance level was fixed at  $p < 0.05$ . All measurements were conducted in triplicate and the results were reported as the mean  $\pm$  SD.

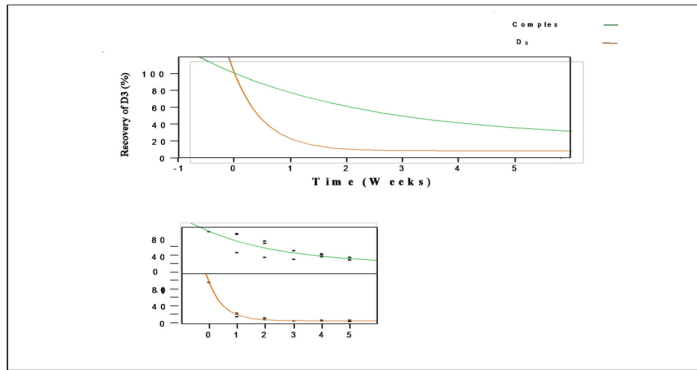
## 5.4. Results and Discussion

### 5.4.1. Stability of the $\beta$ lg/D<sub>3</sub> complex in refrigerated conditions

The stability of the  $\beta$ lg/D<sub>3</sub> complex was assessed at 4°C, which represents the normal storage temperature for milk and most dairy products. The stability of the  $\beta$ lg/D<sub>3</sub> complex was compared to that of the vitamin alone over a period of five weeks. The exponential 3P model ( $R^2 = 0.954$ ) was used to analyze the recovery of D<sub>3</sub> presented in Figure 5.1A. The negative growth rate explains the degradation of the vitamin over time and it should be mentioned that the degradation rate of D<sub>3</sub> in its free form is almost six times faster than in the  $\beta$ lg/D<sub>3</sub> complex. Therefore, the complexation with  $\beta$ lg significantly improves ( $p < 0.05$ ) the stability of D<sub>3</sub> compared to that of the free vitamin in refrigerated conditions, as further shown by the equivalence test in Figure 5.1B.

**A**

versus the  $\beta$ lg/D<sub>3</sub> Complex

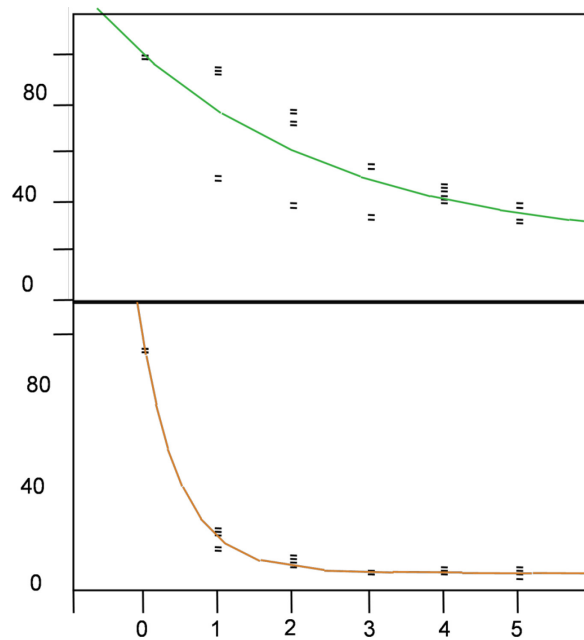


**Time (Weeks)**

**Recovery of D3 (%)**

$\beta$ lg/D3 complex (—) :  $y = 22.83 + 77.80^{-0.35 \times \text{Time (Weeks)}}$

D3 (—) :  $y = 8.73 + 91.25^{-1.87 \times \text{Time (Weeks)}}$



**Time (Weeks)**

**B**

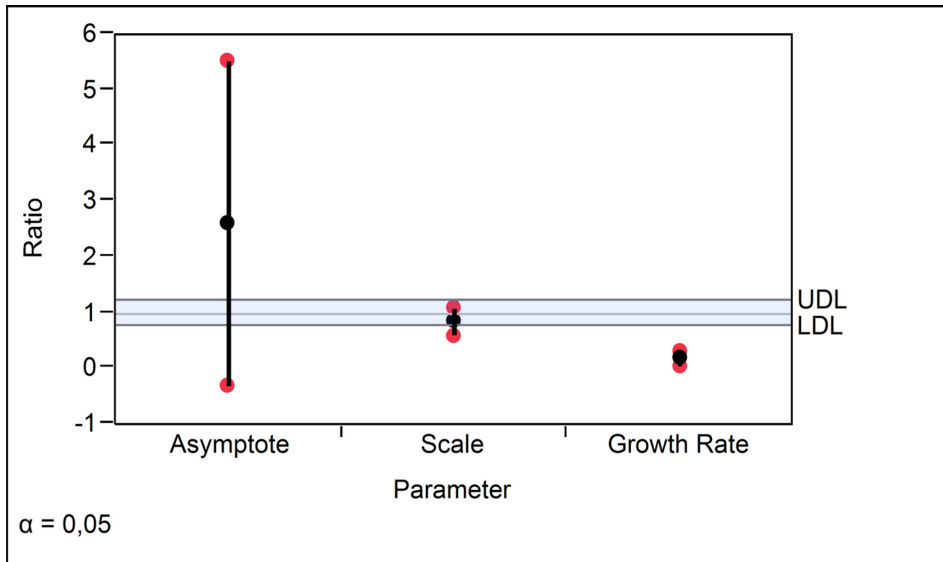


**Figure 5.1. Stability of  $D_3$  and the  $\beta Ig/D_3$  complex in refrigerated conditions ( $4^\circ C$ ) during five weeks. A : Plot of the fitted curves of  $D_3$  and the  $D_3/\beta Ig$ . B. Equivalence between  $D_3$  and the  $D_3/\beta Ig$ . The level of  $\alpha$  was set at 0.05. The lower decision limit (LDL) was 0.8 and the upper decision limit (UDL) was set at 1.25 (representing 25% difference).**

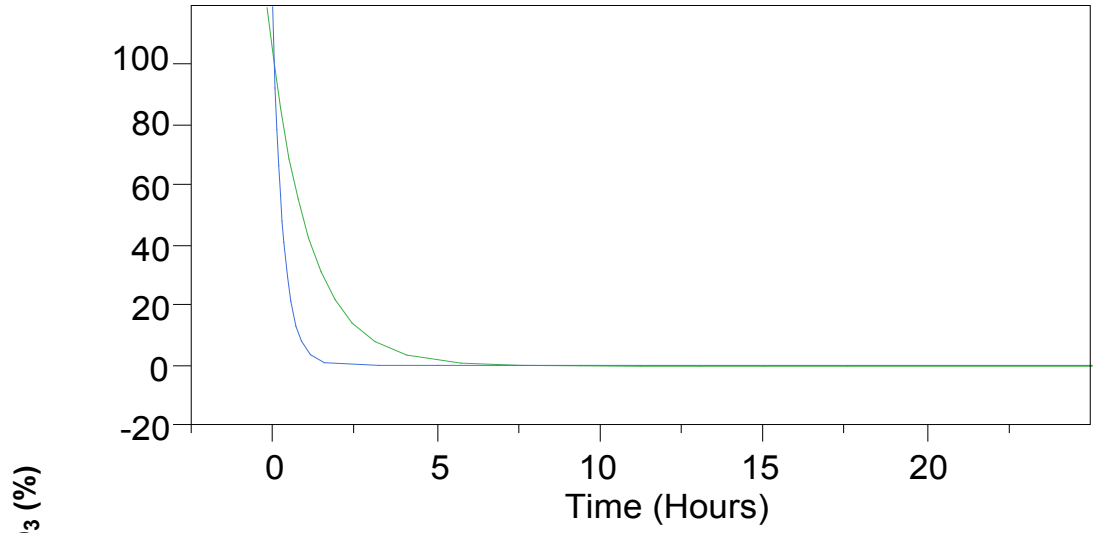
Immediately after the first week of conservation at 4 °C, the amount of D<sub>3</sub> decreased sharply to 21.5 ± 6.3 % for the free vitamin compared to 93.6 ± 0.3 % for the βlg/D<sub>3</sub> complex, before reaching a plateau between weeks 4 and 5 for both. At week 5, only 8.3 ± 2.3 % of the free vitamin D<sub>3</sub> remained, which represents a loss of over 91 % of the initial amount. However, at the end of the five weeks at 4 °C, there was still 43.0 ± 5.1 % remaining for the βlg/D<sub>3</sub> complex, representing a loss of just over half of the initial amount of D<sub>3</sub> (Figure 5.1A). These results indicate that when prepared before incorporation into dairy products and possibly other foodstuffs, the βlg/D<sub>3</sub> complex can improve the stability and extend the shelf-life of D<sub>3</sub> in refrigerated conditions. This is probably due to the strong binding affinity of βlg for D<sub>3</sub> as previously demonstrated [61]. Milk whey is a by-product of cheese production. It becomes undesirable in the case of cheese fortification with D<sub>3</sub> because of the loss of 7 to 9 % D<sub>3</sub> in the whey [14, 15]. The sustained stability of D<sub>3</sub> when bound to βlg can represent an added-value to whey products for the food industry, which would be even more significant if the protective effect of βlg is extended to extreme storage conditions such as during periods of exposure to the damaging effects of UV light.

#### **5.4.2. UV light - stability of the βlg/D<sub>3</sub> complex**

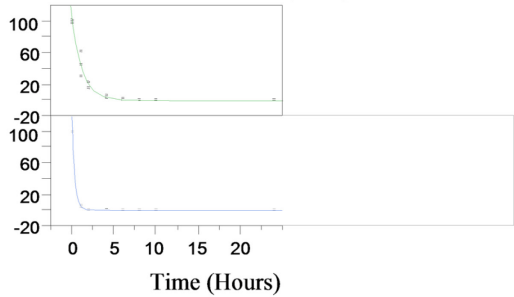
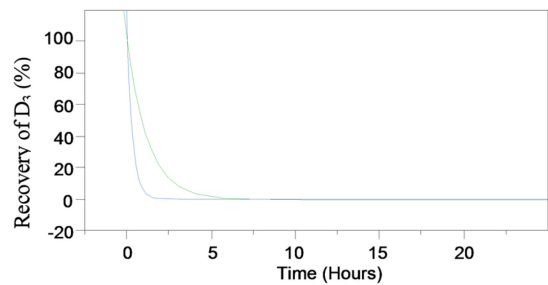
The protection of D<sub>3</sub> from photochemical degradation was studied by exposing the free vitamin and the βlg/D<sub>3</sub> complex to UV-C light irradiation at 254 nm. The residual D<sub>3</sub> was recovered every two hours over a period of 24 hours of irradiation. The rate of degradation was obtained by fitting the non-linear exponential 3P model ( $R^2$  0.98). Here again, the degradation rate of the free vitamin is about three times faster than that of the βlg/D<sub>3</sub> complex. This can be observed in Figure 5.2A where there was a significant difference in the rate of photochemical degradation between the free D<sub>3</sub> and the βlg/D<sub>3</sub> complex during the first few hours (1, 2 and 4) of the irradiation. The equivalence test (Figure 5.2B) did not find any difference between the free and the bound vitamin for the scale. However, the growth rate

was significantly different ( $p < 0.05$ ), confirming our observations of a protective effect against photochemical degradation due to the binding of D<sub>3</sub> to βlg.

**A**



$\beta\text{Ig}/D_3$  complex (—) :  $y = -0.08 + 100.34^{[-0.81 \times \text{Time (Hours)}]}$   
D3 (—) :  $y = 0.19 + 99.81^{[-3.04 \times \text{Time (Hours)}]}$



**Time (Hours)**

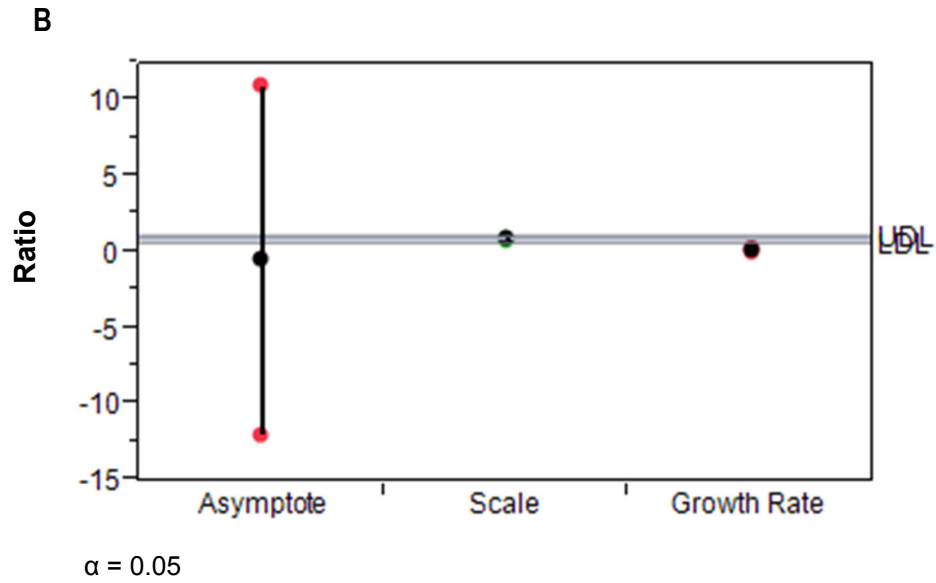


**Figure 5.2. UV-light Stability of D<sub>3</sub> and the  $\beta$ Ig/D<sub>3</sub> complex during 24 hours ( $\lambda = 254$  nm). A: Graph of the stability and B. the equivalence between D<sub>3</sub> and the  $\beta$ Ig/D<sub>3</sub> complex.**

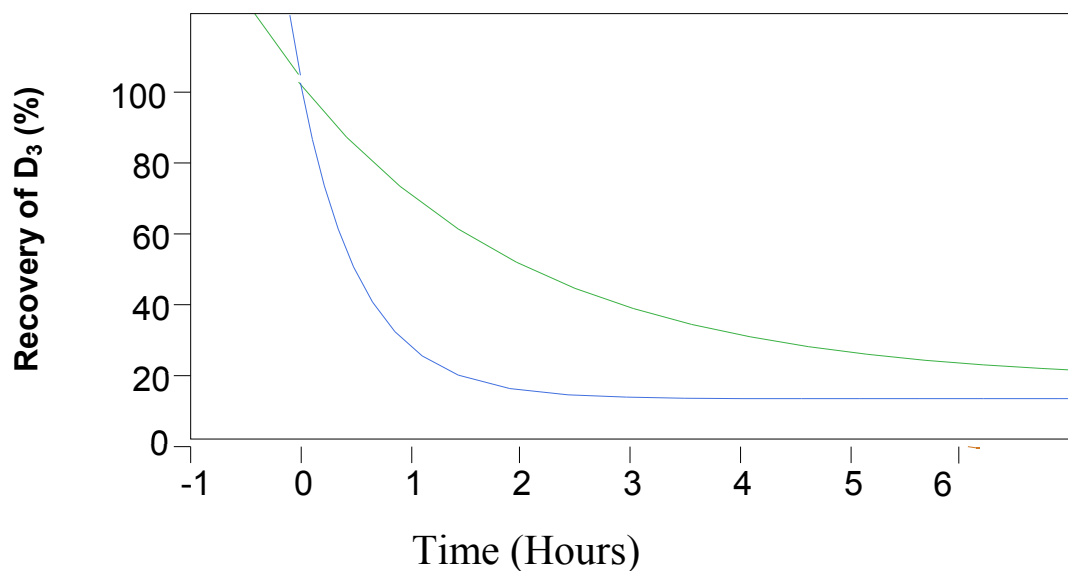
D<sub>3</sub> is susceptible to the action of both oxygen and light, with light producing the greatest loss [203]. In the present study, the photochemical degradation assay was performed with UV-C light at 254 nm, which would be an unusual storage condition. In regular storage conditions, opaque packaging can provide some protection against light to D<sub>3</sub> fortified milk and dairy products [203]. On the other hand, milk casein proteins may provide a 'shade' effect which protects vitamin D<sub>2</sub> against UV-light, and casein micelles absorb more light than the vitamin in its free form [130]. However, after only 3 hours, the micelles did not prevent a loss of over 80 % of D<sub>2</sub> while over 99.5 % of the free D<sub>2</sub> was lost. In the current study, similar results were found after 4 hours where the loss of the free D<sub>3</sub> reached 99.7 ± 0.08 %. For the βlg/D<sub>3</sub> complex, this level of loss was attained only after 8 hours of irradiation (98.9 ± 0.61 %). Although the casein micelles are nanostructured vehicles, and despite the slight structural difference between vitamin D<sub>2</sub> and D<sub>3</sub> (the double bond between C22 and C23 in D<sub>2</sub>), the photochemical degradation of the two vitamins might follow similar pathways [102]. Therefore, in the current study that the βlg/D<sub>3</sub> complex provides improved protection to D<sub>3</sub> against UV-light degradation. If the βlg/D<sub>3</sub> complex is efficient in protecting D<sub>3</sub> during storage, the fate of the complex in the GI still remains unknown. In that regard, the *in vitro* study in simulated intestinal fluids might provide information on the response of the βlg/D<sub>3</sub> complex to digestive proteases.

#### **5.4.3. Intestinal stability of the βlg/D<sub>3</sub> complex**

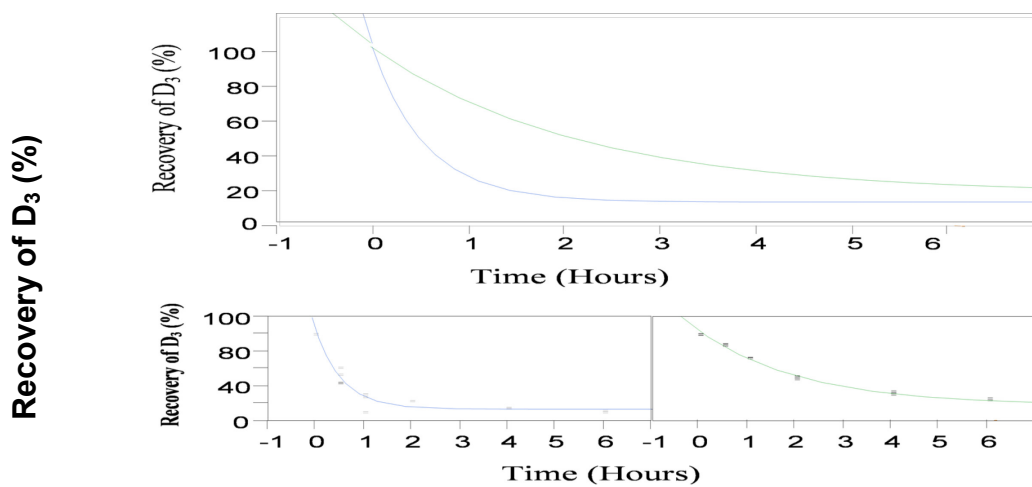
The effect of the simulated intestinal fluid (SIF) at pH 6.8 on the βlg/D<sub>3</sub> complex was compared to that of the free D<sub>3</sub> in the presence (Figure 5.3) and absence of proteases (Figure 5.4). The exponential 3P was used to analyze the intestinal stability of D<sub>3</sub> ( $R^2 = 0.98$ ). Surprisingly, the resistance of the βlg/D<sub>3</sub> complex to proteolytic action was improved, with a subsequent significant improvement in the stability of D<sub>3</sub> compared to the free vitamin (Figures 5.3A and 5.4A). The

equivalence test shows that the values of the asymptote and growth rate are significantly different between the complex and the free  $D_3$  in the presence as well as in the absence of pancreatin (Figures 5.3B and 5.4B).

**A**



$\beta$ Ig/D3 complex (—) :  $y = 18.78 + 83.25^{-0.46 \times \text{Time (Hour)}}$   
D3 (—) :  $y = 13.93 + 86.60^{-1.80 \times \text{Time (Hours)}}$



**B**

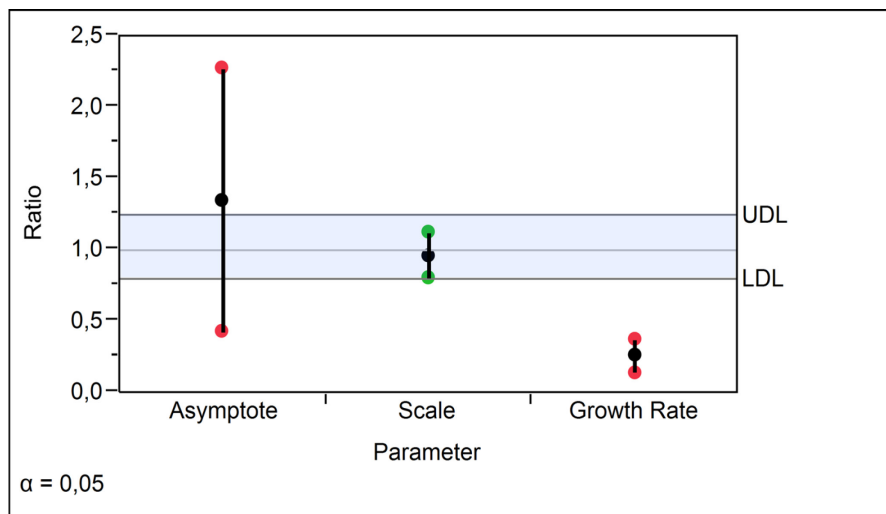
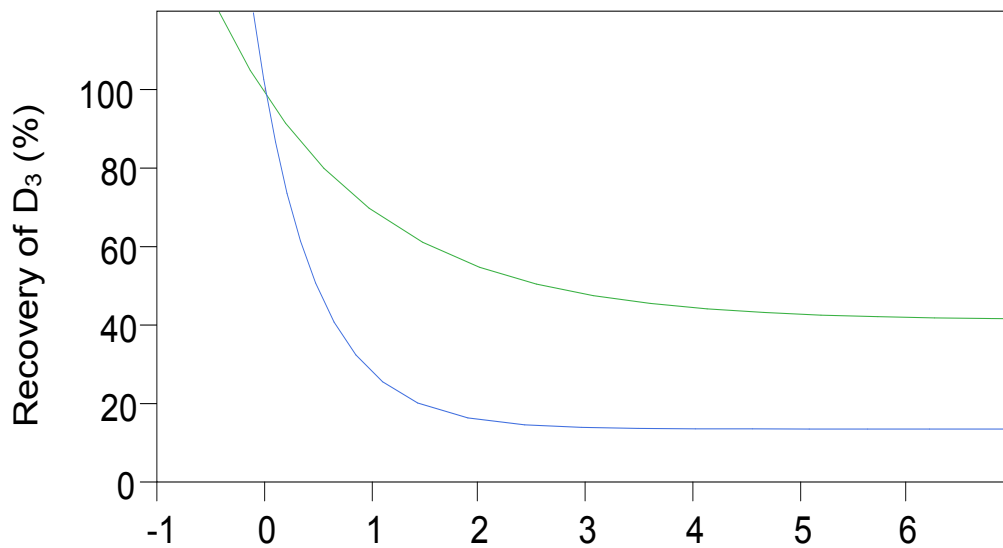


**Figure 5.3. Stability of  $D_3$  and the  $D_3/\beta Ig$  complex in Simulated Intestinal Fluid without pancreatin at pH 6.8, 37°C (USP-2 apparatus). A: Graph of the intestinal stability and B. The equivalence between  $D_3$  and the  $\beta Ig/D_3$  complex.**

The estimate for the scale was not significantly different between  $D_3$  and the  $\beta\text{lg}/D_3$  complex in the absence of pancreatin but was significantly lower in presence of the proteases. After six hours of digestion, there was  $10.9 \pm 0.93$  % of free  $D_3$  remaining in the media whereas  $24.5 \pm 0.73$  % and  $40.9 \pm 0.71$  % of  $D_3$  were recovered for the  $\beta\text{lg}/D_3$  complex in the absence and presence of pancreatin, respectively. These results indicate that in the presence of proteases on top of trypsin and chymotrypsin, the amount of  $D_3$  recovered was about four times higher for the  $\beta\text{lg}/D_3$  complex than without  $\beta\text{lg}$ .

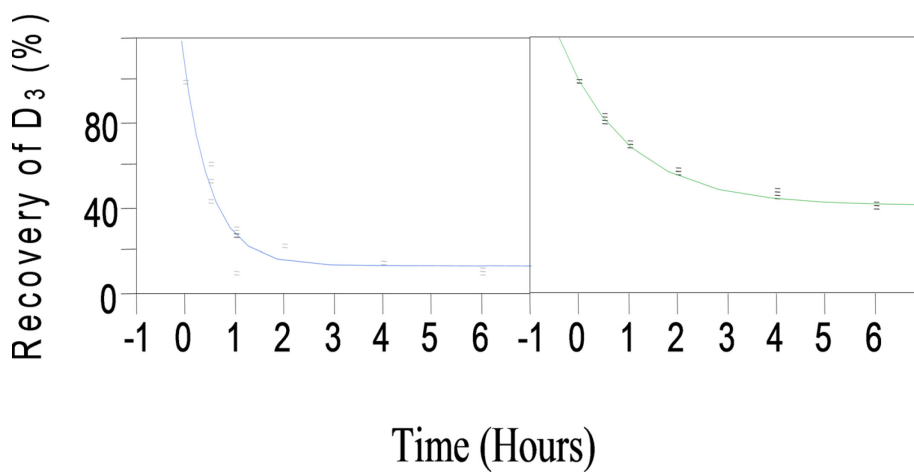
The findings presented in this study are important because  $\beta\text{lg}$  is well known to undergo structural modification at the intestinal pH, which makes it susceptible to intestinal enzymes, both of which are present in pancreatin [204-206]. It can be suggested from the present study that the binding of  $D_3$  to  $\beta\text{lg}$  results in a reciprocal beneficial effect regarding its stability in SIF and its resistance to proteolysis. The increased resistance of  $\beta\text{lg}$  to pancreatin might be attributed to the strong binding affinity of  $D_3$  to the central calyx and to the surface hydrophobic pocket, as was observed for fatty acids [207].

**A**



$\beta$ Ig/D3 complex (—) :  $y = 41.64 + 57.52^{-0.72 \times \text{Time (Hours)}}$

D3 (—) :  $y = 13.93 + 86.60^{-1.80 \times \text{Time (Hours)}}$



**B**

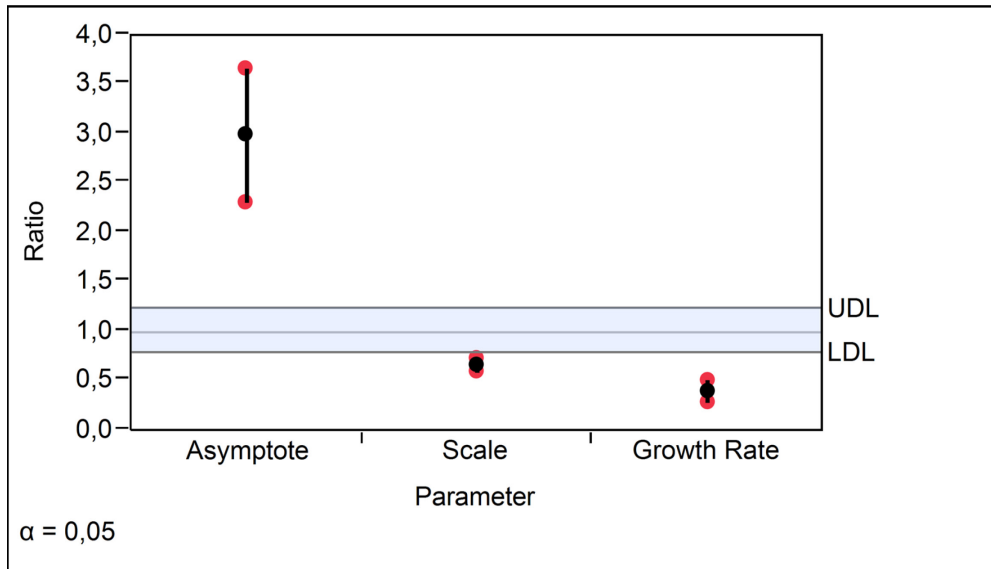


**Figure 5.4. Stability of  $D_3$  and the  $D_3/\beta Ig$  complex in Simulated Intestinal Fluid with pancreatin at pH 6.8, 37°C (USP-2 paddle apparatus). A: Graph of the intestinal stability and B. The equivalence between  $D_3$  and the  $\beta Ig/D_3$  complex.**

The structure of  $\beta$ lg is likely stable at gastric pH and resistant to pepsin digestion because of increased hydrogen bonding which limits the access of pepsin to its target sites located in the hydrophobic cavity [208, 209]. In previous work, the  $\beta$ lg/D<sub>3</sub> complex was proven stable at gastric pH [200]. Therefore, it can be assumed that the  $\beta$ lg/D<sub>3</sub> complex would also be resistant to pepsin digestion as was observed by other hydrophobic ligands [210, 211]. In the present study, the  $\beta$ lg/D<sub>3</sub> complex was shown to be resistant throughout the GI tract in the presence of proteolytic enzymes. Hence, one can suggest that the  $\beta$ lg/D<sub>3</sub> complex-containing products may represent a good vehicle to increase the uptake of D<sub>3</sub>. To test this assertion, the permeability of the  $\beta$ lg/D<sub>3</sub> complex was assessed *in vitro*, and an *in vivo* experiment was carried out to evaluate the efficiency of the  $\beta$ lg/D<sub>3</sub> complex in improving the bioavailability of D<sub>3</sub>.

#### **5.4.4. *In vitro* study of the permeability of the $\beta$ lg/D<sub>3</sub> complex**

The permeability of the  $\beta$ lg/D<sub>3</sub> complex was studied using CaCo-2 cells, used as an *in vitro* model for human intestinal absorption. The amount of D<sub>3</sub> (21.17  $\mu$ g) used was reduced in order to maintain cell viability. During the sampling periods (60 and 120 min) as well as at the end of the experiment, it was not possible to detect D<sub>3</sub> neither at the apical site nor at the basolateral media of the monolayer. This result is not surprising given that D<sub>3</sub> is highly sensitive to oxygen and that considerable manipulation of the cell culture plates occurred during the measurement of the TEER and sampling periods. Thus, in the present study it is not known if the mechanism of the transepithelial passage of D<sub>3</sub> was due to paracellular diffusion, transcellular diffusion, or to transcellular carrier-mediated pathways [212]. However, it is well documented that D<sub>3</sub> is incorporated into chylomicrons and transported from the intestines via the lymphatic system into the bloodstream. Subsequently, it binds with vitamin D-binding protein, which later transports it to the liver where it is converted to the physiologically-active form 25(OH)D<sub>3</sub> [102]. Therefore, the transcellular carrier-mediated pathway might be the

most probable transport route for D<sub>3</sub> to cross the intestinal epithelial barrier, as was shown for oleic acid, cholesterol, phospholipids and vitamin E [213].

It is important to mention that βlg was found at the basolateral site (data not shown), which might imply that the βlg/D<sub>3</sub> complex may have crossed the monolayers. Indeed, βlg was proven to enhance the intestinal uptake of retinol most probably because of the presence of a receptor for βlg at the brush border membrane of the intestinal cells [214]. Accordingly, it can be suggested that βlg might also carry D<sub>3</sub> through the intestinal epithelial barrier. Furthermore, the initial value of TEER significantly decreased ( $p < 0.001$ ) immediately after the βlg/D<sub>3</sub> complex was directly added onto the apical side of the cells, indicating some loosening of the monolayers (Table 5.1).

**Table 5.1. TEER of the Caco-2 cells monolayers**

Treatment	<sup>a</sup> Values of the TEER ( $\Omega \cdot \text{cm}^2$ )						
	TEER measurement periods (hours) before and after the experiment						
	- 24	0	0.5	1	1.5	2	48
<b>D<sub>3</sub></b>	664 ± 35	162 ± 67	124 ± 1	115 ± 2	114 ± 0.4	106 ± 0.4	442 ± 0.8
<b><math>\beta</math>Ig/D<sub>3</sub> complex</b>	887 ± 119	234 ± 3	133 ± 2	124 ± 2.3	125 ± 1.7	116 ± 1.5	619 ± 89

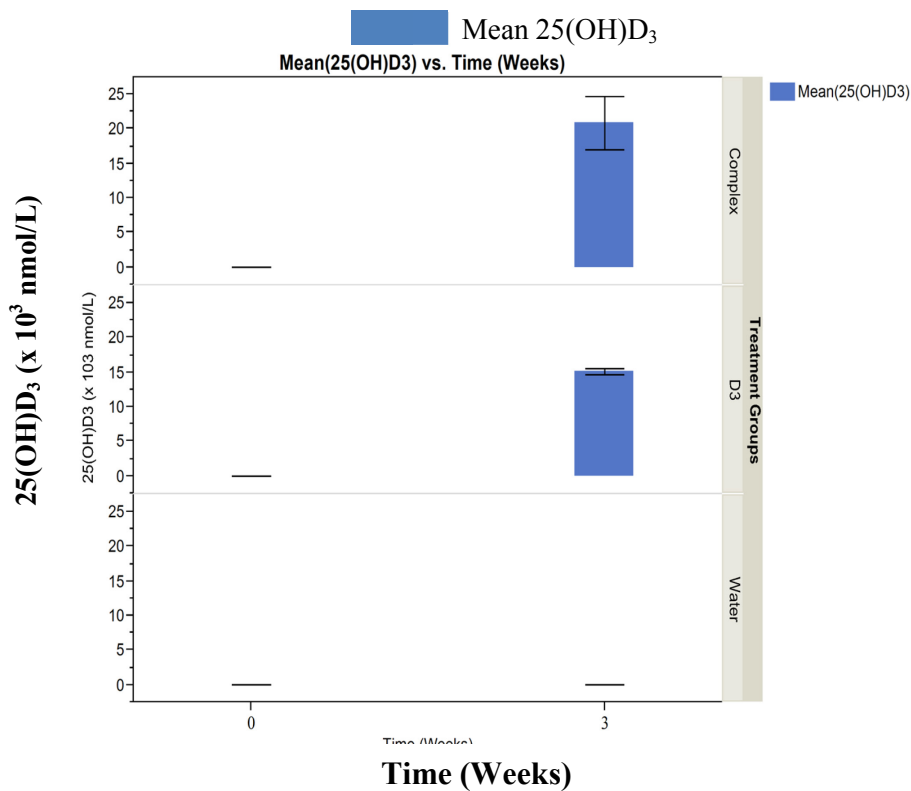
<sup>a</sup>Values are expressed as mean ± SEM

This opening of the tight junctions may have allowed the  $\beta$ lg/D<sub>3</sub> complex through the monolayers even though D<sub>3</sub> was not detected in the basolateral media. Interestingly, there was no significant difference between the values of TEER from 0 to 2 h during the experiment ( $p = 0.24$ ) for the free D<sub>3</sub>. This result shows that the passage of the free D<sub>3</sub> does not result in any loss of integrity of the monolayers; rather, it could confirm the transcellular carrier-mediated pathway. At 48 h after the experiment, the values of the TEER increased to  $442 \pm 0.8$  and  $619 \pm 89 \Omega \cdot \text{cm}^2$  for D<sub>3</sub> and  $\beta$ lg/D<sub>3</sub> complex, respectively (Table 5.1). About four days after the experiment, the values of TEER further increased to levels similar to that of the initial values (data not shown), indicating that the treatment was not toxic for the Caco-2 cells [212]. Given that the mechanism of the passage of D<sub>3</sub> through the monolayers was not clearly distinguished in the present study, an *in vivo* experiment using rats was undertaken to provide further insight into the effects of  $\beta$ lg/D<sub>3</sub> complex on the uptake and bioavailability of D<sub>3</sub>.

#### **5.4.5. *In vivo* study of the intestinal absorption of the $\beta$ lg/D<sub>3</sub> complex**

Male rats received a dose of 77  $\mu$ g by gavage corresponding to 3080 IU of D<sub>3</sub> every day for three weeks. All the animals survived at the end of the experiment, with a total weight gain ranging from  $17.5 \pm 4.73$  to  $20.8 \pm 5.5$  g per rat. The biomarker of D<sub>3</sub> was quantified in plasma samples of the three different groups of rats consisting of the control (water), D<sub>3</sub> and  $\beta$ lg/D<sub>3</sub> complex (Figure 5.5).

**A**



**B**

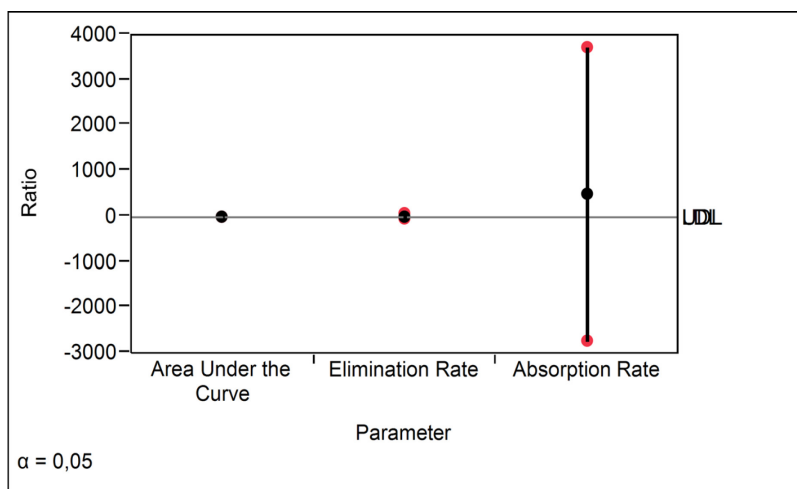


**Figure 5.5 A.** Mean 25(OH)D<sub>3</sub> in the plasma samples of the rats receiving water (control), D<sub>3</sub> and the  $\beta$ Ig/D<sub>3</sub> complex. Each error bar is constructed using 1 standard error from the mean (JMP, SAS Institute, Inc.). **B.** The equivalence between D<sub>3</sub> and the  $\beta$ Ig/D<sub>3</sub> complex.

The pharmacokinetic model with one compartment oral dose was selected to model the concentration of 25(OH)D<sub>3</sub> in the rats. The parameter estimates (data not shown) were used to compute the values of 25(OH)D<sub>3</sub> at week 3, which were 15.12 x 10<sup>3</sup> nmol/L for D<sub>3</sub> and 20.26 x 10<sup>3</sup> nmol/L for the βlg/D<sub>3</sub> complex. The experimental data obtained at the end of the animal study were 15.12 ± 1.0 x 10<sup>3</sup> nmol/L for D<sub>3</sub> and 20.9 ± 8.61 x 10<sup>3</sup> nmol/L for the βlg/D<sub>3</sub> complex. The great similarity between the experimental data and the results from the curve-fitted model formula confirms the accuracy of the pharmacokinetic model.

At the end of the study, there was a striking difference in the plasma concentration of the biomarker 25(OH)D<sub>3</sub> between the control and the rats fed D<sub>3</sub> and the βlg/D<sub>3</sub> complex (Figure 5.5A). While the mean concentration of 25(OH)D<sub>3</sub> was 28 ± 0.0 nmol/L for the control, it was 15.12 ± 1.0 x 10<sup>3</sup> nmol/L for D<sub>3</sub> and 20.9 ± 8.61 x 10<sup>3</sup> nmol/L for the βlg/D<sub>3</sub> complex. This discrepancy is probably due to the fact that the rats were fed a commercial standard diet that was exposed to 12 h of light per day and to air, which are damaging to D<sub>3</sub>. Conversely, the test solutions consisting of D<sub>3</sub> and the βlg/D<sub>3</sub> complex were effectively protected from light and the access to oxygen was reduced to a minimal. All the rats were fed a commercial standard diet that contained D<sub>3</sub> at a dose of 1000 UI/Kg of diet. The average daily feed intake ranges from 25 to 30 g/rat [202]. Hence, the animals in the control group may have received less D<sub>3</sub> than 30 UI per day, taking into consideration losses from degradation. Although the rats in the control group received between 120 and 205 times less D<sub>3</sub> than the ones in the test groups, the approximately 1000 fold increase in the concentration of 25(OH)D<sub>3</sub> remains important.

The equivalence test represented in Figure 5B indicates that the concentration of 25(OH)D<sub>3</sub> is significantly higher for the rats fed the βlg/D<sub>3</sub> complex than those fed free D<sub>3</sub>. This finding is important since it demonstrates that the βlg/D<sub>3</sub> complex increased the bioavailability of D<sub>3</sub>. In light of these considerations, the present study advocates the use of the βlg/D<sub>3</sub> complex in the fortification of dairy products and a wider range of foods with low fat content. In fact, there are an increasing

number of reports indicating that current supplementation and food fortification practices are not sufficient to maintain the normal range of circulating 25(OH)D<sub>3</sub> in populations with reduced exposure to sun light [149]. Wagner and co-workers have reported that during cheese fortification with D<sub>3</sub>, the binding of the vitamin to milk serum proteins affects its bioavailability and thus represents a loss of profit for the dairy industry [15]. However, the data generated in the current study demonstrate that complexation with the major bovine milk protein βlg increases the bioavailability of D<sub>3</sub>.

## 5.5. Conclusion

The complexation of D<sub>3</sub> with βlg improved the stability of the vitamin in regular and excessive storage conditions. The βlg/D<sub>3</sub> complex was resistant to proteases in simulated intestinal fluid, which implies that binding of D<sub>3</sub> to βlg has a dual and reciprocal protective effect on both the molecules. Furthermore, the bioavailability of D<sub>3</sub> was significantly higher for the rats fed the βlg/D<sub>3</sub> complex than the rats that received the free vitamin. The fortification of milk products and low-fat content foods with the βlg/D<sub>3</sub> complex could be recommended as a possible mean to improve the intake of this vitamin. Consequently, the βlg/D<sub>3</sub> complex-containing products could be manufactured accordingly to ensure delivery of proper amounts of D<sub>3</sub> to consumers. An improved bioavailability of D<sub>3</sub> may increase its skeletal and many non-skeletal effects on health, including its beneficial actions on the cardiovascular system, lung immunity, and respiratory diseases [184], and against various types of cancers affecting the breast and colon [181, 182].

## **5.6. Acknowledgements**

This work was supported by the Natural Sciences and Engineering Research Council of Canada (NSERC) through the Vanier Canada Graduate Scholarships (F. Diarrassouba) and the Canada research chair in protein, biosystem and functional food physical chemistry. The authors would like to thank Mr Pascal Dubé, Ms Diane Gagnon (Institut de recherche sur les nutraceutiques et les aliments fonctionnels, Université Laval, Québec, QC, Canada) and the EA-CIDAM's team members (Biopharmacie lab, Faculté de Pharmacie, Clermont-Ferrand, France).

## Contextual transition

The following chapter corresponds to the fourth specific objective of the study. The hypothesis is that the  $\beta$ -lactoglobulin – vitamin D<sub>3</sub> complex can auto-associate under mild acidic condition to form a food grade matrix within which, vitamin D<sub>3</sub> can be encapsulated at high efficiency. The rationale for the auto-association of the  $\beta$ -lactoglobulin – vitamin D<sub>3</sub> complex relies on the functional properties of the protein including its ability to auto-aggregate under varying conditions such as pH and protein concentration. This work reports the formation and optimization of a  $\beta$ -lactoglobulin – based coagulum for the encapsulation of vitamin D<sub>3</sub>. The auto-aggregation of the  $\beta$ -lactoglobulin – vitamin D<sub>3</sub> complex was triggered by mild acidification. The stability of both the entrapped vitamin D<sub>3</sub> and coagulum were evaluated during shelflife and *in vitro* digestion. The bioavailability of vitamin D<sub>3</sub> was assayed by performing an *in vivo* experiment using rats.

## CHAPTER 6

# Increased Water Solubility, Stability and Bioavailability of Vitamin D3 Upon Sequestration in $\beta$ -lactoglobulin - Based Coagulum

A version of this manuscript was submitted to the Journal of Controlled Release

By :

Fatoumata Diarrassouba<sup>a</sup>, Ghislain Garrait<sup>b</sup>, Gabriel Remondetto<sup>b</sup>, Pedro Alvarez<sup>a</sup>,  
Eric Beyssac<sup>b</sup> and Muriel Subirade<sup>a</sup>

<sup>a</sup>Chaire de recherche du Canada sur les protéines, les bio-systèmes et les aliments fonctionnels, Institut de recherche sur les nutraceutiques et les aliments fonctionnels (INAF/STELA), Université Laval, Québec, QC, Canada.

<sup>b</sup>EA-CIDAM, Lab Biopharmacie, Faculté de Pharmacie, 28 Place Henri Dunant, 63001, Clermont-Ferrand, France.

<sup>c</sup>Centre de recherche et développement, Agropur Coopérative. 4700 rue Armand Frappier, St-Hubert, QC, J3Z 1G5, Canada.

## 6.1. Abstract

Evidence strongly suggests that the fortification of staple foods is insufficient to prevent vitamin D<sub>3</sub> deficiency among population groups living in northern altitudes regardless of age or skin type, especially when exposure to sun light is reduced. This work reports the sequestration of D<sub>3</sub> within a water soluble matrix formed using the major bovine whey  $\beta$ -lactoglobulin ( $\beta$ lg). The self-aggregation of the  $\beta$ lg/D<sub>3</sub> complex was triggered by mild acidification using glucono- $\delta$ -lactone. The capacity of the  $\beta$ lg-based coagulum to increase the long term stability of D<sub>3</sub> in cold storage and upon exposure to intensive UV-light was evaluated. Additionally, the intestinal stability of the D<sub>3</sub>-enriched coagulum in the presence and absence of proteases was determined using the USP-2 apparatus. Most importantly, the impact of the sequestration of D<sub>3</sub> within the matrix of  $\beta$ lg-based coagulum on its bioavailability was determined *in vivo* with force-fed rats. When the pH reached the *pI* of  $\beta$ lg, coagulation of the protein was initiated, ending at pH 4.7 and concomitantly entrapping D<sub>3</sub> with an encapsulation efficiency (EE) of 94.5  $\pm$  1.8 %. Consequent to this high EE, the water solubility of D<sub>3</sub> significantly increased. Moreover, the sequestration of D<sub>3</sub> in the  $\beta$ lg-based coagulum significantly improved the long-term storage and UV-light stability of D<sub>3</sub> ( $p < 0.0001$ ). The  $\beta$ lg-based coagulum was not rapidly disrupted by the proteases in the intestines, leading to a slow release of D<sub>3</sub> and increased uptake of D<sub>3</sub>. As a result, there was a striking enhancement of the bioavailability of D<sub>3</sub> in rats fed the D<sub>3</sub>-loaded  $\beta$ lg-based coagulum compared to those fed the control consisting of D<sub>3</sub> or water ( $p < 0.0001$ ). To our knowledge, this is the first report of the use of  $\beta$ lg-based coagulum to enhance the uptake and bioavailability of D<sub>3</sub>.

## 6.2. Introduction

The beneficial effects of higher intake of vitamin D<sub>3</sub> (D<sub>3</sub>) have been well established in countless skeletal and extra-skeletal diseases [102, 215]. The annual economic burden of D<sub>3</sub> deficiency in Canada has been estimated to be about 14.4 \$ billion, which includes direct costs such as hospitals, drugs, physician care, as well as indirect costs such as mortality, long-term diseases and transient disability [215]. In Western Europe, adequate D<sub>3</sub> status is associated with an estimated reduction of 187 billion € per year [216]. The main indicator for D<sub>3</sub> status is serum 25-hydroxyvitamin D<sub>3</sub> (25(OH)D<sub>3</sub>) [15], which is generally considered optimal above 50 to 72 nmol/L, despite some controversy about this threshold [102]. Reports indicate that benefits in disease reduction may start from a mean serum 25(OH)D<sub>3</sub> level above 100 nmol/L [215, 216]. However, for most people living in northern latitudes, irrespective of age or skin type, this threshold is not reached when exposure to sun light is minimum [102, 149, 187, 217]. Despite the fortification of staple foods such as fluid milk, margarine or breakfast cereals, the elevated prevalence of hypovitaminosis D<sub>3</sub> indicates the inability of food fortification programs to achieve adequate intake [187]. In addition to insufficient sun exposure and dietary intake of fortified foods, this failure can also be ascribed to the fact that the retention of D<sub>3</sub> in food is problematic [218]. As such, overages of 30% for D<sub>3</sub> are usually considered consistent with good manufacturing practices by some trade associations [219]. However, this decision does not seem to be sufficient to maintain appropriate levels of D<sub>3</sub> at the time of ingestion, indicating that the incorporation of adequate amounts of D<sub>3</sub> in foods is indeed challenging. D<sub>3</sub> is fat-soluble, requiring the use of lipidic foods for fortification purposes, which is not compatible with consumers' demand for foods with low fat content. In addition, because D<sub>3</sub> is highly sensitive to light and oxygen it is easily degraded. Consequently, deviation of label declarations from actual amounts of D<sub>3</sub> in foods are common [219].

Attempts have been made to incorporate D<sub>3</sub> into other dairy products such as cheese for improved retention and stability. However, prodigious amounts of D<sub>3</sub> in

powder, emulsion or oil forms are used to fortify milk with low yields in the cheese, when compared to the initial concentration incorporated into the milk batch [15, 218, 220]. This implies great profit losses for the industry, given the fact that to date, cheese fortification does not improve the bioavailability of D<sub>3</sub> compared to supplements [15]. Important losses of D<sub>3</sub> may occur due to its affinity with milk whey proteins, which are considered as cheesemaking waste products [15, 218]. Bovine milk  $\beta$ -lactoglobulin ( $\beta$ lg) accounts for about 60 % of the proteins in whey [221]. Recent report indicates that  $\beta$ lg binds D<sub>3</sub> to form a complex that is resistant to pH variation from 1.5 to 8, including that prevailing in the gastro-intestinal tract [222]. Most importantly, the highest stability of the  $\beta$ lg/D<sub>3</sub> complex was observed at pH 5, close to the isoelectric point (pI) of the protein. Therefore, in the current work, acid coagulation of the  $\beta$ lg/D<sub>3</sub> complex was triggered by slowly decreasing the pH close to the pI of  $\beta$ lg using a mild acidifying agent. The  $\beta$ lg/D<sub>3</sub> complex was also shown to significantly improve the solubility of D<sub>3</sub>, implying that higher amounts of the vitamin can be incorporated within the coagulum matrix [222]. Hence, the D<sub>3</sub>-fortified coagulum can later be incorporated into cheese or other dairy products such as yogurt during processing to improve the retention, uptake and bioavailability of D<sub>3</sub>. This may allow cheese fortification with realistic amounts of D<sub>3</sub> [218, 223]. The aim of the present work was to investigate the capacity of the  $\beta$ lg-based coagulum, produced in a mild acidic condition, to entrap and retain D<sub>3</sub> within the protein matrix. The impact of the sequestration of D<sub>3</sub> in the coagulum on the long-term stability during cold storage and upon light irradiation was evaluated. The intestinal stability of the D<sub>3</sub>-enriched coagulum and its resistance to proteolytic activity were examined *in vitro*. Most importantly, an *in vivo* experiment using rats was carried out to study the impact of the sequestration of D<sub>3</sub> within the coagulum matrix on the bioavailability of D<sub>3</sub> by dosage of serum 25(OH)D<sub>3</sub> levels in animals. To our knowledge, this work is the first report of the use of  $\beta$ lg-based coagulum to enhance the solubility, stability and bioavailability of D<sub>3</sub> for improved D<sub>3</sub> encapsulation.

## **6.3. Experimental Section**

### **6.3.1. Materials**

$\beta$ Ig (B variant, purity  $\geq 90$  % PAGE) from bovine milk, D<sub>3</sub> (purity  $\geq 98$  %, HPLC) and glucono- $\delta$ -lactone (GDL, USP specified) were obtained from Sigma–Aldrich Chemical Company (St. Louis, MO, USA) and used without further purification. Methanol (MeOH, HPLC grade) and the Trifluoroacetic Acid (TFA) were purchased from EMD International (Gibbstown, NJ, USA).

### **6.3.2. Sample preparation**

$\beta$ Ig stock solution concentrated at 20 % (w/v) was made daily by dissolving  $\beta$ Ig in MilliQ water under mild stirring conditions for 2 h at room temperature and then stored overnight at 4°C to allow complete rehydration. Stock solutions of D<sub>3</sub> concentrated at 1 mM were prepared daily by dissolving 10 mg of the vitamin in 25 mL of methanol followed by a dilution with MilliQ water to an initial concentration of 220  $\mu$ M [188]. All D<sub>3</sub>-containing solutions were protected from light by preparing them in a dark room and further protected using an aluminum foil wrapping

### **6.3.3. Encapsulation of D<sub>3</sub> in the $\beta$ Ig-based coagulum**

The  $\beta$ Ig/D<sub>3</sub> coagulum was firstly prepared by mixing the same volume of  $\beta$ Ig and D<sub>3</sub> solutions in order to obtain a final concentration of 110  $\mu$ M for the vitamin. The  $\beta$ Ig/D<sub>3</sub> mixture was then incubated for 2 h at room temperature, before adding GDL at a concentration of 2 % (w/v) for an additional 2 h of incubation. The head space in the conical tubes containing the samples was reduced to minimum in order to limit oxidative degradation of D<sub>3</sub> by the air. The coagulum was completely formed when phase separation occurred around pH 4.7, with the creamy-colored

coagulum at the bottom layer of the conical tube and clear serum at the top. The serum was separated from the coagulum after centrifugation at 15,500 x g/5 min and the coagulum was disrupted by rapidly decreasing the pH below the pI of  $\beta$ lg using HCL [17]. D<sub>3</sub> was determined in both fractions by HPLC, as previously described [200]. The encapsulation efficiency (EE) was computed using the following formula:

$$EE (\%) = \frac{\text{Total amount of D3 in the coagulum}}{\text{Total amount of D3}} \times 100$$

#### **6.3.4. Stability of D<sub>3</sub> during long term storage at 4 °C**

The stability of D<sub>3</sub> entrapped in the coagulum at 4 °C was determined over five weeks. The initial concentration of encapsulated D<sub>3</sub> was determined after 24 h, as described in section 6.3.3. Samples corresponding to weeks 1 to 5 were stored at 4 °C in a fridge. Each week, a sample was withdrawn for determination of the amount of D<sub>3</sub> remaining in solution by HPLC, as described elsewhere [200]. Solutions of D<sub>3</sub> diluted in MilliQ water were prepared and analyzed under the same conditions.

#### **6.3.5. Stability of D<sub>3</sub> to UV-light irradiation**

The D<sub>3</sub>-containing coagulum and D<sub>3</sub> solutions were exposed to UV light (254 nm, 15 W) in order to assess the UV-light stability of D<sub>3</sub> over 24 h [130]. At each sampling time consisting of t 0, 1, 2, 4, 6, 8, 10 and 24 h, the amount of D<sub>3</sub> remaining in the microspheres was determined, as indicated in the previous sections.

### 6.3.6. Kinetic release of D<sub>3</sub> in simulated intestinal fluid

The release of D<sub>3</sub> in simulated intestinal fluid (SIF) was investigated using a USP-2 paddles apparatus (SOTAX Corporation, Westborough, MA, USA). The release media consisted of the simulated intestinal fluid (SIF) as described in the US Pharmacopeia with or without 1.0 % pancreatin (w/v) at pH 6.8. Each of the solutions of D<sub>3</sub>-enriched coagulum or D<sub>3</sub> at the same concentration was incubated in one of two release media (100 mL) with continuous agitation (at ~ 50 rpm) at 37 °C [224]. Samples withdrawn at half-hour or 2-h intervals over 6 hours were centrifuged (5,000 x *g*/5 min) and the concentration of D<sub>3</sub> in the supernatant was determined [200]. A control with and without enzyme was also run.

### 6.3.7. *In vivo* study of the intestinal absorption of the D<sub>3</sub> containing βlg/Lyso

Animal studies were conducted at the 'Unité de Stabulation Animale, Ethic Committee-CE-42-12' (Université d'Auvergne, Clermont-Ferrand, France). Adult male Wistar rats (*n* = 25; Elevage Dépré, St. Doulichard, France) weighing 300 ± 20 g at the beginning of the experiment were used. Housing characteristics, accommodation and the average feed intake are described elsewhere [19]. After the acclimation period, two or three rats were housed per cage for three weeks. The animals had access to feed and water *ad libitum*. The rats (*n* = 15) were divided into three groups (*n* = 5) each receiving one of the treatments consisting of MilliQ water (control), D<sub>3</sub> or D<sub>3</sub>-enriched βlg-based coagulum with the same final concentration of D<sub>3</sub> (110 μM or 77 μg). Blood samples were collected at t 0 after three weeks in 0.5 mL conical tubes pre-coated with 10 μL of sodium heparin (0.1 IU). The plasma was separated by centrifugation at 1000 x *g* for 10 min. Plasma samples were stored at - 20 °C until analysis of 25(OH)D<sub>3</sub> in rat plasma was performed using the 25-Hydroxy Vitamin D Direct EIA kit (IDS Diagnostics, Fountain Hills, AZ, USA) according to the manufacturer's instructions. Additionally,

the concentration of 25(OH)D<sub>3</sub> in rats fed the D<sub>3</sub>-enriched βlg-based coagulum was compared to that of rats fed the βlg/D<sub>3</sub> complex, which is the basic building block for the formation of D<sub>3</sub>-entrapped coagulum. The formation of the βlg/D<sub>3</sub> complex is described elsewhere [19].

### **6.3.8. Statistical analysis**

Statistical analysis was performed using SAS version 12.0 (SAS Institute Inc., Cary, NC, USA). ANOVA and the Least Significant Difference (LSD) were used to determine differences among means and the significance level was fixed at  $p < 0.05$ . All measurements were performed in triplicate.

## **6.4. Results and Discussion**

### **6.4.1. Encapsulation efficiency of D<sub>3</sub> in the βlg-based coagulum**

The bovine milk βlg was used to prepare a coagulum by mild acidification. Coagulation started when the pH reached the  $pI$  of the protein and was terminated at pH 4.7. The capacity of the βlg-based coagulum to encapsulate D<sub>3</sub> was investigated by inducing the auto-association of the βlg/D<sub>3</sub> complex using GDL at room temperature. The βlg-based coagulum successfully entrapped D<sub>3</sub> and the encapsulation efficiency (EE) was  $94.5 \pm 1.8 \%$ , the remaining D<sub>3</sub> being recovered in the serum. Similar EE was also obtained for higher amounts of D<sub>3</sub>, ranging from 250 μM to 1 mM (data not shown). The EE level obtained in the current work is superior to that obtained with zein-based nanoparticles without (52.2 %) and with (71.5 %) a carboxymethyl chitosan coating, which increased to 87.9 % after calcium addition [225]. Alginate-based nanoparticles with a hydrophobic core were used to encapsulate D<sub>3</sub> with a resulting loading efficiency ranging from  $45.8 \pm 1.55 \%$  to  $67.6 \pm 2.76$  [226]. More recently, an EE of 96.9 % was obtained using zein-

based hydrogel beads, which is closer to that of the current work. However, this elevated EE required the use of the toxic crosslinking agent glutaraldehyde in addition to a 30 % alcohol concentration, which are not compatible with food administration [227].

In the current work, water soluble  $\beta$ lg-based coagulum was used to entrap  $D_3$  at a high EE using food grade GDL. As a result, the solubility of the fat-soluble vitamin increased upon sequestration within the protein matrix. Therefore, the  $D_3$  enriched coagulum can be used to increase the uptake of the vitamin in dairy products such as cheese or yogurt and other food types with a zero to low fat content in fortification programs. Gelation of whey proteins and  $\beta$ lg can be induced by salt, pressure, temperature or acidification [17]. The rate of gelation of  $\beta$ lg above the critical concentration increases exponentially and is irreversible at higher temperature [17]. It is important to note that in the current work, irreversible gelation of native  $\beta$ lg occurred at refrigerated temperature (data not shown) while the milky-colored coagulum was formed at room temperature. Although the mechanisms underlining the irreversible cold gelation of non-denatured  $\beta$ lg are still under investigation,  $D_3$  may have played a major role in the cold gelation of native  $\beta$ lg.  $D_3$  is highly sensitive to environmental conditions including light irradiation and oxygen. Therefore, before proposing the  $D_3$ -loaded  $\beta$ lg-based coagulum as a functional food ingredient, it is important to carry out stability studies during long term storage conditions.

#### **6.4.2. Impact of the $\beta$ lg-based coagulum on the long term stability of $D_3$**

The stability of the free  $D_3$  during storage under refrigerated conditions was compared to that of the vitamin sequestered in the  $\beta$ lg-based coagulum over five weeks (Figure 6.1).

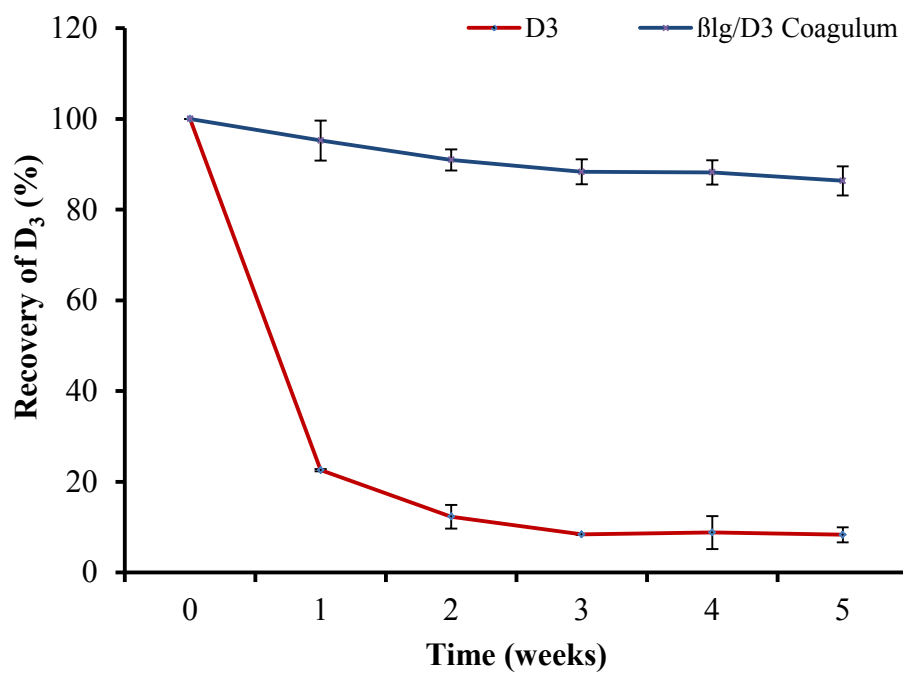


**Figure 6.1. Long term stability of D<sub>3</sub> and the D<sub>3</sub>-loaded  $\beta$ lg-based coagulum in refrigerated conditions (4°C).**

All the conical tubes used during the experiment were filled with D<sub>3</sub>-containing solutions to reduce the head space in order to minimize oxidative degradation. Nevertheless, after the first week of storage in the fridge, only 22.5 ± 0.2 % of the free D<sub>3</sub> remained in solution (Figure 6.1). There was over 91 % of vitamin loss after the third week in the fridge and at the end of the five week period only 8.3 ± 1.7 % of the free D<sub>3</sub> remained in solution (Figure 6.1). Compared to the free vitamin, the D<sub>3</sub> sequestered within the βlg- based coagulum was significantly more stable ( $p < 0.0001$ ). At week 1, 95.2 ± 4.4 % of the D<sub>3</sub> was intact (Figure 6.1). This amount decreased to 88.3 ± 2.7 % at week 3 and after five weeks at 4°C, 86.3 ± 3.2 % of D<sub>3</sub> still remained in the coagulum, which represents a loss of only 13.6 % (Figure 6.1). The coagulum demonstrated an important capacity to protect D<sub>3</sub> and prolong its shelf-life during cold storage.

The recovery of D<sub>3</sub> in the coagulum was 10-fold higher than with the unprotected vitamin and was improved compared to casein micelles [228]. The protective effect of the coagulum can be ascribed in part to the antioxidant activity of the free thiol groups of βlg [129]. In fact, the coagulum was prepared using a final βlg concentration of 10 % (w/v), which certainly encompasses a large number of free thiol groups. In addition, mobility of D<sub>3</sub> entrapped within the coagulum matrix might be impaired, thus provoking the immobilization of the vitamin, which on one hand reduces its reactivity but also reduces access of oxidizing agents to D<sub>3</sub> [20]. This finding implies that sequestration of the D<sub>3</sub> in the βlg-based coagulum can significantly improve the retention of the vitamin and protect it from oxidative degradation over time, which may consequently greatly increase its uptake. Exposure to UV-light over time also greatly damages D<sub>3</sub>-containing food products. It is thus important to evaluate the efficiency of the coagulum in protecting the vitamin during storage.

#### **6.4.4. Impact of the $\beta$ lg-based coagulum on the UV-light stability of D<sub>3</sub>**

The photochemical stability of unprotected D<sub>3</sub> was compared to that of the vitamin sequestered within the  $\beta$ lg-based coagulum matrix during 24 h of intensive UV-light irradiation. As shown in Figure 6.2, the protection effect of the coagulum on D<sub>3</sub> during UV-light irradiation was important.

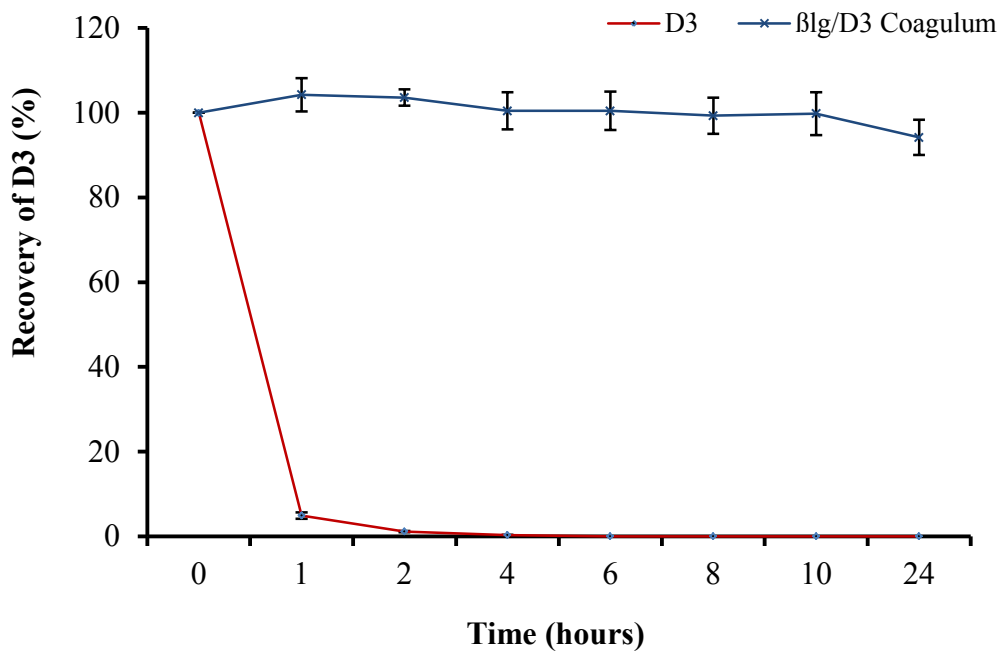


**Figure 6.2.** Photo-degradation of D<sub>3</sub> and the D<sub>3</sub>-loaded βlg-based coagulum upon exposure to UV-light ( $\lambda = 254$  nm).

Only  $5.0 \pm 0.7$  % of the unprotected  $D_3$  remained in solution after the first hour of exposure to light and after the second hour, almost 99 % of the free vitamin was degraded. The  $D_3$  entrapped in the coagulum remained intact even after 10 h of irradiation (Figure 6.2). After 24 h of irradiation,  $94.2 \pm 4.1$  % of  $D_3$ -entrapped in the  $\beta$ lg-based coagulum was still intact. The good protective effect obtained in the current work is higher than that reported in the literature [225]. This important shielding effect against photochemical degradation can be ascribed to several factors. The abundant of aromatic side chains and double bonds in  $\beta$ lg-based coagulum might absorb much of the UV-light and, thus impair the absorption of  $D_3$  [20, 225]. Furthermore, the physical immobilization of  $D_3$  within the coagulum matrix reduces its reactivity and restricts its access to oxidizing agents, as explained above. The present work demonstrates the efficiency of the  $\beta$ lg-based coagulum in protecting and improving the stability of  $D_3$  during long term storage in the cold and upon intensive UV-light irradiation, all of which occurs before ingestion. However, after ingestion, proteolytic enzymes prevailing in the stomach and intestines might destabilize  $\beta$ lg and thus affect the ability of the coagulum to retain  $D_3$  within the coagulum matrix. Therefore, it is important to study the behavior of the  $D_3$ -entrapped  $\beta$ lg-based coagulum during transit in the gastrointestinal (GI) tract.

#### **6.4.5. Impact of the $\beta$ lg-based coagulum on the intestinal kinetic release of $D_3$**

In the present work,  $D_3$  was entrapped in the  $\beta$ lg-based coagulum by inducing the self-aggregation of the  $\beta$ lg/ $D_3$  complex upon mild acidification close to the  $pI$  of the protein (pH 4.7). The  $D_3$ -entrapped  $\beta$ lg-based coagulum might persist in the stomach due to the fact that the  $\beta$ lg/ $D_3$  complex is stable at the gastric pH (Chapter 4, Section 4.4.2). This is further supported by the fact that the structure of native  $\beta$ lg remains intact under the acidic conditions and pepsin concentrations in the stomach [54]. Furthermore, after food ingestion, the pH of the stomach is between 4.5 to 6.0, which encompasses the pH of the coagulum [86]. Therefore, the present

work assumed that when administrated post-prandially, the  $\beta$ lg-based coagulum might not be significantly affected by the gastric pH, with or without pepsin and thus, can remain stable in the stomach. However, this may not be true for the intestinal pH in the presence of the proteases.

The capacity of the  $\beta$ lg-based coagulum to release  $D_3$  in the simulated intestinal fluid (SIF) in the presence and absence of pancreatin was evaluated. Figure 6.3 represents the kinetic release of the unprotected  $D_3$  and  $D_3$ -entrapped in the  $\beta$ lg-based coagulum during digestion. The integrity of the coagulum was well preserved, with a loss of only  $3.7 \pm 2.7$  % and  $17.4 \pm 0.1$  % in presence and absence of pancreatin, respectively, after six hours in SIF (Figure 6.3).

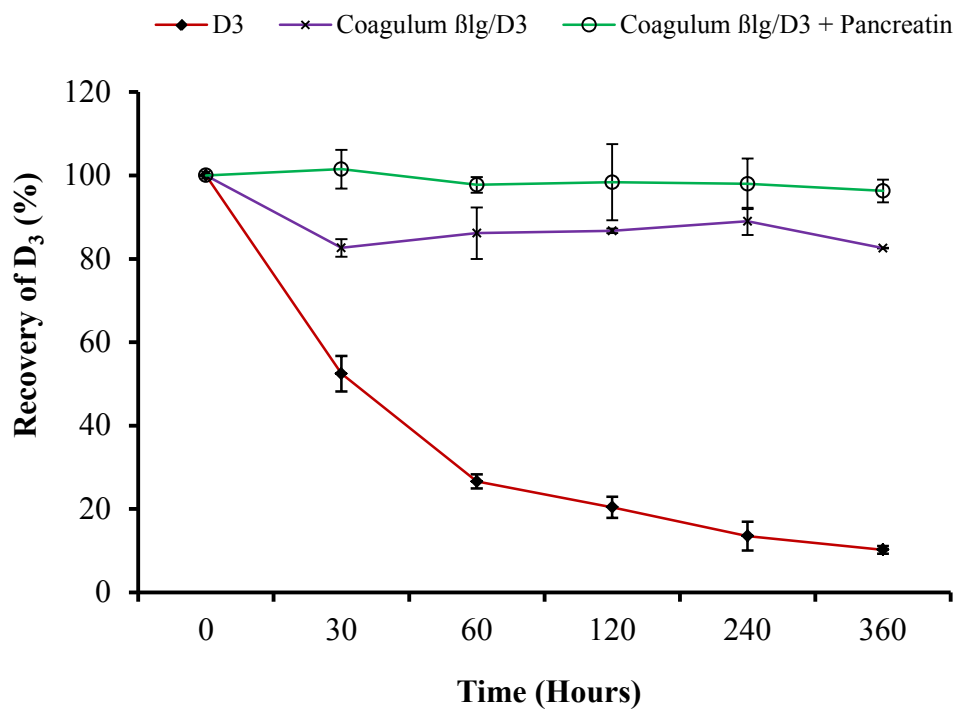


**Figure 6.3. Stability of D<sub>3</sub> and the D<sub>3</sub>-loaded βlg-based coagulum in the simulated intestinal fluid without and with pancreatin at 37°C.**

The unprotected D<sub>3</sub> was almost completely degraded at the end of the digestion with a loss of 90.0 ± 1.3% (Figure 6.3). It is important to note that the release of D<sub>3</sub> was slower in the presence of pancreatin than in its absence. A similar result was previously observed for the βlg/D<sub>3</sub> complex which was significantly more stable ( $p < 0.05$ ) in the presence of pancreatin than in its absence (Chapter 4, Section 4.4.2). Although no clear explanation can be provided, this finding implies that the resistance of the βlg-based coagulum to proteolytic attack was improved. Normally, the structure of βlg is modified at the intestinal pH, resulting in an increased susceptibility to the enzymes [54, 229]. The βlg-based coagulum is a water-soluble matrix that could serve for the oral delivery of D<sub>3</sub>, and consequently, could enhance the bioavailability of D<sub>3</sub>, as determined by the serum level of its biological marker 25(OH)D<sub>3</sub>.

#### **6.4.6. *In vivo* study of the bioavailability of D<sub>3</sub>**

An *in vivo* experiment was carried out to evaluate the impact of the entrapment of D<sub>3</sub> in the βlg-based coagulum on its bioavailability. The rats received by forced feeding the unprotected D<sub>3</sub>, D<sub>3</sub>-entrapped βlg-based coagulum and water supplemented with 0.09% NaCl as the control. The effects of these treatments on the bioavailability of D<sub>3</sub> were compared to that of the βlg/D<sub>3</sub> complex, which by auto-aggregation led to the formation of the D<sub>3</sub>-entrapped βlg-based coagulum [19]. As presented in Figure 8.4, there was a significant difference between the mean 25(OH)D<sub>3</sub> in the rats fed the D<sub>3</sub>-containing treatments compared to the control group ( $p < 0.0001$ ), with a baseline of about 0.02 nmol/L (Figure 6.4).

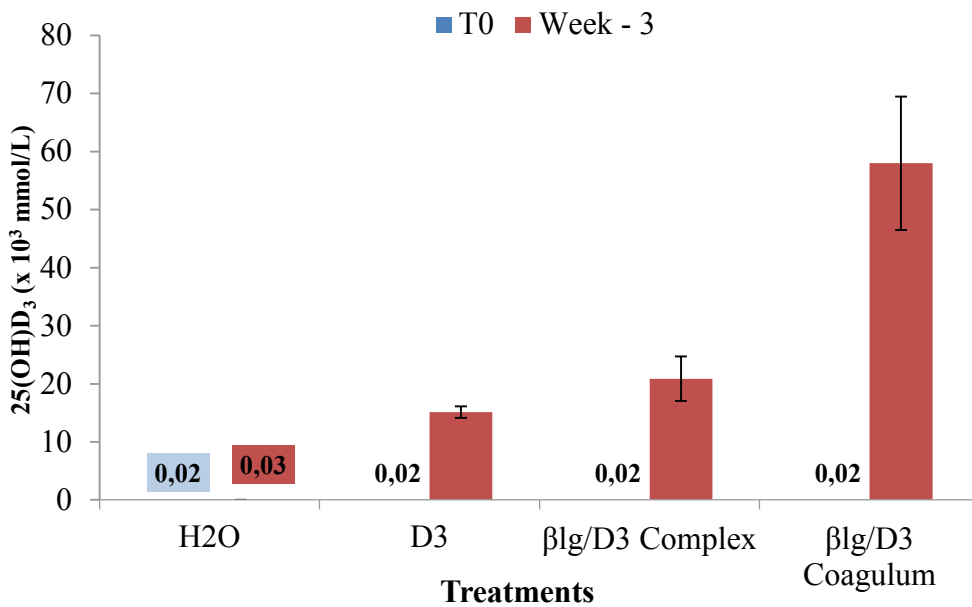
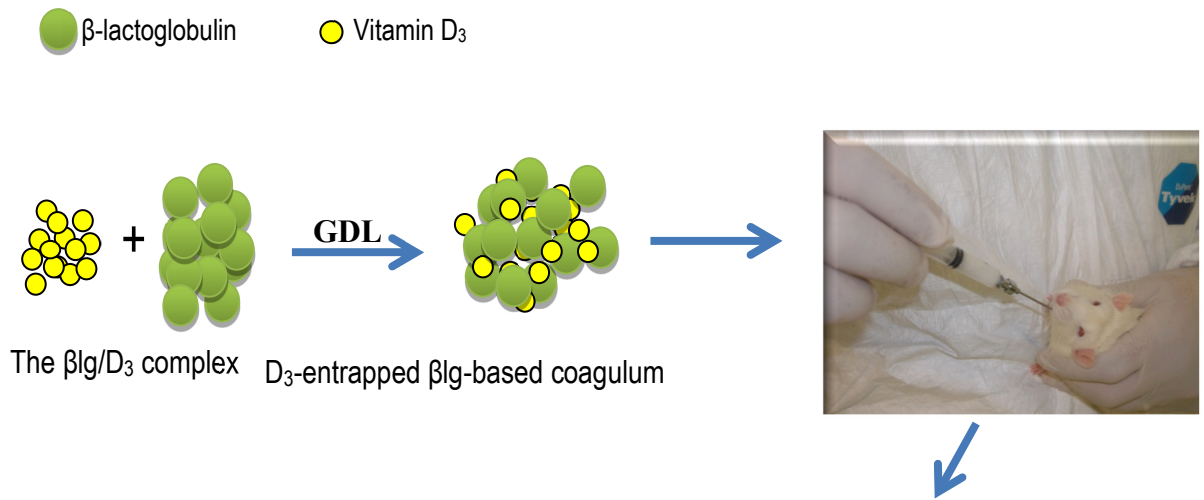


**Figure 6.4. Bioavailability of D<sub>3</sub> in the rat experiment. Mean 25(OH)D<sub>3</sub> ( $\pm$  SEM) in rats forced fed the water (control), D<sub>3</sub>, the  $\beta$ lg/D<sub>3</sub> complex and D<sub>3</sub>-loaded  $\beta$ lg-based coagulum. D<sub>3</sub> was measured by dosage of the serum level of the 25(OH)D<sub>3</sub> was significantly enhanced for the D<sub>3</sub> entrapped in the  $\beta$ lg-based coagulum.**

The serum level of 25(OH)D<sub>3</sub> of the rats fed the D<sub>3</sub>-entrapped coagulum ( $58.0 \pm 11.5 \times 10^3$  nmol/L) was significantly higher ( $p < 0.0001$ ) than those fed the  $\beta$ lg/D<sub>3</sub> complex ( $20.9 \pm 3.8 \times 10^3$  nmol/L) and unprotected D<sub>3</sub> ( $15.1 \pm 11.5 \times 10^3$  nmol/L). The enhancement of the bioavailability of D<sub>3</sub> upon sequestration in the  $\beta$ lg-based coagulum can be ascribed to several factors. Firstly, the  $\beta$ lg-based coagulum entrapped D<sub>3</sub> with a high EE, consequently increasing the water solubility of the vitamin [226]. Despite the fact that the unprotected D<sub>3</sub>,  $\beta$ lg/D<sub>3</sub> complex and D<sub>3</sub>-entrapped  $\beta$ lg-based coagulum had equivalent initial concentrations of D<sub>3</sub>, the  $\beta$ lg-based coagulum actually encapsulated a higher amount of D<sub>3</sub> corresponding to the high EE ( $94.5 \pm 1.8$  %). Therefore, the intake of D<sub>3</sub> by the animals fed the D<sub>3</sub> enriched coagulum was higher than that of those fed the unprotected D<sub>3</sub> or  $\beta$ lg/D<sub>3</sub> complex. Another explanation might be the increased stability of the D<sub>3</sub>-entrapped  $\beta$ lg-based coagulum at intestinal pH and in presence of proteases, as indicated in section 6.4.5. Finally, the water soluble character of the  $\beta$ lg-based coagulum is totally compatible with the aqueous nature of the lining of the digestive tract, which can also contribute to the enhancement of the bioavailability of D<sub>3</sub> [131, 226].

Reports indicate that the loss of D<sub>3</sub> in whey proteins during cheesemaking is problematic because it results in lower retention of the vitamin in the curd matrix and subsequently, in cheese [15, 218]. Herein, the high affinity of D<sub>3</sub> for the major whey protein  $\beta$ lg was exploited to form a D<sub>3</sub>-entrapped  $\beta$ lg-based coagulum which in turn, significantly increased the uptake and bioavailability of D<sub>3</sub> in rats. Powder, ethanol or oil-based vehicles are usually used to evaluate the impact of the carried substances on D<sub>3</sub> bioavailability, with a greater 25(OH)D<sub>3</sub> response for oil-based vehicles because D<sub>3</sub> is fat soluble [218, 230]. To our knowledge this work is the first report of the use of a water soluble  $\beta$ lg-based matrix to improve the bioavailability of D<sub>3</sub>. Despite the difficulty in recovering whey protein in cheese, it has been suggested that coagulate whey proteins can be formed independently followed by entrapment in a casein coagulum [231]. The D<sub>3</sub> entrapped in the  $\beta$ lg-based coagulum can be used in such a procedure to enrich casein coagulum in cheesemaking or other dairy products such as yogurts. Given that whey protein-

based gels and aggregates are used in many food applications as foaming or emulsifying agents or as, films and coatings, one could suggest that other types of semi-solid or solid foods and beverages can also be fortified using the D<sub>3</sub>-entrapped coagulum [2, 17].

## 6.5. Conclusion

In the current work, D<sub>3</sub> was successfully encapsulated in a  $\beta$ lg-based coagulum obtained by triggering the self-aggregation of the  $\beta$ lg/D<sub>3</sub> complex by mild acidification. The  $\beta$ lg-based coagulum is a water soluble matrix that entrapped D<sub>3</sub> with a high EE ( $94.5 \pm 1.8$  %), subsequently increasing the solubility of this fat soluble vitamin. The sequestration of D<sub>3</sub> in the coagulum matrix significantly increased its stability during long term cold storage. Furthermore, D<sub>3</sub> was stable to photochemical degradation after overnight exposure to intensive UV-light. The compactness of the matrix of the  $\beta$ lg-based coagulum provided a protective barrier against degradation by intestinal proteases, resulting in a longer residence time for D<sub>3</sub> in the intestines. Finally, the animal experiment demonstrated that the entrapment of D<sub>3</sub> in the  $\beta$ lg-based coagulum significantly enhanced its bioavailability due to increased water solubility of D<sub>3</sub> and concomitant prolonged intestinal uptake. The findings presented in the current work are important for public health as well as the food industry. Indeed, the high prevalence of D<sub>3</sub> deficiency among populations of all age groups, especially those living in northern latitudes, is well established [102, 232]. This deficiency has been implicated in various skeletal and non-skeletal diseases, such as cancer, cardiovascular diseases, and diabetes and bacterial infections [102, 233-235]. As such, a 2.5-fold increase in the dietary intake of D<sub>3</sub> has been recommended to achieve adequate intake [232]. This work suggests that the D<sub>3</sub>-entrapped  $\beta$ lg-based coagulum may be used for the oral delivery and improved uptake and bioavailability of D<sub>3</sub>. This may help alleviate the economic burden of D<sub>3</sub> deficiency and improve a number of

disease conditions related to D<sub>3</sub> deficiency. To a broader extent, this water soluble matrix may be used as a food grade oral delivery system for fat-soluble nutraceuticals. Rheological analysis and infra-red spectroscopic studies on the formation of the cold gelation of the  $\beta$ Ig/D<sub>3</sub> complex are currently in progress in order to understand the impact of D<sub>3</sub>, temperature and pH on the microstructure, in addition to the rate of gelation.

## **6.6. Acknowledgements**

This work was supported by the Natural Sciences and Engineering Research Council of Canada (NSERC) through the Vanier Canada Graduate Scholarships (F. Diarrassouba) and the Canada research chair in protein, biosystem and functional food physical chemistry. The authors would like to thank Mr Pascal Dubé, Ms Diane Gagnon (Institut de recherche sur les nutraceutiques et les aliments fonctionnels, Université Laval, Québec, QC, Canada) and the EA-CIDAM's team members (Biopharmacie lab, Faculté de Pharmacie, Clermont-Ferrand, France).

## Contextual transision

In the previous chapters, the interaction of  $\beta$ -lactoglobulin with an amphiphilic nutraceuticals (riboflavin) was investigated and the impact on the biological activity of the ligand was evaluated. Then the stability of the  $\beta$ -lactoglobulin – vitamin D<sub>3</sub>, a model hydrophobic bioactive was evaluated. The following chapter broadens the spectrum of interactions to larger size biomacromolecules. Chapter seven covers parts of the fourth objective of this thesis. Due to the presence of charged functional groups in its structure,  $\beta$ -lactoglobulin can exhibit both positive and negative charges in solution, depending on the pH of the media. The isoelectric point of egg white lysozyme is much higher than that of  $\beta$ -lactoglobulin. Furthermore, lysozyme also has different functional groups in its structure, which can interact with that of  $\beta$ -lactoglobulin. Hence, electrostatic complexes were promoted between  $\beta$ -lactoglobulin and lysozyme to form a food grade matrix which was proposed as a carrier for bioactives. The resulting supramolecular structure was characterized by a series of techniques including turbidity measurements, laser diffraction and static light scattering for size and zeta potential of the protein particles. HPLC was performed to determine the optimal protein molar ratio to form a protein-based vehicle for the encapsulation of vitamin D<sub>3</sub>, used here as a model nutraceuticals, since it is a known ligand for  $\beta$ -lactoglobulin. Transmission and scanning electron microscopy were used to determine the interior and surface morphology of the self-assembled particles, respectively.

## CHAPTER 7

# Self-Assembly of $\beta$ -lactoglobulin and Egg White Lysozyme as a Potential Carrier for Nutraceuticals

A version of this work was submitted to the  
Journal of Physical Chemistry B. Manuscript ID jp-2013-08298b

By :

Fatoumata Diarrassouba<sup>a</sup>, Gabriel Remondetto<sup>b</sup>, Ghislain Garrat<sup>c</sup>, Pedro Alvarez<sup>a</sup>,  
Eric Beyssac<sup>c</sup> and Muriel Subirade<sup>a</sup>

<sup>a</sup>Chaire de recherche du Canada sur les protéines, les bio-systèmes et les aliments fonctionnels, Institut de recherche sur les nutraceutiques et les aliments fonctionnels (INAF/STELA), Université Laval, Québec, QC, Canada.

<sup>b</sup>Centre de recherche et développement, Agropur Coopérative. 4700 rue Armand Frappier, St-Hubert, QC, Canada.

<sup>c</sup>EA-CIDAM, Lab Biopharmacie, Faculté de Pharmacie, 28 Place Henri Dunant, 63001, Clermont-Ferrand, France.

## 7.1. Abstract

Proteins can interact with various ingredients in food, affecting characteristics such as texture, flavor and appearance. However, information on protein-protein interactions occurring in foodstuffs is scarce. In the current study, electrostatic interactions were promoted between oppositely charged bovine milk protein,  $\beta$ -lactoglobulin ( $\beta$ lg) and egg protein Lysozyme (Lyso) to induce a spontaneous self-assembly of the proteins.  $\beta$ lg:Lyso concentration ratios (v/v) of 30:1, 10:1, 5:1, 3:1, 2:1, 1.8:1, 1.5:1, 1.2:1, 1:1, 1:2, 1:3 were essayed at pH 6.8 to select the optimal ratio for the proteins self-assembly, which behavior was then studied at varying pH (4, 5, 6.8, 7.5, 8, 9, 10 and 11). Turbidity measurements demonstrated  $\beta$ lg/Lyso concentration ratio of 2:1 (v/v) prepared at pH 7.5 was the optimal condition for the self-assembly of the proteins.  $\beta$ lg and Lyso self-assembled to form microspheres as showed by the SEM image. The TEM image showed that the interior of the  $\beta$ lg/Lyso microspheres was composed of dispersed granular aggregates. The size distribution of the  $\beta$ lg/Lyso microspheres were  $d(0.1, 1.2 \mu\text{m})$ ,  $d(0.5, 4.0 \mu\text{m})$  and  $d(0.9, 11.7 \mu\text{m})$ , with a volume mean diameter of  $7.1 \mu\text{m}$  and a span of  $2.5 \mu\text{m}$ . The surface charge of the microspheres was  $-0.9 \pm 0.02 \text{ mV}$  at pH 7.5. Vitamin D<sub>3</sub>, used as a model nutraceutical, was successfully entrapped in the  $\beta$ lg/Lyso microspheres with an encapsulation efficiency of  $90.8 \pm 4.8 \%$ . The present work suggests that  $\beta$ lg/Lyso microspheres can serve as a potential food-grade vehicle for nutraceuticals in the formulation of food products and pharmaceuticals.

## 7.2. Introduction

Food proteins are generally recognized as safe (GRAS), which makes them excellent materials for the formulation of oral delivery systems [2]. In addition to high nutritional value, functional properties such as gelation, foaming and water binding capacity, food-derived proteins are attracting increasing interest due to their ability to establish a wide range of interactions with other compounds. They can form simple complexes with ligands and gel networks through hydrophobic interactions, covalent and hydrogen bonding, in addition to more elaborate structures such as coacervates with polysaccharides or polyelectrolytes, through electrostatic interactions [236]. Food-derived protein-protein interactions (FPPI) were first suggested by Howell in 1995, between  $\beta$ -lactoglobulin and egg protein Lysozyme [21]. It was observed that  $\beta$ -lactoglobulin ( $\beta$ lg) and Lysozyme (Lyso) can form insoluble but reversible complexes, depending on the pH, ionic force and concentration of the individual protein. Later, Howell and Li-Chan used Raman spectroscopy to confirm the involvement of electrostatic interactions between the oppositely charged globular proteins in addition to minor hydrophobic interactions, which confer more stability to the resultant precipitate [140]. Moreover, it was proven that Lyso from egg white can form electrostatic complexes with negatively charged egg proteins at low ionic strength [237]. More recently, Desfougeres et al. demonstrated that size difference plays a key role in predicting the optimal pH and protein molar ratio for microsphere formation between proteins of opposite charge [139]. These studies suggest the possibility of using food proteins as building blocks for novel biocompatible architectures which may find applications in both the medical and non-medical fields [238]. However, to date, there is no report on FPPI-based vehicles that can be used as oral delivery systems for biologically active molecules. FPPI-based oral delivery systems can form excellent GRAS vehicles for controlled delivery of bio-actives. Indeed, protein-based carriers can be used in controlled and site-specific drug release as they can inherit characteristics such as pH and ionic strength sensitivity, swelling, water binding and gel network formation from constituting proteins [105]. In addition, the physical entrapment and reduced

mobility of light or oxygen sensitive bioactives within the protein matrix might provide additional resistance to oxidizing agents such as oxygen or free radicals by restricting their access to the encapsulated bioactive molecule [20]. The ability of proteins to absorb UV-light can also contribute in improving the light stability of the entrapped bioactives that absorb at a proximate wavelength range [130].

Milk protein  $\alpha$ -lactalbumin and Lyso have been used to form coacervate-like structures but only after prior denaturation of the milk protein by depletion of the central calcium that stabilizes the two domains of the protein in addition to mild heat treatment [238]. Conversely, for  $\beta$ lg from bovine milk, structural integrity is a key requirement for its role as transporter for small nutraceuticals and other biologically active ligands [7]. Furthermore, it was shown that the kinetics of proteolytic degradation of a dense cross-linking protein matrix is considerably reduced since it is difficult for the enzymes to penetrate into the particles. Such a dense protein network can be created by conveniently promoting the interactions between  $\beta$ lg and Lyso, which can offer improved resistance against proteases when kept in the native state, thus retarding access to sensitive amino acids and prolonging the residence time in the intestines [21, 105, 139]. Therefore, in the present work, native  $\beta$ lg from bovine milk and Lyso from egg white were used to form a FPPI-based oral delivery vehicle that could be used as a carrier for nutraceuticals. Turbidity measurements, charge and size determination, and reversed-phase high performance liquid chromatography were performed to determine the optimal protein molar ratio to form a protein-based vehicle for the encapsulation of vitamin D<sub>3</sub> (D<sub>3</sub>), a model nutraceutical. Transmission and scanning electron microscopy were used to determine the interior morphology and external aspect of the  $\beta$ lg/Lyso self-assembled particles, respectively.

## 7.3. Experimental Section

### 7.3.1. Materials

$\beta$ -lactoglobulin ( $\beta$ lg) was purchased from Davisco Foods International, Inc. (Le Sueur, MN, USA). High purity  $\beta$ -lactoglobulin (B variant, purity  $\geq 90\%$ ), Lysozyme (Lyso) from chicken egg white (lyophilized powder, protein  $\geq 90\%$ ,  $\geq 40,000$  units/mg protein) and vitamin D<sub>3</sub> (purity  $\geq 98\%$ , HPLC) were obtained from Sigma-Aldrich Chemical and Co (Oakville, ON, Canada). The proteins were used without further purification. Acetonitrile (ACN, HPLC grade), methanol (MeOH, HPLC grade) and trifluoroacetic acid (TFA) were purchased from EMD International (Gibbstown, NJ, USA).

### 7.3.2. Sample preparation

Protein stock solutions (0.2 %) were prepared by dissolving the powder in MilliQ water under mild stirring conditions for 2 h at room temperature to allow complete rehydration[31]. All protein solutions were filtered through a 0.2  $\mu$ m low binding syringe filter to remove protein aggregates and other impurities. The protein concentrations were not significantly different before and after filtration. Each of the  $\beta$ lg and Lyso solution initially concentrated at 0.1 % were mixed in various proportions for protein co-precipitation at pH 6.8 [21]. Basically, different volumes of Lyso solution (0.1, 0.3, 0.6, 1.0, 1.5, 1.6, 2.0, 2.5, 3.0, 4.0 and 6.0 mL) were added to each one of the 11 vials containing 3 mL of  $\beta$ lg, corresponding to the  $\beta$ lg:Lyso concentration ratios of 30:1, 10:1, 5:1, 3:1, 2:1, 1.8:1, 1.5:1, 1.2:1, 1:1, 1:2, 1:3. Solutions of  $\beta$ lg and Lyso were used as controls.

$\beta$ lg variant B from Sigma-Aldrich was used as a reference because it generates only one peak on the HPLC graph and the concentration was determined spectrophotometrically (HP 8453 UV–Visible, spectrophotometer, Palo Alto, CA) using a molar extinction coefficient of  $17,600 \text{ M}^{-1} \text{ cm}^{-1}$  at 278 nm [6]. Vitamin D<sub>3</sub>

(D<sub>3</sub>) stock (1 mM) was prepared daily by dissolving 10 mg in 25 mL in MeOH [188]. Working solutions of D<sub>3</sub> were obtained by diluting the stock solution in MilliQ water.

### **7.3.3. Effect of protein ratio on the formation of the $\beta$ Ig/Lyso co-precipitate**

In order to determine the ratio at which protein self-assembly occurs,  $\beta$ Ig (0.1%) and Lyso (0.1%) solutions were mixed at different ratios (*v/v*), as described in Section 7.3.2. The mixture at the 1:3 ratio of  $\beta$ Ig/Lyso was clear. Therefore, it was not necessary to further reduce this ratio value. The initial pH of  $\beta$ Ig was 6.6 while the pH of Lyso was 4.2. Immediately after mixing of the protein solutions at varying ratios, the pH of the mixture was adjusted to 6.8 with NaOH [21]. Turbidity measurements were performed at least three times at 600 nm by spectrophotometry 15 min after pH adjustment (HP 8453 UV–Visible, spectrophotometer, Palo Alto, CA). The ratio  $\beta$ Ig/Lyso (*v/v*) at which the value of turbidity was the highest, hence where maximum interaction between  $\beta$ Ig and Lyso occurred, was selected to study the effect of pH on the formation of the protein aggregates.

### **7.3.4. Effect of the pH on the formation of the $\beta$ Ig/Lyso co-precipitate**

The pH of the  $\beta$ Ig and Lyso mixture at the selected ratio was adjusted to pH 4, 5, 6.8, 7.5, 8, 9, 10 or 11, immediately after mixing the protein solutions. The pH was adjusted using NaOH or HCl and the solutions were allowed to stabilize for about 15 min before the turbidity was measured at 600 nm (HP 8453 UV–Visible, spectrophotometer, Palo Alto, CA, USA). Each measurement was repeated at least three times. The data generated allowed the selection of the  $\beta$ Ig/Lyso ratio and pH at which the formation of  $\beta$ Ig/Lyso self-assembly is optimal for further characterization of the co-precipitates.

### **7.3.5. Characterization of the $\beta$ Ig/Lyso co-precipitate**

#### **7.3.5.1 Size and surface charge**

For size and charge distribution analysis, the  $\beta$ Ig and Lyso mixture was kept at 4°C. Measurements of the size (static light scattering) and zeta potential (electrophoretic mobility) of the protein particles were performed using laser diffraction method using a Mastersizer 2000 and Zetasizer Nano ZS, respectively (Malvern Instruments, Southborough, MA, USA). All size measurements were performed using a 90° scattering angle at 25°C with 180 s of recording. The effect of agitation on the formation of  $\beta$ Ig/Lyso self-assembly was evaluated under mild stirring conditions (~ 100 rpm) on each selected protein ratio and at specific pH values. The mean hydrodynamic diameter was generated by cumulative analysis. The zeta potential was measured using an aqueous dip cell in the automatic mode. All samples were analyzed at least three times. The pH value at which the net surface charge of the self-assembled protein particles was near the zwitterion was selected for further surface and interior characterization by electron microscopy.

#### **7.3.5.2 Scanning and transmission electron microscopy for the determination of surface and interior morphology**

Transmission electron microscopy (TEM) and scanning electron microscopy (SEM) were used to observe the interior and surface morphology of the protein aggregates, respectively. Briefly, each sample was placed on a copper grid covered with nitrocellulose. The samples were stained with neutral dye to avoid interaction with the surface charge of the protein particles, and dried at room temperature. For observation of the interior structure by TEM, the samples were embedded in Epon, thinly sectioned, and stained with 1% sodium phosphotungstate. Samples were viewed at 80 kV using a JEOL 1200EX (JEOL Ltd., Akishima, Japan) instrument. The surface appearance was determined by

SEM after each sample was critical-point-dried and sputter-coated with 30 nm of gold/palladium. Samples were viewed at 30 kV using a JEOL JSM 35CF instrument. The samples were analyzed using an SEM system combined with EDS, also known as energy-dispersive X-ray analysis (EDXA) from Noran Instruments (Middleton, Wis., USA).

### **7.3.6. Model nutraceutical loading studies**

The possible binding of two molecules of  $D_3$  to  $\beta$ lg is well described in the literature [79]. Furthermore, preliminary results obtained by spectroscopic investigation proved that  $D_3$  can also bind Lyso. Therefore,  $D_3$  was used as the model nutraceutical for loading studies in the  $\beta$ lg/Lyso self-assembled structure. The  $\beta$ lg/ $D_3$  complex was first formed with a final concentration of 110  $\mu$ M for the vitamin and 0.1%  $\beta$ lg, which corresponds to about 55  $\mu$ M of  $\beta$ lg and thus a  $\beta$ lg: $D_3$  ratio of 1:2. Lyso was incorporated into the  $\beta$ lg- $D_3$  complex solution and the pH of the  $\beta$ lg/ $D_3$ /Lyso mixture was adjusted under a mild nitrogen flow to avoid loss of  $D_3$ . The mixture was allowed to stand for 24 hours at 4°C to allow binding of  $D_3$  to the protein self-assembled structure. After incubation, the  $\beta$ lg/ $D_3$ /Lyso mixture was quickly vortexed and 1.0 mL was sampled into conical tubes and spun at a speed of 5,000 x g for 5 min. The supernatant was directly transferred into amber vials for High performance liquid chromatography (HPLC) analysis. The protein pellet was disrupted to allow the release of the  $D_3$ . The pellet was resuspended in 495  $\mu$ L of MilliQ water and vigorously mixed with 5  $\mu$ L of HCL 1 N to lower the pH and 500  $\mu$ L of MeOH to further provoke its release from  $\beta$ lg. The concentration of  $D_3$ ,  $\beta$ lg, and Lyso in both the supernatant and pellet were determined by HPLC. HPLC measurements were performed on a Phenomenex Kinetex 2.6  $\mu$ m 4.6 x 75 mm C18 column (Torrance, California, USA) using an Agilent 1260 HPLC Series system equipped with a diode Array detector (Agilent technologies, Palo Alto, CA, USA). The elution gradient was 0–2 min, 20–65% B ; 2–2.25 min, 65–100% B; 2.25–4.85 min isocratic 100% B; 4.85–5 min, 100–20% B; 5–8 min isocratic 20% B.

Mobile phases were A: H<sub>2</sub>O+0.1% TFA and B: acetonitrile+0.1% TFA (v/v), both at a flow rate of 0.4 mL min<sup>-1</sup>. After separation on the Kinetex column, detection was achieved by setting the detector at 280 nm for βlg and Lyso, and 265 nm for D<sub>3</sub>. The encapsulation efficiency (EE) was calculated with the following equation:

$$EE (\%) = \frac{\text{Total amount of D3 in the } \beta\text{lg/Lyso microspheres}}{\text{Total amount of D3}} \times 100$$

### **7.3.7. Statistical analysis**

Statistical analysis was performed using the SAS software version 12.0 (SAS Institute Inc., Cary, NC, USA). ANOVA and the Least Square Difference (LSD) were used to determine the significant differences between the means. The significance level was fixed at  $p < 0.05$ . All measurements were conducted in triplicate and the results were reported as the mean  $\pm$  SD.

## **7.4. Results and Discussion**

### **7.4.1. Effect of the protein concentration on the formation of the βlg-Lyso co-precipitates**

The ability of the two proteins to self-assemble through electrostatic forces was exploited to form βlg/Lyso self-assembly observed by measuring the turbidity at 600 nm at pH 6.8 (Figure 7.1).

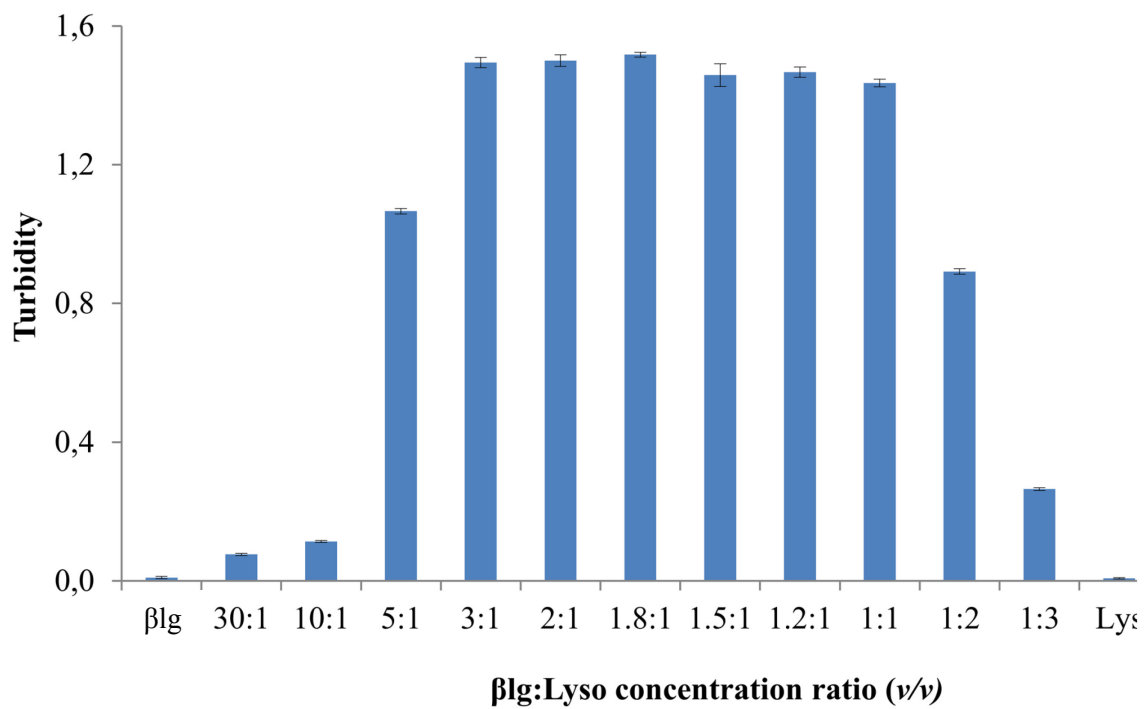


**Figure 7.1. Impact of the βlg:Lyso concentration ratio (v/v) on the protein self-assembly determined by the turbidity at 600 nm.**

At this pH value,  $\beta$ lg, which is close to the well-known Tanford transition [54, 60], bears a net negative charge of  $-22 \pm 3.5$  mV while Lyso carries a net positive charge of about  $+9 \pm 1.0$  mV (Figure 7.2). The turbidity of the mixture of the two proteins increases from a  $\beta$ lg:Lyso concentration ratios 30:1 to 5:1, reaches a plateau at 3:1 to 1:1, and declines when the concentration of Lyso is in excess (Figure 7.1).

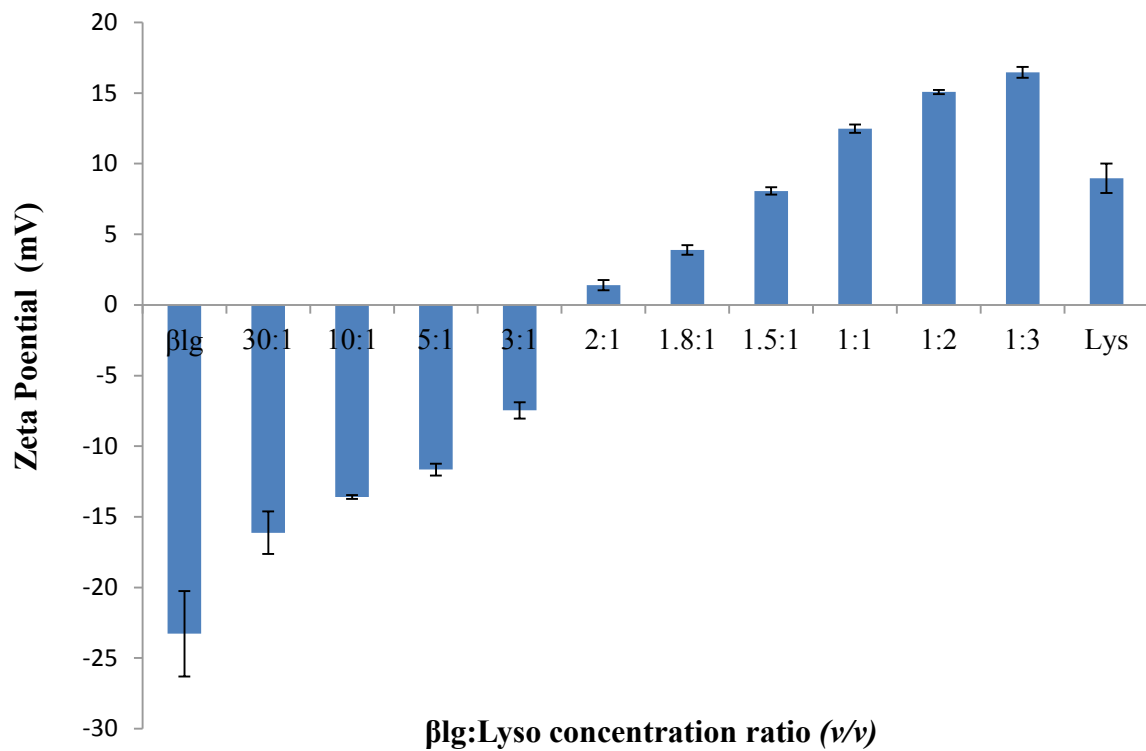


**Figure 7.2. Impact of the  $\beta$ Ig:Lyso concentration ratio (v/v) on the surface charge of the protein self-assembly at pH 6.8.**

It should be noticed that the presence of larger protein aggregates might also explain the plateau in the turbidity, which in fact could resemble to signal saturation if the values of turbidity were not below the signal threshold of the spectroscopic instruments used. Further characterization of the  $\beta$ Ig/Lyso self-assembly will allow the selection of the optimal ratio.

The sharp decrease in turbidity when Lyso is in excess can be explained by the lack of  $\beta$ Ig in solution to form co-precipitates as well as a predominant positive electrostatic repulsion. This finding confirms the observation of Howell and coworkers who also found that absence of  $\beta$ Ig in solution resulted in lower turbidity values [21]. Another theory suggests that 'size difference between protein couples (acidic and basic) is a key element that defines the optimal pH value for microsphere formation and the protein molar ratio in the formed microspheres'[139]. It was indicated that protein self-assembly can only be formed when the molar ratio is 1:1, such as for the binary systems of  $\alpha$ -lactalbumin (14 KDa) and Lyso (14.4 KDa) or avidin (67 KDa) and ovalbumin (45.5 KDa) or a molar ratio of 2:1, with the smallest protein at the highest concentration. Given that the weight difference between  $\beta$ Ig and Lyso is much less than that between avidin and ovalbumin, this theory should also be true for the  $\beta$ Ig/Lyso couple. The highest turbidity value was observed at a  $\beta$ Ig/Lyso ratio of 2:1, in favour of  $\beta$ Ig (18.3 KDa) which is obviously larger than Lyso. This ratio represents the initial concentration of the proteins and might not reflect the actual molar ratio of the  $\beta$ Ig/Lyso couple. Current ongoing studies in our lab might shed the light on the exact final molar ratio of both proteins in the  $\beta$ Ig/Lyso self-assembly.

It was also observed that  $\beta$ Ig and Lyso self-assemble for protein concentration ratios as high as 50:1, 10:1, intermediate ratios (data not show) and all the way to 1:3, although for higher ratio values, the turbidity is much lower than that of the plateau region ( 3:1, 2:1, 1.8:1, 1.5:1 and 1:1). These data suggest the involvement of other types of interactions, such as hydrophobic interactions, which can become predominant when  $\beta$ Ig is in excess, and also to minor changes in the protein

structures and other types of unspecific bonding. This finding is in good agreement with the results of Howell and Li-Chan (1996) who used spectroscopic methods to prove the participation of a small range of hydrophobic interactions in addition to strong electrostatic attraction, changes in the protein secondary structure, and disulphide bonds all contributing to the stability of the co-precipitates [140]. Indeed, the ability of Lyso to form spontaneous electrostatic complexes with negatively charged proteins including egg proteins in the presence of low ionic strength is believed to be responsible for the excellent foaming property of egg white [237, 239]. Nevertheless, electrostatic and hydrophobic interactions in addition to minor changes in the protein secondary structure cannot fully explain the appearance of turbidity over a wide range of  $\beta$ lg:Lyso ratios. In Figure 7.2, the net charge of Lyso at pH 6.8 is significantly lower than that of the  $\beta$ lg/Lyso self-assembly (ratios 1:1 to 1:3). Furthermore, at a ratio of 2:1, where the net charge is supposed to be negative due to an excess of  $\beta$ lg, the self-assembly bears net positive charge of  $1 \pm 0.3$  mV, which is close to the zwitterion (Figure 7.2). At  $\beta$ lg:Lyso ratios of 1.8:1, 1.5:1 and 1:1, the charges of co-precipitates are  $8 \pm 0.2$ ,  $12 \pm 0.2$  and  $15 \pm 0.1$  mV, respectively (Figure 7.2). This finding implies that charge compensation occurs when  $\beta$ lg and Lyso are mixed at an initial concentration ratio of 2:1, which might not represent the final concentration of the proteins in the self-assembly.

Taking into account the results obtained from the turbidity measurement at pH 6.8, where  $\beta$ lg is a dimer, one can suggest that the spontaneous self-assembly of  $\beta$ lg and Lyso molecules may result from a modification of the structure of either  $\beta$ lg or both proteins, with concomitant exposure of charged amino acids which may also contribute to the electrostatic interactions between the two proteins. In fact, molecular modelling studies suggested that electrostatic interactions between glutamate 35 and aspartate 53 in the catalytic binding site on Lysozyme and Lysoine 138 and 141 at the dimerization site of  $\beta$ lg may be responsible for the  $\beta$ lg/Lyso self-assembly[21]. This indicates that the monomer contact site might be implicated in the binding of Lyso to  $\beta$ lg, consequently affecting the structure of  $\beta$ lg during the co-precipitates formation and confirming the results obtained in the

present study. Therefore, for further characterization of  $\beta$ lg/Lyso self-assembly, the protein concentration ratio of 2:1 was selected to study the effect of pH on the co-precipitates.

#### **7.4.2. Effect of the pH on the formation of the $\beta$ lg-Lyso co-precipitates**

Electrostatic attraction is the main interactive force involved in the formation of the  $\beta$ lg/Lyso co-precipitates. Therefore, the study of the effect of pH on protein self-assembly is crucial to determine the stability range and optimal conditions for co-precipitation. The  $\beta$ lg/Lyso ratio of 2:1 was selected to evaluate the effect of pH (4, 5, 6.8, 7.5, 8, 9, 10 and 11) on the self-assembly of the proteins, measured by turbidity at 600 nm and net charge of the protein co-precipitates. Figure 7.3 shows the effect of pH variation on the turbidity of  $\beta$ lg/Lyso co-precipitates. Interestingly,  $\beta$ lg and Lyso self-assemble over a wide range of pH values (6.8, 7.5, 8, 9 and 10), while at pH 5 and 11, close to the  $pI$  of  $\beta$ lg and Lyso, respectively, there was no co-precipitation of the two proteins. One would expect greater co-precipitation at pH 6.8, 7.5 and 8 where both proteins bear net negative ( $\beta$ lg) and positive (Lyso) charges, so it is surprising that almost no turbidity was observed at pH 5 (Figure 7.3).

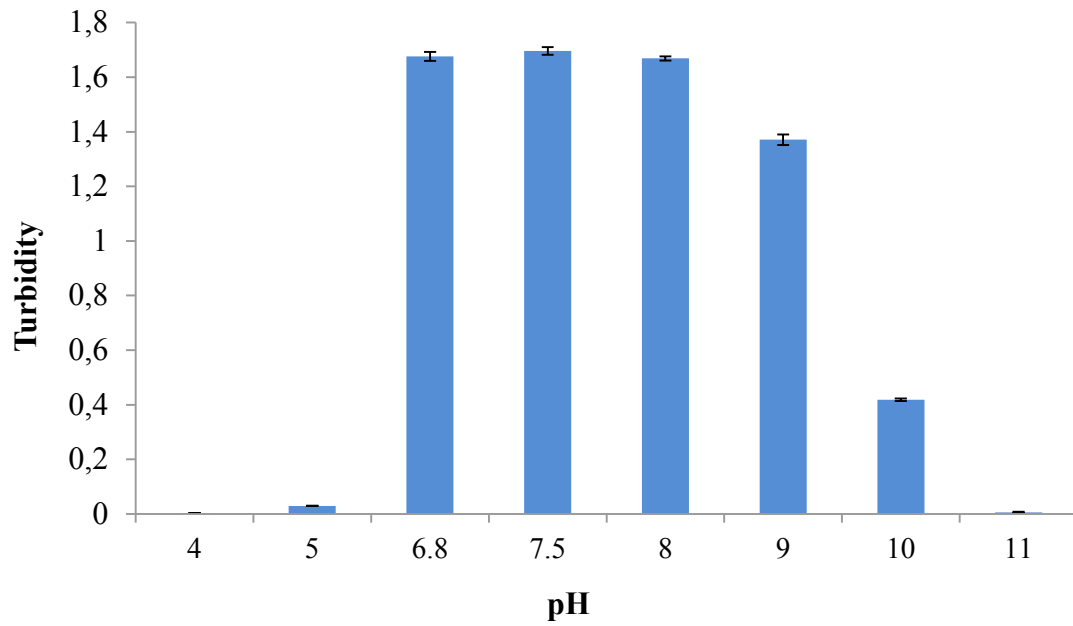


**Figure 7.3. Impact of the pH on the formation of  $\beta$ Ig/Lyso self-assembly as determined by turbidity at 600 nm. The  $\beta$ Ig:Lyso concentration ratio was 2:1 and the pH values were 4, 5, 6.8, 7.5, 8, 9, 10 and 11.**

At pH close to the  $pI$  in a single protein system, auto-aggregation and an increase of the solution's turbidity are expected to occur [60]. Indeed, the solution with only  $\beta Ig$  was turbid at pH 5 (data not shown), which is not the case for the mixture of  $\beta Ig$  and Lyso (ratio 2:1) at the same pH (Figure 7.3). This finding confirms that the binding of Lyso to  $\beta Ig$  might involve some changes in the structure of  $\beta Ig$ , thus disallowing auto-aggregation at pH close to the  $pI$  of the protein. Additionally, it is well documented that at pH 9 and above,  $\beta Ig$  undergoes irreversible base-induced transition with concomitant loss of its structure [54, 60]. Above pH 9, where the base-induced transition occurs,  $\beta Ig$  is highly negatively charged and consequently has a strong electrostatic repulsion between charged side-chains, leading to its denaturation [54]. At pH 9 and 10, Lyso bears positive charges and can still interact with the negatively charged  $\beta Ig$ , which explains the formation of the  $\beta Ig$ /Lyso co-precipitates. Although pH 10 is close to the  $pI$  of Lyso ( $pI = 10.7$ ), Lyso might still carry some positive charge [239]. However, at pH 11, there is no co-precipitation probably due to electrostatic repulsion, given that both  $\beta Ig$  and Lyso bear negative charges.  $\beta Ig$  and Lyso co-precipitation occurs at pH 6.8, 7.5 or 8, within which interval  $\beta Ig$  undergoes the Tanford transition, with minor impact on its structure. Further surface and size characterization were performed in order to determine the optimal pH value for  $\beta Ig$ /Lyso co-precipitation.

#### **7.4.3. Surface charge and size of the $\beta Ig$ -Lyso co-precipitates**

The optimal pH for  $\beta Ig$ /Lyso self-assembly at a  $\beta Ig$ :Lyso ratio of 2:1 was determined by performing zeta potential measurements at each pH value (Figure 7.4).

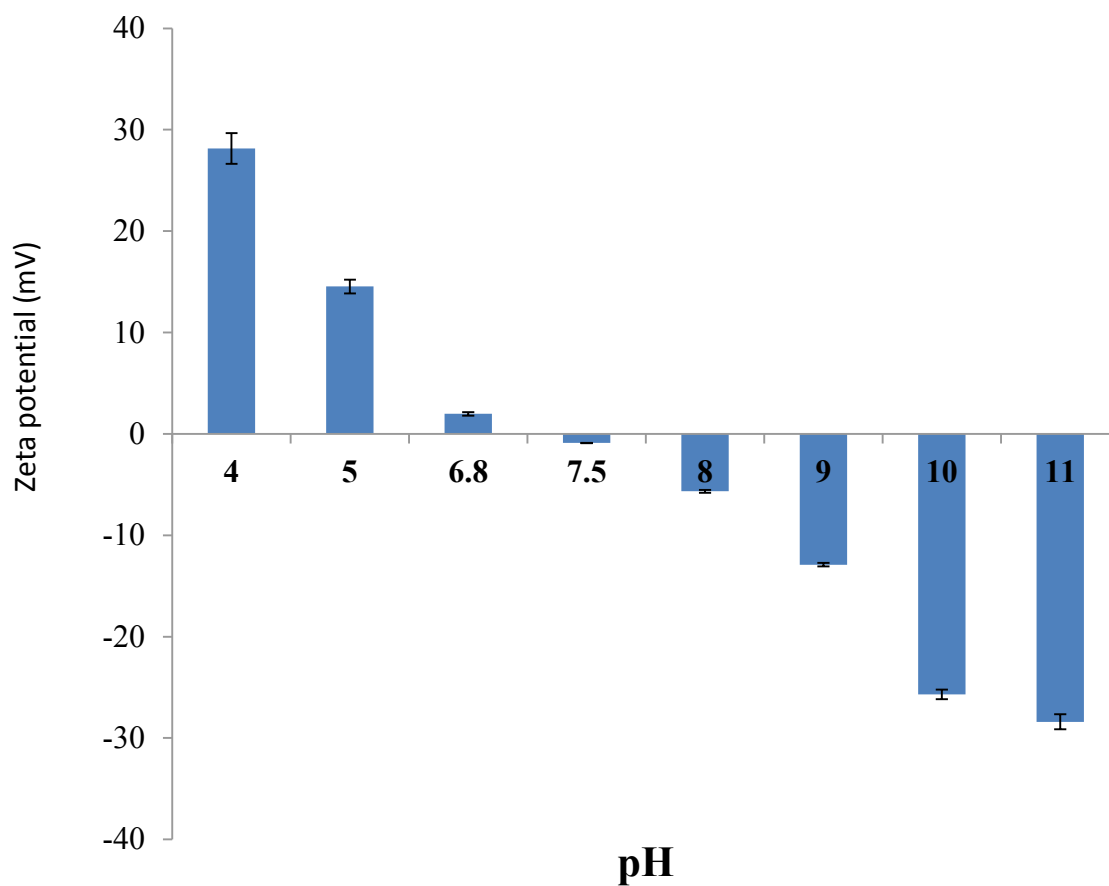


**Figure 7.4. Impact of pH on the charge of the  $\beta$ Ig/Lyso self-assembly at varying pH: 4, 5, 6.8, 7.5, 8, 9, 10 and 11. The  $\beta$ Ig:Lyso concentration ratio was 2:1.**

It should be indicated that a particulate solution is considered colloidally stable if the value of the zeta potential is above +30 mV or below -30 mV [143], the zeta potential being defined as the potential at the slipping plane, which is the layer of resident counter ions in the double electrical diffuse layer. It is a good measurement of the stability of the system, therefore if the zeta potential is zero or close to it, the system is prone to sedimentation. At pH 4, 5 and 6.8 the protein self-assembly carries a net positive charge of  $28.1 \pm 1.5$ ,  $14.5 \pm 0.7$  and  $1.9 \pm 0.1$  mV, respectively. At pH 8, 9, 10 and 11, the protein self-assembly were negatively charged, with the zeta potential values being  $-5.7 \pm 0.1$ ,  $-13.0 \pm 0.2$ ,  $-25.7 \pm 0.5$  and  $-28.4 \pm 0.7$  mV, respectively (Figure 7.4). These results are not surprising since predominantly positive species are in solution at pH 4 and 5 while negatively charged species predominate above pH 6.8. At pH 6.8, the overall charge of the protein self-assembly comes close to the zwitterion point, due to charge compensation accompanied by structural modification of  $\beta$ lg which was explained previously. In summary, the surface charge data confirm that self-assembly occurs between pH 6.8 and 8, with the zwitterion being close to pH 7.5 where the net charge of the  $\beta$ lg/Lyso self-assembly is  $-0.9 \pm 0.02$  mV (Figure 7.4).

The size measurement of the protein self-assembly was performed at pH 6.8, 7.5 and 8 using the  $\beta$ lg/Lyso ratio of 2:1, before and after mild stirring. Before agitation, large particle sizes were observed only at pH 6.8, and with a surprising narrow span (Table 7.1). Agitation has a drastic impact on the size of the  $\beta$ lg/Lyso self-assembly at pH 6.8, with almost a 50-fold reduction in the size after mild agitation, but with a similar span (Table 7.1).

**Table 7.1. Average Size (three measurements) of the  $\beta$ lg/Lyso self-assembly at ratio 2:1 and different pH values before and after overnight agitation**

pH	<sup>a</sup> d (0.1)	d (0.5)	d (0.9)	<sup>b</sup> D [4, 3]	<sup>c</sup> Span
<b>Particle size (<math>\mu</math>m) before agitation</b>					
6.8	2.7	890.4	1567.3	695.6	2.5
7.5	1.2	4.0	11.7	7.1	2.5
8.0	0.8	2.3	5.6	7.0	2.0
<b>Particle size (<math>\mu</math>m) after agitation</b>					
6.8	2.4	10.2	24.5	12.1	2.1
7.5	0.9	2.7	7.5	7.1	2.4
8.0	1.0	2.9	7.0	5.7	1.9

**Notes:** Size measured by static light scattering. Mild agitation was carried out at 4 °C overnight. The speed of the pump and stirring was set at 2000 rpm.

<sup>a</sup>**d (0.1), d (0.5) and d (0.9)** represent the percent of the size distribution lying below 10 %, 50 % and 90 %, respectively.

<sup>b</sup>**D [4, 3]** : the volume mean diameter of the distribution.

<sup>c</sup>**Span** : the width of the distribution. Span = [d (0.9) - d (0.1)] / d (0.5).

This result is in accordance with the suggestion that the binding of Lyso promotes structural change in  $\beta$ lg, probably uncovering additional charged patches for protein self-assembly which are easily disrupted by mild agitation. However, the agitation does not seem to affect the size distribution of the  $\beta$ lg/Lyso self-assembly at pH 7.5 and 8. The mean volume diameter of the distribution is similar for both pH values before and after agitation, with the most consistent average size was observed at pH 7.5 as shown in Table 1. The size distribution of the  $\beta$ lg and Lyso formed microspheres were  $d(0.1, 1.2 \mu\text{m})$ ,  $d(0.5, 4.0 \mu\text{m})$  and  $d(0.9, 11.7 \mu\text{m})$  with a volume mean diameter of  $7.1 \mu\text{m}$  and a span of  $2.5 \mu\text{m}$ . Thus, pH 7.5 and a  $\beta$ lg:Lyso ratio of 2:1, which are the optimal conditions for  $\beta$ lg/Lyso self-assembly, were selected to determine the surface and internal morphology of the microparticles.

#### **7.4.4. Characterization of the $\beta$ lg/Lyso co-precipitates**

##### **7.4.4.1 Scanning and transmission electron microscopy of surface and interior morphology**

The SEM and TEM observations show that the  $\beta$ lg/Lyso self-assembled structure is regular and spherical in shape, with a uniform distribution of the proteins inside the spheres (Figure 7.5A and 7.5B). The TEM image shown in Figure 7.5A is that of typical granular protein aggregates [240]. The spheres have a mean diameter of about  $1 \mu\text{m}$  or less, although larger aggregates of a few microns can be observed on the image (Figure 7.5B). This mean diameter is much smaller than the  $7.1 \mu\text{m}$  diameter provided by the hydrodynamic size measurements, likely due to the fact that sample preparation for TEM and SEM images requires a dehydration step leading to smaller microspheres as previously reported [241]. Therefore, in the present study,  $\beta$ lg and Lyso self-assemble to form microspheres of size varying from less than  $1$  to about  $7.1 \mu\text{m}$ , inside of which the self-aggregated proteins are homogeneously distributed.

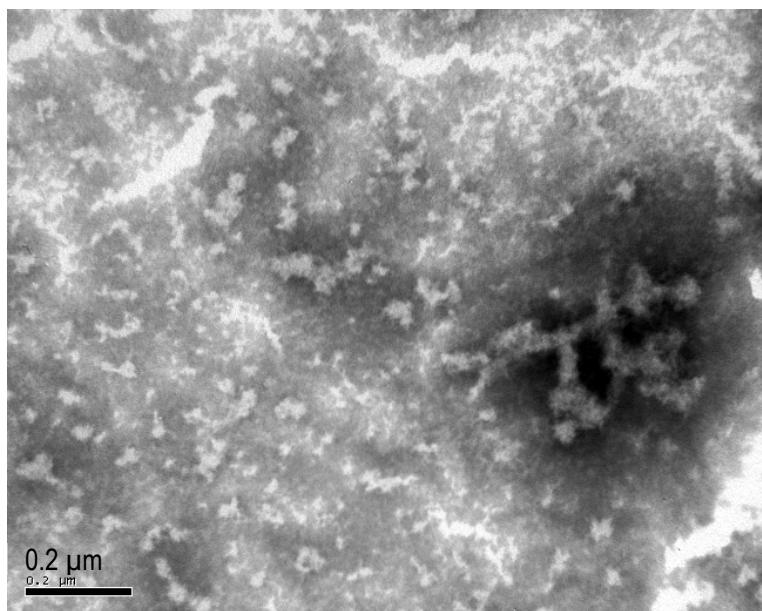


**Figure 7.5A. TEM image of the  $\beta$ Ig/Lyso self-assembly at pH 7.5, ratio 2:1.**

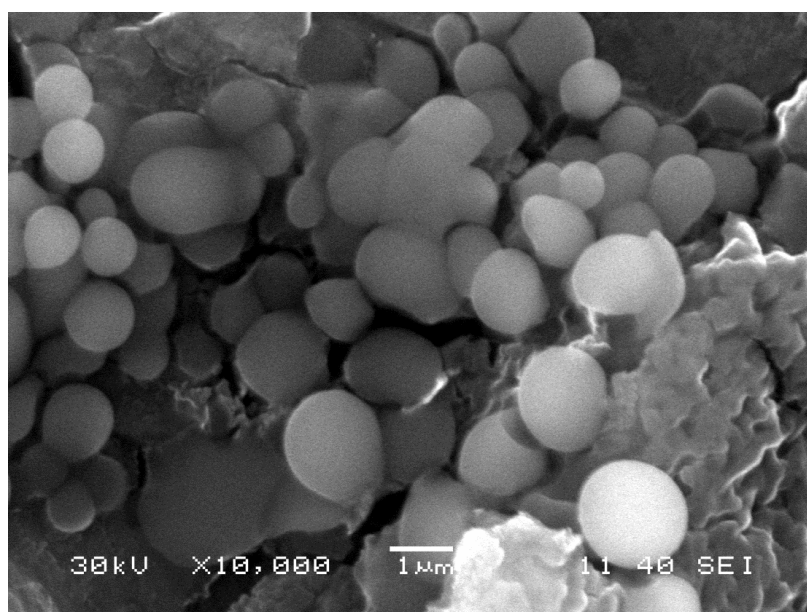


**Figure 7.5B. SEM image of the  $\beta$ Ig/Lyso self-assembly at pH 7.5, ratio 2:1.**

#### **7.4.4.2. Determination of the amounts of proteins in the $\beta$ Ig/Lyso microspheres**

Figure 7.6 represents the HPLC profiles of  $\beta$ Ig and Lyso in the soluble complex present in the supernatant (Figure 7.6A), and in the microspheres that were recovered in the pellet after quick centrifugation at 5,000 x *g*/5 min (Figure 7.6B).

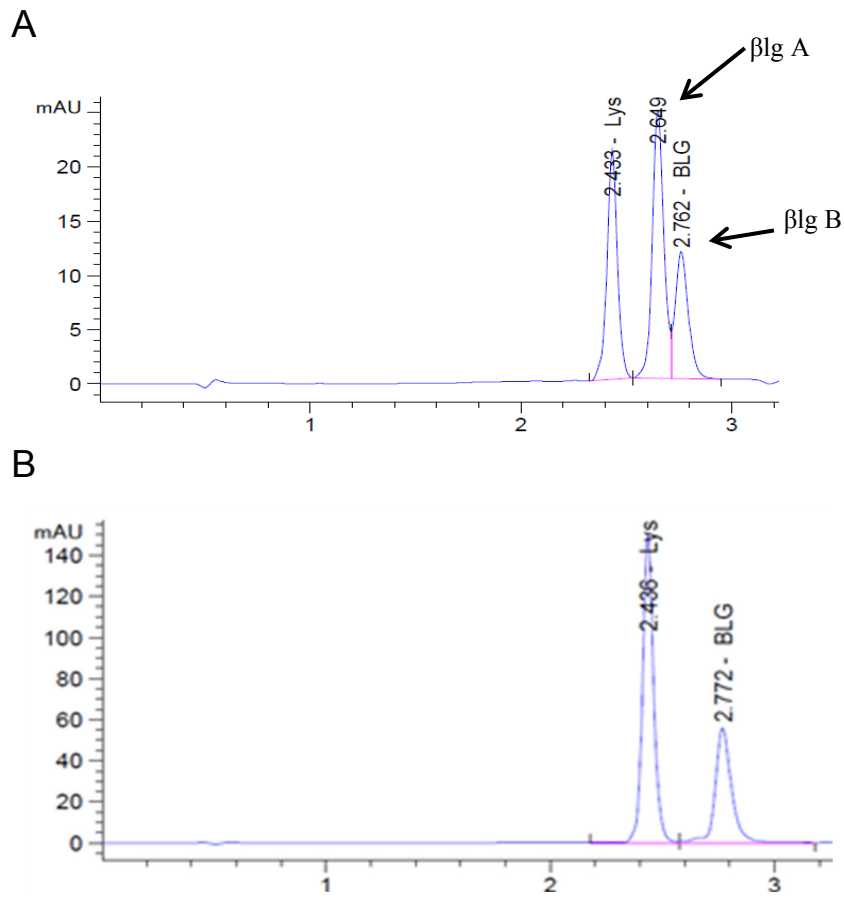


**Figure 7.6. RP-HPLC profiles of amounts of  $\beta$ Ig and Lyso in the supernatant (A) and the pellet (B) after centrifugation (5000 x g for 5 min) of the  $\beta$ Ig/Lyso microspheres prepared using ratio 2:1 at pH 7.5. Absorbance for the proteins at 280 nm and D<sub>3</sub> at 265 nm.**

At pH 7.5,  $\beta$ Ig/Lyso, the microspheres were composed of about 43.1 % Lyso and 45.0 %  $\beta$ Ig, making a total protein content of 88.1 %. This result confirms the theory that protein self-assembly are formed when the molar ratio is 1:1 for the binary systems [139]. The soluble complex recovered in the supernatant was composed of 7.8 %  $\beta$ Ig and 3.0 % Lyso, which is about 10.8% of total soluble protein. Overall, about 98.9 % of the initial protein concentration was recovered by HPLC, the remaining 1.1 % lost due to operator and instrument related errors. Interestingly, the genetic variant  $\beta$ Ig 'A' (retention time at 2.65 min) remains soluble and is entirely recovered in the supernatant indicating that the 'B' variant of  $\beta$ Ig (retention time at 2.76 min) is the one involved in the formation of the  $\beta$ Ig/Lyso microspheres (Figure 7.6B). Most importantly, the present work reports the development and optimization of a rapid HPLC technique which separates and successfully identifies the genetic variants 'A' and 'B' of  $\beta$ Ig from a commercial product without prior denaturation nor hydrolysis. This result is significant because numerous attempts have been made with little success to separate and identify the two genetic variants of native  $\beta$ Ig using HPLC [242].

The purpose of the present study was to prepare an efficient FPPI-carrier for the oral delivery of nutraceutical with excellent drug loading capacity. At the zwitterion point (pH 7.5),  $\beta$ Ig and Lyso at the initial concentration ratio of 2:1 possesses a similar number of oppositely charged residues. This allows charge compensation to occur and the creation of maximum self-association regions between the two proteins where large amounts of drugs may be entrapped. Therefore, a  $\beta$ Ig:Lyso ratio of 2:1 at pH 7.5 may be optimal for bioactives loading studies.

#### **7.4.5. Vitamin D<sub>3</sub> encapsulation in $\beta$ Ig/Lyso microspheres**

In the present study the capacity of the  $\beta$ Ig/Lyso microspheres to encapsulate D<sub>3</sub> was evaluated. Figure 7.7A represents the amount of D<sub>3</sub> remaining in the

supernatant after centrifugation of the  $\beta$ lg/Lyso microspheres, suggesting that almost all  $D_3$  present in the solution was entrapped in the microspheres.

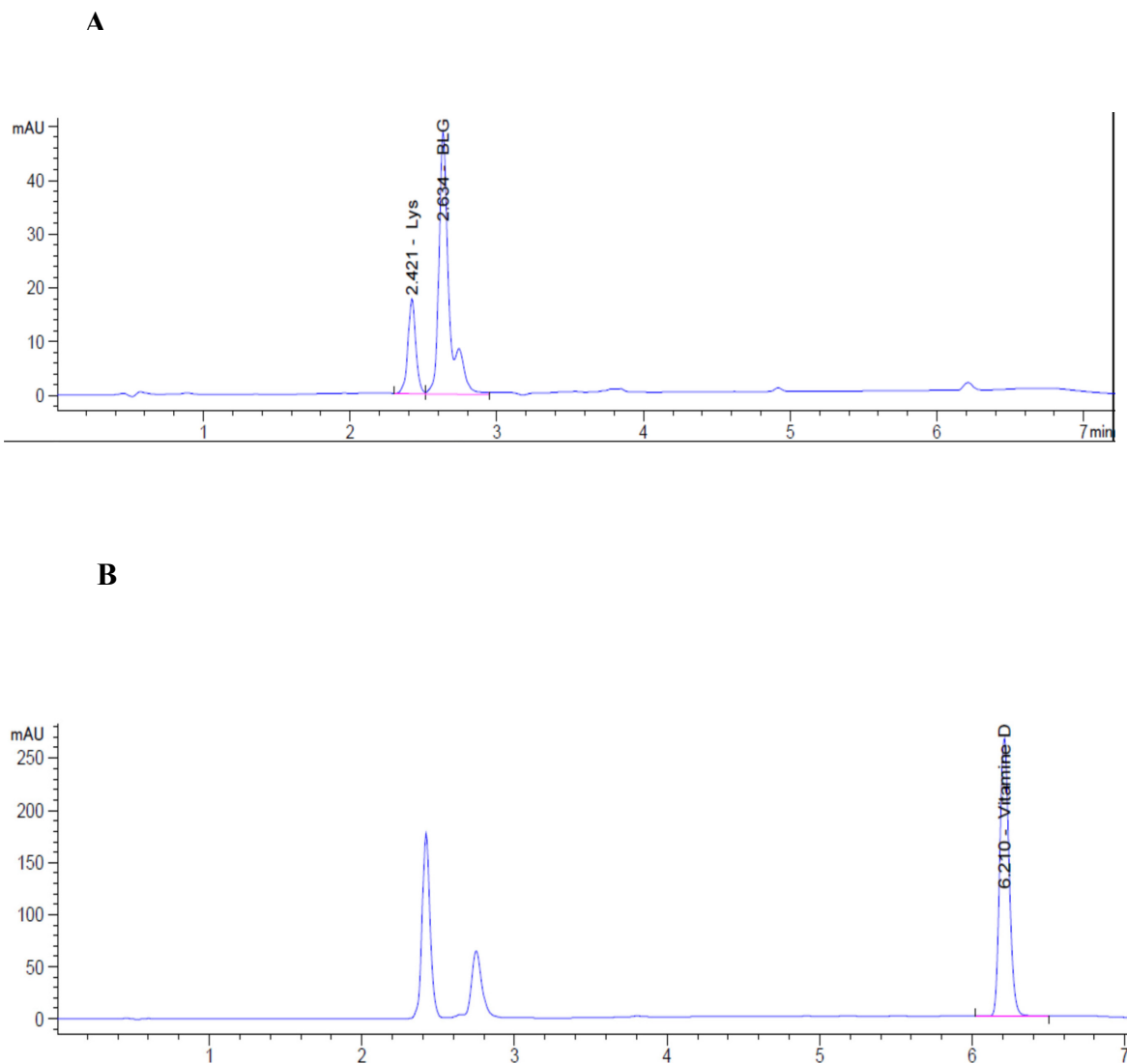


**Figure 7.7. RP-HPLC profiles of D<sub>3</sub> recovered from the supernatant (A) and the pellet (B) after centrifugation (5000 x g for 5 min) of  $\beta$ lg/Lyso microspheres - containing D<sub>3</sub>. Absorbance for the proteins at 280 nm and D<sub>3</sub> at 265 nm.**

This result is confirmed in Figure 7.7B which shows the amounts of  $\beta$ lg, Lyso and  $D_3$  recovered in the pellet. This result was later confirmed by the calculation of the EE which was  $90.8 \pm 4.8$  %. The findings presented in the current study are important since public health authorities are currently being required to increase the daily recommended intake of  $D_3$  from 400 to at least 1000 IU/day for adults and children aged 1 year and older, given the role of  $D_3$  deficiencies in conditions such as cancer, chronic degenerative diseases and various autoimmune disorders [102]. The present study suggests that the  $\beta$ lg/Lyso microspheres can be used as a potential food grade vehicle for  $D_3$ .

## **7.5. Conclusion**

The present study reports that electrostatic interactions between oppositely charged  $\beta$ lg and Lyso induced the formation of microsphere structures that can be used as a versatile food-grade vehicle for nutraceuticals. pH and  $\beta$ lg/Lyso ratios were key factors in the formation of the microspheres. The findings indicate that the optimal initial protein concentration  $\beta$ lg:Lyso ratio (v/v) was 2:1. The  $\beta$ lg/Lyso microspheres successfully encapsulated  $D_3$ , used as a model nutraceutical. Further characterization is ongoing to determine additional information such as the structural changes of the proteins, size distribution and stoichiometry of the complexation. The stability of  $\beta$ lg/Lyso microspheres, during long term storage in the cold and in simulated intestinal fluid, and their ability to protect  $D_3$  from the damaging effects of UV-light are also currently under investigation. The electrostatically-driven process leading the formation of the  $\beta$ lg/Lyso microspheres is an illustration that can serve as model for the aggregation of food proteins which can then be used for the optimization of sustainable platforms to encapsulate a biological active of nutritional interest.

## **7.6. Acknowledgments**

This study was funded by the Canada Research Chair on Proteins, Biosystems and Functional Foods and the Natural Sciences and Engineering Research Council of Canada (NSERC) through the Vanier Canada Graduate Scholarships (Diarrassouba, F.). The authors would like to thank D. Gagnon, A. Gaudreau (Faculté des Sciences de l'Agriculture et de l'Alimentation, Université Laval, Québec, Q.C., Canada) and Pascal Dubé (Institut de recherche sur les nutraceutiques et les aliments fonctionnels (INAF/STELA), Université Laval, Québec, QC, Canada) and the EA-CIDAM staff members (Faculté de Pharmacie, Clermont-Ferrand, France) for their valuable technical assistance.

## Contextual transition

The following chapter encompasses experimental work performed to achieve the fourth objective of the present thesis and provide added-value to the findings obtained from chapter seven. An electrostatically-driven process was used to trigger the aggregation of oppositely charged food grade proteins  $\beta$ -lactoglobulin and egg white Lysozyme. The capacity of the obtained microspheres to protect and stabilize vitamin D<sub>3</sub>, used as model biological active of nutritional interest, during cold storage and when exposed to damaging UV-light was evaluated. The passage of the microspheres through the intestinal membrane was investigated using CaCo-2 cells. The impact of encapsulation of vitamin D<sub>3</sub> in the  $\beta$ -lactoglobulin - Lysozyme microspheres on the bioavailability of the vitamin was assessed by force-feeding rats in an *in vivo* experiment.

## CHAPTER 8

# Food Proteins-Based Microspheres for Increased Uptake of Vitamin D3

A version of this work was submitted to in the Journal of Controlled Release

By

Fatoumata Diarrassouba<sup>a</sup>, Ghislain Garrat<sup>b</sup>, Gabriel Remondetto<sup>c</sup>, Pedro Alvarez<sup>a</sup>,  
Eric Beyssac<sup>b</sup> and Muriel Subirade<sup>a\*</sup>

<sup>a</sup>Chaire de recherche du Canada sur les protéines, les bio-systèmes et les aliments fonctionnels, Institut de recherche sur les nutraceutiques et les aliments fonctionnels (INAF/STELA), Université Laval, Québec, QC, Canada.

<sup>b</sup>EA-CIDAM, Lab Biopharmacie, Faculté de Pharmacie, 28 Place Henri Dunant, 63001, Clermont-Ferrand, France.

<sup>c</sup>Centre de recherche et développement, Agropur Coopérative. 4700 rue Armand Frappier, St-Hubert, QC, J3Z 1G5.

## 8.1. Abstract

Evidence suggests that food supplementation with the current levels of vitamin D<sub>3</sub> (D<sub>3</sub>) cannot address most disease conditions which require increased amounts of D<sub>3</sub> such as breast or colon cancer, bacterial infections or cardiovascular illnesses. Furthermore, label values commonly underestimate the actual amount of D<sub>3</sub> in food products probably due to the fact that D<sub>3</sub> is labile and easily degraded by light and oxygen. Therefore, increasing the stability of D<sub>3</sub> should enhance its intestinal uptake and bioavailability. The efficiency of D<sub>3</sub>-entrapped microspheres previously formed using bovine protein  $\beta$ -lactoglobulin ( $\beta$ lg) and Lysozyme (Lyso) from egg white, to protect D<sub>3</sub> during cold storage and upon exposure to UV-light, was evaluated. The behavior of the  $\beta$ lg/Lyso microspheres in simulated intestinal fluid and their impact on the kinetic release of D<sub>3</sub> were determined. The permeability of the D<sub>3</sub>-loaded  $\beta$ lg/Lyso microspheres using Caco-2 cells was studied. An *in vivo* experiment was carried out to evaluate the impact of the D<sub>3</sub>-loaded  $\beta$ lg /Lyso microspheres on the bioavailability of the vitamin by force-feeding rats. The data indicate that the  $\beta$ lg/Lyso microspheres effectively improved the stability of D<sub>3</sub> during cold storage and exposure to UV-light irradiation. D<sub>3</sub> was readily released in the intestines and the release kinetics was accelerated in presence of proteolytic enzymes. The protein-based microspheres were able to cross the CaCo-2 cells. The absorption and and bioavailability of D<sub>3</sub> were improved, as confirmed by the significant increase in the serum levels of the biomarker 25-hydroxy-D<sub>3</sub> in rats. In the current work, water soluble food protein-based microspheres were used to substantially increase the bioavailability of the lipophilic vitamin, and thus can serve in the oral delivery of D<sub>3</sub>. The enhanced bioavailability of D<sub>3</sub> has applications in the food industry and direct implications for public health.

## 8.2. Introduction

In addition to their classical actions on calcium and phosphorus homeostasis regulation, vitamin D<sub>3</sub> (D<sub>3</sub>) and derived metabolites affect both innate and adaptive immune response, regulation of blood glucose and insulin level, the cardiovascular system, lung immunity and respiratory diseases, and offer protection against bacterial infections, breast and colon cancers, leukemia, tuberculosis, multiple sclerosis, various autoimmune disorders and degenerative diseases; the list is not exhaustive [181-183, 243]. However, D<sub>3</sub> deficiency is quite common among populations worldwide. In addition to insufficient dietary intake, it can occur as a consequence of life and clothing styles, skin types, age, culture, geographic location or displacements to temperate latitudes, all resulting in reduced exposure to sun light [199, 244]. Reports indicate that the current US/Canadian fortification practices are ineffective in preventing hypovitaminosis D in vulnerable populations insufficiently exposed to sunlight [148, 187, 215]. Furthermore, results from cross-sectional, meta-analysed, randomized controlled trials indicate that milk supplementation with D<sub>3</sub> is insufficient to produce significant health benefits other than against bone diseases [215]. Therefore, milk supplementation with the current levels of D<sub>3</sub> cannot address most disease conditions which require increased amounts of D<sub>3</sub> such as breast or prostate cancer or cardiovascular illnesses.

It has been found that labels are often misleading and commonly misrepresent the actual amount of D<sub>3</sub> in food products [244, 245]. This is probably be due to the fact that D<sub>3</sub> is a reactive vitamin that is easily degraded by light and oxygen overtime [244]. For example, a four year survey in the US showed that over half of the milk sampled in dairy processing plants were non-compliant and under-fortified [244, 245]. The poor water solubility of D<sub>3</sub> restricts its applications mostly to foods with some degree of fat content, which may negatively affect the uptake of D<sub>3</sub>, taking into account new consumer requirements for food products with no to low fat content. Furthermore, while in the US, dairy products, breakfast cereals and orange juices are fortified with D<sub>3</sub>, in Canada, milk and margarine are enriched,

which is apparently not sufficient to meet the current recommended intake of D<sub>3</sub> from food [187, 246]. Therefore, strategies aiming at improving D<sub>3</sub> intake by increasing both its amount in foods and the range of candidate foods for fortification are highly encouraged in order to maintain its biological responses on hard and soft tissues. One way to achieve this goal is through binding of D<sub>3</sub> to the major whey protein  $\beta$ -lactoglobulin ( $\beta$ lg) from bovine milk, which is a by-product of cheesemaking.

It has been established that  $\beta$ lg binds and transports D<sub>3</sub> at a  $\beta$ lg:D<sub>3</sub> ratio of 1:2 to form a complex via a static quenching mechanism [13, 61, 79, 176]. Similarly to resveratrol and  $\alpha$ -tocopherol, the  $\beta$ lg/D<sub>3</sub> complex was shown to increase the solubility of D<sub>3</sub> and its stability at gastro-intestinal pH values [6, 8, 200]. As well, a 'green method' was developed to fabricate food protein-based microspheres with high D<sub>3</sub> encapsulation efficiency [224]. The authors used oppositely charged food proteins  $\beta$ lg and egg Lysozyme (Lyso) to form microspheres in aqueous solution without the use of any chemical or cross-linking agents. Electron micrographs have shown that  $\beta$ lg and Lyso can self-assemble to form microspheres smaller than 7.1  $\mu$ m. Therefore,  $\beta$ lg/Lyso-based microspheres were proposed as GRAS (generally recognized as safe) carriers for nutraceuticals and pharmaceuticals. This concept was validated with the entrapment of D<sub>3</sub> in the  $\beta$ lg/Lyso microspheres at encapsulation efficiency greater than 90 %. Therefore, microspheres were suggested as a carrier and protective system that could be used to increase the amount of D<sub>3</sub> in foods, especially those with no or low fat content, which is compatible with current consumer requirements for high nutritional foods with low fat contents. However, D<sub>3</sub> stability studies have not yet been carried out and the mechanism of passage of the D<sub>3</sub>-loaded microspheres through the intestinal epithelium and subsequent impact on the uptake and bioavailability of D<sub>3</sub> is still unknown. Therefore, the aim of the present study was to investigate the stability of D<sub>3</sub>-loaded  $\beta$ lg/Lyso microspheres during cold storage, upon exposure to UV-light irradiation, and in simulated intestinal fluid. The intestinal uptake of D<sub>3</sub> was studied *in vitro* using CaCo-2 cells and *in vivo* using animals.

## **8.3. Experimental Section**

### **8.3.1. Materials**

$\beta$ -lactoglobulin ( $\beta$ lg) was purchased from Davisco Foods International, Inc. (Le Sueur, MN, USA). High purity  $\beta$ -lactoglobulin (B variant, purity  $\geq 90\%$ ), Lysozyme (Lyso) from chicken egg white (lyophilized powder, protein  $\geq 90\%$ ,  $\geq 40,000$  units/mg protein) and vitamin D<sub>3</sub> (purity  $\geq 98\%$ , HPLC) were obtained from Sigma-Aldrich Chemical and Co (Oakville, ON, Canada). The proteins were used without further purification. Acetonitrile (ACN, HPLC grade), methanol (MeOH, HPLC grade) and trifluoroacetic acid (TFA) were purchased from EMD International (Gibbstown, NJ, USA).

### **8.3.2. Sample preparation**

Samples stock solutions consisting of  $\beta$ lg 0.2 % (w/v) and Lyso 0.1 % (w/v) were prepared as previously described [224]. Vitamin D<sub>3</sub> (D<sub>3</sub>) stock (1 ppm) was prepared daily by dissolving 10 mg in 25 mL MeOH [188]. Working solutions of D<sub>3</sub> were obtained by diluting the stock solution in MilliQ water. All D<sub>3</sub>-containing solutions were protected from light by preparing them in a dark room and further protected using an aluminium foil wrapping.

### **8.3.3. Encapsulation of D<sub>3</sub> in the $\beta$ lg/Lyso microspheres**

The  $\beta$ lg/D<sub>3</sub> complex at a  $\beta$ lg (0.1 %, w/v):D<sub>3</sub> (110  $\mu$ M) ratio (v/v) of 1:2 was formed using a procedure previously described [200]. Then Lyso concentrated at 0.1 % (w/v) was added to the  $\beta$ lg/D<sub>3</sub> complex using a  $\beta$ lg:D<sub>3</sub>:Lyso ratio (v:v) of 2:4:1. The pH of the mixture was adjusted to 7.5 under continuous nitrogen flow. The resulting ternary system ( $\beta$ lg/D<sub>3</sub>/Lyso) was incubated at 4 °C in the dark for 24h. The

encapsulation efficiency (EE) was calculated using a method described elsewhere [224].

#### **8.3.4. Stability of D<sub>3</sub> during long term storage at 4 °C**

The stability of D<sub>3</sub> encapsulated in the  $\beta$ lg/Lyso microspheres at 4 °C was determined over a five week period. The initial concentration of encapsulated D<sub>3</sub> was determined after 24 h, as described in section 3. Samples corresponding to weeks 1 to 5 were stored at 4 °C. Each week, a sample was withdrawn for determination of the amount of D<sub>3</sub> remaining in solution for each condition. Solutions of D<sub>3</sub> diluted in MilliQ water were prepared and analyzed under the same conditions.

#### **8.3.5. Stability of D<sub>3</sub> to UV-light irradiation**

The D<sub>3</sub>-loaded  $\beta$ lg/Lyso microspheres and D<sub>3</sub> solutions were exposed to UV light (254 nm, 15 W) in order to assess the UV-light stability of D<sub>3</sub> over 24 h [130]. At each sampling time consisting of t 0, 1, 2, 4, 6, 8, 10 and 24 h, the amount of D<sub>3</sub> remaining in the microspheres was determined.

#### **8.3.6. Kinetic release of D<sub>3</sub> in simulated intestinal fluid**

The release of D<sub>3</sub> in simulated intestinal fluid (SIF) was investigated using a USP-2 paddle apparatus (SOTAX Corporation, Westborough, MA, USA). The release media consisted of the simulated intestinal fluid (SIF) as described in the US Pharmacopeia in the presence and absence of 1.0 % pancreatin (w/v) at pH 6.8. Each of the solutions containing either D<sub>3</sub> (100 mL) or the D<sub>3</sub>-loaded  $\beta$ lg/Lyso

microspheres was incubated in one of two release media with continuous agitation (at ~ 50 rpm) at 37 °C [224]. Samples withdrawn at regular intervals over 6 hours were centrifuged (5,000 x *g*/5 min) and the concentration of D<sub>3</sub> in the supernatant was determined. A control with and without enzyme was also run.

### **8.3.7. *In vitro* study of the permeability of the D<sub>3</sub>**

The human Caucasian colon adenocarcinoma cells (CaCo-2) were sourced from the American Type Culture Collection (ATCC, Rockville, MD, USA) at passage 17. Cell maintenance during culture was described elsewhere [19]. Solutions (0.5 mL) of D<sub>3</sub> and the D<sub>3</sub>-containingβlg/Lyso microspheres were deposited on the apical side of the monolayer membrane while the basolateral area was submerged in 1.5 mL of the culture media, as previously described [224]. The final concentration of D<sub>3</sub> on the cells was 21.17 µg. DPBS (0.5 mL) was used on cells as a control. RP-HPLC was used to monitor the amount of D<sub>3</sub> recovered in the basolateral site. Trans Epithelial Electric Resistance (TEER) measurements (EVOM - World Precision Instruments (WPI), Inc., Sarasota, FL, USA) were taken to determine cell integrity before and after the experiment. The toxicity of the test solutions was determined by measuring the TEER at 30, 60, 90, 120 min and t 24 and 48 h after the experiment.

### **8.3.8. *In vivo* study of the intestinal absorption of the D<sub>3</sub> containing βlg/Lyso**

Animal studies were conducted at the 'Unité de Stabulation Animale, Ethic Committee-CE-42-12' (Université d'Auvergne, Clermont-Ferrand, France). Adult male Wistar rats (*n* = 25; Elevage Dépré, St. Doulchard, France) weighing 300 ± 20 g at the beginning of the experiment were used. Housing characteristics, accommodation and the average feed intake are described elsewhere [19]. After

the acclimation period, two or three rats were housed per cage for three weeks. The animals had access to feed and water *ad libitum*. The rats ( $n = 15$ ) were divided into three groups ( $n = 5$ ) each receiving one of the treatments consisting of MilliQ water supplemented with 0.09 % NaCl (control),  $D_3$ , and the  $D_3$ -containing  $\beta$ lg/Lyso microspheres with the same final concentration of  $D_3$  (110  $\mu$ M or 77  $\mu$ g). Blood samples were collected at  $t_0$  and at three weeks in 0.5 mL conical tubes pre-coated with 10  $\mu$ L of sodium heparin (0.1 IU). The plasma was separated by centrifugation at 1000  $\times g$  for 10 min. Plasma samples were stored at -20 °C until analysis of 25(OH) $D_3$  in rat plasma was performed using the 25-Hydroxy Vitamin D Direct EIA kit (IDS Diagnostics, Fountain Hills, AZ, USA) according to the manufacturer's instructions.

### **8.3.9. Statistical analysis**

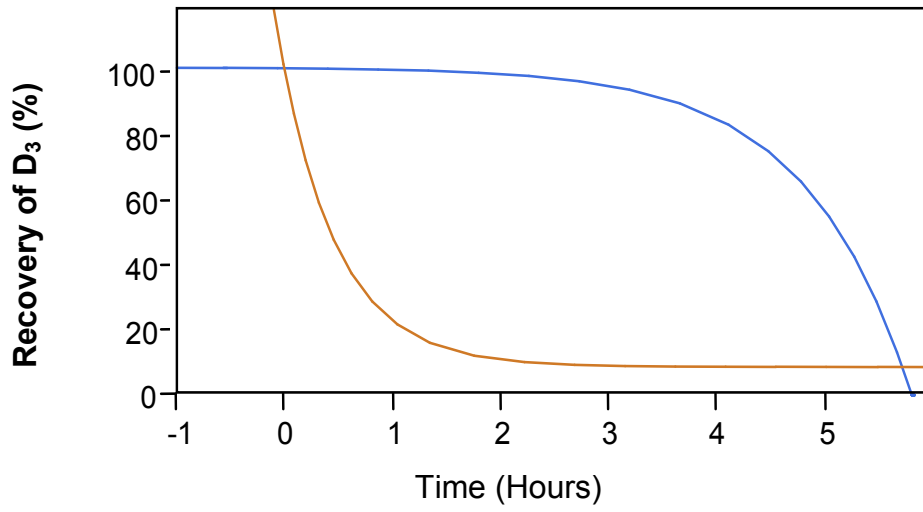
Statistical analysis and  $D_3$  release kinetics were performed using JMP statistical discovery software (JMP 10, SAS Institute Inc., Cary, NC, USA). Nonlinear regression was performed using the built-in models for nonlinear curve fitting. The Equivalence test was also performed to provide an analysis for testing the equivalence of models across levels of the grouping variable ( $D_3$  and the  $D_3$ -containing  $\beta$ lg/Lyso microspheres). The purpose of this test was to assess whether there was a practical difference between means. The equality of the parameters was tested by analyzing the ratio of the parameters. The decision lines were placed at ratio values of 0.8 and 1.25, representing a 25 % difference. The significance level was fixed at  $p < 0.05$ . All measurements were conducted in triplicate and the results were reported as the mean  $\pm$  SD.

## **8.4. Results and Discussion**

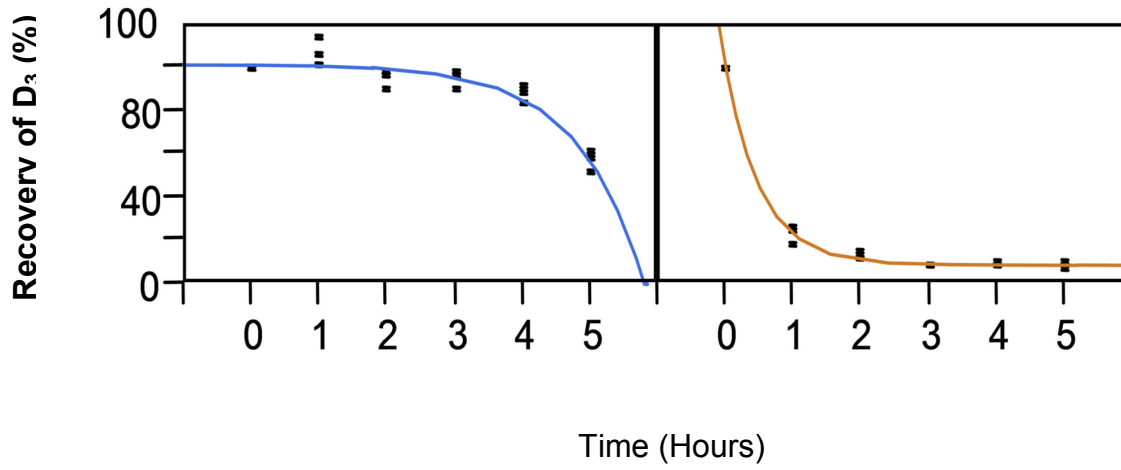
### **8.4.1. Stability of D<sub>3</sub> during long-term storage at 4 °C**

The long-term stability of D<sub>3</sub> during storage in refrigerated conditions was determined over a period of five weeks. The recovery of D<sub>3</sub> in the microspheres was compared to that of the free vitamin as presented in Figure 8.1, representing the fit curves obtained from the non-linear regression model used to analyze the recovery of the D<sub>3</sub>.

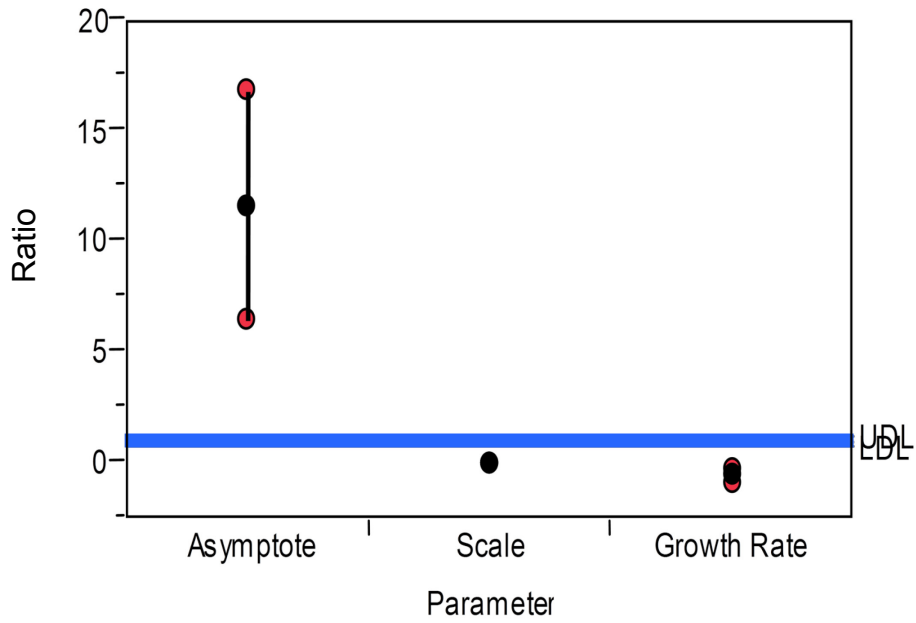
**A**



$\beta$ gl/D<sub>3</sub>/Lyso microspheres (—) :  $y = 101.68 - 0.26 \times 10^{-1.03 x}$   
D<sub>3</sub> (—) :  $y = 8.73 + 91.25 \times 10^{-1.87 x}$



**B**



$\alpha = 0.05$

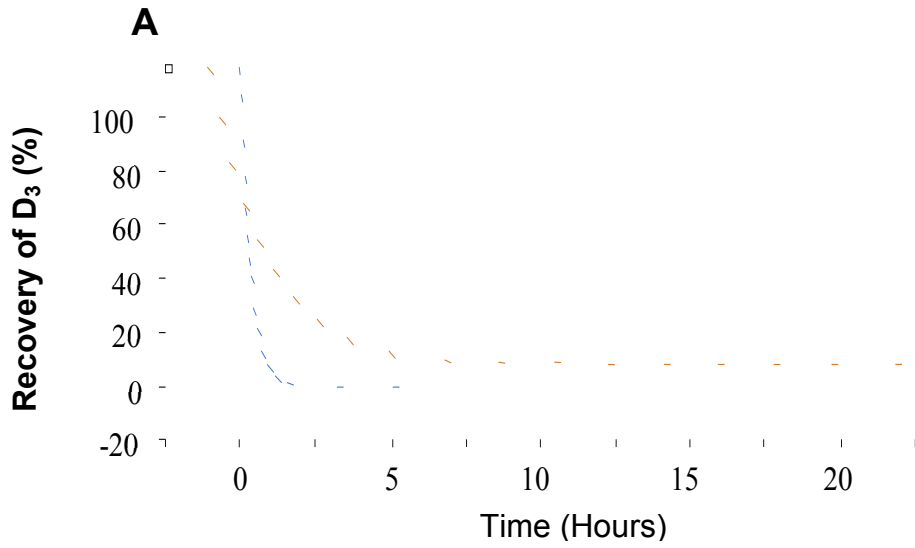
**Figure 8.1. Stability of  $D_3$  and the  $\beta$ lg/ $D_3$ /Lyso microspheres in refrigerated conditions ( $4^\circ\text{C}$ ) during five weeks. A: Plot of the fitted curves of  $D_3$  and the  $\beta$ lg/ $D_3$ /Lyso microspheres. B. Equivalence between  $D_3$  and the  $\beta$ lg/ $D_3$ /Lyso microspheres. The level of  $\alpha$  was set at 0.05. The lower decision limit (LDL) was 0.8 and the upper decision limit (UDL) was set at 1.25 (representing 25% difference).**

After two weeks of storage at 4°C,  $87.7 \pm 2.0$  % of the free D<sub>3</sub> was already lost and at the end of the five weeks, only  $8.3 \pm 2.3$  % remained in solution, which represents a loss of over 91%. Conversely,  $95.0 \pm 2.5$  % and  $56.0 \pm 4.3$  % of D<sub>3</sub> were recovered after two and five weeks, respectively, of cold storage of the vitamin-loaded  $\beta$ lg/Lyso microspheres. This represents a 6-fold increase in D<sub>3</sub> recovered from the protein microspheres compared to the free D<sub>3</sub> treatment stored for the same period. The D<sub>3</sub> entrapped in the  $\beta$ lg/Lyso microspheres was significantly more stable than the free vitamin (Figure 8.1A) as confirmed by the equivalence test (Figure 8.1B). Therefore, the  $\beta$ lg/Lyso microspheres effectively protected D<sub>3</sub> against degradation during storage at 4°C, which represents regular storage conditions of most dairy products. Therefore, during cold storage at pH 7.5 and in absence of any light source, the main degradation mechanism can be ascribed to oxygen and free radical generation [20, 247]. Furthermore, the protein matrix consisting of entangled  $\beta$ lg and Lyso that entraps the vitamin might protect D<sub>3</sub> against oxidative degradation, in addition to the protective anti-oxidative activity of  $\beta$ lg [20, 129]. Long-term stability of D<sub>3</sub> is important in the manufacturing and consumption of food products to ensure that labeling accurately reflects the actual D<sub>3</sub> content [218]. Light is one of the most potent factors to affect D<sub>3</sub> degradation during storage. Thus, it is important to determine the efficiency of the  $\beta$ lg/Lyso microsphere to protect D<sub>3</sub> when exposed to light.

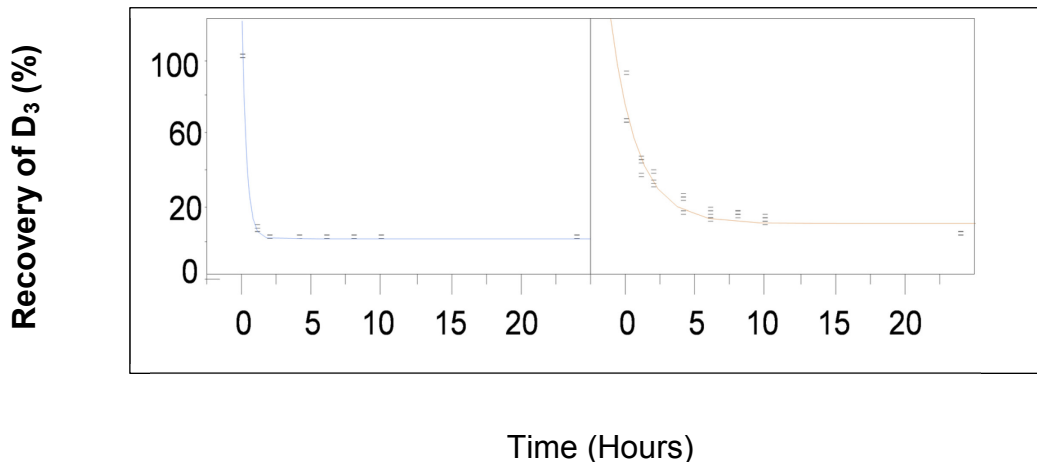
#### **8.4.2. Stability of D<sub>3</sub> in response to UV-light irradiation**

The protective effect of  $\beta$ lg/Lyso microspheres against photochemical degradation of D<sub>3</sub> was assessed by exposing the D<sub>3</sub>-loaded  $\beta$ lg/Lyso microspheres and unprotected D<sub>3</sub> to intensive UV-light for 24 h. The fitted curves obtained from non-linear regression are presented in Figure 2. After 2 h of exposure to UV-light, about 98.8 % of the unprotected D<sub>3</sub> was degraded while 35 % of entrapped-D<sub>3</sub> in the  $\beta$ lg/Lyso microspheres still remained intact. Total loss was obtained after 6 h of

irradiation for the unprotected D<sub>3</sub> while it was only after 24 h that 97 % of D<sub>3</sub> entrapped in the  $\beta$ Ig/Lyso microspheres was degraded (Figure 8.2A).



$\beta$ gal/D3/Lyso microspheres (—) :  $y = 8.64 + 61.03^{-0.52 \times \text{Time (Hours)}}$   
 D<sub>3</sub> (—) :  $y = 0.2 + 99.81^{-3.04 \times \text{Time (Hours)}}$



**B**

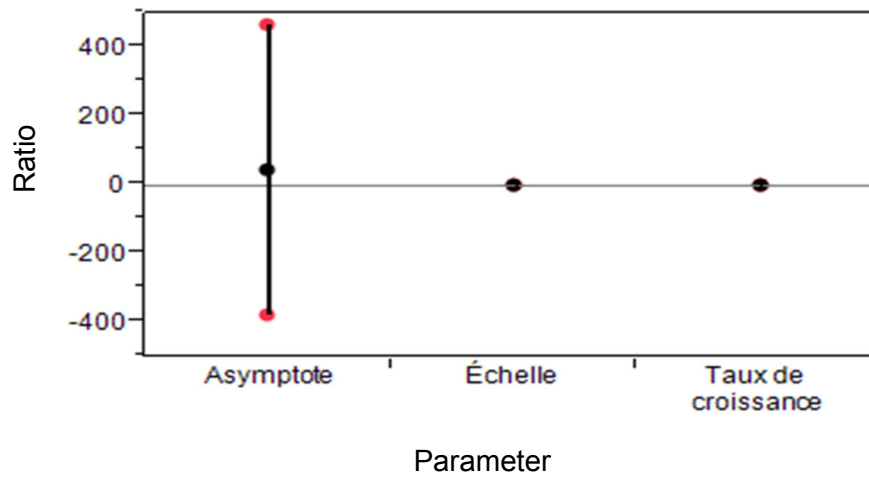


**Figure 8.2. UV-light stability of D<sub>3</sub> and the  $\beta$ lg/D<sub>3</sub>/Lyso microspheres over 24 hours ( $\lambda = 254$  nm). A: Graph of the stability of D<sub>3</sub>. B. The equivalence between D<sub>3</sub> and the  $\beta$ lg/D<sub>3</sub>/Lyso microspheres.**

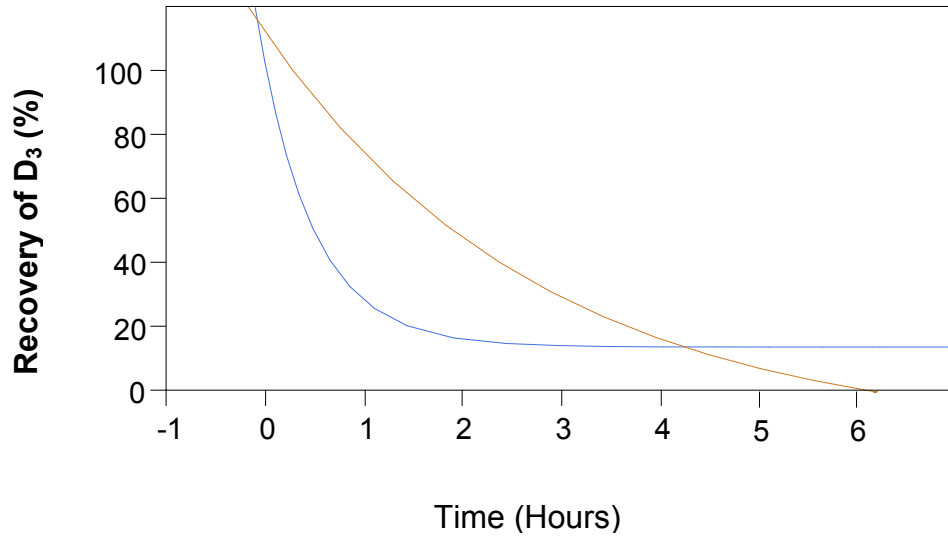
It is important to note that the wavelength used in this work was 254 nm, which is quite damaging to biological systems and commonly used to disinfect surfaces. Even in case of accidental light exposure, D<sub>3</sub>-containing products would be exposed to milder light irradiation; usually higher UV-light wavelengths (e.g. 352 nm) are used to analyze D<sub>3</sub> stability [225]. The rapid degradation of the unprotected D<sub>3</sub> and the importance of the shielding effect of the  $\beta$ lg/Lyso microspheres is confirmed by the Equivalence test (Figure 8.2B). The protective effect of the  $\beta$ lg/Lyso microspheres against the photochemical degradation of D<sub>3</sub> can also be attributed to the dense protein matrix composed of amino acids with aromatic side groups and double bonds which can absorb UV-light and thus reduce the absorption of UV-light by the vitamin [225]. The entrapment of D<sub>3</sub> in the protein microsphere might also provide additional protection by decreasing the mobility of the vitamin, consequently limiting its reactivity [20]. The free thiol responsible of the antioxidant activity of  $\beta$ lg might also contribute to improved stability of D<sub>3</sub> [129].

Attempts to encapsulate D-vitamins in bio-polymeric matrices such as proteins or protein-polysaccharide complexes have been made [20, 130, 225]. However, very few studies have investigated the fate and stability of these biomacromolecules in the gastro-intestinal tract (GI), where digestive enzymes might impede the release of the vitamin from the carrier system. We have previously demonstrated that the stability of  $\beta$ lg/D<sub>3</sub> complex was improved at higher pH and in the presence of proteases in the intestines due to a mutual protective effect [19, 200]. However, the formation of the microspheres between the  $\beta$ lg/D<sub>3</sub> complex and Lyso mainly through electrostatic and hydrophobic interactions might lead to some structural modification of  $\beta$ lg [140], which may affect the release of D<sub>3</sub> during transit in the GI tract. Therefore, it is important to investigate the stability of the  $\beta$ lg/Lyso microspheres in the GI tract.

### **8.4.3. Kinetic release of D<sub>3</sub> in simulated intestinal fluid**

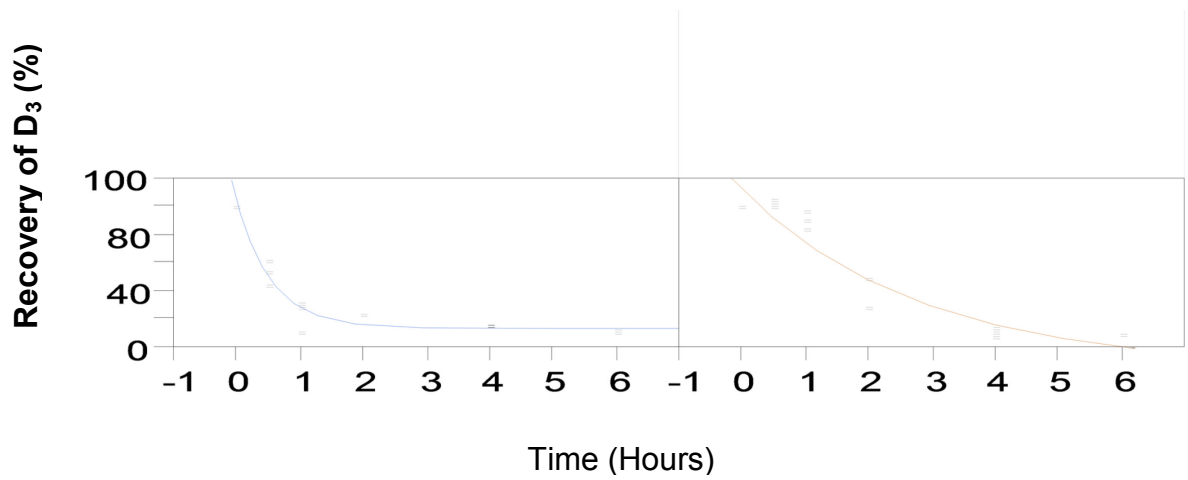
The fitted curves generated by the nonlinear regression models shown in Figures 3 and 4 represent the kinetic release of D<sub>3</sub> in simulated intestinal fluid (SIF) at pH 6.8, with or without pancreatin, respectively. At the end of the six hours of experiment, over 90 % of the D<sub>3</sub> was degraded probably due to oxidation and free radical formation, as was explained above. However, Figure 8.3A shows that the βlg/Lyso microspheres provided some protection to D<sub>3</sub> for up to four hours; following that, the release and/or degradation rate was not statistically different from that of the free vitamin as shown by the scale on the equivalence test (Figure 8.3B).

**A**



$\beta\text{Ig}/\text{D}_3/\text{Lyso microspheres}$  (—)  $y: -14.3 + 126.2^{(-0.35 \times \text{Time (Hours)})}$

$\text{D}_3$  (—)  $y: 13.9 + 86.6^{(-1.8 \times \text{Time (Hours)})}$



**B**

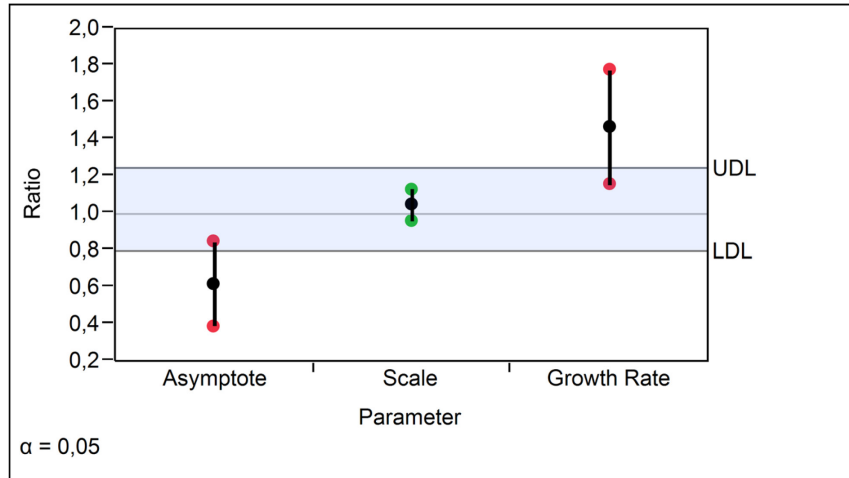
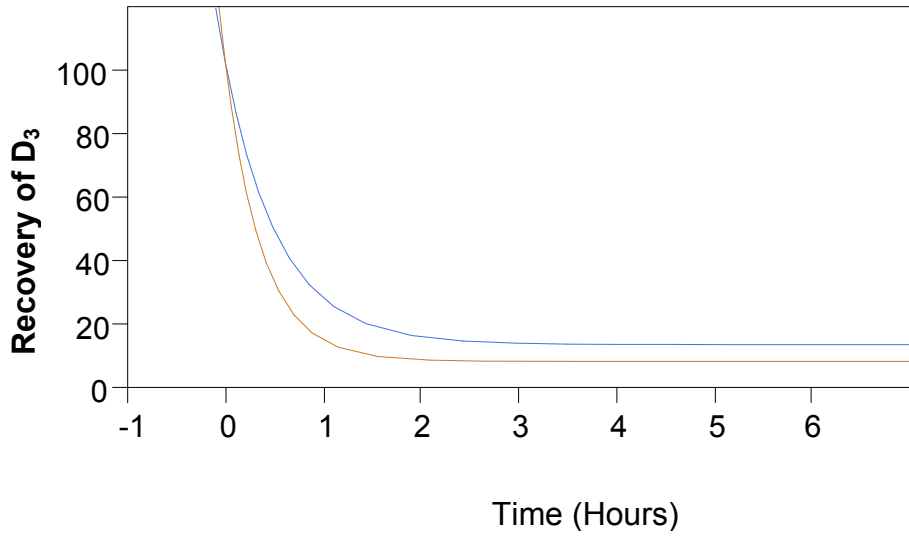


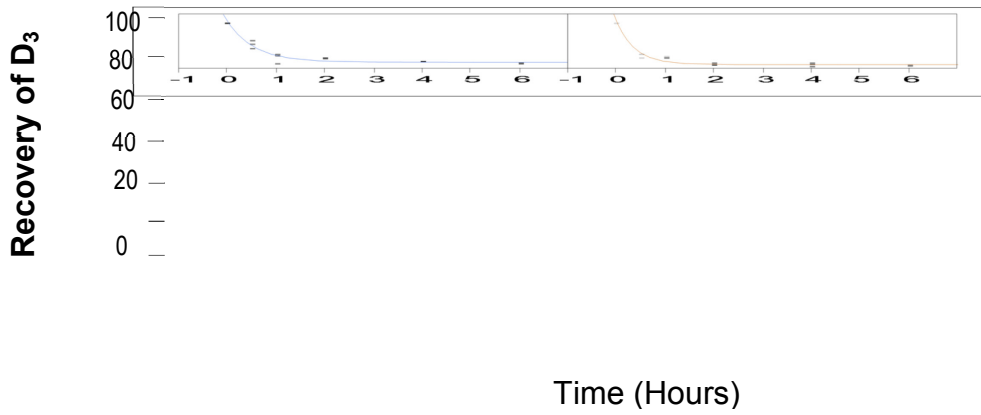
**Figure 8.3. Stability of  $D_3$  and the  $\beta$ Ig/ $D_3$ /Lyso microspheres in Simulated Intestinal Fluid without pancreatin at pH 6.8, 37°C (USP-2 apparatus). A: Graph of the intestinal stability and B. The equivalence between  $D_3$  and the  $\beta$ Ig/ $D_3$ /Lyso microspheres.**

In the presence of pancreatin (Figure 8.4A), the  $\beta$ lg/Lyso microspheres offered little protection to D<sub>3</sub> due to the rapid release of the vitamin. Indeed, after the first hour of digestion over 75 % of the vitamin was released from the  $\beta$ lg/Lyso microspheres.

**A**



$\beta\text{Ig}/\text{D}_3/\text{Lyso microspheres}$  (—)  $y = 8.6 + 90.7^{(-2.64 \times \text{Time (Hours)})}$   
 $\text{D}_3$  (—)  $y = 13.9 + 86.6^{(-1.80 \times \text{Time (Hours)})}$



**B**

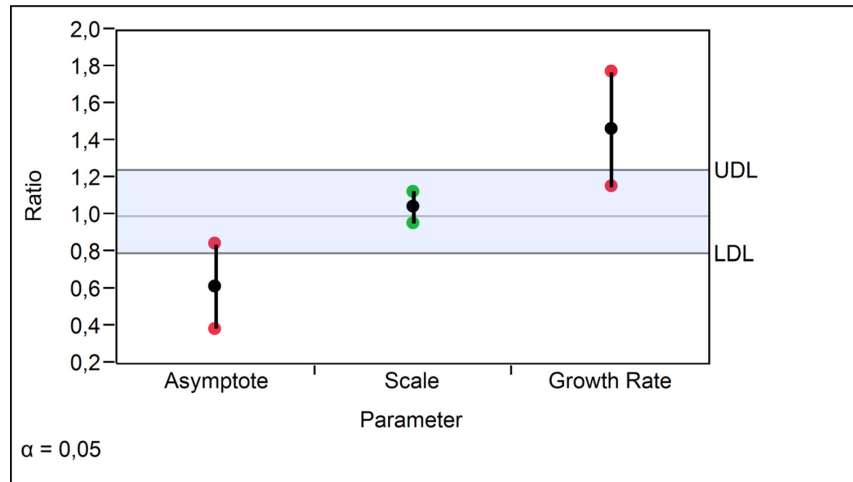


**Figure 8.4. Stability of D<sub>3</sub> and the  $\beta$ Ig/D<sub>3</sub>/Lyso microspheres in Simulated Intestinal Fluid with pancreatin at pH 6.8, 37°C (USP-2 apparatus). A: Graph of the intestinal stability and B. The equivalence between D<sub>3</sub> and the  $\beta$ Ig/D<sub>3</sub>/Lyso microspheres.**

This result confirms that the formation of the  $\beta$ lg/Lyso microspheres concomitantly leads to a substantial modification of the structure of  $\beta$ lg and/or Lyso [140]. Accordingly, the target amino acids become accessible to trypsin and chymotrypsin, which consequently affects the binding of  $D_3$  to  $\beta$ lg/Lyso complex. In that context, the increased stability of the  $D_3$ -loaded  $\beta$ lg/Lyso microspheres in the absence of pancreatin during the first four hours in SIF can be understood (Figure 8.3A).

The structure of Lyso might also be affected by the interaction with  $\beta$ lg and may undergo proteolysis to some extent since it contains amino acids including arginine, lysine, tryptophan and tyrosine that are targets for trypsin and chymotrypsin [129, 226]. Therefore, the structure of both  $\beta$ lg and Lyso can be affected during the formation of the microspheres, which in turn affects the binding of  $D_3$  to  $\beta$ lg, consequently provoking a rapid release of the vitamin in the presence of pancreatin in SIF.

The  $\beta$ lg/Lyso microspheres may be produced by monitoring the couple pH/isoelectric point ( $pI$ ), which in turn promotes electrostatic interactions between the proteins [224]. At the optimal pH for the interaction, that is pH 7.5,  $\beta$ lg is negatively charged while Lyso carries a net positive charge. The  $pI$  of  $\beta$ lg (5.2) is below pH 7.5 and that of Lyso (11.5) is above pH 7.5 [248]. Hence, at the pH of an empty stomach (pH 1.2), the  $\beta$ lg/Lyso microspheres are disrupted due to strong electrostatic repulsion, with both  $\beta$ lg and Lyso bearing net positive charge resulting in a burst release. Hence, it was unnecessary to carry out further kinetic release studies of  $D_3$  at gastric pH which reproduces a fasting condition. However, dilution and buffering effects temporarily raise the gastric pH post-prandially to values between 4.5 and 6.0 [32]. Therefore, one can assume that the  $D_3$ -loaded  $\beta$ lg/Lyso microspheres might persist longer during transit in the stomach if administered with meals at a higher pH value and then later in the intestines, improving the chances of reaching the blood stream. Hence, the  $\beta$ lg/Lyso microspheres can deliver  $D_3$  to the GI tract, with or without meals, depending on the site of action of the encapsulated bioactive. In case of a post-prandial administration, the intestines

can be targeted, and hence it becomes important to further elucidate the transport mechanism through the intestines using the permeability test.

#### **8.4.4. *In vitro* study of the permeability of D<sub>3</sub>**

The permeability of D<sub>3</sub> through the intestinal membrane was studied using Caco-2 cells, which mimic the epithelial cell wall [249]. At each sampling period (0.5, 1 and 2 h),  $\beta$ lg/Lyso microspheres were detected in the basolateral side, as the HPLC profile was similar to that of the  $\beta$ lg/Lyso microspheres shown on Figure 7.7.B in Section 7.4.5 of Chapter 7 (without the peak of D<sub>3</sub>). This finding is important since it implies that the microspheres could cross the intestinal membrane. This result was confirmed by the values of the TEER measurements, which indicated that a loss of cell integrity might occur during the experiment (Table 8.1). Recently, it was shown that alginate-based nanoparticles ranging from 200 to 400 nm in size were internalized into the Caco-2 cells [131]. The modified alginate-based nanoparticles embedded D<sub>3</sub> and were proposed as carriers for oral delivery of the vitamin. We have previously demonstrated that the  $\beta$ lg/Lyso microspheres are composed of protein aggregates of size varying from a few nanometers to volume mean diameter of 7.1  $\mu$ m and span of 2.5  $\mu$ m [224]. More precisely, the percent of the size distribution lying below 10 % (Dv0.1), 50 % (Dv0.5) and 90 % (Dv0.9) were 1.2  $\mu$ m, 4.0  $\mu$ m and 11.7  $\mu$ m, respectively. It was proved that microparticles varying from 0.1 to 10  $\mu$ m in size were able to cross the Caco-2 cells even though smaller microparticles less than 1  $\mu$ m in diameter had significantly greater uptake [250]. Therefore, in the present work, the  $\beta$ lg/Lyso microspheres could cross the Caco-2 cells, which is the *in vitro* model for the intestinal epithelium. The  $\beta$ lg/Lyso microspheres could be proposed as suitable carriers for delivery of D<sub>3</sub> to the intestines. It should be noted that the unprotected D<sub>3</sub> was not detected at the apical side or at the basolateral side, suggesting that the vitamin was degraded by oxygen or free radicals. Indeed, during the experiment, the samples are exposed to ambient air, which explains the absence of the vitamin in all samples including the

control (unprotected D<sub>3</sub>). The values of the TEER measurements increased after the cells were incubated in regular storage buffer, meaning that the protein-based microspheres were not toxic for the cells (Table 8.1).

**Table 8.1. TEER of the Caco-2 cells monolayers**

Treatment	<sup>a</sup> Values of the TEER ( $\Omega \cdot \text{cm}^2$ )						
	TEER measurement periods (hours) before and after the experiment						
	- 24	0	0.5	1	1.5	2	48
<b>D<sub>3</sub></b>	664 ± 35	162 ± 67	124 ± 1	115 ± 2	114 ± 0	106 ± 0	442 ± 1
<b><math>\beta</math>lg/D<sub>3</sub>/Lyso</b>	917 ± 59	220 ± 44	139 ± 8	130 ± 3	132 ± 2	119 ± 5	315 ± 86

<sup>a</sup>Values are expressed as mean ± SEM

The major hurdles in processing and commercialization of D<sub>3</sub> are its photochemical instability and poor solubility. The improvement in the bioavailability of D<sub>3</sub> relies essentially on the enhancement of its water solubility [131]. In a previous study, we showed that the βlg/Lyso microspheres significantly increased the water solubility of D<sub>3</sub> with an encapsulation efficiency of 90.8 ± 4.8 % [224]. Here, we demonstrate that the food protein-based microspheres could cross the intestinal membrane, which may increase the uptake of D<sub>3</sub>. Consequently, the *in vivo* study of the bioavailability of D<sub>3</sub> was carried out to validate the findings of the present work.

#### **8.4.5. *In vivo* study of the bioavailability of D<sub>3</sub>**

The efficiency of the βlg/Lyso microspheres in enhancing the bioavailability of D<sub>3</sub> was evaluated *in vivo* by force feeding rats with the control (water), D<sub>3</sub> solution or the D<sub>3</sub>-entrapped βlg/Lyso microspheres every day for three weeks. The animals received a dose of 77 μg corresponding to 3080 IU of D<sub>3</sub>. All rats survived at the end of the experiment, with a total weight gain ranging from 17.5 ± 4.73 to 20.8 ± 5.5 g per rat. The biomarker 25(OH)D<sub>3</sub> was then measured in blood samples. The results are presented in Figure 5. The βlg/Lyso microspheres significantly increased the concentration of 25(OH)D<sub>3</sub> in the rats compared to the control and the free vitamin treatments ( $p < 0.001$ ). The mean concentration of 25(OH)D<sub>3</sub> of 22.0 ± 0.02 nmol/L, 15.12 ± 1.0 × 10<sup>3</sup> nmol/L and 42.4 ± 8.17 × 10<sup>3</sup> nmol/L were obtained for the control, D<sub>3</sub> and the D<sub>3</sub>-entrapped βlg/Lyso microspheres, respectively (Figure 8.5).

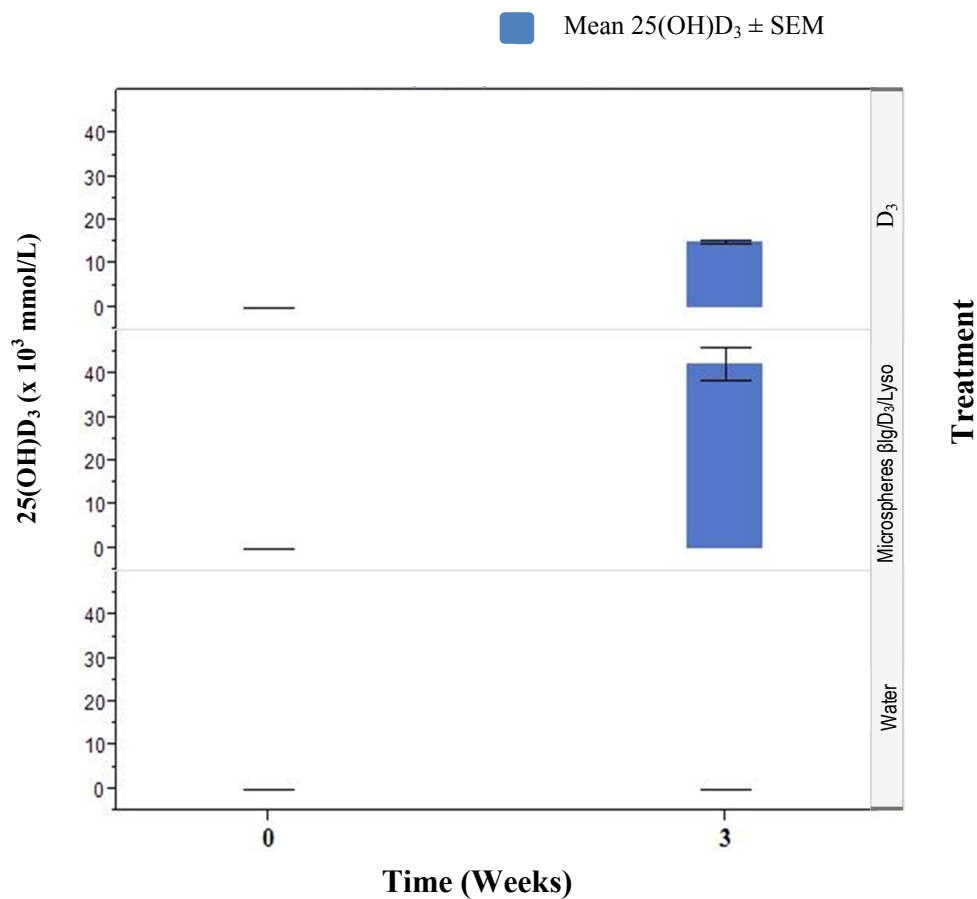


**Figure 8.5. Bioavailability of D<sub>3</sub> in the rat experiment. Mean 25(OH)D<sub>3</sub> in rats forced fed the water (control), D<sub>3</sub> and D<sub>3</sub> - entrapped βIg/Lyso microspheres. Each error bar is constructed using 1 standard error from the mean.**

## 8.5. Conclusion

The present study reports that electrostatic interactions between oppositely charged  $\beta$ lg and Lyso induced the formation of microsphere structures that can be used as a versatile food-grade vehicle for nutraceuticals. pH and  $\beta$ lg/Lyso ratios were key factors in the formation of the microspheres. The findings indicate that the optimal initial protein concentration  $\beta$ lg:Lyso ratio (v/v) was 2:1. The  $\beta$ lg/Lyso microspheres successfully encapsulated D<sub>3</sub>, used as a model nutraceutical. Further characterization is ongoing to determine additional information such as the structural changes of the proteins, size distribution and stoichiometry of the complexation. The stability of  $\beta$ lg/Lyso microspheres, during long term storage in the cold and in simulated intestinal fluid, and their ability to protect D<sub>3</sub> from the damaging effects of UV-light are also currently under investigation. The electrostatically-driven process leading the formation of the  $\beta$ lg/Lyso microspheres is an illustration that can serve as model for the aggregation of food proteins which can then be used for the optimization of sustainable platforms to encapsulate a biological active of nutritional interest.

## 8.6. Acknowledgments

This study was funded by the Canada Research Chair on Proteins, Biosystems and Functional Foods and the Natural Sciences and Engineering Research Council of Canada (NSERC) through the Vanier Canada Graduate Scholarships (Diarrassouba, F.). The authors would like to thank D. Gagnon, A. Gaudreau (Faculté des Sciences de l'Agriculture et de l'Alimentation, Université Laval, Québec, Q.C., Canada) and Pascal Dubé (Institut de recherche sur les nutraceutiques et les aliments fonctionnels (INAF/STELA), Université Laval, Québec, QC, Canada) and the EA-CIDAM staff membres (Faculté de Pharmacie, Clermont-Ferrand, France) for their valuable technical assistance.

## Contextual transition

The following chapter is a comparative study between the free vitamin D<sub>3</sub> and the different  $\beta$ -lactoglobulin-based scaffolds, including the  $\beta$ -lactoglobulin/D<sub>3</sub> complex,  $\beta$ -lactoglobulin/D<sub>3</sub> coagulum and  $\beta$ -lactoglobulin - Lysozyme microspheres. The long term storage and light stability and solubility of vitamin D<sub>3</sub> were determined as well as the serum levels of 25-hydroxy-vitamin D<sub>3</sub> after an *in vivo* experiment with force-fed rats. This comparative study summarizes the experimental work performed in the current thesis and shows that the  $\beta$ -lactoglobulin – based carriers have potential in the protection, stabilization and enhancement of the bioavailability of vitamin D<sub>3</sub>.

## CHAPTER 9

# Comparative Study between different $\beta$ -Lactoglobulin-based scaffolds for the delivery of Vitamin D3

Manuscript in preparation

By :

Fatoumata Diarrassouba<sup>a</sup>, Ghislain Garrat<sup>b</sup>, Gabriel Remondetto<sup>c</sup>  
and Muriel Subirade<sup>a</sup>

<sup>a</sup>Chaire de recherche du Canada sur les protéines, les bio-systèmes et les aliments fonctionnels, Institut de recherche sur les nutraceutiques et les aliments fonctionnels (INAF/STELA), Université Laval, Québec, QC, Canada.

<sup>b</sup>EA-CIDAM, Lab Biopharmacie, Faculté de Pharmacie, 28 Place Henri Dunant, 63001, Clermont-Ferrand, France.

<sup>c</sup>Centre de recherche et développement, Agropur Coopérative. 4700 rue Armand Frappier, St-Hubert, QC, J3Z 1G5, Canada.

## 9.1. Abstract

The maximum stability of the  $\beta$ -lactoglobulin/vitamin D<sub>3</sub> ( $\beta$ lg/D<sub>3</sub>) complex was obtained close to the pI of  $\beta$ lg. Additionally, it was demonstrated that egg white lysozyme (Lyso) could form an electrostatic-driven complex with the  $\beta$ lg/D<sub>3</sub> complex, hence encapsulating the vitamin with high efficiency ( $90.8 \pm 4.8$  %). This encapsulation efficiency was higher with the coagulum  $\beta$ lg/D<sub>3</sub> formed by triggering the auto-association of the  $\beta$ lg/D<sub>3</sub> complex ( $94.5 \pm 1.8$  %). In the current work, the effectiveness of the  $\beta$ lg/D<sub>3</sub> and  $\beta$ lg/D<sub>3</sub>/Lyso complexes as well as  $\beta$ lg/D<sub>3</sub> coagulum to enhance the long term, light and intestinal stability of D<sub>3</sub> was compared to that of the free D<sub>3</sub>. The serum levels of the 25-hydroxy-D<sub>3</sub> was assayed in plasma samples of rats force-fed each of the  $\beta$ lg-based scaffolds, the free D<sub>3</sub> and the rats included the control group were fed the physiological serum. The findings reveal that the  $\beta$ lg-based scaffolds increased significantly the long term and light stability of D<sub>3</sub> compared to the free vitamin ( $p < 0.05$ ). The  $\beta$ lg/D<sub>3</sub>/Lyso complex was disrupted in the simulated intestinal fluid in presence of pancreatin, resulting in a lower stability of the vitamin compared to the free D<sub>3</sub>,  $\beta$ lg/D<sub>3</sub> complex and  $\beta$ lg/D<sub>3</sub> coagulum. After 24 h of UV-light irradiation, over 94 % of D<sub>3</sub> was still remaining for the  $\beta$ lg/D<sub>3</sub> coagulum, compared to about 2.8 % for the  $\beta$ lg/D<sub>3</sub>/Lyso complex and 0.0 % for the  $\beta$ lg/D<sub>3</sub> complex and the free D<sub>3</sub>. The serum levels of 25(OH)D<sub>3</sub> were ranked as follows:  $\beta$ lg/D<sub>3</sub> coagulum >  $\beta$ lg/D<sub>3</sub>/Lyso complex >  $\beta$ lg/D<sub>3</sub> complex > D<sub>3</sub> > control. In the present study, the effectiveness of the  $\beta$ lg-based scaffolds, more specifically the  $\beta$ lg/D<sub>3</sub>/Lyso complex and the  $\beta$ lg/D<sub>3</sub> coagulum to enhance the bioavailability of D<sub>3</sub> in rats is probably due to their high encapsulation efficiency of D<sub>3</sub>, thus increasing its water solubility and uptake.

## 9.2. Introduction

Bovine milk  $\beta$ lg is the major protein in whey [57]. This globular protein is amphiphilic, mainly composed of  $\beta$ -sheets and two disulfide bridges in addition to one free thiol group [17]. Upon heat treatment, the polypeptide chains unfold, exposing the initially buried hydrophobic residues. The exposure of the nonpolar regions leads to the formation of intermolecular  $\beta$ -sheets as a result of non-covalent interactions and SS (disulfide) or SH interchange from the free thiol group [253]. The establishment of covalent bonds stabilizes the protein aggregates. The pH and ionic strength control the equilibrium between attractive and repulsive forces, responsible for gel or aggregate formation. Gels of  $\beta$ lg produced by acidification are stronger than those produced by modulation of the ionic strength [17]. The maximum strength is obtained around the  $pI$  of the protein, probably due to the fact that electrostatic attraction between the oppositely charged residues contributes to increased gel strength [254].

Vitamin D<sub>3</sub> (D<sub>3</sub>) was selected as ligand model that is known to have high affinity with  $\beta$ lg [200]. The effects of higher intake of D<sub>3</sub> have been well established in numerous skeletal and extra-skeletal diseases [102]. The role of D<sub>3</sub> in conditions such as cancer, cardiovascular diseases, diabetes and bacterial infections is well described in the literature [102, 233-235]. Evidence also suggests that the intake of D<sub>3</sub> is insufficient despite the fortification of staple foods such as fluid milk, margarine or breakfast cereals [187]. The D<sub>3</sub> deficiency was ascribed to insufficient sun exposure and inadequate dietary intake of fortified foods. Additionally, this lipophilic vitamin is labile making its retention in foods, especially those with low fat content, challenging and highly reactive and degrades easily when exposed to light or oxygen. This might explain deviation of label declarations from actual amounts in foods. Therefore, increased solubility, retention and stability of D<sub>3</sub> in food products are crucial for improved food intake.

D<sub>3</sub> binds βlg through hydrophobic interactions to form the βlg/D<sub>3</sub> complex. We have recently demonstrated (Chapter 4, Section 4.4.2) that maximum stability of the βlg/D<sub>3</sub> complex was obtained at pH 5, near the pI of βlg. In the current work, GDL (2 %, w/v) was used to induce the auto-aggregation of the βlg/D<sub>3</sub> complex. As a result, coagulation of the βlg/D<sub>3</sub> complex occurred at room temperature whereas a firmer gel was obtained in refrigerated conditions. D<sub>3</sub> might act as cement that favors the stacking of the protein side-chains. This in turn, allows for the establishment of non-covalent interactions including electrostatic interactions and hydrogen bonding between acidic and basic side chains of the protein at the pI of βlg, which increases the strength of the gel [17]. Consequently, free thiol groups become physically closer to the disulfide bonds, which predictably promote the formation of disulfide bridges. Finally, the establishment of disulfide bonds stabilizes the protein network and induces gel hardening [17, 254]. In absence of D<sub>3</sub>, gel hardening in refrigerated conditions does not occur, implying that the role of D<sub>3</sub> in this two-stage gelation process is crucial. Reports indicate that in the absence of ionic strength, fine stranded or filamentous gels are formed at more extreme pH values while opaque or particulate gels are obtained at pH values around the pI of βlg [57, 190]. In the present work, opaque gels were obtained, thus corroborating previous findings. Destabilizing agents such as urea, 2-mercaptoethanol or sodium dodecyl sulfate can be used to identify the contribution of specific interactions [57]. Hence, no further explanation can be provided on the mechanism of cold gelation of the βlg/D<sub>3</sub> complex without the conventional heat-induced pre-denaturation step of βlg. Nevertheless, the coagulation or gelation of native βlg without any heat treatment can be attractive for the food industry since heat sensitive products can be enriched with the D<sub>3</sub> entrapped coagulum. The high-efficient encapsulation of D<sub>3</sub> within the coagulum matrix represents an innovative method to improve the uptake of this fat-soluble vitamin and concomitant beneficial effects on health.

The isoelectric point (pI) of βlg (18.3 KDa) is around 5.2 [37]. Lyso from egg white is a smaller protein with a molecular weight of 14.4 KDa, a strong basic character

and a *pI* at 10.7 [239]. Below the isoelectric point (*pI*) of  $\beta$ Ig (5.2), at pH 4, both the proteins bear strong positive charges while above pH 11, repulsive negative forces become predominant and lead to formation of monomeric structures of the protein [54]. At pH above 5.2,  $\beta$ Ig is negatively charged whereas Lyso still bears overall positive charge up to a pH of 11, which corresponds to the *pI* of Lyso [139]. Thus, between the *pI* of the two food proteins, electrostatic complexes can be formed, which was the case with between the  $\beta$ Ig/D<sub>3</sub> complex and Lyso leading to the formation of microcrosspheres. This was achieved probably because of the fact D<sub>3</sub> binds the  $\beta$ Ig through hydrophobic forces, which seem to remain stable after the formation of the  $\beta$ Ig/Lyso microspheres.

In previous chapters of the current thesis, the long term, light and intestinal stability of the  $\beta$ Ig/D<sub>3</sub> complex as well as that of the D<sub>3</sub> encapsulated in the  $\beta$ Ig/D<sub>3</sub> coagulum and  $\beta$ Ig/D<sub>3</sub>/Lyso microspheres were compared to that of the free vitamin. An *in vivo* experiment was performed by force feeding rats in order to assess the impact of the protein-based scaffolds on the bioavailability of D<sub>3</sub>.

## **9.3. Experimental Section**

### **9.3. Experimental Section**

#### **9.3.1 Materials**

$\beta$ -lactoglobulin ( $\beta$ Ig) was purchased from Davisco Foods International, Inc. (Le Sueur, MN, USA). High purity  $\beta$ -lactoglobulin (B variant, purity  $\geq$  90 %), Lysozyme (Lyso) from chicken egg white (lyophilized powder, protein  $\geq$  90 %,  $\geq$  40,000 units/mg protein) and vitamin D<sub>3</sub> (purity  $\geq$  98 %, HPLC) were obtained from Sigma-Aldrich Chemical and Co (Oakville, ON, Canada). The proteins were used without further purification. Acetonitrile (ACN, HPLC grade), methanol (MeOH, HPLC grade) and trifluoroacetic acid (TFA) were purchased from EMD International (Gibbstown, NJ, USA).

### 9.3.2 Sample preparation

Protein stock solutions (0.2 %) were prepared by dissolving the powder in MilliQ water under mild stirring conditions for 2 h at room temperature and then stored overnight at 4 °C to allow complete rehydration [31]. Vitamin D<sub>3</sub> (D<sub>3</sub>) stock was prepared daily by dissolving 10 mg in 25 mL MeOH [188]. Working solutions of D<sub>3</sub> were obtained by diluting the stock solution in MilliQ water.

The βlg-based scaffolds, including the βlg/D<sub>3</sub> complex, βlg/D<sub>3</sub> coagulum and βlg/D<sub>3</sub>/Lyso microspheres, were prepared as previously indicated in the Experimental Sections of Chapters 5, 6, 8, respectively. All samples containing D<sub>3</sub> were protected from light by using amber-tinted conical tubes or aluminum foil.

### 9.3.3. Stability in refrigerated conditions

The βlg/D<sub>3</sub> complex was first formed at room temperature as mentioned above by mixing the same volume (7.5 mL) of both βlg (0.2%) and D<sub>3</sub> (220 μM) in six different 15 mL - conical tubes in the dark before covering the tubes with aluminum foil. Each tube corresponded to one of the following sampling periods: week 0, 1, 2, 3, 4 and 5. D<sub>3</sub> concentration on day 0 was immediately determined after the incubation period of about 2 h.

The initial concentration of encapsulated D<sub>3</sub> in the βlg/D<sub>3</sub> coagulum and βlg/Lyso microspheres was determined after 24 h, as described in Section 6.3.3 (Chapter 6) and Section 8.3 (Chapter 8), respectively. Samples corresponding to weeks 1 to 5 were stored at 4 °C. Each week, a sample was withdrawn for HPLC analysis from the D<sub>3</sub> remaining in the tube, as previously described [200]. Solutions of D<sub>3</sub> diluted in MilliQ water were prepared and analyzed under the same conditions. All the experiments were repeated at least three times.

#### **9.3.4. UV – Stability of the $\beta$ Ig-based scaffolds**

Each of the  $\beta$ Ig/D<sub>3</sub> complex,  $\beta$ Ig/D<sub>3</sub> coagulum,  $\beta$ Ig/Lyso microspheres and free D<sub>3</sub> solutions were prepared as mentioned in the preceding section and exposed to UV-C light (254 nm, 15 W) in order to assess the UV-light stability of D<sub>3</sub> over 24 h [130]. At each sampling time (t 0, 1, 2, 4, 6, 8, 10 and 24 h), HPLC analysis was performed for D<sub>3</sub> recovery, which represent the amount of the vitamin remaining in solution, using the procedure presented in Section 9.3. Experiments were repeated three times.

#### **9.3.5. Intestinal stability of the $\beta$ Ig-based scaffolds**

The stability of the the  $\beta$ Ig/D<sub>3</sub> complex,  $\beta$ Ig/D<sub>3</sub> coagulum,  $\beta$ Ig/Lyso microspheres and free D<sub>3</sub> solutions were investigated using a USP-2 paddles apparatus (SOTAX Corporation, Westborough, MA, USA). Each of test solutions were incubated in 95 ml in one of two release media with continuous agitation (at ~ 50 rpm) at 37 °C [18]. In order to minimize D<sub>3</sub> degradation by air, custom-made paraffin discs were used to occlude the top of the mini-vessels with just enough space to allow for the rotation of the paddles. The release media consisted of the simulated intestinal fluid (SIF) as described in the US Pharmacopeia with and without 1.0% pancreatin (w/v) at pH 6.8. Samples (~ 0.1 mL) withdrawn at half-hour or 1-h intervals over 6 h were centrifuged (5,000 x g /5 min) and the concentration of D<sub>3</sub> in the supernatant was determined by HPLC as indicated above. A control with and without enzyme was also run.

### **9.3.6. *In vivo* study of the bioavailability of D<sub>3</sub>**

#### **9.3.6.1. Animal models**

Animal studies were conducted at the 'Unité de Stabulation Animale, Ethic Committee-CE-42-12' (Université d'Auvergne, Clermont-Ferrand, France). Adult male Wistar rats ( $n = 25$ ; Elevage Dépré, St. Doulichard, France) weighing  $300 \pm 20$  g at the beginning of the experiment were used. They were housed for an acclimation period of one week in a temperature-controlled room ( $22 \pm 3^{\circ}\text{C}$ ) and maintained on a 12 h light/12 h dark cycle (lights on from 8:00 a.m. to 8:00 p.m.). Animals were allowed free access to a commercial standard diet (A04, lot 21206, UAR, Epinay-sur-Orge, France) and tap water, as previously reported [201]. The estimated average daily amount of feed intake per adult rat ranged from 25 to 30 g [202].

#### **9.3.6.2. *In vivo* experiments**

After the acclimation period, two or three rats were housed per cage for three weeks. The animals had access to feed and water *ad libitum*. The rats ( $n = 15$ ) were divided into 3 groups ( $n = 5$ ) each receiving one of the treatments consisting of MilliQ water supplemented with 0.09 % NaCl (control), the  $\beta\text{lg}/\text{D}_3$  complex,  $\beta\text{lg}/\text{D}_3$  coagulum,  $\beta\text{lg}/\text{Lyso}$  microspheres and free  $\text{D}_3$  solutions with the same final concentration of  $\text{D}_3$  ( $110 \mu\text{M}$  or  $77 \mu\text{g}$ ). Blood samples were collected at T 0, week 1, 2 and 3 in 0.5 mL conical tubes pre-coated with 10  $\mu\text{L}$  of sodium heparin (0.1 IU). The plasma was separated by centrifugation at  $1000 \times g$  for 10 min. Plasma samples were stored at  $-20^{\circ}\text{C}$  until analysis of  $25(\text{OH})\text{D}_3$  in rat plasma was performed using the 25-Hydroxy Vitamin D Direct EIA kit (IDS Diagnostics, Fountain Hills, AZ, USA) according to the manufacturer's instructions.

### 9.3.7. Statistical analysis

Statistical analysis was performed using SAS version 12.0 (SAS Institute Inc., Cary, NC, USA). ANOVA and the Least Significant Difference (LSD) were used to determine differences among means and the significance level was fixed at  $p < 0.05$ . All measurements were performed in triplicate.

## 9.4. Results and discussion

Compared to the unprotected vitamin, the  $\beta$ lg – based platforms, including the  $\beta$ lg/D<sub>3</sub> complex,  $\beta$ lg/D<sub>3</sub> coagulum and the  $\beta$ lg/D<sub>3</sub>/Lyso microspheres significantly improved the stability of D<sub>3</sub> during long term storage in the cold ( $p < 0.05$ ), as shown on Figure 9.1. Among the different protein-based platforms tested in the current work, the  $\beta$ lg/D<sub>3</sub> coagulum showed the highest stability for D<sub>3</sub> after 5 weeks à 4 °C, with  $86.3 \pm 3.2$  % of D<sub>3</sub> was still remaining compared to  $8.3 \pm 2.3$  % for the unprotected vitamin (Figure 9.1). The  $\beta$ lg/D<sub>3</sub>/Lyso microspheres ( $56.0 \pm 4.4$  %) and  $\beta$ lg/D<sub>3</sub> complex ( $43.0 \pm 5.1$  %) significantly improved the stability of the free D<sub>3</sub> after 5 weeks of storage in the cold. These results are important since they imply that  $\beta$ lg – based platforms, especially when prepared prior to incorporation in foods such as dairy products may extend the shelf life of D<sub>3</sub> in refrigerated conditions.

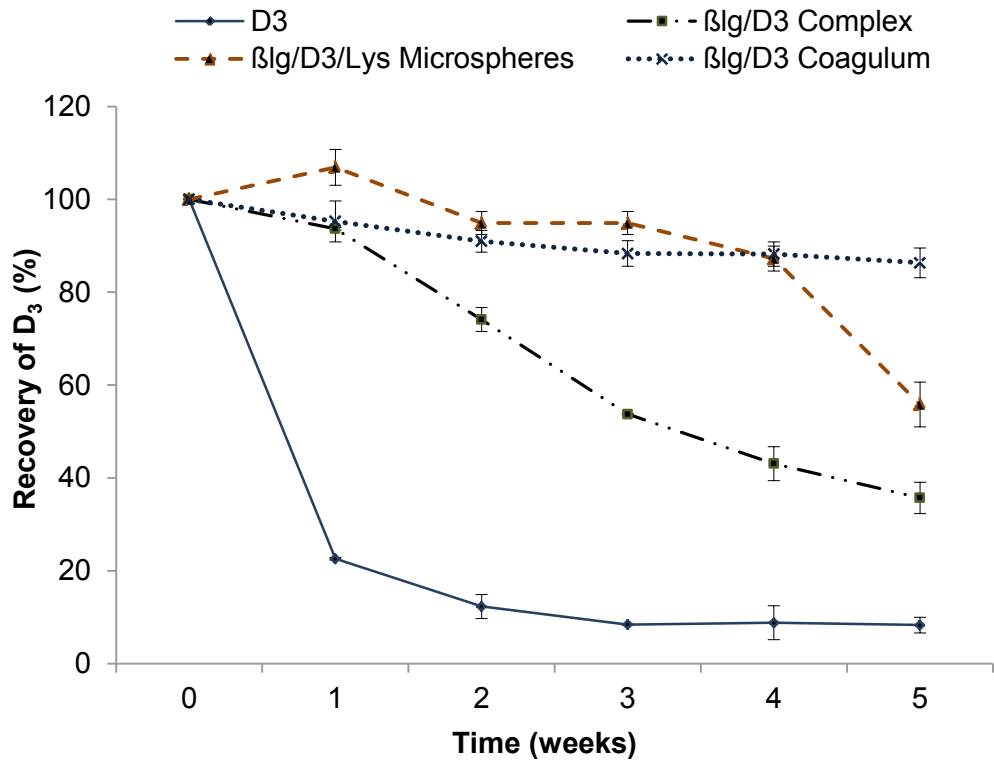


**Figure 9.1. Stability of the unprotected D<sub>3</sub> and in the  $\beta$ Ig/D<sub>3</sub> complex,  $\beta$ Ig/D<sub>3</sub>/Lyso microspheres and  $\beta$ Ig-based coagulum. and the  $\beta$ Ig/D<sub>3</sub>/Lyso microspheres in refrigerated conditions (4 °C) during five weeks.**

The  $\beta$ lg/D<sub>3</sub> complex and  $\beta$ lg/D<sub>3</sub>/Lyso microspheres showed some protection against UV-light degradation of D<sub>3</sub> during the first 2 h of the irradiation (Figure 9.2). Compared to the unprotected vitamin for which, over 95 % of the initial amount was lost after 2 h of light exposure, about 35.0 % and 17.8 % of D<sub>3</sub> remained in solution for the  $\beta$ lg/D<sub>3</sub> complex and  $\beta$ lg/D<sub>3</sub>/Lyso microspheres, respectively. After 24 h of UV-light exposure, only the  $\beta$ lg/D<sub>3</sub> coagulum showed a good stability, with  $94.2 \pm 4.1$  % of D<sub>3</sub> still intact, representing a loss of only about 5.8 % of the initial amount of the vitamin (Figure 9.2). The protective effect of the  $\beta$ lg/D<sub>3</sub> coagulum is probably due to the density of the protein matrix, which may physically entrapment D<sub>3</sub> and thus may provide a shielding effect against the UV-light [20, 225].

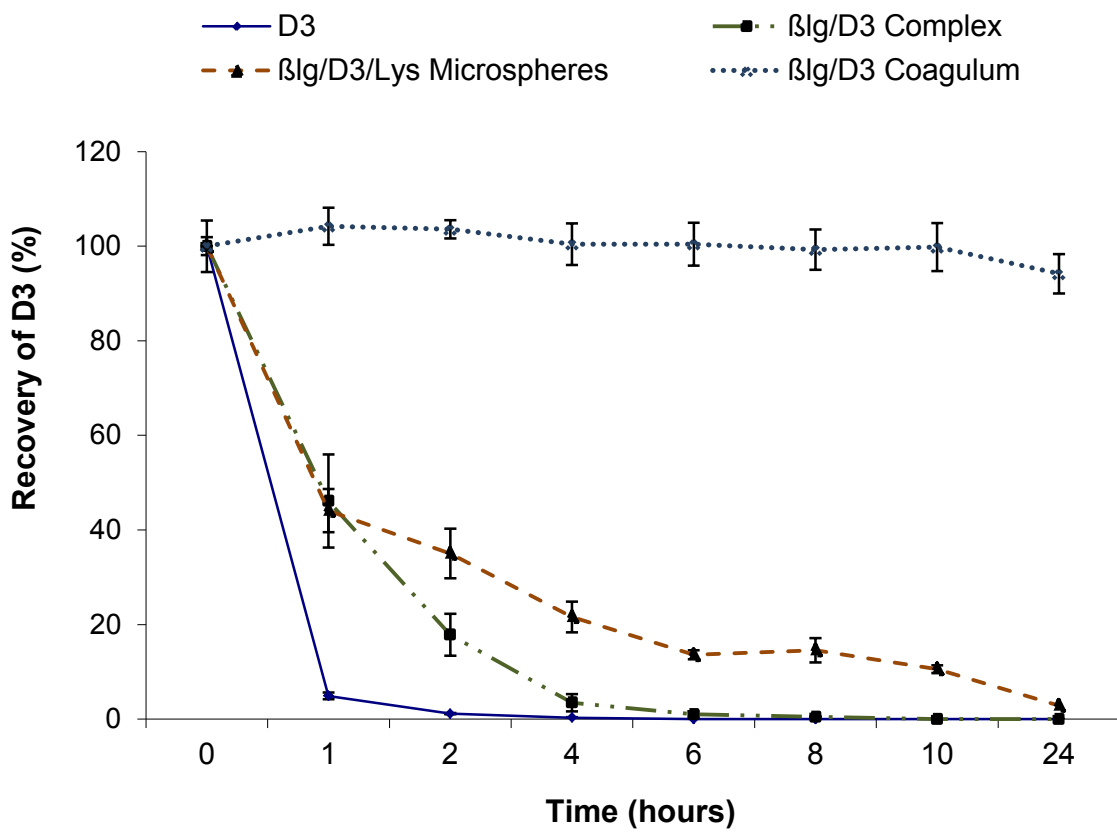


**Figure 9.2. UV-light stability of D<sub>3</sub> of the unprotected D<sub>3</sub> and in the  $\beta$ Ig/D<sub>3</sub> complex,  $\beta$ Ig/D<sub>3</sub>/Lyso microspheres and  $\beta$ Ig-based coagulum.**

Overall, in the simulated intestinal fluid, with or without pancreatin, the  $\beta$ lg/D<sub>3</sub> complex and  $\beta$ lg/D<sub>3</sub> coagulum exhibited an improved stability compared to the  $\beta$ lg/D<sub>3</sub>/Lyso microspheres and free D<sub>3</sub>. The dense matrix of the coagulum composed of numerous long polypeptide and side chains may impede access of the proteases to their target amino acids (Figures 9.3 and 9.4). Whereas, the binding of D<sub>3</sub> to  $\beta$ lg may provide a mutual protection to both molecules against enzymes attack, thus improving the intestinal stability compared to the free vitamin. Finally, the formation of electrostatic complexes between  $\beta$ lg and Lyso may probably affect the structural integrity of the former protein, hence explaining the disruption of the microspheres in the simulated intestinal conditions [140].

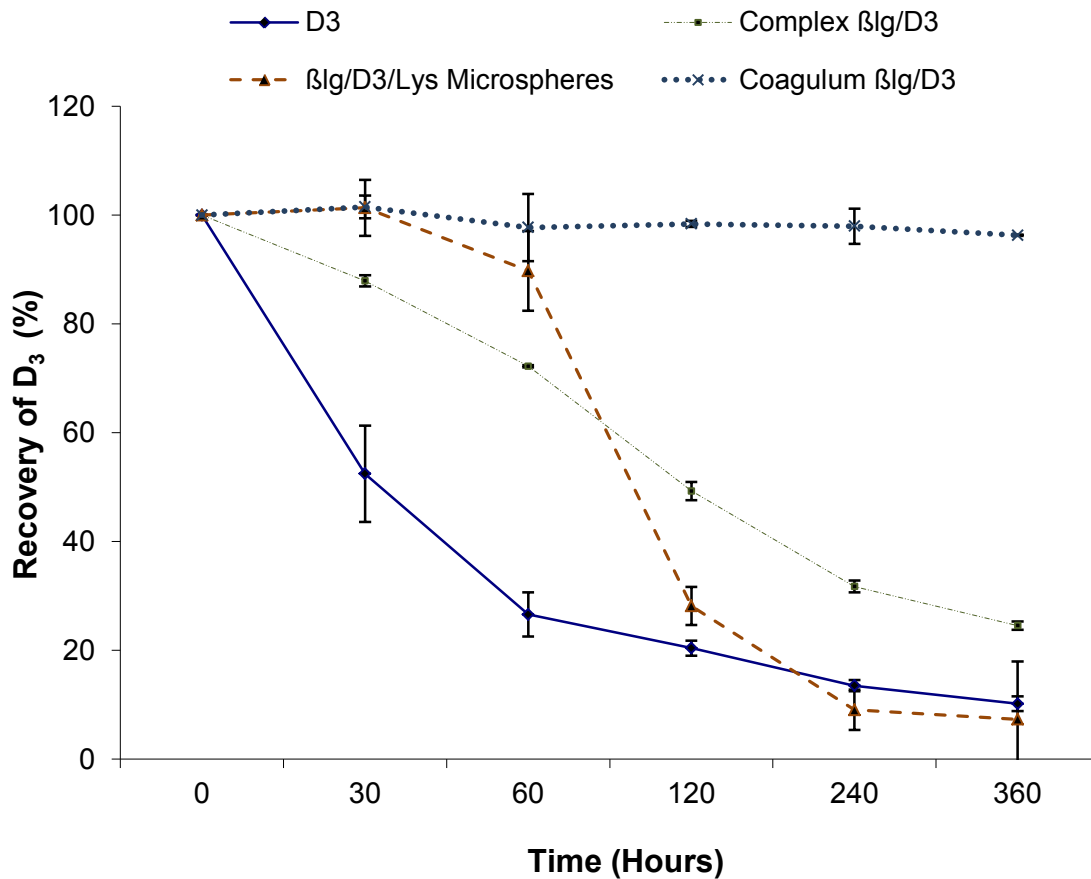


**Figure 9.3. Stability of the unprotected D<sub>3</sub> and in the βlg/D<sub>3</sub> complex, βlg/D<sub>3</sub>/Lyso microspheres and βlg-based coagulum in Simulated Intestinal Fluid without pancreatin at pH 6.8, 37 °C (USP-2 apparatus).**

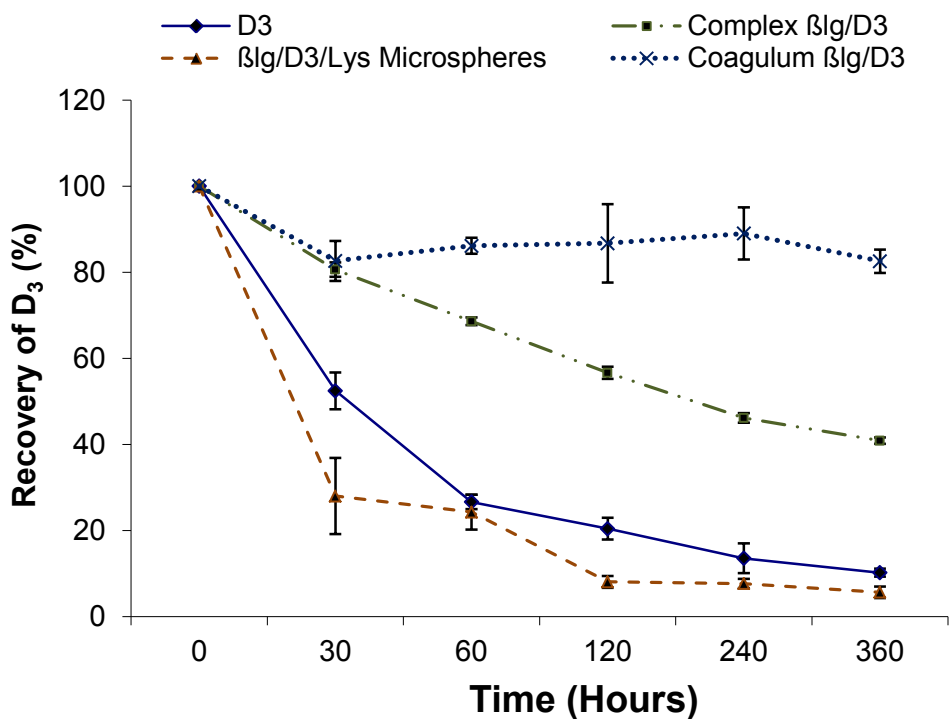


**Figure 9.3. Stability of the unprotected D<sub>3</sub> and in the  $\beta$ Ig/D<sub>3</sub> complex,  $\beta$ Ig/D<sub>3</sub>/Lyso microspheres and  $\beta$ Ig-based coagulum in Simulated Intestinal Fluid with pancreatin at pH 6.8, 37 °C (USP-2 apparatus).**

Rats were force-fed with the free D<sub>3</sub>, βlg/D<sub>3</sub> complex, βlg/D<sub>3</sub> coagulum, the βlg/D<sub>3</sub>/Lyso microspheres and water (with NaCl 0.09 %) as the control. It is important to note that the lethal dose (LD<sub>50</sub>) for the rat is 42 mg of D<sub>3</sub> per kg, corresponding to about 12.6 mg for a rat weighing 300 mg (US Pharmacopeia). The rats included in the present study received about 2.2 mg per day, well below the LD<sub>50</sub>.

The serum levels of the 25(OH)D<sub>3</sub> were significantly higher in rats fed the D<sub>3</sub> – containing treatment compared to the control group ( $p < 0.0001$ ), as shown on Figure 9.5.

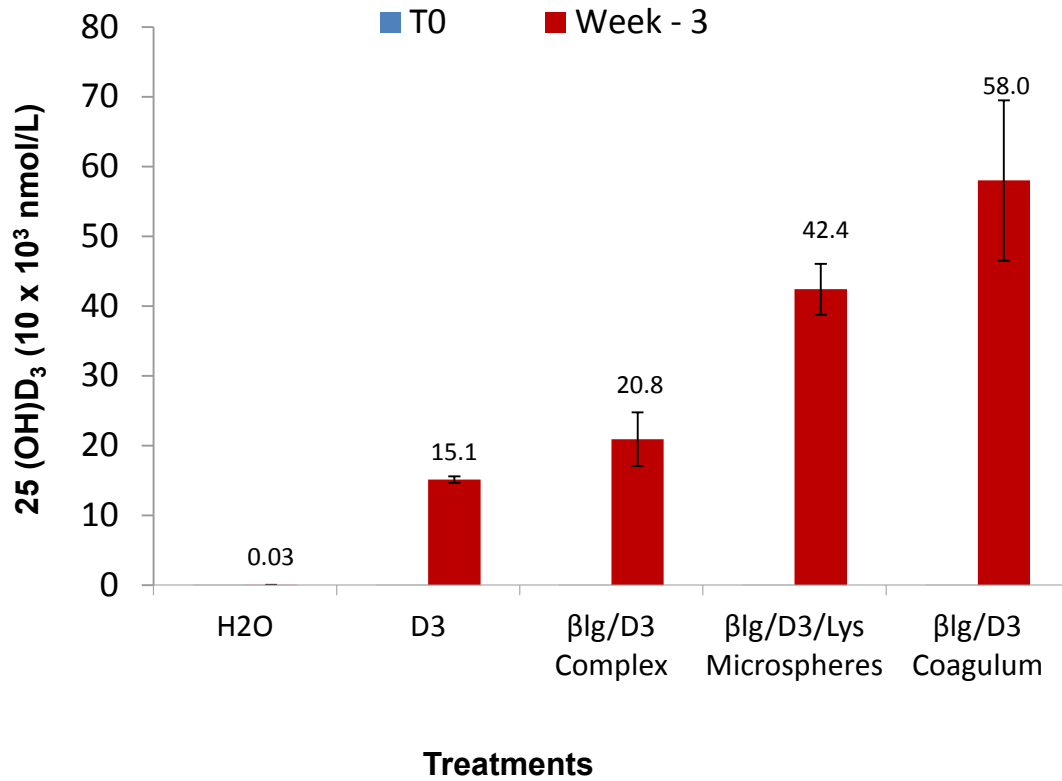


**Figure 9.5.** *In vivo* experiment of the bioavailability of D<sub>3</sub>. Mean 25(OH)D<sub>3</sub> in rats forced fed the water (control), unprotected D<sub>3</sub>,  $\beta$ Ig/D<sub>3</sub> complex,  $\beta$ Ig/D<sub>3</sub>/Lyso microspheres and  $\beta$ Ig-based coagulum in the rat experiment. Each error bar is constructed using 1 standard error from the mean.

The levels of the D<sub>3</sub> biomarker was significantly higher ( $p < 0.0001$ ) in rats fed the  $\beta$ lg/D<sub>3</sub> coagulum ( $58.0 \pm 11.5 \times 10^3$  nmol/L) than in the rats fed the  $\beta$ lg/D<sub>3</sub>/Lyso microspheres ( $42.4 \pm 8.17 \times 10^3$  nmol/L),  $\beta$ lg/D<sub>3</sub> complex ( $\pm 8.17 \times 10^3$  nmol/L) and the free D<sub>3</sub> ( $15.1 \pm 1.0 \times 10^3$  nmol/L). In the rats fed the control (water), the serum level of 25(OH)D<sub>3</sub> was only  $22.0 \pm 0.02$  nmol/L. The enhancement of the bioavailability of D<sub>3</sub> could be explained by the high encapsulation efficiency of the coagulum ( $94.5 \pm 1.8$  %) and microspheres ( $90.8 \pm 4.8$  %), which in turn might increase the water solubility of D<sub>3</sub>. While the binding ratio may explain the improved bioavailability of D<sub>3</sub> in rats fed the  $\beta$ lg/D<sub>3</sub> complex. The large difference between the control and the D<sub>3</sub>-containing treatments may be explained by the fact that the test solutions were effectively protected from light and access to oxygen was reduced to a minimum whereas the rats in the control group were fed food that was exposed to 12 hours of light per day and to air. Most importantly, oil, powder or ethanol-based substances serve as common vehicles to improve the bioavailability of D<sub>3</sub> [230].

The data presented in the current study are important since they indicate a significant increase in serum levels of 25(OH)D<sub>3</sub> and consequently, an enhancement of the uptake and bioavailability of D<sub>3</sub> in rats. In fact, it was reported that individuals who received cheddar or low-fat cheese fortified with a dose of 28,000 IU of D<sub>3</sub> (equivalent to 100  $\mu$ g/day) did not show any significant difference in the serum level of 25(OH)D<sub>3</sub> compared to those who received a liquid D<sub>3</sub> supplement [15]. Another report indicates that serum levels of 25(OH)D<sub>3</sub> in elderly people consuming D<sub>3</sub>-fortified cheese for two months did not increase even during limited sunlight exposure [251].

All the  $\beta$ lg-based platforms studied in the current work showed potential in the stability and improvement of the uptake of D<sub>3</sub>. However, the  $\beta$ lg/D<sub>3</sub> coagulum remains the most promising  $\beta$ lg-based scaffold for the protection, stability, enhancement of the solubility and bioavailability of D<sub>3</sub>, and consequently, may represent a good delivery system for this vitamin. Giving the fact that retention of

D<sub>3</sub> in the curd matrix during cheesemaking is problematic, the optimization of the  $\beta$ lg – based coagulum enriched with D<sub>3</sub> represents an innovative platform for the fortification of cheese, yogurt and other semi-fluid or solid foods.

## 9.6. Conclusion

In the current study, water soluble food protein-based microspheres with high D<sub>3</sub> encapsulation efficiency were used to substantially increase the bioavailability of the lipophilic vitamin. The increased solubility of D<sub>3</sub> is advantageous for fortification of foods with low or no fat content. The improved bioavailability of D<sub>3</sub> has direct implications on health and on non-skeletal conditions such as cancer, cardiovascular diseases, bacterial infections, skeletal afflictions such as bone fractures, and multiple sclerosis [102, 252].

Public health authorities now recommend that the daily intake of vitamin D<sub>3</sub> be raised from 400 to 1000 IU/day for adults and children aged 1 year and older, which might save the lives of at least 56,000 people each year in the USA [182]. Therefore, improving the uptake and bioavailability of D<sub>3</sub> are important goals. It is urgent to formulate a versatile D<sub>3</sub> delivery system that can utilize different properties, including (i) the encapsulation of accurate amounts of D<sub>3</sub> with concomitant increase in its solubility, (ii) increased stability and protection of D<sub>3</sub> against adverse environmental conditions during food or supplement manufacturing and storage, and (iii) the delivery of D<sub>3</sub> to the absorption site in the intestines for enhanced uptake and bioavailability. In the current study, water-soluble food protein-based platforms were used to improve the stability of D<sub>3</sub> on exposure to UV-light and to extend the shelf-life of D<sub>3</sub> under regular storage condition in the fridge. The  $\beta$ lg/Lyso microspheres released the vitamin in the intestines, which makes them a good GRAS carrier system for oral delivery. Overall, the  $\beta$ lg – based coagulum offered the best protective scaffold for D<sub>3</sub> and significantly enhanced the serum concentration of 25(OH)D<sub>3</sub> compared the free

vitamin,  $\beta$ lg/D<sub>3</sub> complex and  $\beta$ lg/Lyso microspheres. The findings of this work can have direct applications in D<sub>3</sub> fortification programs and important implications for public health.

### **9.7. Acknowledgments**

This study was funded by the Canada Research Chair on Proteins, Biosystems and Functional Foods and the Natural Sciences and Engineering Research Council of Canada (NSERC) through the Vanier Canada Graduate Scholarships (Diarrassouba, F.). The authors would like to thank D. Gagnon, A. Gaudreau (Faculté des Sciences de l'Agriculture et de l'Alimentation, Université Laval, Québec, Q.C., Canada) and Pascal Dubé (Institut de recherche sur les nutraceutiques et les aliments fonctionnels (INAF/STELA), Université Laval, Québec, QC, Canada) and the EA-CIDAM staff members (Faculté de Pharmacie, Clermont-Ferrand, France) for their valuable technical assistance.

## **CHAPTER 10**

### **CONCLUDING CHAPTER**

## 10.1. Research outcome

In recent years, considerable interest has been ascribed to the development of colloidal carrier systems. Food grade delivery platforms are attractive due to their non-toxicity, biocompatibility and biodegradability [39, 150]. Specifically, food proteins offer important avenues in the formulation innovative delivery scaffolds owing to their structural and physicochemical properties, in addition to high nutritional value. Among animal proteins, milk and milk whey proteins have been the focus of tremendous research. Milk proteins are considered as natural occurring carriers which deliver essential micronutrients, building blocks such as amino acids and immune system constituents from mother to the newborn [39]. Milk whey proteins, especially  $\beta$ lg, exhibit properties such as binding of small bioactives, surface and self-assembly, heat-induced gelation or cold-set gelation for heat sensitive bioactive compounds, pH-induced structural changes, all of which are convenient for interactions with other biopolymers, electrostatic complexes formation and controlled release [5, 39].

The first objective of this study was to investigate the interactions between riboflavin and  $\beta$ lg using spectroscopic methods. The findings revealed that  $\beta$ lg can bind riboflavin, an endogenous photosensitizer also known as vitamin B2. The structure of  $\beta$ lg was little affected by the association, which is beneficial for its carrier function. As a photosensitizer, riboflavin can interact with biological systems upon light activation and induce damages leading to cell toxicity. This property is useful in photodynamic therapy to treat affections such as cancer, inhibit the growth of harmful bacteria and sanitize. The anti-proliferative activity of riboflavin on skin melanoma cancer cell lines was not affected by the binding to  $\beta$ lg. Moreover, the  $\beta$ lg/riboflavin nanocomplex, resulting from the interaction between the two compounds, showed important anti-proliferative activity in the micromolar range, possibility due to the generation of reactive radical and oxygen species. The findings of this work are far-reaching since the development of light activated drug is attracting increasing interest in both oncology and non-oncologic clinical

applications. Although still in its infancy, the use of food grade compounds in photodynamic therapy for the treatment of malignant cells is a good alternative to chemical photosensitizers such as Porfimer-sodium and 5-aminolevulinic acid currently used in clinic which are toxic and mutagenic. Biocompatible and biodegradable photosensitizers like riboflavin will certainly gain in popularity in the near future. The use of food grade compounds in photodynamic therapy will likely uncover new research possibilities for the food industry, in controlling microbial growth during food processing and at the retail market, which ultimately will contribute to offer safer and good quality food products to the consumers.

Vitamin D<sub>3</sub> (D<sub>3</sub>) is a highly hydrophobic molecule that binds to the central cavity and surface hydrophobic pocket in the groove between the  $\beta$ -barrel and  $\alpha$ -helix of  $\beta$ lg [79]. Previous reports on the  $\beta$ lg/D<sub>3</sub> complex focused only on the binding capacity of  $\beta$ lg at varying pH values before complex formation, and the experiments were performed during the Tanford transition when the EF flap is in the 'open conformation' to allow the entrance of D<sub>3</sub> inside the central cavity of  $\beta$ lg [79, 176]. Experimentations related to the second objective of the current work showed that the  $\beta$ lg/D<sub>3</sub> complex was resistant to pH variation from pH 1.2 to 8, comprising that of the stomach and intestines. This implies that  $\beta$ lg constitutes a good carrier which can deliver D<sub>3</sub> in the intestines where the vitamin could be released upon proteolytic degradation. The uptake of D<sub>3</sub> might in turn be enhanced, which is highly sought in food fortification programs. The solubility of D<sub>3</sub> was increased as a consequence of the binding to  $\beta$ lg, which is important for the formulation of beverages or foods with high water contents and for the production of foods with low fat content.

In order to push further the studies on the  $\beta$ lg/D<sub>3</sub> complex, the auto-aggregation property of  $\beta$ lg was exploited to form upon mild acidification using glucono- $\delta$ -lactone. The experimental work addressing the third objective of the present thesis revealed that the pH of the  $\beta$ lg/D<sub>3</sub> complex was decreased near the pI of the protein, which triggered the auto-aggregation of the complex and concomitant

encapsulation of D<sub>3</sub> within the dense βlg network. The encapsulation efficiency was 94.5 ± 1.8 %, which is important compared to previous published works using mixed polymeric systems with toxic components [225].

The fourth objective of the current work was addressed by carrying out experiments that resulted in the promotion of electrostatic interactions between oppositely charged βlg and egg white Lysozyme (Lyso). βlg and Lyso self-assembled to form a supramolecular structure with a spherical shape and interior composed of dispersed granular protein aggregates. The volume mean size of the βlg/Lyso self-assembly was around 7.1 μm, ascribing the status of food grade microsphere to the protein electrostatic complex. D<sub>3</sub> was successfully encapsulated in the βlg/Lyso microspheres with a high encapsulation efficiency of 90.8 ± 4.8 %. The choice of Lyso relies on the fact that preliminary spectroscopic investigation (data not shown) indicates that D<sub>3</sub> also binds Lyso, which explains well the important encapsulation rate of the vitamin within the protein electrostatic complex. Stability studies were performed to demonstrate that the βlg/Lyso microspheres conferred increased stability to D<sub>3</sub> in the cold, to UV light. Despite the rapid degradation of the βlg/Lyso microspheres by the proteases in the intestines, the permeability studied performed using Caco-2 cells revealed that the βlg/Lyso microspheres could cross the intestinal barrier. This, in turn could increase the uptake and bioavailability of D<sub>3</sub>, as shown by the *in vivo* animal experiment. Overall, the findings of this work indicate that the βlg/D<sub>3</sub> coagulum and βlg/Lyso microspheres can serve as a good carrier to protect and stabilize D<sub>3</sub> during storage and to deliver the vitamin to the intestines when administered postprandially.

The hypothesis of the present study hypothesized was that β-lactoglobulin can serve in the formulation of food grade delivery systems, consequently improving the biological activity of the bound nutraceuticals. The present work demonstrates that βlg can transport riboflavin. Although the anti-proliferative activity of the βlg/riboflavin nanocomplex on skin melanoma cancer cell lines was not significantly higher than that of the free riboflavin, its (nanocomplex) showed important anti-

proliferative activity in the micromolar range. In another hand, the stability, solubility and bioavailability of D<sub>3</sub> was improved upon binding to βlg. Moreover, β-lactoglobulin was capable to auto-aggregate and co-precipitate with egg white Lysozyme to form microspheres which successfully encapsulated D<sub>3</sub> with a high efficiency. Therefore, the present study confirms the hypothesis that βlg can be used to formulate GRAS scaffolds for the delivery of bioactives which can then be used for the development of food products with improved health benefits.

## 10.2. Perspectives and Future trends

The use of food proteins to prepare versatile delivery scaffolds is advantageous on numerous aspects. The presence of charged and hydrophobic functional groups confers unique surface properties which can be judiciously exploited to form interactions involving covalent and non-covalent forces with small bioactives as well as with larger size biomacromolecules. The resulting devices can be tailor made to exhibit characteristics such nano or micro-meter size, controlled delivery and modulation of the release of the payload at specific target sites in the body.

To our knowledge, this work is the first report on the stability of the βlg/D<sub>3</sub> complex formed beforehand, to varying pH and its impact on the solubility of D<sub>3</sub>. The use of a native βlg – based coagulum, formed in mild acidic condition, as delivery platform for D<sub>3</sub> has not been reported before. Neither was the use of the βlg/Lyso electrostatic complexes in the delivery the delivery of bioactives. Despite the originality of the present work, the use of food proteins and specially βlg as delivery platform presents important drawbacks that need to be rightfully addressed.

In general, proteins are sensitive to proteolytic degradation in the GI tract. The acid and pepsin resistance of βlg is useful when targeting the stomach but becomes inadequate when the bioactive is degraded or require a prolong residence time in the intestines. Both βlg and Lyso are known food allergens and their application in

foods might be restricted to non-allergenic people. Additionally,  $\beta$ lg originates from bovine milk whey and is therefore an animal protein. The association of animal proteins to the dissemination of prion related diseases such as bovine spongiform encephalopathy known as Creutzfeldt-Jacob disease in humans raised the apprehension of health care professional and the general population. Research for good alternative to animal proteins is ongoing. The use of vegetable proteins, the development of biotechnology engineered proteins and recombinant technology, constitute examples of avenues where innovation meets motivation and great insights to overcome challenges and create smart delivery scaffolds.

The present thesis is a contribution to the ever-evolving controlled delivery technology. It is not an exhaustive work nor does it pretend to fully address all issues pertaining to the vast field of food grade delivery technology. The delivery platforms developed in the current work and the data reported will certainly gain in clarity, accuracy and wholeness, when the following in-depth research will be performed:

- ◆ Information concerning the aggregation of the  $\beta$ lg/D<sub>3</sub> complex, self-assembly of  $\beta$ lg and Lyso, can be obtained by Fourier transform infrared (FT-IR) absorption spectroscopy. The data can be completed by techniques that probe at a macroscopic or microscopic scale, such as rheology or microscopy, respectively.
- ◆ The spectroscopic investigation on the interaction between Lyso and D<sub>3</sub>, for instance using fluorescence spectroscopy and circular dichroism.
- ◆ The role of D<sub>3</sub>, temperature and protein concentration in the auto-aggregation of the leading to the formation of the coagulum can be determined using FT-IR and rheology and destabilizing agents to investigate participating forces.

- ◆ The concept of the use of the  $\beta$ Ig-based coagulum and  $\beta$ Ig/Lyso microspheres in delivery technology can be validated using other bioactives such as retinol, fatty acids and  $\alpha$ -tocopherol, which are known to bind  $\beta$ Ig.

Despite these shortcomings, the findings of the present thesis are far-reaching and possibly open a whole boulevard of research. The development of proteomics and protein biotechnology will allow outstanding discoveries in the near future and increase our knowledge on the structure and functionality of proteins, which in turn will help in the manufacturing of intelligent and programmable delivery devices.

## References

- [1] E. Acosta, Bioavailability of nanoparticles in nutrient and nutraceutical delivery, *Curr. Opin. Colloid Interface Sci.*, 14 (2009 ) 3-15.
- [2] L. Chen, G.E. Remondetto, M. Subirade, Food protein-based materials as nutraceutical delivery systems, *Trends Food Sci Tech*, 17 (2006) 272-283.
- [3] H. Canada, A new approach to natural health products, in: D.a.H. Products (Ed.), 2012
- [4] A.J. Núñez Sellés, Natural Health Products (NHPs), in: J.O. Nriagu (Ed.) *Encyclopedia of Environmental Health*, Elsevier, Burlington, 2011, pp. 33-43.
- [5] L. Sawyer,  $\beta$ -Lactoglobulin in: P.F.F. Paul L. H. McSweeney (Ed.) *Advanced dairy chemistry*, Springer US, 2013, pp. 211-259.
- [6] L. Liang, H.A. Tajmir-Riahi, M. Subirade, Interaction of  $\beta$ -Lactoglobulin with Resveratrol and its Biological Implications, *Biomacromolecules*, 9 (2008) 50-56.
- [7] L. Liang, M. Subirade,  $\beta$ -lactoglobulin/folic acid complexes: formation, characterization, and biological implication, *J. Phys. Chem. B*, 114 (2010) 6707-6712.
- [8] L. Liang, V. Tremblay-Hebert, M. Subirade, Characterisation of the beta-lactoglobulin/alpha-tocopherol complex and its impact on alpha-tocopherol stability, *Food Chem.*, 126 (2011) 821-826.
- [9] Y.A. Khan, R.T. Kashiwabuchi, S.A. Martins, J.M. Castro-Combs, S. Kalyani, P. Stanley, D. Flikier, A. Behrens, Riboflavin and Ultraviolet Light A Therapy as an Adjuvant Treatment for Medically Refractive Acanthamoeba Keratitis: Report of 3 Cases, *Ophthalmology*, 118 (2011) 324-331.
- [10] J. Baier, T. Maisch, M. Maier, E. Engel, M. Landthaler, W. Baumler, Singlet oxygen generation by UVA light exposure of endogenous photosensitizers, *Biophysical journal*, 91 (2006) 1452-1459.
- [11] E. Silva, R. Ugarte, A. Andrade, A.M. Edwards, Riboflavin-sensitized photoprocesses of tryptophan, *J. Photoch. Photobio. B.*, 23 (1994) 43-48.
- [12] A.M. Edwards, E. Silva, B. Jofré, M.I. Becker, A.E. De Ioannes, Visible light effects on tumoral cells in a culture medium enriched with tryptophan and riboflavin, *J Photoch Photobio B*, 24 (1994) 179-186.
- [13] M.C. Yang, H.H. Guan, J.M. Yang, C.N. Ko, M.Y. Liu, Y.H. Lin, Y.C. Huang, C.J. Chen, S.J.T. Mao, Rational design for crystallization of  $\beta$ -lactoglobulin and

- vitamin D3 complex: Revealing a secondary binding site *Cryst. Growth Des.*, 8 (2008) 4268-4276.
- [14] D. Wagner, D. Rousseau, G. Sidhom, M. Pouliot, P. Audet, R. Vieth, Vitamin D-3 fortification, quantification, and long-term stability in cheddar and low-fat cheeses, *J. Agric. Food Chem.*, 56 (2008) 7964-7969.
- [15] D. Wagner, G. Sidhom, S.J. Whiting, D. Rousseau, R. Vieth, The bioavailability of vitamin D from fortified cheeses and supplements is equivalent in adults, *J Nutr*, 138 (2008) 1365-1371.
- [16] T. Nicolai, D. Durand, Controlled food protein aggregation for new functionality, *Curr. Opin. Colloid Interface Sci.*, 18 (2013) 249-256.
- [17] T. Nicolai, M. Britten, C. Schmitt,  $\beta$ -Lactoglobulin and WPI aggregates: formation, structure and applications, *Food Hydrocoll*, 25 (2011) 1945-1962.
- [18] L. Chen, M. Subirade, Chitosan/ $\beta$ -lactoglobulin core-shell nanoparticles as nutraceutical carriers, *Biomaterials*, 26 (2005) 6041-6053.
- [19] F. Diarrassouba, G. Garrait, G.E. Remondetto, P. Alvarez, E. Beyssac, M. Subirade, Increased stability and protease resistance of the  $\beta$ -Lactoglobulin/vitamin D3 complex *Food Chem* (2013) *In press*.
- [20] N. Ron, P. Zimet, J. Bargarum, Y.D. Livney, Beta-lactoglobulin-polysaccharide complexes as nanovehicles for hydrophobic nutraceuticals in non-fat foods and clear beverages, *Int. Dairy J.*, 20 (2010) 686-693.
- [21] N.K. Howell, N.A. Yeboah, D.F.V. Lewis, Studies on the electrostatic interactions of lysozyme with  $\alpha$ -lactalbumin and  $\beta$ -lactoglobulin, *Int. J. Food Sci. Technol.*, 30 (1995) 813-824.
- [22] T. Ganz, Lysozyme, in: J.L. Geoffrey, D.S. Steven (Eds.) *Encyclopedia of Respiratory Medicine*, Academic Press, Oxford, 2006, pp. 649-653.
- [23] E.F. Franssen, R.M. van Amsterdam, J. Visser, F. Moolenaar, D. de Zeeuw, D.F. Meijer, Low molecular weight proteins as carriers for renal drug targeting: naproxen-lysozyme, *Pharm Res*, 8 (1991) 1223-1230.
- [24] P. Qin, B. Su, R. Liu, Probing the binding of two fluoroquinolones to lysozyme: a combined spectroscopic and docking study, *Molecular BioSystems*, 8 (2012) 1222-1229.
- [25] K.K. Kim, D.W. Pack, *Microspheres for Drug Delivery*  
*BioMEMS and Biomedical Nanotechnology*, in: M. Ferrari, A.P. Lee, L.J. Lee (Eds.), Springer US, 2006, pp. 19-50.

- [26] V. Ranade, V., J. Cannon, B., Oral Drug Delivery in: C. Press (Ed.) Drug Delivery Systems, CRC Press Talyors & Francis Group, Boca Raton, FL, USA, 2011, pp. 169-238.
- [27] G. Santus, R.W. Baker, Pharmaceuticals, Controlled Release of, in: A.M. Editor-in-Chief: Robert (Ed.) Encyclopedia of Physical Science and Technology (Third Edition), Academic Press, New York, 2003, pp. 791-803.
- [28] H.A. Schiffter, 5.46 - The Delivery of Drugs – Peptides and Proteins, in: M.-Y. Editor-in-Chief: Murray (Ed.) Comprehensive Biotechnology (Second Edition), Academic Press, Burlington, 2011, pp. 587-604.
- [29] C.H. Weiss, P. Takhistov, D.J. McClements, Functional materials in food nanotechnology, J. Food Sci., 71 (2006) R107-116.
- [30] IFST, Nanotechnology. Information Statement, in: P.A.a.T.L. Committees (Ed.), Institute of Food Science & Technology, London, UK, 2006.
- [31] G. Hebrard, V. Hoffart, J.M. Cardot, M. Subirade, E. Beyssac, Development and characterization of coated-microparticles based on whey protein/alginate using the Encapsulator device, Drug development and industrial pharmacy, (2013) 128-137.
- [32] L. Chen, M. Subirade, Alginate-whey protein granular microspheres as oral delivery vehicles for bioactive compounds, Biomaterials, 27 (2006) 4646-4654.
- [33] G. Hebrard, V. Hoffart, E. Beyssac, J.M. Cardot, M. Alric, M. Subirade, Coated whey protein/alginate microparticles as oral controlled delivery systems for probiotic yeast, Journal of microencapsulation, 27 (2010) 292-302.
- [34] G. Hebrard, V. Hoffart, J.M. Cardot, M. Subirade, M. Alric, E. Beyssac, Investigation of coated whey protein/alginate beads as sustained release dosage form in simulated gastrointestinal environment, Drug development and industrial pharmacy, 35 (2009) 1103-1112.
- [35] G. Hebrard, S. Blanquet, E. Beyssac, G. Remondetto, M. Subirade, M. Alric, Use of whey protein beads as a new carrier system for recombinant yeasts in human digestive tract, J Biotechnol, 127 (2006) 151-160.
- [36] L. Beaulieu, L. Savoie, P. Paquin, M. Subirade, Elaboration and characterization of whey protein beads by an emulsification/cold gelation process: application for the protection of retinol, Biomacromolecules, 3 (2002) 239-248.
- [37] J. O'Regan, M.P. Ennis, D.M. Mulvihill, Milk proteins, in: P.A.W. G. O. Phillips (Ed.) Handbook of hydrocolloids, Woodhead Publishing Limited. , Cambridge, UK, 2009, pp. 298-358.

- [38] M. Boland, Whey proteins, in: G.O.W. Phillips, P. A (Ed.) Handbook of Food Proteins, Woodhead Publishing, 2011, pp. 32-55.
- [39] Y.D. Livney, Milk proteins as vehicles for bioactives, *Curr. Opin. Colloid In.*, 15 (2010) 73-83.
- [40] G.O. Phillips, P.A. Williams, Introduction to food proteins, in: G.O.W. Phillips, P. A (Ed.) Handbook of Food Proteins, Woodhead Publishing, 2011, pp. 1-12.
- [41] R. Mehra, B.T. O'Kennedy, Separation of  $\beta$ -Lactoglobulin from Whey: Its Physico-Chemical Properties and Potential Uses in: C.I.O.a.P.J. Huth (Ed.) Whey Processing, Functionality and Health Benefits, Wiley-Blackwell, Oxford, UK., 2009, pp. 39-62.
- [42] H.F. Alomirah, I. Alli, Separation and characterization of  $\beta$ -lactoglobulin and  $\alpha$ -lactalbumin from whey and whey protein preparations, *Int. Dairy J.*, 14 (2004) 411-419.
- [43] L.M. Bonnaillie, P.M. Tomasula, Whey protein fractionation in: C. Onwulata, P. Huth (Eds.) Whey Processing, Functionality and Health Benefits, John Wiley & Sons, 2009, pp. 15-38.
- [44] A. Albrecht, I. Vovk, Applicability of analytical and preparative monolithic columns to the separation and isolation of major whey proteins, *Journal of chromatography. A*, 1227 (2012) 210-218.
- [45] V. Bonfatti, L. Grigoletto, A. Cecchinato, L. Gallo, P. Carnier, Validation of a new reversed-phase high-performance liquid chromatography method for separation and quantification of bovine milk protein genetic variants, *Journal of chromatography. A*, 1195 (2008) 101-106.
- [46] G. Kontopidis, C. Holt, L. Sawyer, Invited review:  $\beta$ -lactoglobulin: binding properties, structure, and function, *Journal of dairy science*, 87 (2004 ) 785-796.
- [47] J. Loch, A. Polít, A. Górecki, P. Bonarek, K. Kurpiewska, M. Dziejicka-Wasylewska, K. Lewiński, Two modes of fatty acid binding to bovine  $\beta$ -lactoglobulin—crystallographic and spectroscopic studies, *J. Mol. Recognit.*, 24 (2011) 341-349.
- [48] K.M.G. Oliveira, V.L. Valente-Mesquita, M.M. Botelho, L. Sawyer, S.T. Ferreira, I. Polikarpov, Crystal structures of bovine  $\beta$ -lactoglobulin in the orthorhombic space group C2221, *Eur J Biochem*, 268 (2001) 477-484.
- [49] M.M. Botelho, V.L. Valente-Mesquita, K.M.G. Oliveira, I. Polikarpov, S.T. Ferreira, Pressure denaturation of  $\beta$ -lactoglobulin, *Eur J Biochem*, 267 (2000) 2235-2241.

- [50] L. Liang, M. Subirade, Study of the acid and thermal stability of  $\beta$ -lactoglobulin–ligand complexes using fluorescence quenching, *Food Chem.*, 132 (2012) 2023-2029.
- [51] K. Sakurai, Y. Goto, Dynamics and mechanism of the tanford transition of bovine  $\beta$ -lactoglobulin studied using heteronuclear NMR spectroscopy, *J Mol Biol*, 356 (2006) 483-496.
- [52] S. Uhrínová, M.H. Smith, G.B. Jameson, D. Uhrín, L. Sawyer, P.N. Barlow, Structural changes accompanying pH-induced dissociation of the  $\beta$ -lactoglobulin dimer, *Biochemistry*, 39 (2000) 3565-3574.
- [53] K. Sakurai, Y. Goto, Principal component analysis of the pH-dependent conformational transitions of bovine  $\beta$ -lactoglobulin monitored by heteronuclear NMR, *Proc Natl Acad Sci U S A*, 104 (2007) 15346-15351.
- [54] N. Taulier, T.V. Chalikian, Characterization of pH-induced transitions of  $\beta$ -lactoglobulin: ultrasonic, densimetric, and spectroscopic studies, *J Mol Biol*, 314 (2001) 873-889.
- [55] P.E. Morris, R.J. FitzGerald, *Whey Proteins and Peptides in Human Health*, in: C. Onwulata, P. Huth (Eds.) *Whey Processing, Functionality and Health Benefits*, John Wiley & Sons, 2009, pp. 285-384.
- [56] M.H. Tunick, *Whey protein production and utilization: a brief history*, in: C.I.O.a.P.J. Huth (Ed.) *Whey Processing, Functionality and Health Benefits*, Wiley-Blackwell, Oxford, UK., 2009, pp. 1-13.
- [57] G.E. Remondetto, M. Subirade, Molecular mechanisms of Fe<sup>2+</sup>-induced beta-lactoglobulin cold gelation, *Biopolymers*, 69 (2003) 461-469.
- [58] L.K. Creamer, S.M. Loveday, L. Sawyer, *Milk Proteins |  $\beta$ -Lactoglobulin*, in: W.F. Editor-in-Chief: John (Ed.) *Encyclopedia of Dairy Sciences (Second Edition)*, Academic Press, San Diego, 2011, pp. 787-794.
- [59] K. Sakurai, T. Konuma, M. Yagi, Y. Goto, Structural dynamics and folding of beta-lactoglobulin probed by heteronuclear NMR, *BBA. General subjects*, 1790 (2009) 527-537.
- [60] B.Y. Qin, M.C. Bewley, L.K. Creamer, H.M. Baker, E.N. Baker, G.B. Jameson, Structural basis of the tanford transition of bovine  $\beta$ -lactoglobulin, *Biochemistry*, 37 (1998) 14014-14023.
- [61] M.C. Yang, N.C. Chen, C.J. Chen, C.Y. Wu, S.J. Mao, Evidence for beta-lactoglobulin involvement in vitamin D transport in vivo--role of the gamma-turn (Leu-Pro-Met) of beta-lactoglobulin in vitamin D binding, *FEBS*, 276 (2009) 2251-2265.

- [62] M. Collini, L. D'Alfonso, H. Molinari, L. Ragona, M. Catalano, G. Baldini, Competitive binding of fatty acids and the fluorescent probe 1-8-anilinonaphthalene sulfonate to bovine  $\beta$ -lactoglobulin, *Protein Sci*, 12 (2003) 1596-1603.
- [63] L.H. Riihimäki, M.J. Vainio, J.M.S. Heikura, K.H. Valkonen, V.T. Virtanen, P.M. Vuorela, Binding of phenolic compounds and their derivatives to bovine and reindeer  $\beta$ -lactoglobulin, *J Agric Food Chem*, 56 (2008) 7721-7729.
- [64] L. Ragona, F. Fogolari, M. Catalano, R. Ugolini, L. Zetta, H. Molinari, EF loop conformational change triggers ligand binding in  $\beta$ -lactoglobulins, *J Biol Chem*, 278 (2003) 38840-38846.
- [65] J.R. Lakowicz, Principles of Fluorescence Spectroscopy, in: J.R. Lakowicz (Ed.), Springer US, Baltimore, MD, USA, 2006.
- [66] M. Rouabhia, V. Gilbert, H. Wang, M. Subirade, In vivo evaluation of whey protein-based biofilms as scaffolds for cutaneous cell cultures and biomedical applications, *Biomed Mater*, 2 (2007) S38-44.
- [67] H. Zhao, M. Ge, Z. Zhang, W. Wang, G. Wu, Spectroscopic studies on the interaction between riboflavin and albumins, *Spectrochim. Acta A*, 65 (2006) 811-817.
- [68] M. van de Weert, Fluorescence quenching to study protein-ligand binding: common errors *J fluoresc*, 20 (2010) 625-629.
- [69] X.J. Guo, X.D. Sun, S.K. Xu, Spectroscopic investigation of the interaction between riboflavin and bovine serum albumin, *J Mol Struct*, 931 (2009) 55-59.
- [70] J.R. Lakowicz, Energy transfer, in: Springer (Ed.) Principles of fluorescence spectroscopy, New York, USA 2006, pp. 443-475.
- [71] N. Stănciuc, I. Aprodu, G. Râpeanu, G. Bahrim, Fluorescence spectroscopy and molecular modeling investigations on the thermally induced structural changes of bovine  $\beta$ -lactoglobulin, *Innov. Food Sci. Emerg. Technol.*, 15 (2012) 50-56.
- [72] T. Croguennec, D. Molle, R. Mehra, S. Bouhallab, Spectroscopic characterization of heat-induced nonnative beta-lactoglobulin monomers, *Protein Sci.*, 13 (2004) 1340-1346
- [73] P. Busti, S. Scarpeci, C.A. Gatti, N.J. Delorenzi, Use of fluorescence methods to monitor unfolding transitions in  $\beta$ -lactoglobulin, *Food Res Int*, 35 (2002) 871-877.
- [74] R.W. Woody, Electronic circular dichroism of proteins, in: P.L.P. Nina Berova, Koji Nakanishi, Robert W. Woody (Ed.) *Comprehensive Chiroptical Spectroscopy*, John Wiley & Sons, Inc., 2012, pp. 473-497.

- [75] S.M. Kelly, T.J. Jess, N.C. Price, How to study proteins by circular dichroism, *BBA- Proteins Proteom*, 1751 (2005) 119-139.
- [76] T.E. Creighton, Physical and Chemical Basis of Molecular Biology, in: T.E. Creighton (Ed.), Helvetian Press, 2010, pp. 681.
- [77] B. Nina, P.L. Polavarapu, K. Nakanishi, R.W. Woody, Comprehensive Chiroptical Spectroscopy: Applications in Stereochemical Analysis of Synthetic Compounds, Natural Products, and Biomolecules, in: P.L.P. Nina Berova, Koji Nakanishi, Robert W. Woody (Ed.) Comprehensive Chiroptical Spectroscopy, John Wiley & Sons, Inc., 2012.
- [78] G. Mandalari, A.M. Mackie, N.M. Rigby, M.S.J. Wickham, E.N.C. Mills, Physiological phosphatidylcholine protects bovine  $\beta$ -lactoglobulin from simulated gastrointestinal proteolysis, *Mol. Nutr. Food Res.*, 53 (2009) S131-S139.
- [79] M.-C. Yang, H.-H. Guan, M.-Y. Liu, Y.-H. Lin, J.-M. Yang, W.-L. Chen, C.-J. Chen, S.J.T. Mao, Crystal structure of a secondary vitamin D3 binding site of milk  $\beta$ -lactoglobulin, *Proteins*, 71 (2008) 1197-1210.
- [80] A. Divsalar, L. Barzegar, G.R. Behbehani, Thermal study of a newly synthesized Cu(II) complex binding to bovine  $\beta$ -lactoglobulin, in: *J Chem*, 2013.
- [81] G. Kontopidis, C. Holt, L. Sawyer, The ligand-binding site of bovine  $\beta$ -lactoglobulin: evidence for a function?, *J Mol Biol*, 318 (2002) 1043-1055.
- [82] F. Diarrassouba, L. Liang, G.E. Remondetto, M. Subirade, Nanocomplex formation between riboflavin and  $\beta$ -lactoglobulin: Spectroscopic investigation and biological characterization, *Food Res Int*, 52 (2013) 557-567.
- [83] D. Agudelo, M. Beauregard, G. Bérubé, H.-A. Tajmir-Riahi, Antibiotic doxorubicin and its derivative bind milk  $\beta$ -lactoglobulin, *J Photoch Photobio B* 117 (2012) 185-192.
- [84] A. Tromelin, E. Guichard, Interaction between flavour compounds and  $\beta$ -lactoglobulin: approach by NMR and 2D/3D-QSAR studies of ligands, *Flavour Frag J*, 21 (2006) 13-24.
- [85] M. von Staszewski, F.L. Jara, A.L.T.G. Ruiz, R.J. Jagus, J.E. Carvalho, A.M.R. Pilosof, Nanocomplex formation between  $\beta$ -lactoglobulin or caseinomacropeptide and green tea polyphenols: Impact on protein gelation and polyphenols antiproliferative activity, *J Funct Foods*, 4 (2012) 800-809.
- [86] J. Keller, Gastrointestinal Digestion and Absorption, in: J.L. Editors-in-Chief: William, M.D. Lane (Eds.) *Encyclopedia of Biological Chemistry*, Academic Press, Waltham, 2013, pp. 354-359.

- [87] L. Ragona, L. Zetta, F. Fogolari, H. Molinari, D.M. Pérez, P. Puyol, K.D. Kruif, F. Löhr, H. Rüterjans, Bovine  $\beta$ -lactoglobulin: Interaction studies with palmitic acid, *Protein Sci*, 9 (2000) 1347-1356.
- [88] G. Mandalari, A.M. Mackie, N.M. Rigby, M.S.J. Wickham, E.N.C. Mills, Physiological phosphatidylcholine protects bovine  $\beta$ -lactoglobulin from simulated gastrointestinal proteolysis, *Mol Nut Food Res*, 53 (2009) S131-S139.
- [89] C.D. Kanakis, I. Hasni, P. Bourassa, P.A. Tarantilis, M.G. Polissiou, H.-A. Tajmir-Riahi, Milk  $\beta$ -lactoglobulin complexes with tea polyphenols, *Food Chem*, 127 (2011) 1046-1055.
- [90] M. Stojadinovic, J. Radosavljevic, J. Ognjenovic, J. Vesic, I. Prodic, D. Stanic-Vucinic, T. Cirkovic Velickovic, Binding affinity between dietary polyphenols and  $\beta$ -lactoglobulin negatively correlates with the protein susceptibility to digestion and total antioxidant activity of complexes formed, *Food Chem*, 136 (2013) 1263-1271.
- [91] J.P. Tardivo, A. Del Giglio, C.S. de Oliveira, D.S. Gabrielli, H.C. Junqueira, D.B. Tada, D. Severino, R. de Fátima Turchiello, M.S. Baptista, Methylene blue in photodynamic therapy: From basic mechanisms to clinical applications, *Photodiagn Photodyn*, 2 (2005) 175-191.
- [92] C. Lu, W. Lin, W. Wang, Z. Han, S. Yao, N. Lin, Riboflavin (VB2) photosensitized oxidation of 2[prime or minute]-deoxyguanosine-5[prime or minute]-monophosphate (dGMP) in aqueous solution: a transient intermediates study, *Phys Chem Chem Phys*, 2 (2000) 329-334.
- [93] S.G. Baldursdottir, A.L. Kjoniksen, J. Karlsen, B. Nystrom, J. Roots, H.H. Tonnesen, Riboflavin-photosensitized changes in aqueous solutions of alginate. Rheological studies, *Biomacromolecules*, 4 (2003) 429-436.
- [94] J.-Y. Liang, J.-M.P. Yuann, C.-W. Cheng, H.-L. Jian, C.-C. Lin, L.-Y. Chen, Blue light induced free radicals from riboflavin on E. coli DNA damage, *J Photoch Photobio B*, 119 (2013) 60-64.
- [95] K. Sato, N. Sakakibara, K. Hasegawa, H. Minami, T. Tsuji, A preliminary report of the treatment of blue nevus with dermal injection of riboflavin and exposure to near-ultraviolet/visible radiation (ribotherapy), *J Dermatol Sci*, 23 (2000) 22-26.
- [96] B.C. Wilson, Photodynamic therapy: Clinical applications, in: J.R. Bertino (Ed.) *Encyclopedia of Cancer (Second Edition)*, Academic Press, New York, 2002, pp. 453-462.
- [97] D.R. Cardoso, D.W. Franco, K. Olsen, M.L. Andersen, L.H. Skibsted, Reactivity of bovine whey proteins, peptides, and amino acids toward triplet riboflavin as studied by laser flash photolysis, *J Agr Food Chem*, 52 (2004) 6602-6606.

- [98] A. Grzelak, B. Rychlik, G. Bartosz, Light-dependent generation of reactive oxygen species in cell culture media, *Free Radical Bio Med*, 30 (2001) 1418-1425.
- [99] M.J. Davies, Singlet oxygen-mediated damage to proteins and its consequences, *Biochem Bioph Res Co*, 305 (2003) 761-770.
- [100] M.S. Calvo, S.J. Whiting, Public health strategies to overcome barriers to optimal vitamin D status in populations with special needs, *J Nutr*, 136 (2006) 1135-1139.
- [101] D.o.A. U.S. Department of Health and Human Services and U.S. Dietary Guidelines for Americans, 2005. Adequate Nutrients Within Calorie Needs, in: D.o.A. (USDA) (Ed.), U.S. Government Printing Office, Washington DC, 2005, pp. Government Printing Office, January 2005. .
- [102] M.F. Holick, Vitamin D deficiency, *The New England journal of medicine*, 357 (2007) 266-281.
- [103] S.C. Meredith, Protein denaturation and aggregation, *Ann N Y Acad Sci*, 1066 (2006) 181-221.
- [104] E.A. Foegeding, J.P. Davis, Food protein functionality : a comprehensive approach, *Food Hydrocoll*, 25 (2011 ) 1853-1864.
- [105] S. Gunasekaran, S. Ko, L. Xiao, Use of whey proteins for encapsulation and controlled delivery applications, *J Food Eng*, 83 (2007) 31-40.
- [106] G.E. Remondetto, E. Beyssac, M. Subirade, Iron availability from whey protein hydrogels: an in vitro study, *J Agric Food Chem*, 52 (2004) 8137-8143.
- [107] V.L. Sok Line, G.E. Remondetto, M. Subirade, Cold gelation of  $\beta$ -lactoglobulin oil-in-water emulsions, *Food Hydrocoll*, 19 (2005) 269-278.
- [108] M.A. Augustin, P. Sanguansri, Chapter 5 - nanostructured materials in the food industry, in: L.T. Steve (Ed.) *Adv Food Nutr Res*, Academic Press, 2009, pp. 183-213.
- [109] S. Verma, R. Gokhale, D.J. Burgess, A comparative study of top-down and bottom-up approaches for the preparation of micro/nanosuspensions, *Int J Pharm*, 380 (2009) 216-222.
- [110] J. Salazar, A. Ghanem, R.H. Müller, J.P. Möschwitzer, Nanocrystals : comparison of the size reduction effectiveness of a novel combinative method with conventional top-down approaches, *Eur J Pharm Biopharm*, 81 (2012) 82-90.
- [111] H. Singh, Milk Protein Products | Functional Properties of Milk Proteins, in: W.F. Editor-in-Chief: John (Ed.) *Encyclopedia of Dairy Sciences (Second Edition)*, Academic Press, San Diego, 2011, pp. 887-893.

- [112] T. Vo-Dinh, Protein Nanotechnology, in: T. Vo-Dinh (Ed.) Protein Nanotechnology, Humana Press, 2005, pp. 1-13.
- [113] N. Sozer, J.L. Kokini, Nanotechnology and its applications in the food sector, Trends in Biotechnol, 27 (2009) 82-89.
- [114] P.N. Ezhilarasi, P. Karthik, N. Chhanwal, C. Anandharamakrishnan, Nanoencapsulation Techniques for Food Bioactive Components: A Review, Food Bioprocess Technol, 6 (2013) 628-647.
- [115] S. Ko, S. Gunasekaran, Preparation of sub-100-nm  $\beta$ -lactoglobulin (BLG) nanoparticles, J Microencapsul, 23 (2006) 887-898.
- [116] G. Lafitte, Structure of the gastrointestinal mucus layer and implications for controlled release and delivery of functional food ingredients, in: N. Garti (Ed.) Delivery and Controlled Release of Bioactives in Foods and Nutraceuticals, Woodhead Publishing, 2008, pp. 26-52.
- [117] O.G. Jones, E.A. Decker, D.J. McClements, Formation of biopolymer particles by thermal treatment of beta-lactoglobulin-pectin complexes, Food Hydrocoll, 23 (2009) 1312-1321.
- [118] P. Zimet, Y.D. Livney, Beta-lactoglobulin and its nanocomplexes with pectin as vehicles for  $\omega$ -3 polyunsaturated fatty acids, Food Hydrocoll, 23 (2009) 1120-1126.
- [119] S. Ko, S. Gunasekanran. Preparation of sub-100-nm  $\beta$ -lactoglobulin (BLG) nanoparticles. J Microencapsul, 23 (2006) 887-898.
- [120] Z. Teng, Y. Li, Y. Luo, B. Zhang, Q. Wang, Cationic  $\beta$ -Lactoglobulin nanoparticles as a bioavailability enhancer: protein characterization and particle formation, Biomacromolecules, 14 (2013) 2848-2856.
- [121] C.-Y. Yu, B.-C. Yin, W.N. Zhang, S.-X. Cheng, X.-Z. Zhang, R.-X. Zhuo, Composite microparticle drug delivery systems based on chitosan, alginate and pectin with improved pH-sensitive drug release property, Colloids Surf B Biointerfaces, 68 (2009) 245-249.
- [122] M. George, T.E. Abraham, Polyionic hydrocolloids for the intestinal delivery of protein drugs: Alginate and chitosan — a review, J Control Release, 114 (2006) 1-14.
- [123] W. Chanasattru, O.G. Jones, E.A. Decker, D.J. McClements, Impact of cosolvents on formation and properties of biopolymer nanoparticles formed by heat treatment of  $\beta$ -lactoglobuline - Pectin complexes, Food Hydrocoll, 23 (2009) 2450-2457.

- [124] O.G. Jones, E.A. Decker, D.J. McClements, Comparison of protein–polysaccharide nanoparticle fabrication methods: Impact of biopolymer complexation before or after particle formation, *Journal of Colloid and Interface Science*, 344 (2010) 21-29.
- [125] O.G. Jones, U. Lesmes, P. Dubin, D.J. McClements, Effect of polysaccharide charge on formation and properties of biopolymer nanoparticles created by heat treatment of beta-lactoglobulin-pectin complexes, *Food Hydrocoll*, 24 (2010) 374-383.
- [126] C. Schmitt, S.L. Turgeon, Protein/polysaccharide complexes and coacervates in food systems, *Adv. Colloid Interface Sci.*, 167 (2011) 63-70.
- [127] O.G. Jones, D.J. McClements, Biopolymer nanoparticles from heat-treated electrostatic protein–polysaccharide complexes: factors affecting particle characteristics, *J Food Sci*, 75 (2010) N36-N43.
- [128] A. Shpigelman, Y. Cohen, Y.D. Livney, Thermally-induced  $\beta$ -lactoglobulin–EGCG nanovehicles : loading, stability, sensory and digestive-release study, *Food Hydrocoll*, 29 (2012 ) 57-67.
- [129] H.C. Liu, W.L. Chen, S.J.T. Mao, Antioxidant nature of bovine milk  $\beta$ -Lactoglobulin, *Journal of dairy science*, 90 (2007) 547-555.
- [130] E. Semo, E. Kesselman, D. Danino, Y.D. Livney, Casein micelle as a natural nano-capsular vehicle for nutraceuticals, *Food Hydrocoll*, 21 (2007) 936-942.
- [131] F.S. Sun, C.X. Ju, J.H. Chen, S. Liu, N. Liu, K.K. Wang, C.G. Liu, Nanoparticles based on hydrophobic alginate derivative as nutraceutical delivery vehicle : vitamin D-3 loading, *Artif Cells Blood Substit Immobil Biotechnol*, 40 (2012) 113-119.
- [132] E. Acosta, Testing the effectiveness of nutrient delivery systems in: N. Garti (Ed.) *Delivery and controlled release of bioactives in foods and nutraceuticals*, Woodhead Publishing, 2008, pp. 53-106
- [133] A. Nesterenko, I. Alric, F. Silvestre, V. Durrieu, Vegetable proteins in microencapsulation : a review of recent interventions and their effectiveness, *Ind Crops Prod*, 42 (2013) 469-479.
- [134] S.L. Turgeon, S.I. Laneuville, Protein + Polysaccharide Coacervates and Complexes: From Scientific Background to their Application as Functional Ingredients in Food Products, in: K. Stefan, T.N. Ian, I.T.N. Johan B. UbbinkA2 - Stefan Kasapis, B.U. Johan (Eds.) *Modern Biopolymer Science*, Academic Press, San Diego, 2009, pp. 327-363.
- [135] C. Schmitt, L. Aberkane, C. Sanchez, Protein—polysaccharide complexes and coacervates, in: *Handbook of hydrocolloids*, 2009, pp. 420-476.

- [136] C. Schmitt, C. Sanchez, S. Despond, D. Renard, F. Thomas, J. Hardy, Effect of protein aggregates on the complex coacervation between  $\beta$ -lactoglobulin and acacia gum at pH 4.2, *Food Hydrocoll*, 14 (2000) 403-413.
- [137] R. Caillard, M.A. Mateescu, M. Subirade, Maillard-type cross-linked soy protein hydrogels as devices for the release of ionic compounds an in vitro study, *Food Res Int*, 43 (2010) 2349-2355.
- [138] T.J. Wooster, M.A. Augustin,  $\beta$ -Lactoglobulin-dextran Maillard conjugates: their effect on interfacial thickness and emulsion stability, *J Colloid Interf Sci*, 303 (2006) 564-572.
- [139] Y. Desfougeres, T. Croguennec, V. Lechevalier, S. Bouhallab, F. Nau, Charge and size drive spontaneous self-assembly of oppositely charged globular proteins into microspheres, *J Phys Chem B*, 114 (2010) 4138-4144.
- [140] N. Howell, E. LiChan, Elucidation of interactions of lysozyme with whey proteins by Raman spectroscopy, *Int J Food Sci Technol*, 31 (1996) 439-451.
- [141] Y. Desfougères, T. Croguennec, V. Lechevalier, S. Bouhallab, F. Nau, Charge and size drive spontaneous self-assembly of oppositely charged globular proteins into microspheres, *J Phys Chem B*, 114 (2010) 4138-4144.
- [142] H.-C. Mahler, W. Friess, U. Grauschopf, S. Kiese, Protein aggregation: pathways, induction factors and analysis, *J Pharm Sci*, 98 (2009) 2909-2934.
- [143] J. Moore, E. Cerasoli, Particle Light Scattering Methods and Applications, in: L. Editor-in-Chief: John (Ed.) *Encyclopedia of Spectroscopy and Spectrometry* (Second Edition), Academic Press, Oxford, 2010 pp. 2077-2088.
- [144] R.M. Murphy, C.C. Lee, Laser Light Scattering as an Indispensable Tool for Probing Protein Aggregation, in: *Misbehaving Proteins*, Springer New York, 2006, pp. 147-165.
- [145] H.R. Jiang, N. Liu, Self-assembled  $\beta$ -lactoglobulin–conjugated linoleic acid complex for colon cancer-targeted substance, *J Dairy Sci*, 93 (2010) 3931-3939.
- [146] R.M. Faulks, S. Southon, Assessing the bioavailability of nutraceuticals in: N. Garti (Ed.) *Delivery and Controlled Release of Bioactives in Foods and Nutraceuticals*, Woodhead Publishing, 2008, pp. 3-25.
- [147] M.J. Davies, R.J.W. Truscott, Photo-oxidation of proteins and its role in cataractogenesis, *J Photochem Photobio B*, 63 (2001 ) 114-125.
- [148] M.S. Calvo, S.J. Whiting, Prevalence of vitamin D insufficiency in Canada and the United States: importance to health status and efficacy of current food fortification and dietary supplement use, *Nut Rev*, 61 (2003) 107-113.

- [149] S.J. Whiting, T.J. Green, M.S. Calvo, Vitamin D intakes in North America and Asia-Pacific countries are not sufficient to prevent vitamin D insufficiency, *J Steroid Biochem Mol Biol*, 103 (2007) 626-630.
- [150] A.O. Elzoghby, W.M. Samy, N.A. Elgindy, Protein-based nanocarriers as promising drug and gene delivery systems, *J Control Release*, 161 (2012) 38-49.
- [151] T. Dai, Y.Y. Huang, M.R. Hamblin, Photodynamic therapy for localized infections — state of the art, *Photodiagn Photodyn*, 6 (2009) 170-188.
- [152] L.Y. Brovko, A. Meyer, A.S. Tiwana, W. Chen, H. Liu, C.D.M. Filipe, M.W. Griffiths, Photodynamic treatment: a novel method for sanitation of food handling and food processing surfaces, *J Food Prot*, 72 (2009) 1020-1024.
- [153] R.R. Allison, C.H. Sibata, Oncologic photodynamic therapy photosensitizers: a clinical review, *Photodiagn Photodyn*, 7 (2010) 61-75.
- [154] Y. Cheng, C. Burda, Nanoparticles for photodynamic therapy, in: L.A. Editors-in-Chief: David, D.S. Gregory, P.W. Gary (Eds.) *Comprehensive Nanoscience and Technology*, Academic Press, Amsterdam, 2011, pp. 1-28.
- [155] T.J. Dougherty, C.J. Gomer, B.W. Henderson, G. Jori, D. Kessel, M. Korbelik, J. Moan, Q. Peng, Photodynamic therapy, *J Natl Cancer I*, 90 (1998) 889-905.
- [156] I. Roy, T.Y. Ohulchansky, H.E. Pudavar, E.J. Bergey, A.R. Oseroff, J. Morgan, T.J. Dougherty, P.N. Prasad, Ceramic-based nanoparticles entrapping water-insoluble photosensitizing anticancer drugs: a novel drug-carrier system for photodynamic therapy, *J Am Chem Soc*, 125 (2003) 7860-7865.
- [157] Y.N. Konan, R. Gurny, E. Allémann, State of the art in the delivery of photosensitizers for photodynamic therapy, *J Photoch Photobio B*, 66 (2002) 89-106.
- [158] C.J. Bates, Riboflavin, in: B. Caballero (Ed.) *Encyclopedia of human nutrition (Second Edition)*, Elsevier, Oxford, 2005, pp. 100-108.
- [159] A.C. de Souza, L. Kodach, F.R. Gadelha, C.L. Bos, A.D. Cavagis, H. Aoyama, M.P. Peppelenbosch, C.V. Ferreira, A promising action of riboflavin as a mediator of leukaemia cell death, *Apoptosis : an international journal on programmed cell death*, 11 (2006) 1761-1771.
- [160] A. Schrier, G. Greebel, H. Attia, S. Trokel, E.E. Smith, In Vitro Antimicrobial Efficacy of Riboflavin and Ultraviolet Light on *Staphylococcus aureus*, Methicillin-resistant *Staphylococcus aureus*, and *Pseudomonas aeruginosa*, *J Refract Surg*, 25 (2009) S799-S802.

- [161] C.K. Remucal, K. McNeill, Photosensitized amino acid degradation in the presence of riboflavin and its derivatives, *Environ Sci Technol*, 45 (2011) 5230-5237.
- [162] M. Bartosik, V. Ostatna, E. Palecek, Electrochemistry of riboflavin-binding protein and its interaction with riboflavin, *Bioelectrochemistry*, 76 (2009) 70-75.
- [163] S. Fortin, L.H. Wei, E. Moreau, J. Lacroix, M.F. Cote, E. Petitclerc, L.P. Kotra, R. C-Gaudreault, Design, Synthesis, Biological Evaluation, and Structure-Activity Relationships of Substituted Phenyl 4-(2-Oxoimidazolidin-1-yl)-benzenesulfonates as New Tubulin Inhibitors Mimicking Combretastatin A-4, *J. Med. Chem.*, 54 (2011) 4559-4580.
- [164] N.C. Institute, NCI-60 Developmental Therapeutics Program Human Tumor Cell Line Screen in, National Institute of Health, USA, 2012.
- [165] G. Tollin, Magnetic circular dichroism and circular dichroism of riboflavine and its analogs, *Biochemistry-US*, 7 (1968) 1720-1727.
- [166] G. Zandomeneghi, M. Zandomeneghi, Determination of holo- and apo-riboflavin binding protein in avian egg whites through circular dichroism and fluorescence spectroscopy, *J Agr Food Chem*, 57 (2009) 6510-6517.
- [167] E. Dufour, C. Genot, T. Haertle,  $\beta$ -lactoglobulin binding properties during its folding changes studied by fluorescence spectroscopy, *BBA-Protein Struct M*, 1205 (1994) 105-112.
- [168] Q. Wang, J.C. Allen, H.E. Swaisgood, Protein concentration dependence of palmitate binding to  $\beta$ -lactoglobulin, *J Dairy Sci*, 81 (1998) 76-81.
- [169] T. Lefevre, M. Subirade, Interaction of beta-lactoglobulin with phospholipid bilayers: a molecular level elucidation as revealed by infrared spectroscopy, *Intl J Biol Macromol*, 28 (2000) 59-67.
- [170] L. Tavel, C. Moreau, S. Bouhallab, E.C.Y. Li-Chan, E. Guichard, Interactions between aroma compounds and  $\beta$ -lactoglobulin in the heat-induced molten globule state, *Food Chem*, 119 (2010) 1550-1556.
- [171] D. Fessas, S. Lametti, A. Schiraldi, F. Bonomi, Thermal unfolding of monomeric and dimeric  $\beta$ -lactoglobulins, *Eur J Biochem*, 268 (2001) 5439-5448
- [172] F. Tian, K. Johnson, A.E. Lesar, H. Moseley, J. Ferguson, I.D.W. Samuel, A. Mazzini, L. Brancaleon, The pH-dependent conformational transition of [ $\beta$ ]-lactoglobulin modulates the binding of protoporphyrin IX, *BBA. General Subjects*, 1760 (2006) 38-46.
- [173] A. Galat, Interaction of riboflavin binding protein with riboflavin, quinacrine, chlorpromazine and daunomycin, *Int J Biochem*, 20 (1988) 1021-1029.

- [174] D.R. Flower, A.C.T. North, C.E. Sansom, The lipocalin protein family: structural and sequence overview, *BBA-Protein Struct. M.*, 1482 (2000) 9-24.
- [175] J.P. Tardivo, A. Del Giglio, C.S. de Oliveira, D.S. Gabrielli, H.C. Junqueira, D.B. Tada, D. Severino, T.R. de Fatima, M.S. Baptista, Methylene blue in photodynamic therapy: from basic mechanisms to clinical applications, *Photodiagn Photodyn*, 2 (2005) 175-191.
- [176] Q. Wang, J.C. Allen, H.E. Swaisgood, Binding of vitamin D and cholesterol to beta-lactoglobulin, *J Dairy Sci*, 80 (1997) 1054-1059.
- [177] Q. Wang, J.C. Allen, H.E. Swaisgood, Binding of lipophilic nutrients to beta-lactoglobulin prepared by bioselective adsorption, *J Dairy Sci*, 82 (1999) 257-264.
- [178] M. Hattori, A. Watabe, K. Takahashi, beta-lactoglobulin protects beta-ionone related compounds from degradation by heating, oxidation, and irradiation, *Biosci Biotechnol Biochem*, 59 (1995) 2295-2297.
- [179] H. Lal, R. Pandey, S.K. Aggarwal, Vitamin D: non-skeletal actions and effects on growth, *Nut Res*, 19 (1999) 1683-1718.
- [180] M.F. Holick, Importance for monitoring serum 25-hydroxyvitamin D for the prevention of osteoporosis, common cancers, autoimmune diseases and cardiovascular diseases, *Clin Chim Acta*, 355 (2005) S31-S31.
- [181] S.L. Hines, H.K.S. Jorn, K.M. Thompson, J.M. Larson, Breast cancer survivors and vitamin D: A review, *Nutrition*, 26 (2010) 255-262.
- [182] E.D. Gorham, C.F. Garland, F.C. Garland, W.B. Grant, S.B. Mohr, M. Lipkin, H.L. Newmark, E. Giovannucci, M. Wei, M.F. Holick, Vitamin D and prevention of colorectal cancer, *J Steroid Biochem Mol Biol*, 97 (2005) 179-194.
- [183] D.D. Bikle, L. Gerald, Vitamin D regulation of immune function, in: *Vitam. Horm.*, Academic Press, 2011, pp. 1-21.
- [184] S. Hansdottir, M.M. Monick, Vitamin D Effects on Lung Immunity and Respiratory Diseases, *Vitam Horm*, 86 (2011) 217-237.
- [185] M. Hewison, L. Gerald, Vitamin D and innate and adaptive immunity, in: *Vitam. Horm.*, Academic Press, 2011, pp. 23-62.
- [186] S. Ardizzone, A. Cassinotti, M. Bevilacqua, M. Clerici, G.B. Porro, L. Gerald, Vitamin D and inflammatory bowel disease, in: *Vitam. Horm.*, Academic Press, 2011, pp. 367-377.
- [187] M.S. Calvo, S.J. Whiting, C.N. Barton, Vitamin D fortification in the United States and Canada: current status and data needs, *Am J Clin Nutr*, 80 (2004) 1710S-1716S.

- [188] L. Bilodeau, G. Dufresne, J. Deeks, G. Clément, J. Bertrand, S. Turcotte, A. Robichaud, F. Beraldin, A. Fouquet, Determination of vitamin D<sub>3</sub> and 25-hydroxyvitamin D<sub>3</sub> in foodstuffs by HPLC UV-DAD and LC-MS/MS, *J Food Compost Anal*, 24 (2011) 441-448.
- [189] H.L. Casal, U. Köhler, H.H. Mantsch, Structural and conformational changes of  $\beta$ -lactoglobulin B: an infrared spectroscopic study of the effect of pH and temperature, *BBA. Protein structure and molecular enzymology*, 957 (1988) 11-20.
- [190] T. Lefèvre, M. Subirade, Molecular differences in the formation and structure of fine-stranded and particulate  $\beta$ -lactoglobulin gels, *Biopolymers*, 54 (2000) 578-586.
- [191] E.R. Bertone-Johnson, W.Y. Chen, M.F. Holick, B.W. Hollis, G.A. Colditz, W.C. Willett, S.E. Hankinson, Plasma 25-hydroxyvitamin D and 1,25-dihydroxyvitamin D and risk of breast cancer, *Canc Epidemiol Biomarkers Prev*, 14 (2005) 1991-1997.
- [192] M.D. Pérez, M. Calvo, Interaction of  $\beta$ -lactoglobulin with retinol and fatty acids and its role as a possible biological function for this protein: a review, *J Dairy Sci*, 78 (1995) 978-988.
- [193] J.-M. Chobert, M. Dalgalarondo, E. Dufour, C. Bertrand-Harb, T. Haertlé, Influence of pH on the structural changes of  $\beta$ -lactoglobulin studied by tryptic hydrolysis, *BBA. Protein structure and molecular enzymology*, 1077 (1991) 31-34.
- [194] L.K. Creamer, Effect of Sodium Dodecyl Sulfate and Palmitic Acid on the Equilibrium Unfolding of Bovine  $\beta$ -lactoglobulin, *Biochemistry*, 34 (1995) 7170-7176.
- [195] J.I. Loch, A. Polit, P. Bonarek, D. Olszewska, K. Kurpiewska, M. Dziedzicka-Wasylewska, K. Lewiński, Structural and thermodynamic studies of binding saturated fatty acids to bovine  $\beta$ -lactoglobulin, *Int J Biol Macromol*, 50 (2012) 1095-1102.
- [196] P. Busti, S. Scarpeci, C.A. Gatti, N.J. Delorenzi, Binding of alkylsulfonate ligands to bovine  $\beta$ -lactoglobulin: effects on protein denaturation by urea, *Food Hydrocoll*, 19 (2005) 249-255.
- [197] S.J. Fairweather-Tait, S. Southon, Bioavailability of nutrients in: C. Editor-in-Chief: Benjamin (Ed.) *Encyclopedia of Food Sciences and Nutrition* (Second Edition), Academic Press, Oxford, 2003, pp. 478-484.
- [198] R.J. Wood, Bioavailability in: C. Editor-in-Chief: Benjamin (Ed.) *Encyclopedia of Human Nutrition* (Second Edition), Elsevier, Oxford, 2005, pp. 195-201.
- [199] R. Vieth, H. Kris, Vitamin D, in: *International Encyclopedia of Public Health*, Academic Press, Oxford, 2008, pp. 532-537.

- [200] F. Diarrassouba, G.E. Remondetto, L. Liang, G. Garrait, E. Beyssac, M. Subirade, Effects of gastrointestinal pH conditions on the stability of the  $\beta$ -lactoglobulin/vitamin D3 complex and on the solubility of vitamin D3, *Food Res Int*, 52 (2013) 515-521.
- [201] G. Garrait, J.F. Jarrige, S. Blanquet, E. Beyssac, J.M. Cardot, M. Alric, Gastrointestinal absorption and urinary excretion of trans-cinnamic and p-coumaric acids in rats, *J Agric Food Chem*, 54 (2006) 2944-2950.
- [202] M. Ritskes-Hoitinga, A. Chwalibog, Nutrient requirements, experimental design, and feeding schedules in animal experimentation in: J. Hau, G.L.J. Van Hoosier (Eds.) *Handbook of laboratory animal science. Essential principles and practices* CRC Press, Boca Raton, FL, USA, 2003, pp. 282-305.
- [203] S.A. Renken, J.J. Warthesen, Vitamin-D stability in milk, *J Food Sci*, 58 (1993) 552-555.
- [204] J.T.T. Baird, C.S. Craik, Chapter 575 - Trypsin, in: *Handbook of Proteolytic Enzymes*, Academic Press, 2013, pp. 2594-2600.
- [205] L.K. Creamer, H.C. Nilsson, M.A. Paulsson, C.J. Coker, J.P. Hill, R. Jimenez-Flores, Effect of genetic variation on the tryptic hydrolysis of bovine beta-lactoglobulin A, B, and C, *J Dairy Sci*, 87 (2004) 4023-4032.
- [206] L. Gráf, L. Szilágyi, I. Venekei, Chapter 582 - Chymotrypsin, in: *Handbook of Proteolytic Enzymes*, Academic Press, 2013, pp. 2626-2633.
- [207] T. Considine, H.A. Patel, H. Singh, L.K. Creamer, Influence of binding of sodium dodecyl sulfate, all-trans-retinol, palmitate, and 8-anilino-1-naphthalenesulfonate on the heat-induced unfolding and aggregation of  $\beta$ -lactoglobulin B, *J Agric Food Chem*, 53 (2005) 3197-3205.
- [208] J. Mou.écoucou, C. Villaume, C. Sanchez, L. Méjean,  $\beta$ -Lactoglobulin/polysaccharide interactions during in vitro gastric and pancreatic hydrolysis assessed in dialysis bags of different molecular weight cut-offs, *BBA. General subjects*, 1670 (2004) 105-112.
- [209] I.M. Reddy, N.K.D. Kella, J.E. Kinsella, Structural and conformational basis of the resistance of beta-lactoglobulin to peptic and chymotryptic digestion, *J Agric Food Chem*, 36 (1988) 737-741.
- [210] A. Barbiroli, T. Beringhelli, F. Bonomi, D. Donghi, P. Ferranti, M. Galliano, S. Iametti, D. Maggioni, P. Rasmussen, S. Scanu, M.C. Vilaro, Bovine beta-lactoglobulin acts as an acid-resistant drug carrier by exploiting its diverse binding regions, *Biol Chem*, 391 (2010) 21-32.

- [211] L. Ragona, F. Fogolari, L. Zetta, D.M. Perez, P. Puyol, K. De Kruif, F. Lohr, H. Ruterjans, H. Molinari, Bovine beta-lactoglobulin: interaction studies with palmitic acid, *Protein Sci*, 9 (2000) 1347-1356.
- [212] S. Lu, A.W. Gough, W.F. Bobrowski, B.H. Stewart, Transport properties are not altered across Caco-2 cells with heightened TEER despite underlying physiological and ultrastructural changes, *J Pharm Sci*, 85 (1996) 270-273.
- [213] S. Ghoshal, J. Witta, J. Zhong, W. de Villiers, E. Eckhardt, Chylomicrons promote intestinal absorption of lipopolysaccharides, *J Lipid Res*, 50 (2009) 90-97.
- [214] H.M. Said, D.E. Ong, J.L. Shingleton, Intestinal uptake of retinol - enhancement by bovine-milk beta-lactoglobulin, *Am J Clin Nutr*, 49 (1989) 690-694.
- [215] W.B. Grant, G.K. Schwalfenberg, S.J. Genuis, S.J. Whiting, An estimate of the economic burden and premature deaths due to vitamin D deficiency in Canada, *Molecular nutrition & food research*, 54 (2010) 1172-1181.
- [216] W.B. Grant, H.S. Cross, C.F. Garland, E.D. Gorham, J. Moan, M. Peterlik, A.C. Porojnicu, J. Reichrath, A. Zittermann, Estimated benefit of increased vitamin D status in reducing the economic burden of disease in western Europe, *Prog Biophys Mol Biol*, 99 (2009) 104-113.
- [217] W.B. Grant, An estimate of the global reduction in mortality rates through doubling vitamin D levels, *Eur J Clin Nutr*, 65 (2011) 1016-1026.
- [218] M. Tippetts, S. Martini, C. Brothersen, D.J. McMahon, Fortification of cheese with vitamin D3 using dairy protein emulsions as delivery systems, *J Dairy Sci*, 95 (2012) 4768-4774.
- [219] E.A. Yetley, Multivitamin and multimineral dietary supplements: definitions, characterization, bioavailability, and drug interactions, *Am J Clin Nutr*, 85 (2007) 269S-276S.
- [220] B. Ganesan, C. Brothersen, D.J. McMahon, Fortification of cheddar cheese with vitamin D does not alter cheese flavor perception, *J Dairy Sci*, 94 (2011) 3708-3714.
- [221] T. Nicolai, M. Britten, C. Schmitt,  $\beta$ -Lactoglobulin and WPI aggregates: Formation, structure and applications, *Food Hydrocoll*, 25 (2011) 1945-1962.
- [222] F. Diarrassouba, G.E. Remondetto, L. Liang, G. Garrait, E. Beyssac, M. Subirade, Effects of gastrointestinal pH conditions on the stability of the  $\beta$ -lactoglobulin/vitamin D3 complex and on the solubility of vitamin D3, *Food Res Int*, 52(2013):515-521.

- [223] N.I.H. Health, Dietary Supplement FACT Sheet : Vitamin D, in, NIH Office of Dietary Supplements, Bethesda, MD, USA, 2011.
- [224] F. Diarrassouba, G.E. Remondetto, G. Garrait, P. Alvarez, E. Beyssac, M. Subirade, Self-assembly of  $\beta$ -lactoglobulin and egg white lysozyme as a potential carrier for nutraceuticals, (Unpublished) 2013.
- [225] Y. Luo, Z. Teng, Q. Wang, Development of zein nanoparticles coated with carboxymethyl chitosan for encapsulation and controlled release of vitamin D3, *J Agric Food Chem*, 60 (2012) 836-843.
- [226] Q. Li, C.-G. Liu, Z.-H. Huang, F.-F. Xue, Preparation and Characterization of Nanoparticles Based on Hydrophobic Alginate Derivative as Carriers for Sustained Release of Vitamin D3, *J Agric Food Chem.*, 59 (2011) 1962-1967.
- [227] Y. Luo, Z. Teng, X. Wang, Q. Wang, Development of carboxymethyl chitosan hydrogel beads in alcohol-aqueous binary solvent for nutrient delivery applications, *Food Hydrocoll*, 31 (2013) 332-339.
- [228] M. Haham, S. Ish-Shalom, M. Nodelman, I. Duek, E. Segal, M. Kustanovich, Y.D. Livney, Stability and bioavailability of vitamin D nanoencapsulated in casein micelles, *Food Funct*, 3 (2012) 737-744.
- [229] B.Y. Qin, G.B. Jameson, M.C. Bewley, E.N. Baker, L.K. Creamer, Functional implications of structural differences between variants A and B of bovine  $\beta$ -lactoglobulin, *Protein Sci*, 8 (1999) 75-83.
- [230] R.E. Grossmann, V. Tangpricha, Evaluation of vehicle substances on vitamin D bioavailability: a systematic review, *Mol Nutr Food Res*, 54 (2010) 1055-1061.
- [231] S.T. Dybing, D.E. Smith, The ability of phosphates or  $\kappa$ -carrageenan to coagulate whey proteins and the possible uses of such coagula in cheese manufacture, *J Dairy Sci*, 81 (1998) 309-317.
- [232] D.A. Hanley, K.S. Davison, Vitamin D insufficiency in North America, *J Nutr*, 135 (2005) 332-337.
- [233] P. Lips, Vitamin D physiology, *Prog Biophys Mol Biol*, 92 (2006 ) 4-8.
- [234] B. Dawson-Hughes, R.P. Heaney, M.F. Holick, P. Lips, P.J. Meunier, R. Vieth, Estimates of optimal vitamin D status, *Osteoporosis Int*, 16 (2005) 713-716.
- [235] W.C. Byrdwell, J. Devries, J. Exler, J.M. Harnly, J.M. Holden, M.F. Holick, B.W. Hollis, R.L. Horst, M. Lada, L.E. Lemar, K.Y. Patterson, K.M. Philips, M.T. Tarrago-Trani, W.R. Wolf, Analyzing vitamin D in foods and supplements : methodologic challenges, *Am J Clin Nutr*, 88 (2008) 554S-557S.

- [236] C. Schmitt, L. Aberkane, C. Sanchez, Protein—polysaccharide complexes and coacervates, in: P.A.W. G. O. Phillips (Ed.) Handbook of hydrocolloids, Woodhead Publishing Limited. , Cambridge, UK, 2009, pp. 420-476.
- [237] S. Damodaran, K. Anand, L. Razumovsky, Competitive Adsorption of Egg White Proteins at the Air–Water Interface: Direct Evidence for Electrostatic Complex Formation between Lysozyme and Other Egg Proteins at the Interface, *J Agric Food Chem*, 46 (1998) 872-876.
- [238] M. Nigen, T. Croguennec, D. Renard, S. Bouhallab, Temperature Affects the Supramolecular Structures Resulting from  $\alpha$ -Lactalbumin–Lysozyme Interaction, *Biochemistry*, 46 (2007) 1248-1255.
- [239] M. Anton, F. Nau, V. Lechevalier, Egg proteins, in: P.A.W. G. O. Phillips (Ed.) Handbook of hydrocolloids, Woodhead Publishing Limited. , Cambridge, UK, 2009 pp. 359-382.
- [240] M. Bucciantini, E. Giannoni, F. Chiti, F. Baroni, L. Formigli, J. Zurdo, N. Taddei, G. Ramponi, C.M. Dobson, M. Stefani, Inherent toxicity of aggregates implies a common mechanism for protein misfolding diseases, *Nature*, 416 (2002) 507-511.
- [241] J.M. Yu, Y.H. Li, L.Y. Qiu, Y. Jin, Self-aggregated nanoparticles of cholesterol-modified glycol chitosan conjugate: Preparation, characterization, and preliminary assessment as a new drug delivery carrier, *Eur Polym J*, 44 (2008) 555-565.
- [242] S.C. Cheison, E.K. Bor, A.K. Faraj, U. Kulozik, Selective hydrolysis of  $\alpha$ -lactalbumin by Acid Protease A offers potential for  $\beta$ -lactoglobulin purification in whey proteins, *Food Sci Technol-LEB* 49 (2012) 117-122.
- [243] M.F. Holick, Vitamin D: Important for prevention of osteoporosis, cardiovascular heart disease, type 1 diabetes, autoimmune diseases, and some cancers, *South Med J*, 98 (2005) 1024-1027.
- [244] E.A. Yetley, Assessing the vitamin D status of the US population, *Am J Clin Nutr*, 88 (2008) 558S-564S.
- [245] S.C. Murphy, L.J. Whited, L.C. Rosenberry, B.H. Hammond, D.K. Bandler, K.J. Boor, Fluid milk vitamin fortification compliance in New York State, *J Dairy Sci*, 84 (2001) 2813-2820.
- [246] H. Vatanparast, M.S. Calvo, T.J. Green, S.J. Whiting, Despite mandatory fortification of staple foods, vitamin D intakes of Canadian children and adults are inadequate, *J Steroid Biochem Mol Biol*, 121 (2010) 301-303.
- [247] D.C. Woollard, H.E. Indyk, CHOLECALCIFEROL | Properties and Determination, in: C. Editor-in-Chief: Benjamin (Ed.) Encyclopedia of Food

Sciences and Nutrition (Second Edition), Academic Press, Oxford, 2003 pp. 1205-1213.

[248] T. Imoto, Lysozyme, in: eLS, John Wiley & Sons, Ltd, 2001.

[249] P. Artursson, J. Karlsson, Correlation between oral drug absorption in humans and apparent drug permeability coefficients in human intestinal epithelial (Caco-2) cells, *Mol Cell Biol Res Commun*, 175 (1991) 880-885.

[250] M.P. Desai, V. Labhasetwar, E. Walter, R.J. Levy, G.L. Amidon, The mechanism of uptake of biodegradable microparticles in Caco-2 cells is size dependent, *Pharm Res*, 14 (1997) 1568-1573.

[251] J.L. Johnson, V.V. Mistry, M.D. Vukovich, T. Hogue-Lorenzen, B.W. Hollis, B.L. Specker, Bioavailability of vitamin D from fortified process cheese and effects on vitamin D status in the elderly, *J Dairy Sci*, 88 (2005) 2295-2301.

[252] R. Vieth, H. Bischoff-Ferrari, B.J. Boucher, B. Dawson-Hughes, C.F. Garland, R.P. Heaney, M.F. Holick, B.W. Hollis, C. Lamberg-Allardt, J.J. McGrath, A.W. Norman, R. Scragg, S.J. Whiting, W.C. Willett, A. Zittermann, The urgent need to recommend an intake of vitamin D that is effective, *Am J Clin Nutr*, 85 (2007) 649-650.

[253] C. Schmitt, C. Bovay, A.-M. Vuillomenet, M. Rouvet, L. Bovetto, R. Barbar, C. Sanchez, Multiscale Characterization of Individualized  $\beta$ -Lactoglobulin Microgels Formed upon Heat Treatment under Narrow pH Range Conditions, *Langmuir*, 25 (2009) 7899-7909.

[254] A.C. Alting, R.J. Hamer, C.G. de Kruif, R.W. Visschers, Formation of Disulfide Bonds in Acid-Induced Gels of Preheated Whey Protein Isolate, *J Agric Food Chem*, 48 (2000) 5001-5007.



# APPENDICES

## **APPENDIX 1**

### **List of contributions**

## List of manuscripts

1. **Diarrassouba, F.**; Remondetto, G.; Liang, L.; Garrait, G.; Beyssac, E. and Subirade, M. 2013. Effects of Gastrointestinal pH Conditions on the Stability of the  $\beta$ -Lactoglobulin/Vitamin D<sub>3</sub> Complex and on the solubility of Vitamin D<sub>3</sub>. *Food Research International*, 52(2):515-521.
2. **Diarrassouba, F.**; Liang, L.; Remondetto, G. and Subirade, M. 2013. Nanocomplex formation between riboflavin and  $\beta$ -lactoglobulin: Spectroscopic investigation and biological characterization. *Food Research International*, 52(2):557-567.
3. **Diarrassouba, F.**; Garrait, G.; Remondetto, G.; Alvarez, P.; Beyssac, E. and Subirade, M. 2013. Increased Stability and Protease Resistance of the  $\beta$ -Lactoglobulin/Vitamin D<sub>3</sub> Complex. 2014. *Food Chemistry*, 145:646-652.
4. **Diarrassouba, F.**; Remondetto, G.; Garrait, G.; Alvarez, P.; Beyssac, E. and Subirade, M. 2013. Increased Water Solubility, Stability and Bioavailability of Vitamin D<sub>3</sub> Upon Sequestration in  $\beta$ -lactoglobulin - Based Coagulum. Submitted to the *Journal of Controlled Release*.
5. **Diarrassouba, F.**; Garrait, G.; Remondetto, G.; Alvarez, P.; Beyssac, E. and Subirade, M. 2013. Self-Assembly of  $\beta$ -lactoglobulin and Egg White Lysozyme as a Potential Carrier for Nutraceuticals. Submitted to *The Journal of Physical Chemistry B*. JP-2013-08298b.
6. **Diarrassouba, F.**; Garrait, G.; Remondetto, G.; Alvarez, P.; Beyssac, E. and Subirade, M. 2013. Food Proteins-Based Microspheres for Increased Uptake of Vitamin D<sub>3</sub>. Submitted to *The Journal of Controlled Release*.
7. **Diarrassouba, F.**; Remondetto, G.; Alvarez, P. and Subirade, M. 2013. Spectroscopic Investigations on the Interactions between Lysozyme and Vitamin D<sub>3</sub>. *In preparation*.
8. **Diarrassouba, F.**; Remondetto, G. and Subirade, M. 2013.  $\beta$ -Lactoglobulin-based Oral Delivery Systems. (Review paper). Chapter 13. *In Engineering Foods for Bioactives Stability and Delivery*. Yrjö H. Roos and Yoav D. Livney. Ed. Springer. (*In press*).

## Conferences

1. Fatoumata Diarrassouba, Li Liang, Gabriel Remondetto and Muriel Subirade. Formation of Riboflavin/ $\beta$ -lactoglobulin Nanocomplex and Impact on Riboflavin's Photo-Activation. The 39th Annual Meeting & Exposition of the Controlled Release Society, July 15 - 18, 2012, Quebec City, Canada. C&DP: Nutraceuticals and Functional Foods podium session. (Oral presentation, see Appendix 5).

2. Fatoumata Diarrassouba, Ghislain Garrait, Eric Beyssac, Gabriel Remondetto and Muriel Subirade. Effects of Gastrointestinal pH Conditions on the Stability of the  $\beta$ -lactoglobulin/Vitamin D3 Complex and on the Solubility of Vitamin D3. The 39th Annual Meeting & Exposition of the Controlled Release Society (CRS), July 15 – 18, 2012, Québec City, Canada. (Poster presentation, see Appendix 4).

3. Fatoumata Diarrassouba, Li Liang, Gabriel Remondetto and Muriel Subirade. Evidence of the occurrence of efficient energy transfer between  $\beta$ -lactoglobulin and riboflavin and implication for the photo-activation of riboflavin. CIFST's 50<sup>th</sup> National Conference "*Innovation Meets Commercialization*", Niagara Falls, Ontario on May 27-29, 2012. (Poster presentation, see Appendix 5).

4. Fatoumata Diarrassouba, Li Liang, Gabriel Remondetto and Muriel Subirade. The use of riboflavin and  $\beta$ -lactoglobulin in photodynamic therapy: investigation of light energy transfer and its clinical implications. Nutraceuticals & Functional Foods Division Poster Session - Food, Health & Nutrition Track. IFT Annual Meeting being held in New Orleans, LA from June 11 – June 14, 2011. Division poster competition for the International Division: George Stewart graduate paper competition (1st place winner). (Poster presentation, see Appendix 3)

5. Fatoumata Diarrassouba, Li Liang, Gabriel Remondetto and Muriel Subirade. Spectroscopic investigation of the interaction between Riboflavin and  $\beta$ -Lactoglobulin. Nutraceuticals & Functional Foods Division Poster Session - Food, Health & Nutrition Track. IFT Annual Meeting being held in New Orleans, LA from June 11 – June 14, 2011. (Poster presentation, see Appendix 2).

6. Fatoumata Diarrassouba. Protein-ligand Complexes in foodstuff, mechanisms of formation, physicochemical & biological characterization. Student oral professional presentation. IFT Annual Meeting being held in New Orleans, LA from June 11 – June 14, 2011. (Oral presentation).

## **APPENDIX 2**

Spectroscopic investigation of the interaction between  
riboflavin and  $\beta$ -lactoglobulin

**Fatoumata Diarrassouba, Li Liang and Muriel Subirade. (2011)**  
**Book of Abstracts p 77. (Poster)**

**IFT Annual Meeting and Food Expo.,  
New Orleans, Louisiana, USA. June 11-14, 2011.**

# Spectroscopic Investigation of the interaction between Riboflavin and $\beta$ -lactoglobulin



Fatoumata Diarrassouba, Li Liang, Gabriel Remondetto and Muriel Subirade

Canada research chair in protein, biosystem and functional food physical chemistry  
The Institute of Nutraceuticals and Functional Foods (INAF/Stela)



## ABSTRACT

Riboflavin (RF) is essential for living cell growth and development. It is also the precursor of important coenzymes involved in numerous metabolic reactions. However, this vitamin is extremely sensitive to light and can be easily degraded with subsequent loss of its biological properties. On the other hand,  $\beta$ -lactoglobulin ( $\beta$ lg) is well recognized as small ligands transporter, thus allowing protection and preservation of their biological properties. The current study hypothesized that RF can bind to  $\beta$ lg which may result in the preservation of the vitamin biological properties.

Spectroscopic methods, including Circular Dichroism and fluorescence spectroscopy, were used to investigate the interactions between  $\beta$ lg and RF. The far-UV CD data showed minor impact of RF on the secondary structure of  $\beta$ lg while significant modification of the protein tertiary structure was revealed by alteration of the near-UV CD signals. Moreover, the fluorescence of  $\beta$ lg was strongly quenched by RF and the data indicated that RF binds to  $\beta$ lg forming ground stable complexes through static quenching mechanism. The analysis of the binding parameters revealed that RF probably binds at the entrance of the hydrophobic cavity and surface hydrophobic site of the protein. The complex  $\beta$ lg/RF is stabilised by hydrophobic interactions and hydrogen bonds.

The present study demonstrated the occurrence of interactions between RF and  $\beta$ lg at the molecular level. The findings generated are crucial for both the food and pharmaceutical industries, since they imply the potential use of  $\beta$ lg/RF complexes to preserve and improve the biological properties of RF.

## INTRODUCTION

### Riboflavin (RF) (Bates 2005)

- Essential vitamin for physiological functions and the metabolism
- Central component of cofactors FAD and FMN, required for many cellular processes
- Insufficient RF uptake associated with iron deficiency and anaemia, especially in under-developed countries

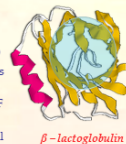
### Problems (Cardoso et al., 2004)

- Photosensitivity: > 80% losses in milk within a few hours
- Fragile and very sensitive: > 20% losses during food processing
- Difficult to stabilize in pharmaceuticals and food products



### $\beta$ -lactoglobuline ( $\beta$ lg) (Liang et al. 2006)

- Transports small hydrophobic ligands (resveratrol, Vitamin D)
- Formation of soluble complexes with bound ligands which can improve their solubility
- Presence of intestinal receptors for  $\beta$ lg, where absorption of RF takes also place
- Interactions between  $\beta$ lg and RF may improve RF biological properties: photosensitivity, stability and bio-availability



Aim : Demonstrate the transport role of  $\beta$ lg which could improve RF absorption and biological properties

## RESULTS AND DISCUSSION

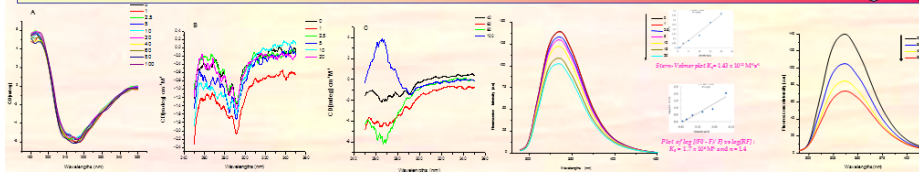


Figure 1: (A) Far-UV; (B) and (C) near-UV CD spectra of  $\beta$ lg in absence and presence of increasing concentration of RF (0 to 100  $\mu$ M) in 10mM phosphate buffer at pH 7.4.  $\beta$ lg 10  $\mu$ M (far-UV region), 20  $\mu$ M (near-UV region).

Figure 2: Fluorescence emission spectra of  $\beta$ lg (10  $\mu$ M) in the presence of different concentrations of RF (0, 1, 2.5, 5, 10, 15 and 20  $\mu$ M).

Figure 3: Fluorescence intensity of  $\beta$ lg (10  $\mu$ M) as a function of temperature (20, 35, 45, 55°C) in phosphate buffer 10mM, pH 7.4.

### Circular Dichroism:

### Fluorescence Spectroscopy:

## MATERIALS AND METHODS

### Circular Dichroism (Jasco J-710 Spectropolarimeter)

- $\beta$ lg secondary far-UV (190 to 250 nm) and tertiary structure near-UV (250 to 350 nm).  $\beta$ lg: 10  $\mu$ M and 20  $\mu$ M. RF: 0, 1, 2.5, 5, 10, 20, 40, 60, 80 and 100  $\mu$ M. Pathlengths: 0.1 cm (far-UV) and 1 cm (near-UV).

### Fluorescence Spectroscopy (Cary Eclipse 300, Varian Inc. USA)

- The fluorescence spectra recorded at different temperatures (20, 35, 45 and 55°C) for  $\beta$ lg 10  $\mu$ M in presence of RF (0, 1, 2.5, 5, 10, 15 and 20  $\mu$ M).
- The fluorescence emission spectra in the range of 290 to 450 nm were recorded (Ex: 280nm); RF no fluorescence in the range of 300–450 nm.

## CONCLUSION

- The fluorescence of  $\beta$ lg strongly quenched by RF: important interactions occur between  $\beta$ lg and RF
- Static quenching mechanism and formation of ground stable complexes.
- Two binding sites for RF: the central hydrophobic cavity and contact site between the two monomers.
- $K_s = 1.7 \times 10^4 \text{ M}^{-1}$ ,  $n = 1.4$  for  $\beta$ lg 10  $\mu$ M.
- Hydrophobic interactions and hydrogen bonds involved in the binding.
- Photodynamic therapy: Upon UV-vis irradiation, RF enters excited states to initiate photo-oxidation process which can lead to degradation of proteins and biological systems.

## REFERENCES

- Bates (2005) Encyclopedia of Human Nutrition (2<sup>nd</sup> Ed.). Pp. 100-108.
- Cardoso et al. (2004). J. Agric. Food Chem. 52:6602-6606.
- Flower et al. (2000) BBA - Protein Struct. Mol. Enzymol. 1482:9-24.
- Lakowicz (2006) Principles of fluorescence spectroscopy, Springer (Ed.). Pp. 443-475. New York, USA.
- Liang et al. (2008) Biomacromolecules. J. Phys. Chem. 9:50-56.
- Tian et al. (2006) BBA - General Subjects. 1760:38-46.
- Wang et al. (2008) J. Mol Struct. 875:509-514.
- Zandomenighi et al. (2009). J. Agric. Food Chem. 57:6510-6517.
- Zhao et al. (2006) Spectrochim. Acta A Mol Biomol Spectro. 65:811-817.

## ACKNOWLEDGEMENT

## **APPENDIX 3**

### **The use of riboflavin and $\beta$ -lactoglobulin in photodynamic therapy: investigation of light energy transfer and its clinical implications**

**1st place – IFT International Division  
George Stewart graduate paper competition at the 2011 Annual Meeting IFT**

**Fatoumata Diarrassouba, Li Liang and Muriel Subirade. (2011). Book of  
Abstracts p 77. (Poster and podium (oral) presentation)**

**IFT Annual Meeting and Food Expo., New Orleans, Louisiana, USA. June 11-  
14, 2011.**

# The Use of Riboflavin and $\beta$ -Lactoglobulin in Photodynamic Therapy: Investigation of Light Energy Transfer and Its Clinical Implications



Fatoumata Diarrassouba, Li Liang, Gabriel Remondetto and Muriel Subirade

Canada research chair in protein, biosystem and functional food physical chemistry; The Institute of Nutraceuticals and Functional Foods (INAF/Stela)

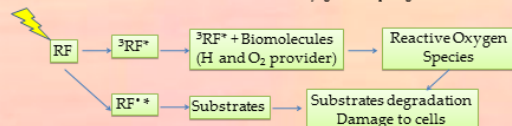


## ABSTRACT

Riboflavin (RF) is crucial for living cell development and conversely, acts as a photosensitizer that can promote damage in biological systems through photo-oxidation processes. The major whey protein,  $\beta$ -Lactoglobulin ( $\beta$ lg), is well recognized as small ligands transporter, thus allowing protection of their biological properties. The current study reports the use of spectroscopic methods to prove the occurrence of interactions and energy transfer between  $\beta$ lg and RF.

The fluorescence of  $\beta$ lg was strongly quenched by RF which forms ground state complexes with the protein through a quenching mechanism that is static. The Förster theory was used to demonstrate the occurrence of efficient energy transfer between the two biomolecules. The data generated in the present study suggest that  $\beta$ lg/RF complexes could be used in photodynamic therapy. Upon appropriate light irradiation, these complexes may generate reactive oxygen and radical species. As a result, protein and other biological systems can be damaged causing subsequent cell death. This is a comprehensive study that provides first hand and accurate information for the potential use of RF alone as endogenous photosensitizer or in combination with  $\beta$ lg to generate photodynamic reaction.

This finding of paramount importance has crucial clinical and biological implications, especially in tumour and cancer cells treatment as well as in the food industry against food pathogens.



## INTRODUCTION

Photodynamic therapy (PDT) is applied in the treatment of various tumors and nonmalignant diseases. PDT involves the use of a photosensitizer, which upon light absorption, triggers cascade biological systems damaging reactions involving the singlet oxygen ( $^1O_2$ ) and biomacromolecules (Tardivo et al. 2005).

PDT is based on the combination of a photosensitizer that is selectively localized in the target tissue and illumination of the lesion with visible light, resulting in photodamage and subsequent cell death (Baldisseri et al. 2003).

**Type I Photooxidation** : formation reactive radicals (Superoxide ion ( $O_2^{\cdot-}$ ), hydroxyl ( $OH^{\cdot}$ ) caused by removal of H or e<sup>-</sup> by  $^3RF^*$  from biomolecules.

**Type II Photooxidation** : energy transfer from  $^3RF^*$  to residual  $O_2$  to form the singlet oxygen state ( $^1O_2$ ) which reacts very strongly with substrates.

## MATERIALS & METHODS

**Fluorescence Spectroscopy** (Cary Eclipse 300, Varian Inc. USA)

The fluorescence spectra recorded for  $\beta$ lg 10  $\mu$ M in presence of RF (0, 1, 2.5, 5, 10, 15, 20  $\mu$ M). Em. 290 to 450 nm, Ex. 280nm; RF has no fluorescence in the range of 300–450 nm.

**Synchronous Fluorescence** (Cary Eclipse 300, Varian Inc. USA)

The fluorescence scans for  $\beta$ lg fluorochromes tyrosine ( $\Delta\lambda=15$  nm) and for Tryptophane ( $\Delta\lambda=60$ nm), were recorded in presence of increasing concentrations of RF.

**Fröster's Theory of Energy Transfer**

Minimal distance from donor to acceptor ( $r$ ) < 8 nm and  $0.5 R_0 < r < 2 R_0$  ( $R_0$  = Fröster distance) for efficient energy transfer.

Efficient Energy Transfer (E)

$$E = 1 - \frac{F}{F_0} = \frac{R_0^6}{R_0^6 + r^6}$$

Integral of the overlapping (J)

$$J = \int_0^\infty F(\lambda) \varepsilon(\lambda) \lambda^4 d\lambda$$

Fröster distance ( $R_0$ )

$$R_0 = 9.78 \times 10^8 \left[ \kappa^2 r^6 J \right]^{-1/6}$$

## RESULTS

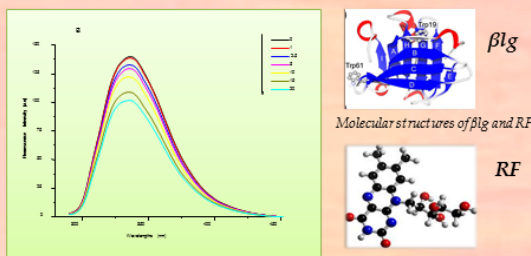


Figure 1: Fluorescence of  $\beta$ lg (10  $\mu$ M) in presence of increasing conc. of RF (0, 1, 2.5, 5, 10, 15 and 20  $\mu$ M) in phosphate buffer 10 mM

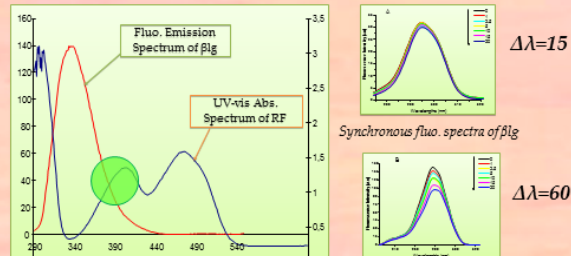


Figure 2: Evidence of efficiency transfer: overlap of the fluorescence emission spectrum of the donor  $\beta$ lg and the UV-vis absorption spectrum of the acceptor RF

Table 1: Energy efficiency transfer (E) and distance between the donor  $\beta$ lg and the acceptor RF

$\beta$ lg ( $\mu$ M)	Ratio RF / $\beta$ lg	E	J ( $10^{18} M^{-1} cm^{-3}$ )	$R_0$ (nm)	r (nm)
10	0.1	0,0087	7,99	1,246	2,706
	0.4	0,058	7,58	1,236	1,936
	0.2	0,086	7,36	1,230	1,797
	1	0,146	6,88	1,216	1,608
	1.5	0,250	6,05	1,190	1,410
	2	0,323	5,45	1,169	1,304

## DISCUSSION

- RF can induce important damage in cells, DNA, proteins and biomolecules, resulting in various lesions to diverse biological systems (Grzelak et al. 2001).
- Proteins (~68%) of the dry weight of cells and tissues, as such, constitute interesting targets for photo-oxidation. Upon UV irradiation, they undergo either direct oxidation (excited states, radicals) or indirect oxidation ( $^1O_2$ ) (Davies & Truscott 2001).
- Singlet oxygen-mediated protein oxidation induces changes to side-chains and backbone of amino acids, peptides, and proteins. Changes in tryptophan provokes formation of reactive peroxide intermediate and sustained cascade cell damage.
- RF binds to  $\beta$ lg near the tryptophan amino acid and efficient energy transfer occurs between the two molecules, making this association interesting alternative to expensive conventional photosensitizers used in photodynamic therapy (Tardivo et al. 2005).

## CONCLUSION

- Important interactions occur between RF and  $\beta$ lg. The fluorescence of  $\beta$ lg is strongly quenched by RF.
- RF binds to  $\beta$ lg in the vicinity of the tryptophanyl amino acid residues
- Efficient energy transfer occurs between  $\beta$ lg and RF according to the Fröster theory of non radiative energy transfer.
- $\beta$ lg and RF complexes can be light activated to generate reactive oxygen species which in turn will create cascade damaging reactions to biological systems.
- $\beta$ lg and RF complexes can be efficiently used in photodynamic therapy to treat tumor tissues and in the food industry to destroy pathogenic cells.

## REFERENCE & ACKNOWLEDGEMENT

### Reference

- Baldisseri et al. (2003). *Biomacromolecules*. 4(2):429–436.
  - Davies & Truscott (2001). *J. Photochem. Photobiol. B: Biol.* 63(1-3):114-125.
  - Grzelak et al. (2001). *Free radic. biol. med* 30:1418-1425.
  - Lakowicz (2006). *Energy transfer*, in: Springer (Ed.), *Principles of fluorescence spectroscopy*, New York, USA, pp. 443-475.
  - Tardivo et al. (2005). *Photodiagnosis and Photodynamic Therapy*. 2(3):175-191.
  - Wang et al. (2008). *J. Molecular Structure* 875:509-514.
- Acknowledgement**
- Canada Research Chair in Protein, Biosystem and Functional Food Physical Chemistry
  - The Vanier Canada Graduate Scholarships – The Natural Sciences and Engineering Research Council of Canada (NSERC) (Fatoumata Diarrassouba)

## **APPENDIX 4**

### **Effects of gastrointestinal pH conditions on the stability of the $\beta$ -lactoglobulin and vitamin D3 complex and on the solubility of vitamin D3**

**Fatoumata Diarrassouba, Li Liang, Ghislain Garrait, Eric Beyssac, Gabriel Remondetto and Muriel Subirade (Poster)**

**The 39th Annual Meeting & Exposition of the Controlled Release Society  
July 15-18, 2012, Centre des congrès de Québec, Québec City, Canada**

# Effects of Gastrointestinal pH Conditions on the Stability of the $\beta$ -lactoglobulin/Vitamin D<sub>3</sub> Complex and on the Solubility of Vitamin D<sub>3</sub>



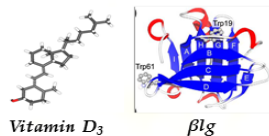
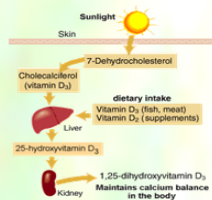
Fatoumata Diarrassouba, Li Liang, Ghislain Garrat, Eric Beyssac, Gabriel Remondetto and Muriel Subirade

Canada research chair in protein, biosystem and functional food physical chemistry; The Institute of Nutraceuticals and Functional Foods (INAF/Stela)



## ABSTRACT

The stability of the complex  $\beta$ lg/vitamin D<sub>3</sub> at pH values varying from 1.2 to 8 was investigated. The complex remained stable at all studied pH values, probably due to the formation of the complex prior to the pH modification. The study also reports the improvement of the solubility of vitamin D<sub>3</sub> as a result of binding to  $\beta$ lg.



Molecular structures of  $\beta$ lg and  $VD_3$

## INTRODUCTION

$\beta$ -lactoglobulin ( $\beta$ lg) has been well recognized as a transporter of small hydrophobic ligands such as vitamin D<sub>3</sub> (Wang et al. 1977; Yang et al. 2008). The binding sites for vitamin D<sub>3</sub> include the central calyx formed by the  $\beta$ -barrel and the surface hydrophobic pocket in the groove between the  $\alpha$ -helix and the  $\beta$ -barrel. The complex  $\beta$ lg-ligand is believed to protect the bound ligand from oxidative degradation and improve some of its solubility (Liang et al. 2008). However, very few studies evaluate the stability of the  $\beta$ lg-ligand complex under gastrointestinal conditions such as pH. Most studies rather evaluate the complex under conditions that can affect the binding capacity of the protein alone, before complexation with the ligand. This can impair the binding efficiency of  $\beta$ lg (Yang et al. 2008). For instance, pH plays a crucial role in controlling the opening and closing of the entrance of the calyx for ligands, the so-called Tanford transition (Qin et al. 1998). As such, at low pH the 'calyx gate' is in a closed configuration which prohibits binding of the ligands.

In addition to its classical action on the regulation of calcium and phosphorus homeostasis, vitamin D<sub>3</sub> has become the new 'miracle drug' that intervenes in the regulation of both innate and adaptive immune response, blood glucose and insulin level, the cardiovascular system, and protection against bacterial infections, inflammatory bowel diseases, breast and colon cancers, and leukemia; the list is not exhaustive (Helick 2007). Therefore, increasing the bioavailability of vitamin D<sub>3</sub> is important. The current study evaluates the stability of the  $\beta$ lg/vitamin D<sub>3</sub> complex under various pH conditions including that of the gastrointestinal tract and examines its effects on the solubility of vitamin D<sub>3</sub>.

## MATERIALS & METHODS

Fluorescence spectroscopy and Synchronous fluorescence were used to study the binding of vitamin D<sub>3</sub> to  $\beta$ lg and to determine the effects of pH (1.2, 2, 3, 5, 6.8, 7 and 8) on the stability of the complex. The excitation wavelength was 280 nm and  $\Delta\lambda$  was 60 nm for the fluorescence scans (Liang et al. 2008).

Fractional residual fluorescence ( $F_{max}/F_0$ ) was used to determine the fraction of the total protein fluorescence that was not quenched, and thus the fraction of  $\beta$ lg not bound to ligand (Liang et al. 2012).  $F$  is fluorescence intensity of  $\beta$ lg versus wavelength;  $F_{max}$  is the intensity at the emission maximum ( $\lambda_{max}$ ), and  $F_0$  is the intensity for  $\beta$ lg at  $\lambda_{max}$  and is proportional to concentration. A low ratio therefore indicates strong binding of the ligand while a ratio of 1 (100%) indicates no binding. The fractional residual fluorescence is a good measure of the stability of the  $\beta$ lg/ligand complex (Liang et al. 2012).

Vitamin D<sub>3</sub> solubility was determined by RP-HPLC. The  $\beta$ lg/ $VD_3$  complex was prepared at different ratios using a static concentration of vitamin D<sub>3</sub> and increasing concentrations of  $\beta$ lg.

## RESULTS

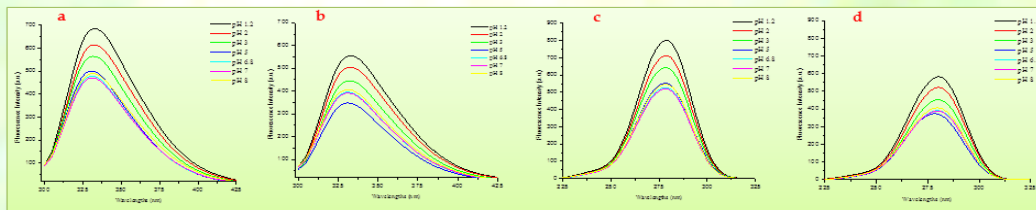


Figure 1: Fluorescence intensity of  $\beta$ lg (a) and the  $\beta$ lg/ $VD_3$  complex (b) at different pH (1.2, 2, 3, 5, 6.8, 7 and 8). Excitation at 290 nm

Figure 2: Synchronous fluorescence of  $\beta$ lg using  $\Delta\lambda = 60$  nm of  $\beta$ lg in absence (c) and presence of vitamin D<sub>3</sub> (d), at different pH (1.2, 2, 3, 5, 6.8, 7 and 8)

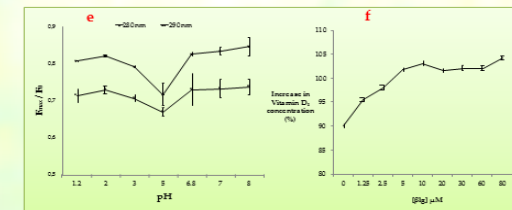


Figure 3: Binding capacity of  $\beta$ lg at different pH (1.2, 2, 3, 5, 6.8, 7 and 8). Excitation at 280 and 290 nm (e); Increase in the solubility Vitamin D<sub>3</sub> after 168 h (f)

## DISCUSSION

$\beta$ lg transports two molecules of vitamin D<sub>3</sub> in the central calyx and at the surface between the  $\alpha$ -helix and the  $\beta$ -barrel. Figure 1(a,b) clearly shows the binding of vitamin D<sub>3</sub> to  $\beta$ lg, with a decrease in the fluorescence intensity of  $\beta$ lg at all pH values. Interestingly, as shown in Figure 1e, the fractional residual fluorescence ( $F_{max}/F_0$ ) was similar for all pH values (0.75), implying that the binding of vitamin D<sub>3</sub> to  $\beta$ lg was not affected by pH. This finding is important, since it has been shown that significant transition of vitamin D<sub>3</sub> binding to  $\beta$ lg occurs at pH values between 6.0 and 8.0, and at pH values below 3, the binding site inside the central calyx is lost due to the Tanford transition effect (Qin et al. 1998).

In the current study, the  $\beta$ lg/vitamin D<sub>3</sub> complex was formed prior to pH modification. With the vitamin being already bound inside the calyx, the closure of the 'gate' did not displace the ligand. Furthermore, it has been shown that  $\beta$ lg retains vitamin D<sub>3</sub> bound to the exosite, even during the Tanford transition. As a result, the interaction between the two molecules did not change and the amount of vitamin D<sub>3</sub> bound to  $\beta$ lg was constant even at pH 1.2 and 6.8, corresponding to gastric and intestinal pH, respectively, and under alkaline conditions (pH 8).

## CONCLUSION

- Concerns about finding the safest and most effective way to increase the uptake of vitamin D<sub>3</sub> are real.
- $\beta$ lg can bind vitamin D<sub>3</sub> at all pH values, from pH 1.2 to pH 8. Therefore, the  $\beta$ lg/vitamin D<sub>3</sub> complex can remain stable in acid beverages, in gastric and intestinal pH and during pH-related structural transitions, including the Tanford transition.
- Increasing the amount of  $\beta$ lg significantly improved the solubility of vitamin D<sub>3</sub> ( $p < 0.0001$ ).
- These results are crucial as they demonstrate that  $\beta$ lg can be used to improve the absorption and thus the uptake of vitamin D<sub>3</sub>, which is involved in countless metabolic pathways needed to maintain or improve human health.

## REFERENCES & ACKNOWLEDGEMENT

**Reference**  
 Wang et al. *J. Dairy Sci.* 1997, 80, 1054-1059.  
 Yang et al. *Process.* 2008, 15, 1197-210.  
 Liang, L. et al. *Food Chem.* 2011, 126, 821-826.  
 Qin et al. *Biochemistry.* 1998, 37, 14014-14023.  
 Wang et al. *J. Dairy Sci.* 1999, 82, 257-264.  
 Helick, M.P. *Engl. J. Med.* 2007, 357, 216-31.  
 Liang and Subirade. *Food Chem.* 2012, 132, 20223-20229.  
 Yang, M.C. et al. *FEBS.* 2009, 276, 2251-2265.

**Acknowledgement**  
 Canada Research Chair in Protein, Biosystem and Functional Food Physical Chemistry  
 The Vaxier-Canada Graduate Scholarships – The Natural Sciences and Engineering Research Council of Canada (NSERC) (Fatoumata Diarrassouba)

## **APPENDIX 5**

# **Evidence of the Occurrence of Efficient Energy Transfer Between $\beta$ -lactoglobulin and Riboflavin and Implication for the Photo-Activation of Riboflavin**

**Fatoumata Diarrassouba, Li Liang, Gabriel Remondetto and Muriel Subirade**

**The 39th Annual Meeting & Exposition of the Controlled Release Society  
July 15-18, 2012, Centre des congrès de Québec, Québec City, Canada**

### **ABSTRACT : Podium (Oral) presentation**

Riboflavin (RF) is crucial for living cell development and conversely, acts as a photosensitizer that can promote damage in biological systems through photo-activation processes. The major whey protein,  $\beta$ -Lactoglobulin ( $\beta$ lg), is well recognized as small ligands transporter, thus allowing protection of their biological properties. The current study reports the use of spectroscopic methods to prove the occurrence of interactions and energy transfer between  $\beta$ lg and RF. The fluorescence of  $\beta$ lg was strongly quenched by RF which forms ground state complex with the protein through a quenching mechanism that is static. The Fröster theory was used to demonstrate the occurrence of efficient energy transfer between the two biomolecules. The data generated in the present study suggest that  $\beta$ lg/RF complex could be used in photodynamic therapy. Upon appropriate light irradiation, this complex may generate reactive oxygen and radical species. As a result, protein and other biological systems can be damaged causing subsequent cell death. This is a comprehensive study that provides first hand and accurate information for the potential use of RF alone as endogenous photosensitizer or in combination with  $\beta$ lg to generate photodynamic reaction. This finding of paramount importance has crucial clinical and biological implications, especially in tumour and cancer cells treatment as well as in the food industry against food pathogens.

## **APPENDIX 6**

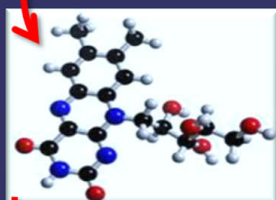
**Prix du public**

**Concours *Votre soutenance en 180 secondes*  
(*MT<sup>MC</sup>*) 2012**

**Finale Université Laval**

**Québec, le 24 avril 2012**

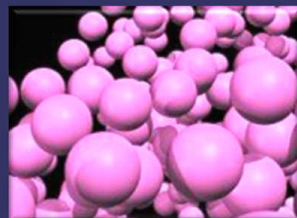
## Thérapie photo-dynamique



Vitamine B2



Protéine du lait



**Nano-complexes**  
Protéine du lait + Vitamine B2

x 1,000,000



2 mm

## Thérapie conventionnelle



**Cancer : Principale cause de mortalité au Canada**



Perte de cheveux



Fatigue

